SOLAR SPECTRUM FORMATION: EXAMPLES

Robert J. Rutten
https://webspace.science.uu.nl/~rutte101

thin: cloud modeling corona chromosphere Rydberg per ALMA?

thick: UV line flip VAL3C temperature VAL3C spectrum Kurucz stars

photospheric lines: inversions bright points reversed granulation Na I D1 MGs limb emission lines

continua from VAL3C: Avrett models versus 3D MHD VAL3C continua VALII budget hydrogen budget all

lines from ALC7: model optical spectrum ultraviolet depletion hydrogen strong lines plot formats pops plot BSJ plot profile plot Mg I 4571 Fe I 6302 Mg I b_2 Na I D_1 Ba II 4554 Ca II 8542 Å Ca II K Mg II k Lyα Hα Hβ He I 584 He I 10830 canonical Hα Na I D_1–Mg I b_2 Lyα–Hα Hα–Ca II 8542 Å Ca II K–Mg II k versus FCHHT-B ALC7–FALC FALC–FALP ALC7–FALP

detour lines: pumping suction

Oslo-simulated dynamic atmosphere: 1D RADYN 3D Bifrost Bifrost line synthesis

LA-conjectured PSBE atmosphere: non-E Hα aureole boosting Hα extinction CE–SB EBs spicules-II contrail ALMA non-E chromosphere?

IRIS diagnostics: overview diagnostics

CLOUD MODELING

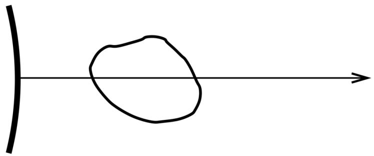

review: Tziotziou 2007ASPC..368..217T

Formal solution for line of sight (LOS) through irradiated cloud

$$I_\nu = I_\nu(0)\,\mathrm{e}^{-\tau_\nu^{\mathrm{c}}} + \int_0^{\tau_\nu^{\mathrm{c}}} S_\nu(t_\nu)\,\mathrm{e}^{-(\tau_\nu - t_\nu)}\,\mathrm{d}t_\nu$$

Homogeneous cloud, Gaussian broadening, parameters $I_0(\Delta\lambda)$, S, τ_0, LOS v

$$I(\Delta\lambda) = I_0(\Delta\lambda)\,\mathrm{e}^{-\tau(\Delta\lambda)} + S\left(1 - \mathrm{e}^{-\tau(\Delta\lambda)}\right) \qquad \tau(\Delta\lambda) = \tau_0\,\mathrm{e}^{-\left(\frac{\Delta\lambda - \lambda_0 v/c}{\Delta\lambda_{\mathrm{D}}}\right)^2}$$

$$C(\Delta\lambda) \equiv \frac{I(\Delta\lambda) - I_0(\Delta\lambda)}{I_0(\Delta\lambda} = \left(\frac{S}{I_0(\Delta\lambda} - 1\right)\left(1 - \mathrm{e}^{-\tau(\Delta\lambda)}\right)$$

Refinements: Voigt, τ-dependent S, wavelength-dependent S (for PRD with $S \approx S^l$)

Interpretation: $S \Rightarrow (T, \rho)$

– Beckers 1968SoPh....3..367B: Giovanelli NLTE hydrogen ionization tables
– Molowny-Horas et al. 1999A&A...345..618M: “inversion” from many model profiles

Problems: impinging profile, sideways irradiation, multi-thread

Hα CLOUD MODELING

Rutten & Uitenbroek *2012A&A...540A..86R*

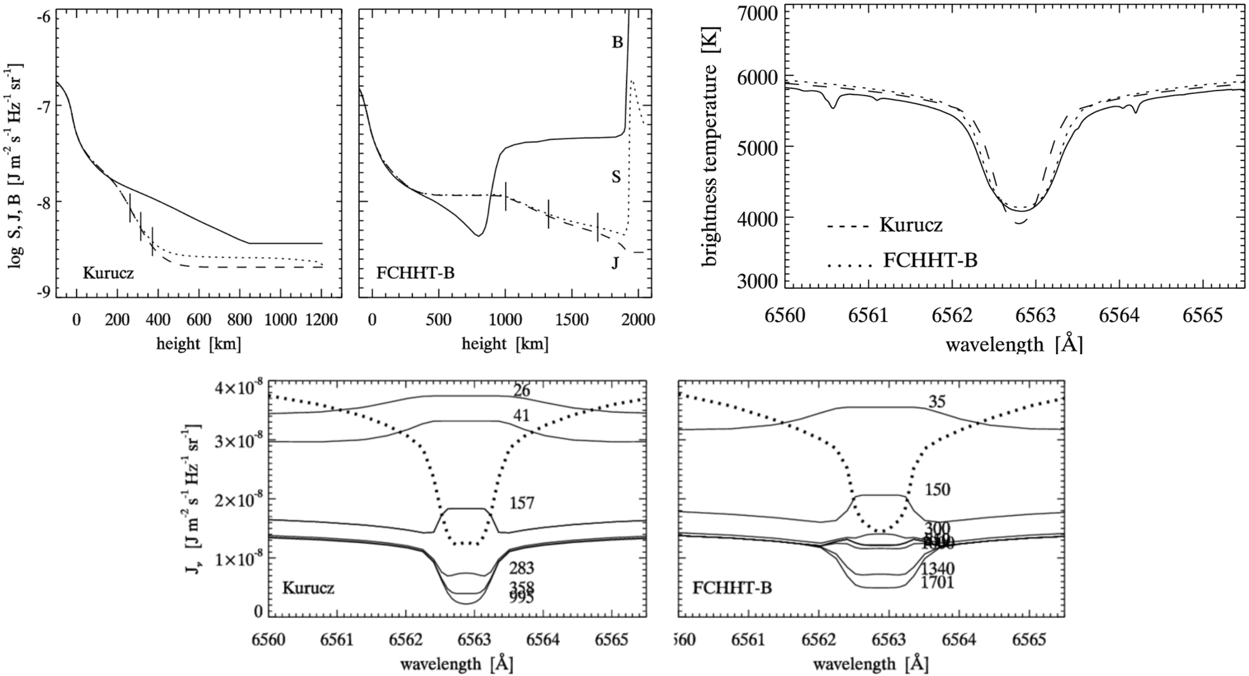

Ha-Ha formation: the Kurucz and FCHHT-B models both reproduce observed Hα

cloud modeling: $I_\nu = I_\nu(0)\,\mathrm{e}^{-\tau_\nu^{\mathrm{c}}} + \int_0^{\tau_\nu^{\mathrm{c}}} S_\nu(t_\nu)\,\mathrm{e}^{-(\tau_\nu - t_\nu)}\,\mathrm{d}t_\nu$

new recipe: for the impinging profile $I_\nu(0)$ take the outward I_ν profile in a RE model at the depth τ_{ν_0} which equals the cloud thickness $\tau_{\nu_0}^{\mathrm{c}}$ (dotted profiles)

SOLAR SPECTRUM FORMATION: EXAMPLES

Robert J. Rutten
https://webspace.science.uu.nl/~rutte101

thin: cloud modeling corona chromosphere Rydberg per ALMA?

thick: UV line flip VAL3C temperature VAL3C spectrum Kurucz stars

photospheric lines: inversions bright points reversed granulation Na I D1 MGs limb emission lines

continua from VAL3C: Avrett models versus 3D MHD VAL3C continua VALII budget hydrogen budget all

lines from ALC7: model optical spectrum ultraviolet depletion hydrogen strong lines plot formats pops plot BSJ plot profile plot Mg I 4571 Fe I 6302 Mg I b_2 Na I D_1 Ba II 4554 Ca II 8542 Å Ca II K Mg II k Lyα Hα Hβ He I 584 He I 10830 canonical Hα Na I D_1–Mg I b_2 Lyα–Hα Hα–Ca II 8542 Å Ca II K–Mg II k versus FCHHT-B ALC7–FALC FALC–FALP ALC7–FALP

detour lines: pumping suction

Oslo-simulated dynamic atmosphere: 1D RADYN 3D Bifrost Bifrost line synthesis

LA-conjectured PSBE atmosphere: non-E Hα aureole boosting Hα extinction CE–SB EBs spicules-II contrail ALMA non-E chromosphere?

IRIS diagnostics: overview diagnostics

SOLAR ECLIPSE VISIBILITY

P. den Hartog

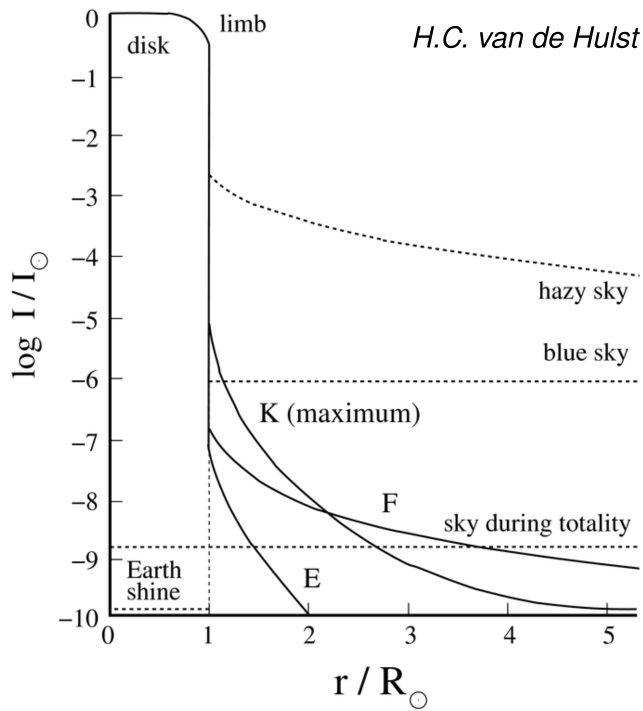

- dusty sky has 0.1 – 0.01% of the solar brighness (10^{-3} – 10^{-4}), brighter closer to Sun
- "coronal" blue sky (Rayleigh scattering) is one millionth (10^{-6}), even distribution across sky
- during totality the sky brightness is only one billionth (10^{-9}), less than the coronal brightness
- "K" = continuum component, "F" = Fraunhofer component, "E" = emission-line component
- earthshine (10^{-10}): new-moon brightness from full-earth-with-spot irradiation

start *index*

CORONAL WHITE LIGHT

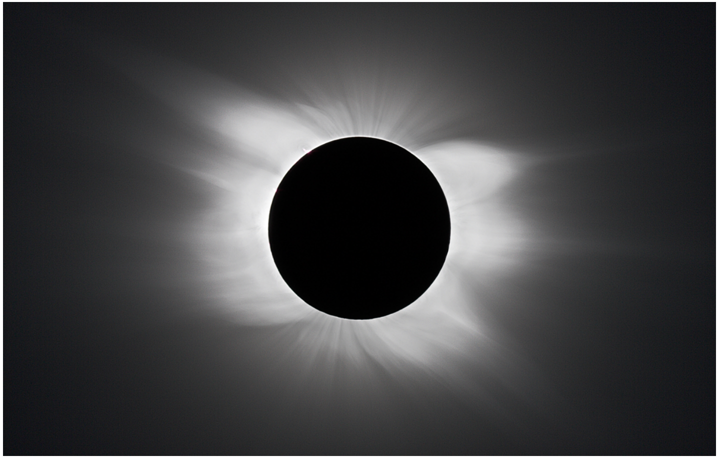

- Walter Grotrian (Potsdam, 1931)
  white ⇒ Thomson scattering of photospheric photons by free electrons
  weak ⇒ low electron density (electron cross-section only 10^{-25} cm^2)
  absence of photospheric Fraunhofer lines ⇒ washed out by large Dopplershifts
  required electron speeds 4000 km/s [⇒ if motions thermal: 1 million degrees !?]
- linear polarisation from right-angle scattering
- fine structure maps variatons in electron density dictated by magnetic fields
- the F component further out results from photon scattering by slower-moving inter-planetary dust particles; its spectrum shows the photospheric Fraunhofer lines

Appreciate that during totality you are illuminated by normal photospheric light — but only a 10^{-7} fraction bounced around the moon, without Fraunhofer lines, and polarized too!

WHITE LIGHT CORONA

M. Stix "The Sun", Section 9.1.3

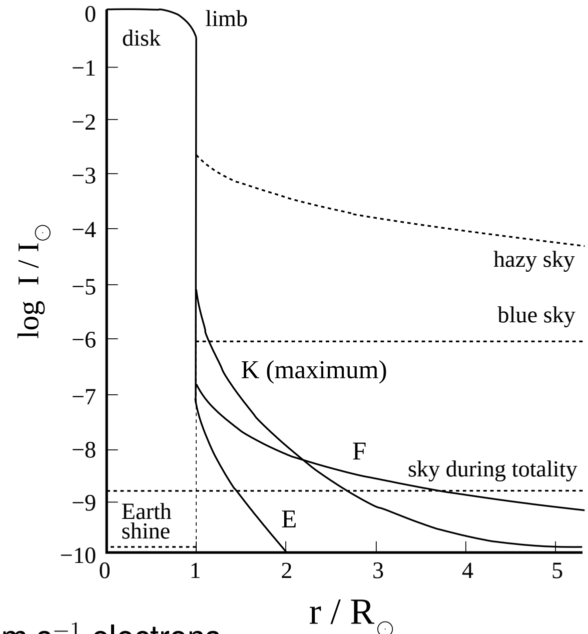

Grotrian (1931): Thomson scattering 8000 km s^{-1} electrons

$$\rho^2 = x^2 + y^2 \qquad I(x) = 2\int_0^\infty j(\rho)\,\mathrm{d}y = 2\int_x^\infty \frac{\rho\, j(\rho)}{\sqrt{\rho^2 - x^2}}\,\mathrm{d}\rho$$

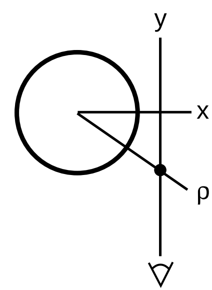

N_e from inverse Abel transform = isotropically scattered irradiation

$$j(\rho) = -\frac{1}{\pi}\int_\rho^\infty \frac{\mathrm{d}I/\mathrm{d}x}{\sqrt{x^2 - \rho^2}}\,\mathrm{d}x = \sigma_\mathrm{T}\, N_\mathrm{e}\, \frac{1}{4\pi}\int I_\odot(\theta)\,\mathrm{d}\Omega$$

“CORONIUM” LINES

M. Stix “The Sun”, Section 9.1.3 *http://laserstars.org/spectra/Coronium.html*

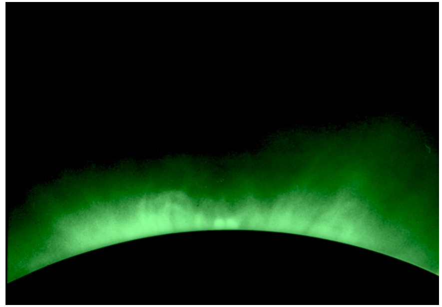

Grotrian (1939), Edlén (1942): forbidden lines high ionization stages (Stix Table 9.2 p. 398)

name	wavelength	identification	$\Delta\lambda_D$	$\overline{v}$	A_{ul}	previous ion	$\chi_{\rm ion}$
green line	530.29 nm	[Fe XIV]	0.051 nm	29 km/s	60 s^{-1}	Fe XIII	355 eV
yellow line	569.45	[Ca XV]	0.087	46	95	Ca XIV	820
red line	637.45	[Fe XI]	0.049	23	69	Fe X	235

Coronal sky at Dome C

EUV CORONA

bf equilibria: collisional ionization = radiative recombination ⇒ only $f(T)$, not $f(N_\mathrm{e})$

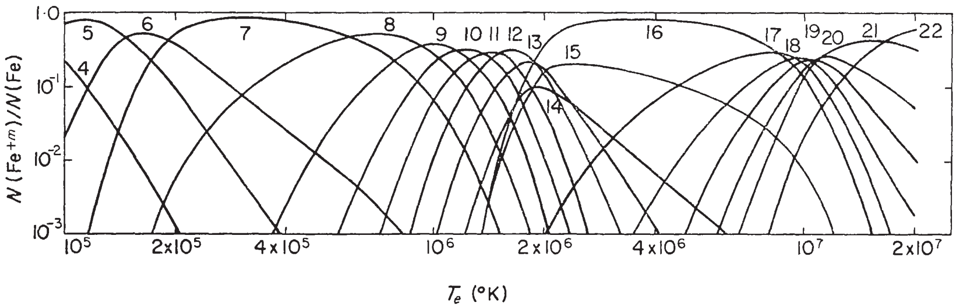

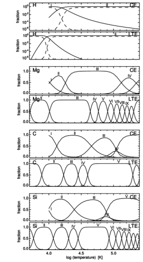

bb equilibria: collisional excitation = spontaneous deexcitation ⇒ $f(T, N_\mathrm{e})$

$$n_l C_{lu} = n_l N_\mathrm{e} \int_{v_0}^{\infty} \sigma_{lu} f(v)\, v \mathrm{d}v \approx n_u A_{ul} \qquad \sum h\nu \propto \int A_\mathrm{elem} N_\mathrm{H} N_\mathrm{e}\, \mathrm{d}z \approx \int N_\mathrm{e}^2 \left(\frac{\mathrm{d}T}{\mathrm{d}z}\right)^{-1} \mathrm{d}T \equiv \mathrm{EM}$$

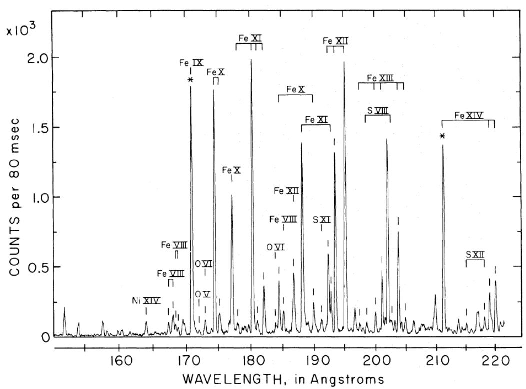

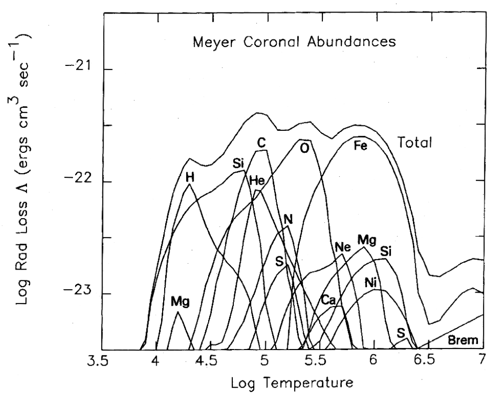

BRIGHT AND DARK IN EUV IMAGES

Rutten *1999ASPC..184..181R*

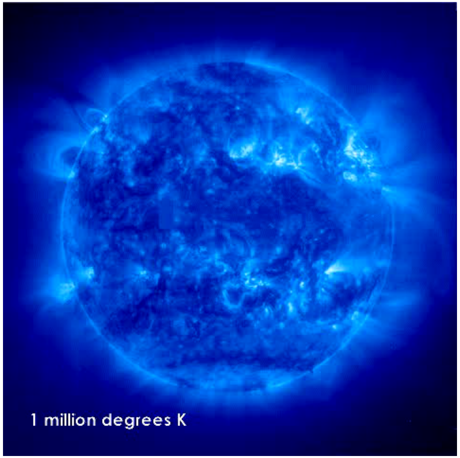

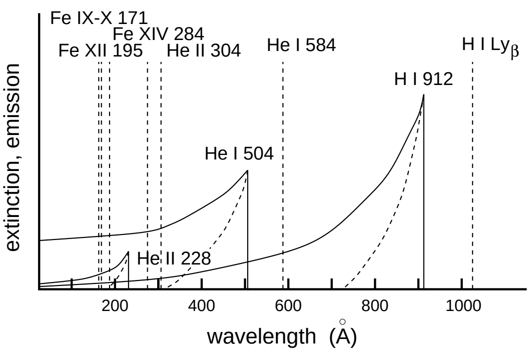

- *iron lines*
  - Fe IX/X 171 Å: about 1.0 MK
  - Fe XII 195 (AIA 193) Å: about 1.5 MK
  - Fe XIV 284 Å: about 2 MK
- *bright*
  - collision up, radiation down
  - thermal photon creation, NLTE equilibrium
  - one line: selected loops = special trees in forest
- *dark*
  - lack of emissivity ("volume blocking"??) or bound-free scattering
  - scattering: radiation up, re-radiation at bound-free threshold = black in narrow passband
  - scattering agents: H I, He I, He II

SOLAR SPECTRUM FORMATION: EXAMPLES

Robert J. Rutten
https://webspace.science.uu.nl/~rutte101

thin: cloud modeling corona chromosphere Rydberg per ALMA?

thick: UV line flip VAL3C temperature VAL3C spectrum Kurucz stars

photospheric lines: inversions bright points reversed granulation Na I D1 MGs limb emission lines

continua from VAL3C: Avrett models versus 3D MHD VAL3C continua VALII budget hydrogen budget all

lines from ALC7: model optical spectrum ultraviolet depletion hydrogen strong lines plot formats pops plot BSJ plot profile plot Mg I 4571 Fe I 6302 Mg I b_2 Na I D_1 Ba II 4554 Ca II 8542 Å Ca II K Mg II k Lyα Hα Hβ He I 584 He I 10830 canonical Hα Na I D_1–Mg I b_2 Lyα–Hα Hα–Ca II 8542 Å Ca II K–Mg II k versus FCHHT-B ALC7–FALC FALC–FALP ALC7–FALP

detour lines: pumping suction

Oslo-simulated dynamic atmosphere: 1D RADYN 3D Bifrost Bifrost line synthesis

LA-conjectured PSBE atmosphere: non-E Hα aureole boosting Hα extinction CE–SB EBs spicules-II contrail ALMA non-E chromosphere?

IRIS diagnostics: overview diagnostics

NORMAN LOCKYER

wikipedia

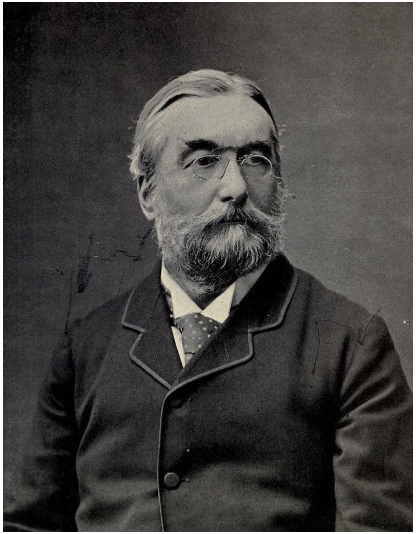

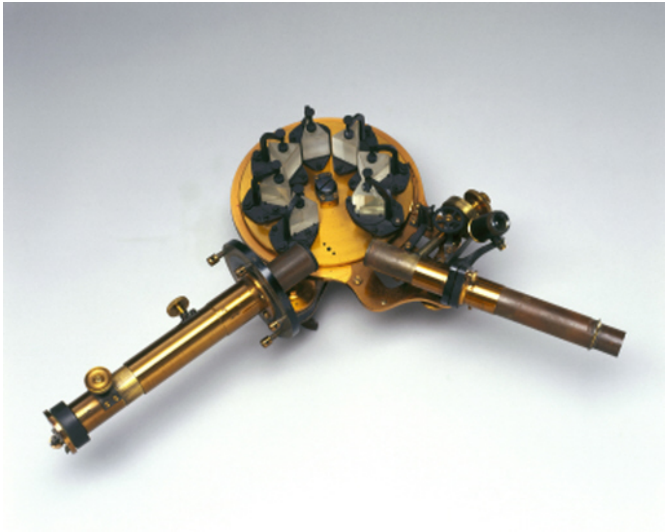

Sir Joseph Norman Lockyer, FRS (17 May 1836 – 16 August 1920), known simply as Norman Lockyer, was an English scientist and astronomer. Along with the French scientist Pierre Janssen he is credited with discovering the gas helium.

In 1885 he became the world's first professor of astronomical physics at the Royal College of Science, South Kensington, now part of Imperial College. At the college, the Solar Physics Observatory was built for him and here he directed research until 1913.

To facilitate the transmission of ideas between scientific disciplines, Lockyer established the general science journal Nature in 1869. He remained its editor until shortly before his death.

CHROMOSPHERE AND HELIUM NAMING

Abstract of Norman Lockyer's paper read Nov. 26, 1868; Procs. Royal Society of London, 17, 131

ADS 1868RSPS...17..131L courtesy Kevin Reardon 9 cites (7 RR)

Details are given of the observations made by the new instrument, which was received incomplete on the 16th of October. These observations include the discovery, and exact determination of the lines, of the prominence-spectrum on the 20th of October, and of the fact that the prominences are merely local aggregations of a gaseous medium which entirely envelopes the sun. The term *Chromosphere* is suggested for this envelope, in order to distinguish it from the cool absorbing atmosphere on the one hand, and from the white light-giving photosphere on the other. The possibility of variations in the thickness of this envelope is suggested, and the phenomena presented by the star in Corona are referred to.

Two of the lines correspond with Fraunhofer's C and F; another lies 8° or 9° (of Kirchhoff's scale) from D towards E. There is another bright line, which occasionally makes its appearance near C, but slightly less refrangible than that line. It is remarked that the line near D has no corresponding line ordinarily visible in the solar spectrum. The author has

Fraunhofer's "C" is Hα, "F" is Hβ. The non-Fraunhofer line near "D" (Na I D$_1$ + Na I D$_2$) for which Lockyer proposed a new element "helios" is He I D$_3$. The occasional "less refrangible" (redward) line near Hα is He I 6678 Å.

SOLAR FLASH SPECTRUM

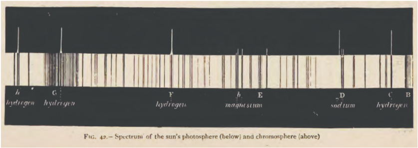

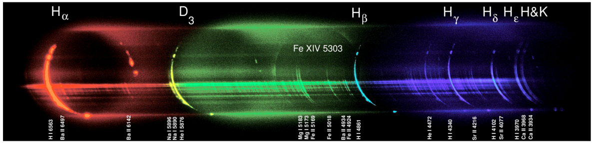

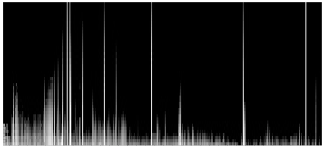

- *chromosphere naming = definition (Lockyer 1868 outside eclipse)*
  - strong: H I Balmer lines, He I D_3, Ca II H & K
  - weaker: Mg I b, Na I D, Sr II, Ba II

- *chromosphere research = flash spectrometry*
  - Menzel thesis = 1898–1908 Campbell 1930PLicO..17....1M (302 pp, on ADS)
  - Thomas & Athay book = 1952 HAO 1961psc..book.....A (422 pp, not on ADS)
  - Dunn et al. = 1962 HAO 1968ApJS...15..275D (275 pp, on ADS; RR digitized)

- *chromosphere = enigma*
  - flash spectrum ≠ reversed disk spectrum
  - both hot (He I D_3) and cool (Na I D_1 & D_2) lines
  - spatial extent exceeds radiative-equilibrum scale height

ECLIPSE WISDOM

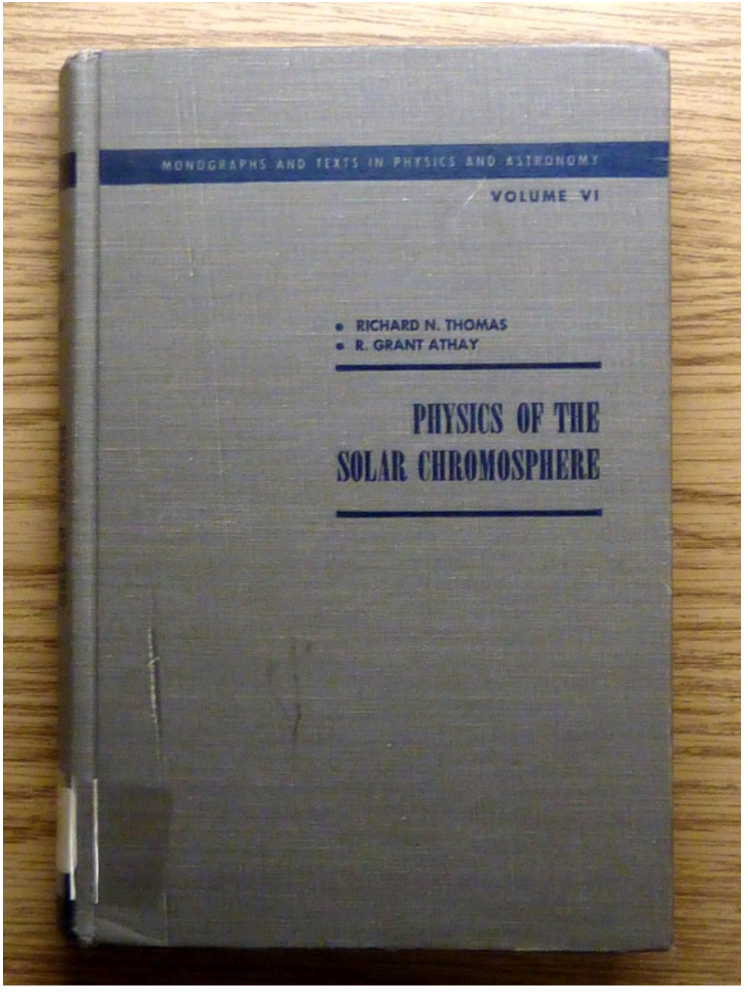

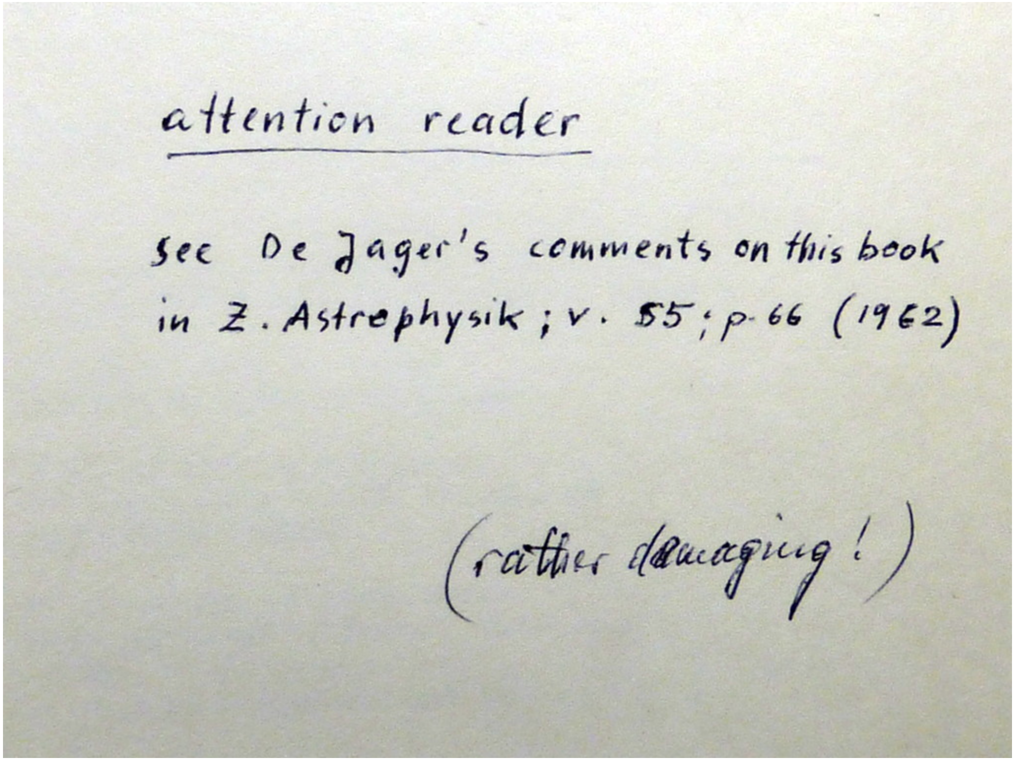
attention reader

see De Jager's comments on this book
in Z. Astrophysik ; v. 55 ; p. 66 (1962)

(rather damaging!)

De Jager's review (1962ZA.....55...66T + 1962ZA.....55...70W)

Besprechungen

THOMAS, R. N., und R. G. ATHAY: *Physics of the Solar Chromosphere.* X + 422 Seiten. Interscience Publishers, Inc., New York 1961. Geb. $ 15.50.

Der Titel des Buches verspricht mehr, als der Inhalt gibt. Jeder, der schon einmal durch ein Hα-Filter oder durch ein Spektroheliοskop die bezaubernde Struktur der Chromosphärenoberfläche gesehen oder das Profil des Sonnenrandes beobachtet hat, wird — sobald er den Titel „Physik der Chromosphäre" hört — an eine Erklärung der Dynamik dieser Gasmassen denken. Er wird an Probleme der Schall-, Stoß- und Gravitationswellen und an die Dissipation von deren Energie denken. Vielleicht wird er sich fragen, was die Autoren von der Rolle halten, die Magnetfelder und magnetohydrodynamische Wellen spielen und in welchem Maße von ihnen die verschiedenen Strukturen der ruhigen bzw. gestörten Gebiete dieses merkwürdigen Teiles der Sonne bestimmt werden.

Von allem dem wird er aber in diesem Buche nichts finden: Die betreffenden Probleme werden kaum erwähnt, geschweige denn besprochen.

und so weiter. . . four pages more

Upshot: the book treats the derivation of a model atmosphere from the spectrograms taken by the 1952 HAO eclipse expedition but ignores the inhomogeneity and dynamics of the chromosphere such as sound, shock, gravity and MHD waves, as well as magnetic fields.

CHROMOSPHERE POTPOURRI

- *line formation theory*
  - flash spectrum @ Harvard, Boulder ⇒ Mihalas (1970, 1978): summary
  - static 1D “standard” models: VALIIIC more Avrett hydrogen exam
  - non-E: detailed balancing 1D Radyn 2D Stagger 3D Bifrost
- *chromosphere diagnostics*

  Na I D_1+Mg I b_2 Lyα+Hα Hα+Ca II 8542 Å Ca II H & K+Mg II h & k
  Si IV mm He I+He II
- *chromospheric & coronal heating ingredients*
  - gravity waves
  - acoustic waves
  - Alfvénic waves
  - reconnection
- *fine structure*
  - sketched: Noyes 1979 Gabriel 1976 Rutten 1998 Wedemeyer 2016 Rutten 2016
  - observed and explained: Ca II grains dynamic fibrils
  - observed but not explained: straws/spicules-II/RBEs/RREs long Hα fibrils
  - fibril-field alignment for NLFFF: yes partly only at launch?

SOLAR SPECTRUM FORMATION: EXAMPLES

Robert J. Rutten
https://webspace.science.uu.nl/~rutte101

thin: cloud modeling corona chromosphere Rydberg per ALMA?

thick: UV line flip VAL3C temperature VAL3C spectrum Kurucz stars

photospheric lines: inversions bright points reversed granulation Na I D1 MGs limb emission lines

continua from VAL3C: Avrett models versus 3D MHD VAL3C continua VALII budget hydrogen budget all

lines from ALC7: model optical spectrum ultraviolet depletion hydrogen strong lines plot formats pops plot BSJ plot profile plot Mg I 4571 Fe I 6302 Mg I b_2 Na I D_1 Ba II 4554 Ca II 8542 Å Ca II K Mg II k Lyα Hα Hβ He I 584 He I 10830 canonical Hα Na I D_1–Mg I b_2 Lyα–Hα Hα–Ca II 8542 Å Ca II K–Mg II k versus FCHHT-B ALC7–FALC FALC–FALP ALC7–FALP

detour lines: pumping suction

Oslo-simulated dynamic atmosphere: 1D RADYN 3D Bifrost Bifrost line synthesis

LA-conjectured PSBE atmosphere: non-E Hα aureole boosting Hα extinction CE–SB EBs spicules-II contrail ALMA non-E chromosphere?

IRIS diagnostics: overview diagnostics

SUMMARY 1D SCATTERING SOURCE FUNCTIONS

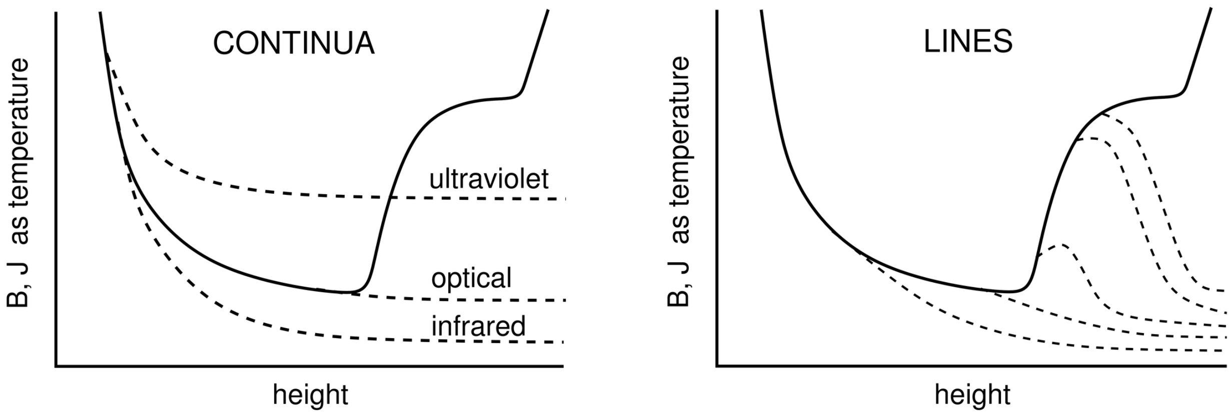

- *continua*
  - optical: $J \approx B$ for radiative equilibrium
  - ultraviolet: $S \approx J > B \rightarrow$ overionization of minority neutrals
  - infrared: $J < B$ but J doesn't matter since $H^-_{\rm ff}$ and $H_{\rm ff}$ have $S = B$
- *lines*
  - $\mathrm{d}B/\mathrm{d}\tau = \mathrm{d}B/\mathrm{d}(\tau^c + \tau^l)$ much less steep, so closer to isothermal $S \approx \sqrt{\varepsilon}\, B$
  - for stronger lines S sees more of the model chromosphere
  - PRD lines have frequency-dependent core-to-wing $S \approx J$ curves like these

EXPLAIN EVERYTHING – INCLUDING SIMILARITIES AND DIFFERENCES

ALC7: 2008ApJS..175..229A *FCHHT-B:* 2009ApJ...707..482F *FALP:* 1993ApJ...406..319F

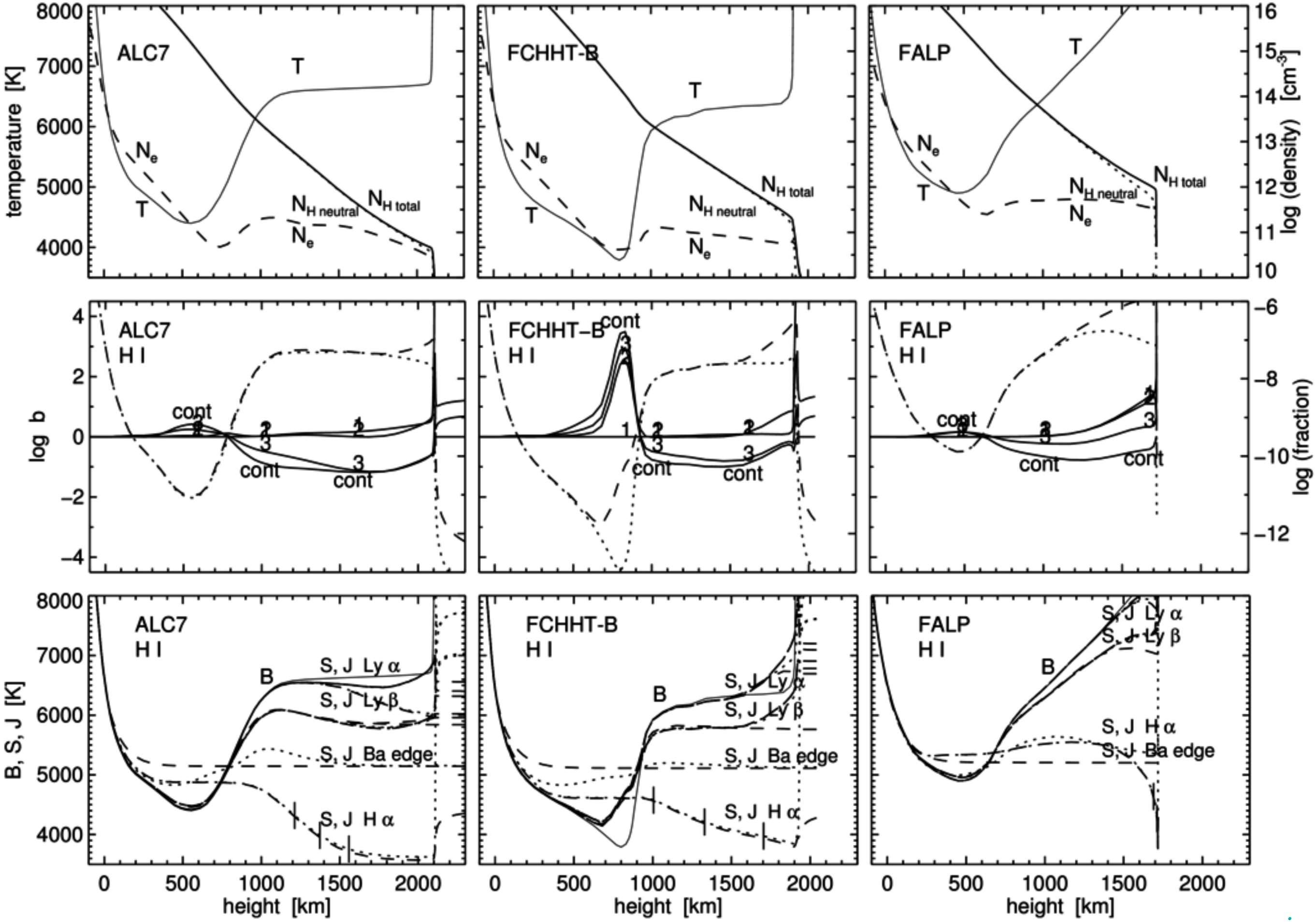

DYNAMIC FIBRILS

Hα: *Hansteen et al.* *2006ApJ...647L..73H*, *De Pontieu et al.* *2007ApJ...655..624D* (plage)
Rouppe van der Voort & De la Cruz Rodiguez *2013ApJ...776...56R* (sunspots)
Ca II 8542: *Langangen et al.* *2008ApJ...673.1194L*
Ly α: *Koza et al.* *2009A&A...499..917K*
non-E 2D MHD simulation: *Leenaarts et al.* *2007A&A...473..625L*

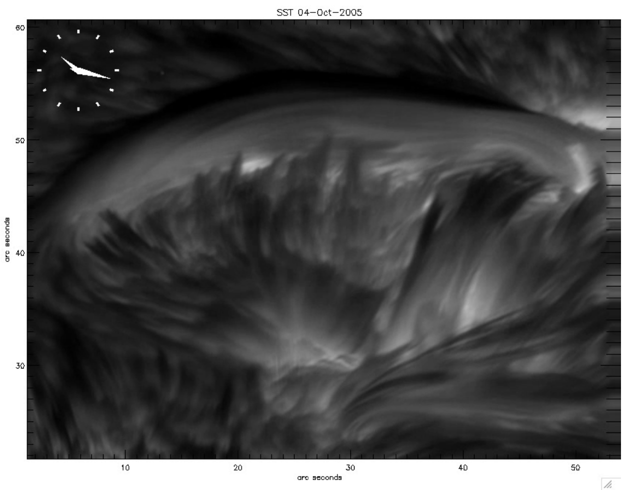

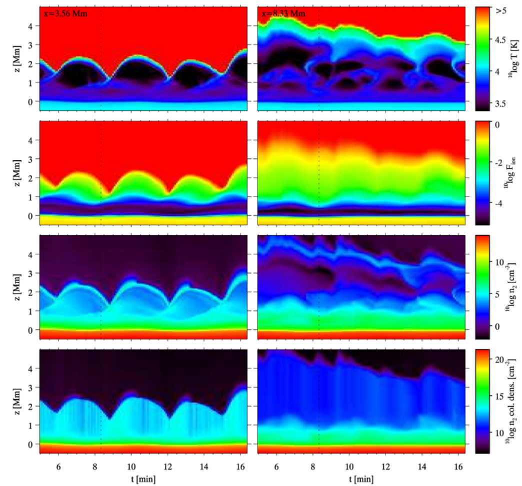

explanation: p-mode-driven 3–5 minute shock waves along inclined field as slanted wave guide with lowered cutoff frequency; fan pattern = surface network strings

Michalitsanos 1973SoPh...30...47M
Bel & Leroy *1977A&A....55..239B*
Suematsu *1990LNP...367..211S*
De Pontieu et al. *2004Natur.430..536D*

1973SoPh...30...47M

THE FIVE-MINUTE PERIOD OSCILLATION IN MAGNETICALLY ACTIVE REGIONS

A. G. MICHALITSANOS* **

Institute of Astronomy, University of Cambridge, Cambridge, England

If we incline the magnetic field (with respect to g) through 45 degrees in Figure 1d, we note that in Region I, $\omega(k_x)$ is no longer asymptotic to ω_s as k_x tends to zero. Therefore, for an inclined magnetic field, magnetosonic waves may propagate vertically at frequencies $\omega < \omega_s$. If in Equation (3) we set $a=0$ and $k_x=0$, and let $b= = -g\gamma/2V_s^2$ we will obtain the critical magnetosonic-gravity frequency ω_c, where

$$\omega_c^2 = \omega_s^2\left(\frac{1}{2} - \frac{1}{\gamma\beta}\right) + \omega_s^2\left[\left(\frac{1}{\gamma\beta} - \frac{1}{2}\right)^2 + \frac{2\cos^2\theta}{\gamma\beta}\right]^{1/2}, \tag{4}$$

and $\theta = \arccos(B_z/B_0)$. Therefore, at levels where $\beta<1$, the critical magnetosonic-gravity frequency is less than the critical sonic-gravity frequency ω_s when the field is inclined from the vertical.

STRAWS / SPICULES-II / RBEs

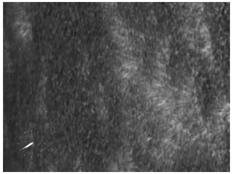

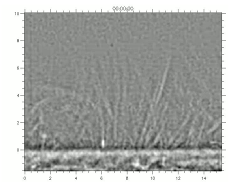

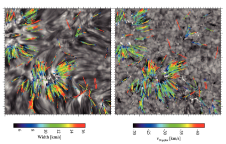

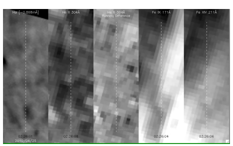

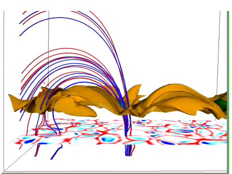

- *observations*
  - "straws", DOT Ca II H
    Rutten *2006ASPC..354..276R*
  - "spicules-II", SST Ca II H
    De Pontieu et al. *2007Sci...318.1574D*
  - on-disk visibility? DOT unpublished
  - "rapid blue excursions", SST Hα
    Rouppe van der Voort et al. *2009ApJ...705..272R*
  - "heating events", Hinode + SDO Hα + EUV
    De Pontieu et al. *2011Sci...331...55D*

- *simulation: Martínez-Sykora et al.* *2011ApJ...736....9M*
  - complex emergence, steep gradients, intense currents
  - spicular Joule heating (green), outflow (blue)
  - nearby coronal loop heating (red)

- *expectations*
  - quiet-sun (also unipolar) coronal heating
  - fast solar wind driving
  - solar wind element segregation

DYNAMIC FIBRILS

Hα: *Hansteen et al.* 2006ApJ...647L..73H, *De Pontieu et al.* 2007ApJ...655..624D (plage)
Rouppe van der Voort & De la Cruz Rodiguez 2013ApJ...776...56R (sunspots)
Ca II 8542: *Langangen et al.* 2008ApJ...673.1194L
Ly α: *Koza et al.* 2009A&A...499..917K
non-E 2D MHD simulation: *Leenaarts et al.* 2007A&A...473..625L

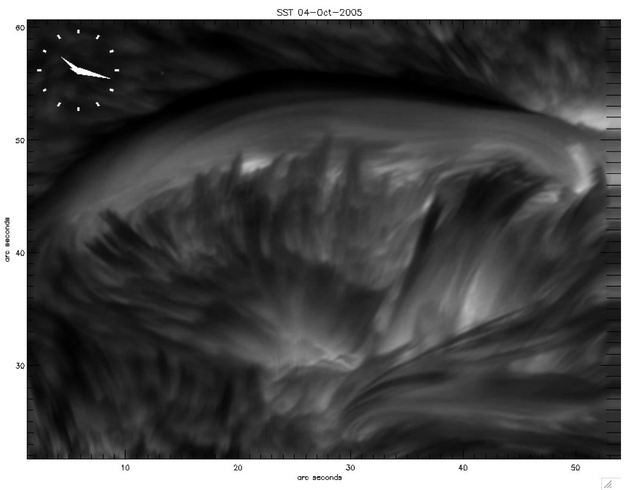

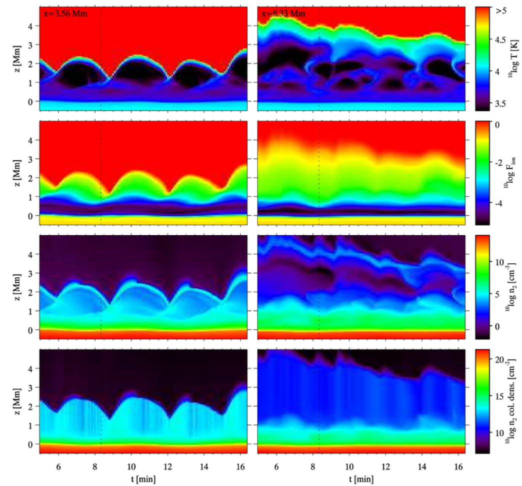

explanation: p-mode-driven 3–5 minute shock waves along inclined field as slanted wave guide with lowered cutoff frequency; fan pattern = surface network strings

Michalitsanos 1973SoPh...30...47M
Bel & Leroy 1977A&A....55..239B
Suematsu 1990LNP...367..211S
De Pontieu et al. 2004Natur.430..536D

FIBRIL–FIELD ALIGNMENT FOR NLFFF LOWER BOUNDARY

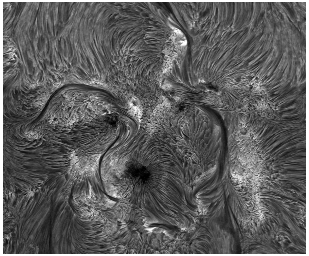

- *NLFFF tests with chromospheric boundary*
  - Na I D_1: Metcalf et al. 1995ApJ...439..474M 2005ApJ...623L..53M
  - Hα: Bobra & van Ballegooijen 2008ApJ...672.1209B Wiegelmann et al. 2008SoPh..247..249W
- *good alignment*
  - Aschwanden et al. 2016ApJ...826...61A
- *partial alignment*
  - de la Cruz Rodríiguez & Socas-Navarro 2011A&A...527L...8D
  - Leenaarts et al. 2015ApJ...802..136L
  - Martínez-Sykora et al. 2016ApJ...831L...1M
  - Asensio Ramos et al. 2016arXiv161206088A
- non-E alignment only at H ionization in propagating heating events?

Na I D_1 AND Mg I b_2

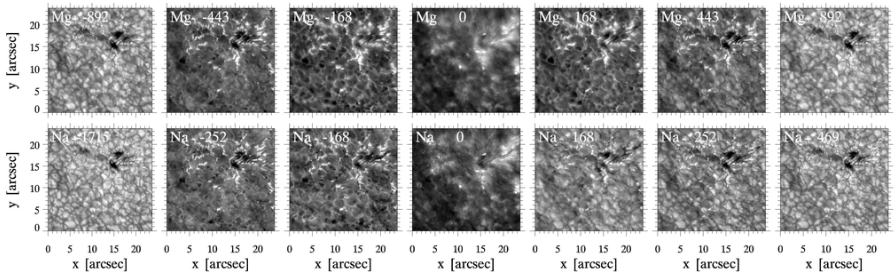

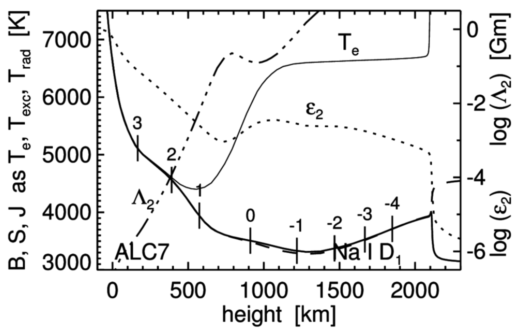

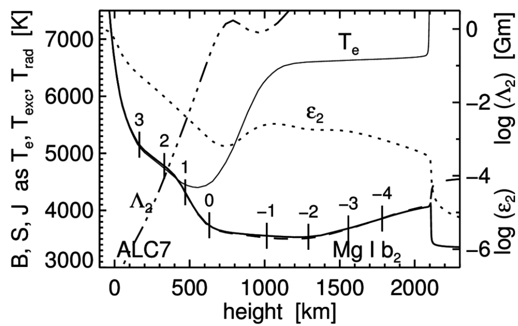

- similar NLTE formation $=$ heavy two-level scattering
- core intensities do not sense ALC7 chromosphere
- narrow Na I D_1 flanks reverse reversed granulation
- non-E? minority stages: recombination $\propto N_e$ senses Lyα settling and scattering
- SST: Dopplergrams $\approx$ unsigned fluxtube magnetograms (Na I D_1 formation)
  non-E enhanced in cooling recombining downflows? (SE $=$ Bifrost snapshot OK)

Lyα and Hα

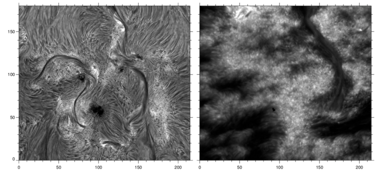

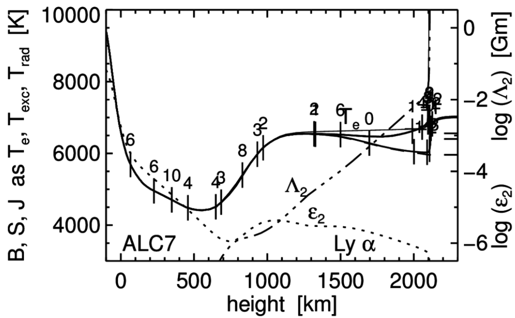

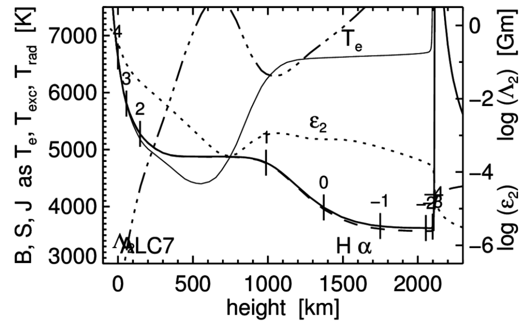

- both: heavy NLTE scatterers with $S{\approx}J$
- Lyα: boxed-in by enormous extinction $\Rightarrow$ radiative detailed balance: $S = J$
  in shocks ($\approx$ ALC7 chromosphere) collisional thermalization: $b_2 \approx b_1$
  in cool gas surroundng hot structures $b_2 \gg 1$ from Lyα surround scattering
  in post-hot cool gas slow $S{\approx}J$ thermalization with $b_2 \gg 1$: S^l memory of hot past
- Hα: photons created in granulation
  scatter 3D across upper-photosphere opacity gap and through chromosphere
  in shocks etc. Boltzmann extinction $b_2{\approx}b_1$
  in post-hot cool gas $b_2 \gg 1$: extinction memory of hot past

Lyα scene: heating events bright down-throat, cooling contrails dark from scattering
Hα scene: RBE/RRE heating events, cooling contrails dark from non-E opacity

start *index*

Hα and Ca II 8542 Å

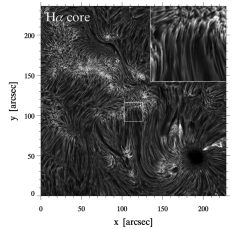

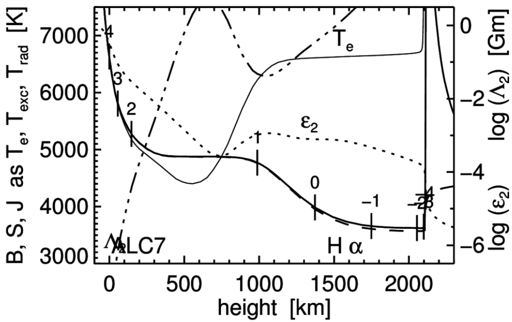

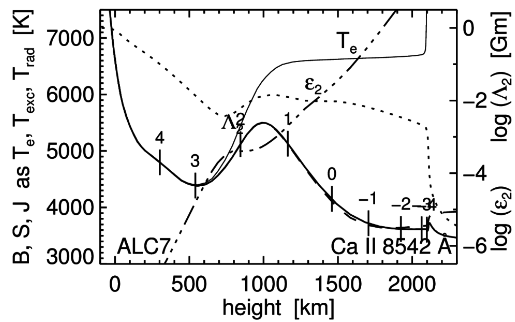

- both: heavy NLTE scatterers with $S \approx J$ sampled at similar $\tau = 1$ heights
- both: Saha-Boltzmann or larger extinction in shocks and ALC7
- core widths: both decrease away from network $=$ decreasing temperature
- Hα fibrils extend further, contradicting Saha-Boltzmann extinction sensitivities

fibril opacity in Ca II 8542 Å instantenous, in Hα post-hot non-E?

Ca II H & K and Mg II h & k

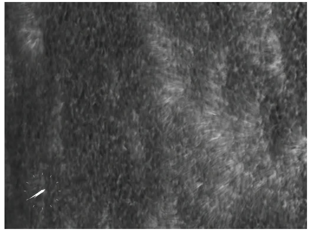

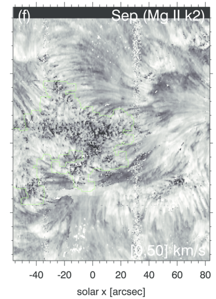

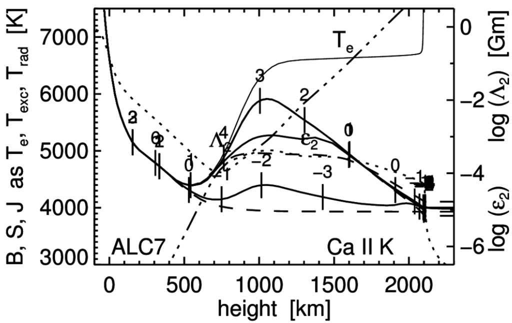

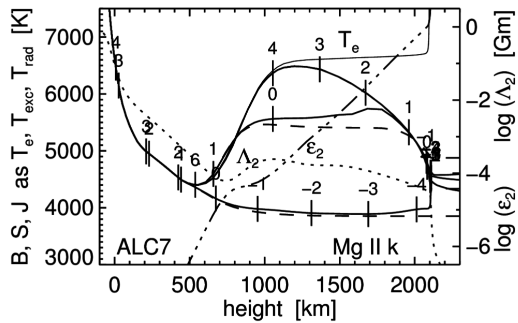

- both: heavy NLTE scatterers with PRD source function splits
- both: near-Saha-Boltzmann extinction everywhere; abundance ratio 18
- both: absence of non-E sensitivities $=$ instantaneous chromosphere
- both: slender fibrils emanating from network, in Ca II H & K better at narrower bandwidth, in Mg II k best in k_2 peak separation

slender fibrils $=$ propagating heating events?

CLOSED AND OPEN QUIET-SUN INTERNETWORK IN Si IV

Peter et al. in preparation

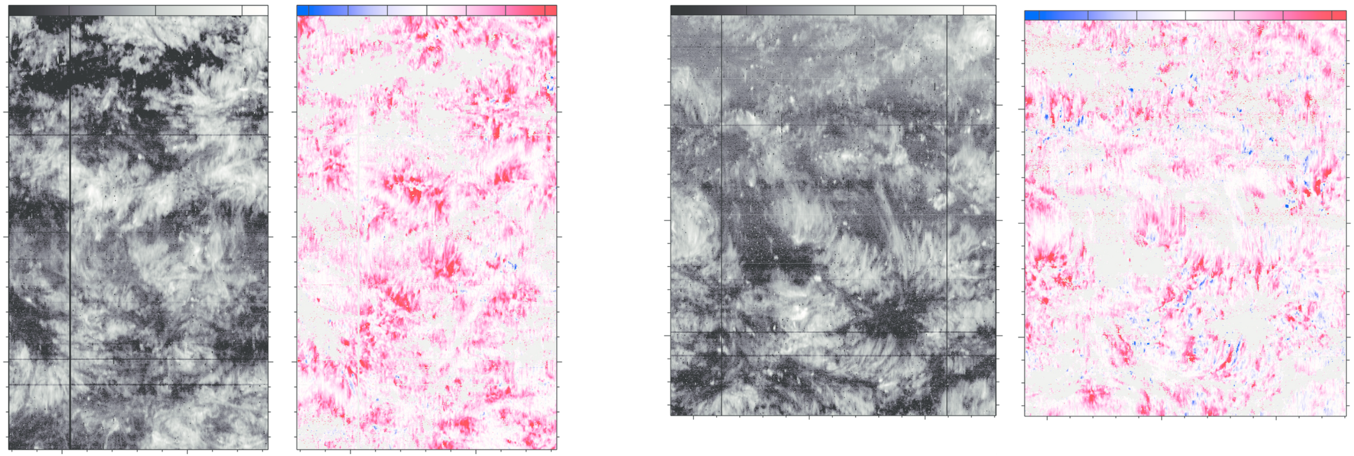

- thin to thickish (ratio $<$ 2) line formation
- Gaussian fits
- widths $\approx$ non-thermal widths

redshifted fibrils away from network $\approx$ recombining Hα contrails?

roundish coronal-hole blueshifts in network $=$ down-throat heating events?

SAHA-BOLTZMANN HYDROGEN EXTINCTION AT ALMA WAVELENGTHS

Rutten *2017A&A...598A..89R* *2017IAUS..327....1R* *(tutorial)*

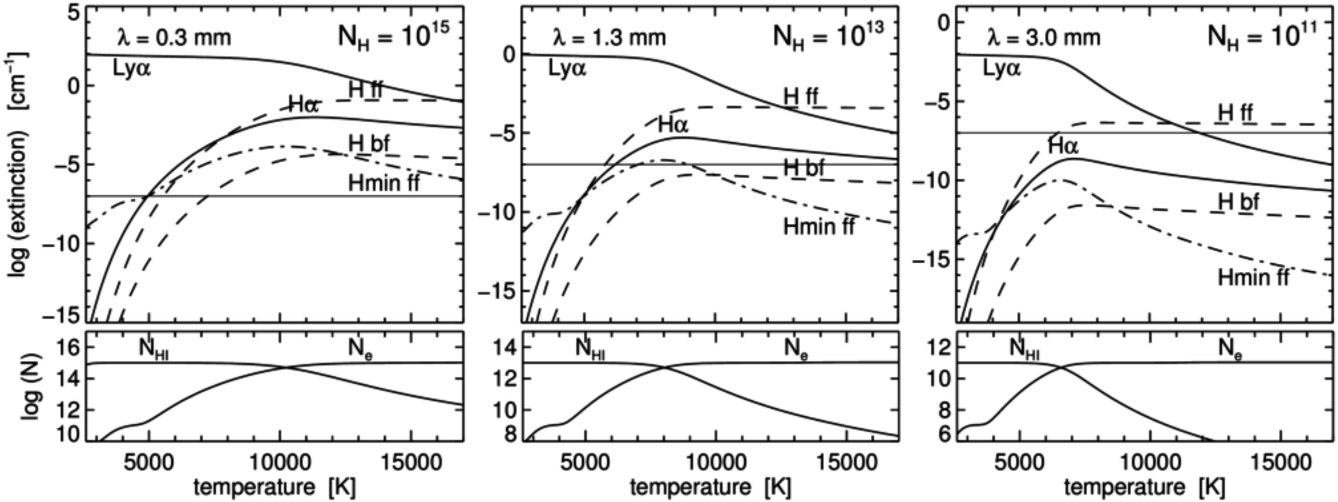

- LTE extinction: Lyα Hα H I continua H$^-$ ff continuum 8542 other lines
- Hα at high T: LTE extinction from $n_2 \approx n_2^{\rm LTE}$ enforced by enclosed Lyα
- H ionization: $n=2$ population fixed by (actually non-E) Lyα; hydrogen top has additional NLTE-SE balancing between Balmer continum and Balmer lines
- Balmer continuum $T_{\rm rad} \approx$ 5250 K: overionization below, underionization above $\Rightarrow$ de-steepening of these LTE H ff Boltzmann increases around 5250 K pivot
- $\alpha_\nu^{\rm ff} \sim \lambda^2 N_{\rm e} N_{\rm ion}\, T^{-3/2}$ (RTSA Eq. 2.79) gives steep H ff increase between ALMA bands
- features with non-E post-hot Hα extinction have larger to very much larger H ff extinction

SOLAR RYDBERG LINES WITH ALMA?

Rutten 2017IAUS..327....1R

- *"linear thermometer"*
  - H^- free-free + H I free-free: $S \equiv B$
  - thick feature: $T_b = T(\tau_\nu = 1)$
  - thin feature: cloud contribution $\Delta T_b = \tau T$
- *solar Rydberg lines so far*
  - in μm range Mg I stronger than H I
  - prediction H I α lines $n = 4 - 18$
  - H I 19α, 21α observed at limb
- *H I Rydberg lines with ALMA?*
  - candidate: H I 30α in Band 6 (1.3 mm)
  - much stronger than above predictions from large post-hot non-E extinction?
  - if so, unblendedly present since Mg I etc are not non-E boosted?
  - on disk as $T(\tau_\mu = 1)$ emission at steep $T(\tau)$ gradient
  - at limb as τT extension
  - Zeeman in I and Stokes: super-sensitive chromospheric magnetometer?

SOLAR ULTRAVIOLET SPECTRUM

Scheffler & Elsässer, courtesy Karin Muglach

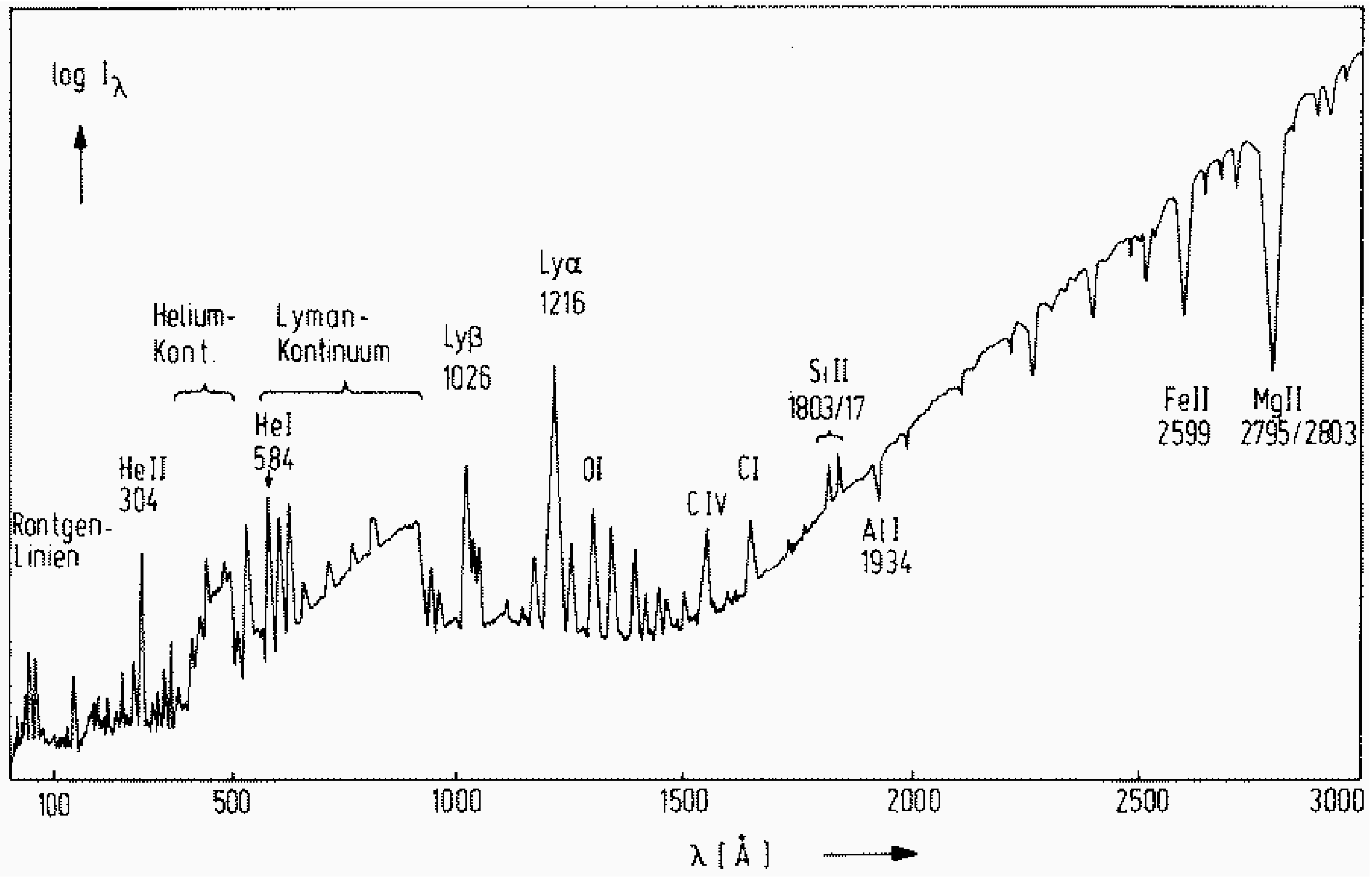

VALIIIC MODEL

Vernazza, Avrett, Loeser *1981ApJS...45..635V*

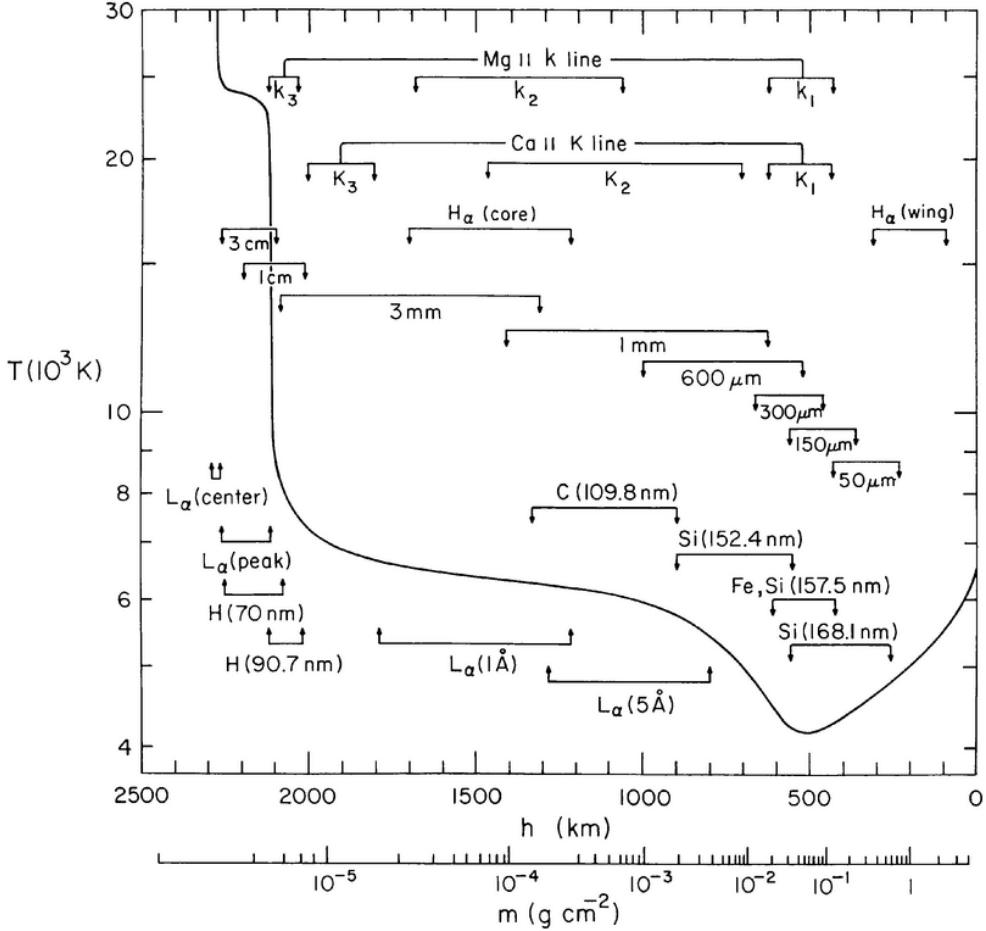

VALIIIC SPECTRUM FORMATION

Avrett *1990IAUS..138....3A*

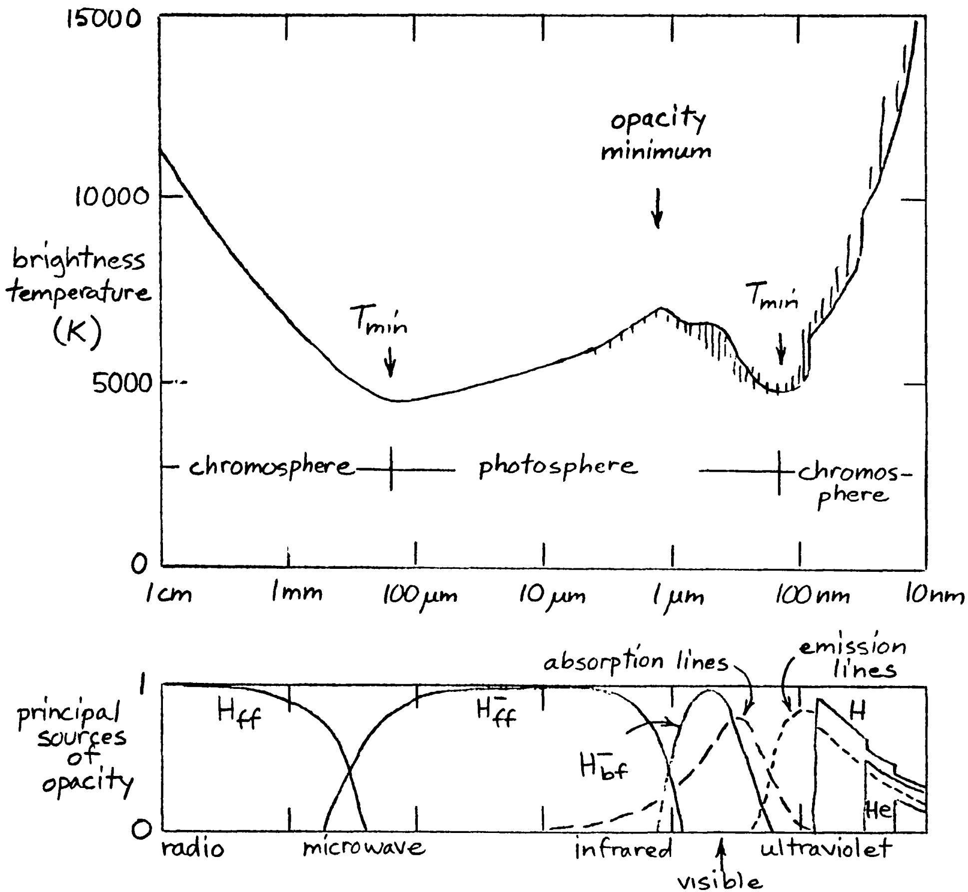

KURUCZ STARS

Kurucz ATMOS program = LTE–RE–HE 1979ApJS...40....1K

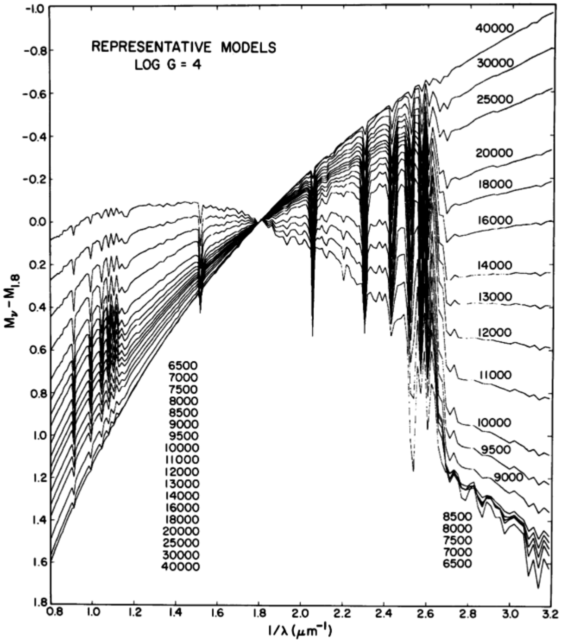

- color $M_V - M_{1.8}$
- $1/\lambda = 1.8\ \mu$m^{-1}: $\lambda = 555$ nm $= UBV$ color V
- Balmer edge at $1/\lambda = 2.74\ \mu$m^{-1}
- Paschen edge at $1/\lambda = 1.22\ \mu$m^{-1}

SOLAR SPECTRUM FORMATION: EXAMPLES

Robert J. Rutten
https://webspace.science.uu.nl/~rutte101

thin: cloud modeling corona chromosphere Rydberg per ALMA?

thick: UV line flip VAL3C temperature VAL3C spectrum Kurucz stars

photospheric lines: inversions bright points reversed granulation Na I D1 MGs limb emission lines

continua from VAL3C: Avrett models versus 3D MHD VAL3C continua VALII budget hydrogen budget all

lines from ALC7: model optical spectrum ultraviolet depletion hydrogen strong lines plot formats pops plot BSJ plot profile plot Mg I 4571 Fe I 6302 Mg I b_2 Na I D_1 Ba II 4554 Ca II 8542 Å Ca II K Mg II k Lyα Hα Hβ He I 584 He I 10830 canonical Hα Na I D_1–Mg I b_2 Lyα–Hα Hα–Ca II 8542 Å Ca II K–Mg II k versus FCHHT-B ALC7–FALC FALC–FALP ALC7–FALP

detour lines: pumping suction

Oslo-simulated dynamic atmosphere: 1D RADYN 3D Bifrost Bifrost line synthesis

LA-conjectured PSBE atmosphere: non-E Hα aureole boosting Hα extinction CE–SB EBs spicules-II contrail ALMA non-E chromosphere?

IRIS diagnostics: overview diagnostics

THE MOST SUCCESSFUL INVERSION EVER

Holweger 1967ZA.....65..365H (243 cites); Holweger & Müller 1974SoPh...39...19H (over 800 cites)

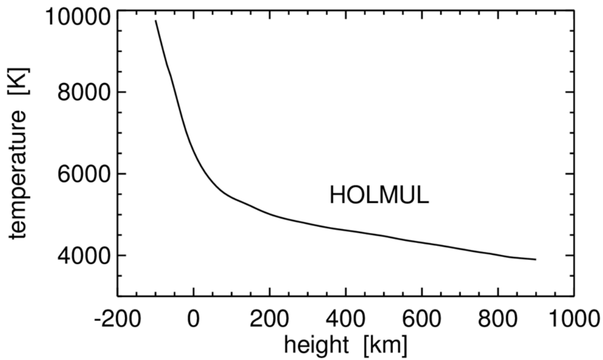

- PhD thesis: empirical LTE fit of the optical continuum and the depths of 900 lines
- very similar to subsequent “theoretical” radiative-equilibrium models
- HOLMUL = update (fitting Ba II lines) prefered in all pre-Asplund abundance determinations *because* it has no chromosphere – but also no granulation
- *“[. . .] Among the problems that need further study are deviations from LTE. Unfortunately, these are easily arising in the computer if important collisional processes are neglected, or if radiative rates are not realistic. In cool stars, collisional excitation by hydrogen atoms is generally neglected [. . .] However, in the Sun, hydrogen atoms outnumber the free electrons by a factor of 10000. The UV radiation field is complicated by a vast number of absorption lines . . . ”*

NLTE MASKING

Rutten & Kostik 1982A&A...115..104R

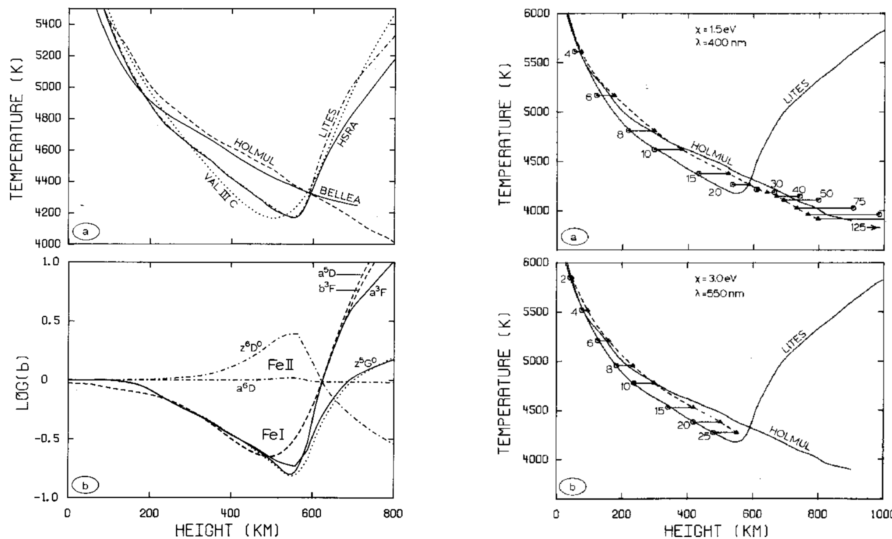

- VALIIIC ≈ LITES steeper decline than HOLMUL ≈ BELLEA
- ultraviolet bf scattering causes Fe I underopacities
- strong-line bb scattering causes Fe I source function deficits
- ultraviolet bb pumping causes Fe II source function excesses
- empirical LTE line depth fitting á la Holweger:
  - opacity-deficient Fe I cores suggest too small height
  - scattering Fe I cores suggest too low temperature
  - pumped Fe II cores suggest too high temperature

MILNE-EDDINGTON APPROXIMATION IN A MURaM SIMULATION

Vitas et al. 2009A&A...499..301V

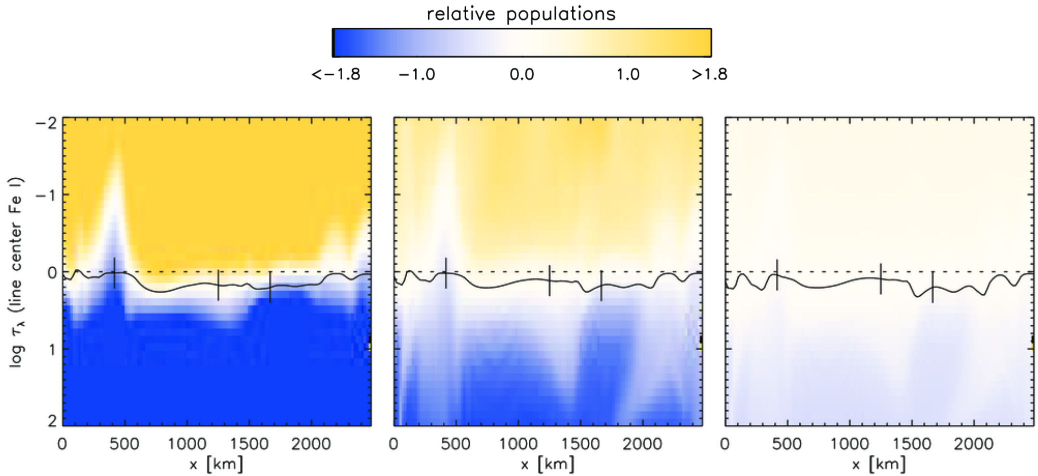

- representative weak Fe I line with excitation energy 0, 3, and 6 eV; transition probability scaled to obtain the same emergent line strength
- dotted curve: line-center $\tau = 1$ (normalization)
  solid curve: continuum $\tau = 1$. Its modulation represents line-core Doppler brightening. The line vanishes from ionization within a magnetic concentration at $x = 400$ km
- first panel: increasing Fe ionization and corresponding H^- increase at larger depth cause very steep gradients in normalized populations $\sim \eta \equiv \alpha^l/\alpha^c$
- other panels: increasing compensation from Boltzmann excitation factor
- upshot: Milne-Eddington approximation better at higher excitation

ULTRAVIOLET DEPLETION IN THE ALC7 ATMOSPHERE

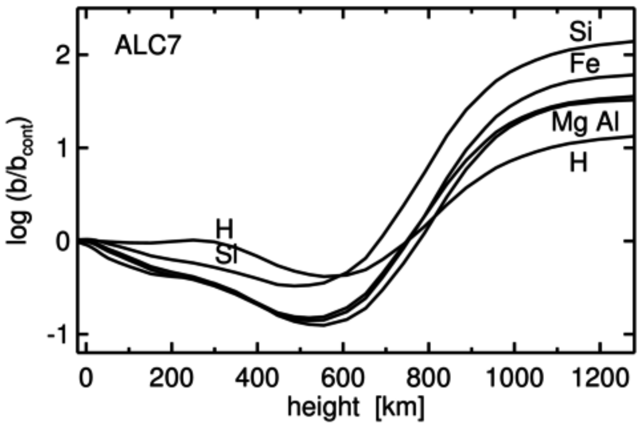

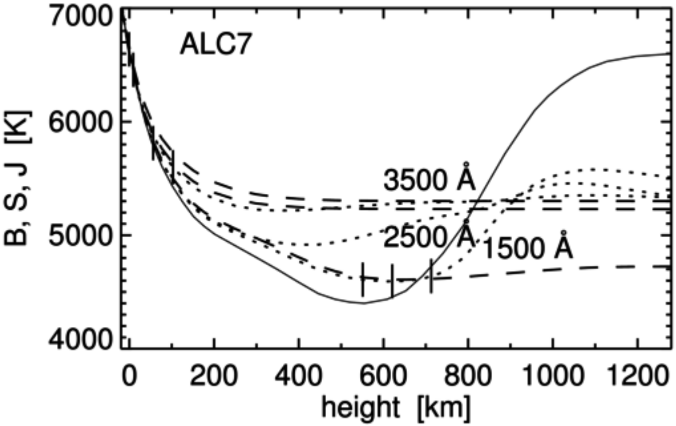

minority atoms: photospheric extinction depletion by ultraviolet bound-free scattering

- ultraviolet bound-free edges produce scattering continua
- $J > B$ from:
  - $T(h)$ gradient defined by radiative equilibrium for the optical
  - $B(h)$ steeper in the ultraviolet due to Wien nonlinearity
  - Λ operator gives $J > S$ for steep $S(\tau)$
  - deep escape from small H I bf extinction
- $b_1/b_{\rm cont}$ for electron donors Mg I, Fe I, Si I and Al I imply b_1 population depletion across photosphere because $b_{\rm cont} \approx 1$
- their photospheric lines have increasing extinction deficits compared to LTE
- $b_2/b_{\rm cont}$ for H I shows similar behavior for the top of the hydrogen atom starting at $n=2$

SOLAR SPECTRUM FORMATION: EXAMPLES

Robert J. Rutten
https://webspace.science.uu.nl/~rutte101

thin: cloud modeling corona chromosphere Rydberg per ALMA?

thick: UV line flip VAL3C temperature VAL3C spectrum Kurucz stars

photospheric lines: inversions bright points reversed granulation Na I D1 MGs limb emission lines

continua from VAL3C: Avrett models versus 3D MHD VAL3C continua VALII budget hydrogen budget all

lines from ALC7: model optical spectrum ultraviolet depletion hydrogen strong lines plot formats pops plot BSJ plot profile plot Mg I 4571 Fe I 6302 Mg I b_2 Na I D_1 Ba II 4554 Ca II 8542 Å Ca II K Mg II k Lyα Hα Hβ He I 584 He I 10830 canonical Hα Na I D_1–Mg I b_2 Lyα–Hα Hα–Ca II 8542 Å Ca II K–Mg II k versus FCHHT-B ALC7–FALC FALC–FALP ALC7–FALP

detour lines: pumping suction

Oslo-simulated dynamic atmosphere: 1D RADYN 3D Bifrost Bifrost line synthesis

LA-conjectured PSBE atmosphere: non-E Hα aureole boosting Hα extinction CE–SB EBs spicules-II contrail ALMA non-E chromosphere?

IRIS diagnostics: overview diagnostics

FLUX TUBES

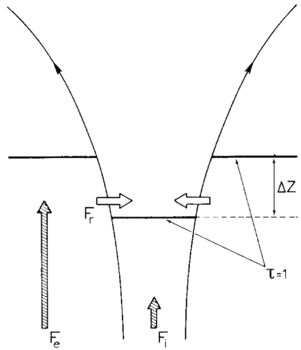

- *1970s: Utrecht fluxtube paradigm*
  - magnetostatic equilibrium: flaring
  - evacuation: Wilson depression
  - thin tube: hot walls bright, brighter limbwards

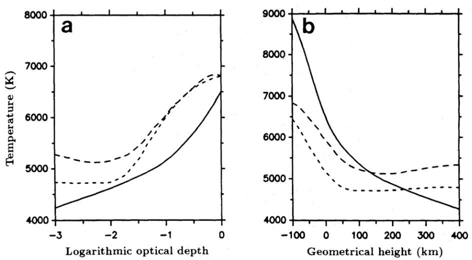

- *1980s: Zürich unsharp 1.5D models*
  - McMath-Pierce FTS Fe I & Fe II Stokes V
  - assume magnetostatic geometry
  - spatially-averaged LTE Stokes profile fitting
  - flatter-than-RE temperature gradient

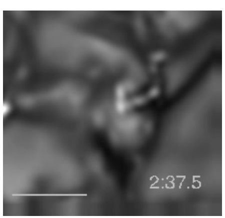

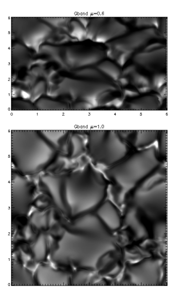

- *1990s+: sharp observations and simulations*
  - enhanced contrast in G band, strong-line wings
  - rapid morphology change, much vorticity
  - near-limb faculae: see-through into granules

1970s magnetostatic fluxtubes

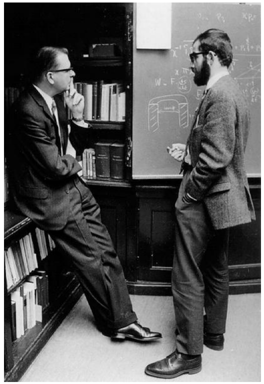

Kees Zwaan & Hans Rosenberg

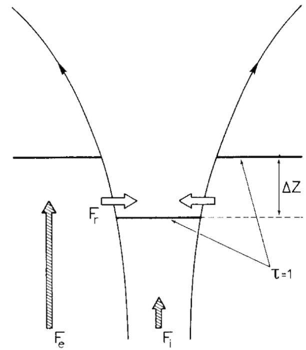

Zwaan 1978SoPh...60..213Z

PRESSURE EQUILIBRIUM AND ENERGY BALANCE OF SMALL PHOTOSPHERIC FLUXTUBES

H. C. SPRUIT
The Astronomical Institute of the University of Utrecht, The Netherlands

(Received 12 July, 1976)

Abstract. Field configurations and temperature distributions of axially symmetric fluxtubes are determined on the basis of pressure equilibrium and energy balance of the tubes. The description concentrates on layers below ≈600 km above the photosphere; a magnetostatic field, and energy transport by a diffusion process are assumed. It is assumed also that the magnetic field of the tubes prevents convective flow across the field lines, so that only radiative energy exchange between the tube and the convection zone is present. A set of model tubes is presented ranging in size from facular points (150 km) to small pores (1000 km), for different values of the field amplitude and the asymptotic energy flux F_0 flowing along the tube from the deeper layers. Radial influx of heat into the tube at the photospheric level influences the temperature in the tube strongly for all these models. For a pore-like tube $F_0 = 0.25$ (similar to the flux from a spot umbra) seems appropriate (F_0 in units of the normal photospheric flux). If in the smallest fluxtubes F_0 is also 0.25, a comparison of the intensity contrast with observations of facular points indicates that the radius of tubes corresponding to facular points is 50–100 km. In the continuum the structure looks like a depression in the photosphere (similar to the Wilson depression of spots). The magnitude of this depression is ≈200 km for pores of 1000 km diameter and ≈100 km for facular points. The walls of the hole created by the depression contribute considerably to the contrast of structures observed near the solar limb. It is shown how this contribution may explain the centre to limb behaviour of facular contrast as seen in the continuum, and why the continuum CLV differs so strongly from that in line cores. Over the first 400 km above the photosphere the tube expands by a factor of ≈2 for all the tubes calculated.

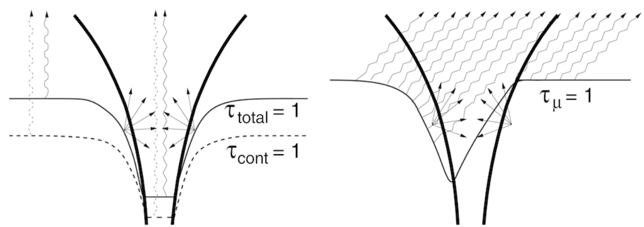

Spruit 1976SoPh...50..269S

Rutten 1999ASPC..184..181

MAGNETIC BRIGHT POINTS

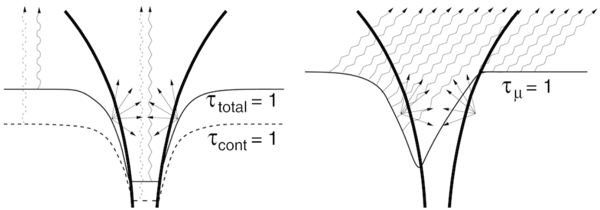

- *high-resolution observation*
  - Berger et al. 2004A&A...428..613B: G-band bright points as ribbons and flowers
- *high-resolution simulation*
  - Keller et al. 2004ApJ...607L..59K: continuum faculae simulation
  - Carlsson et al. 2004ApJ...610L.137C: G-band faculae simulation
- *bright points in Hα*
  - DOT Hα movie 2004-10-06
  - Leenaarts et al. 2006A&A...449.1209L: bright points in Hα
  - Leenaarts et al. 2006A&A...452L..15L: comparison of bright-point diagnostics
- *less bright points in "normal" lines*
  - Vitas et al. 2009A&A...499..301V: only Mn I lines are not mucked up by granulation

MODELING NETWORK / PLAGE MAGNETISM FOR SPECTRAL IRRADIANCE

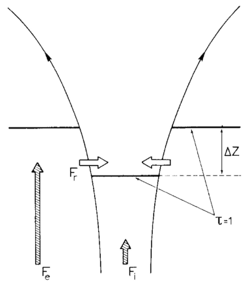

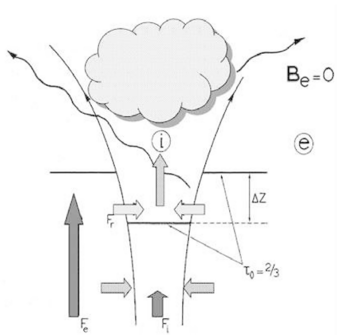

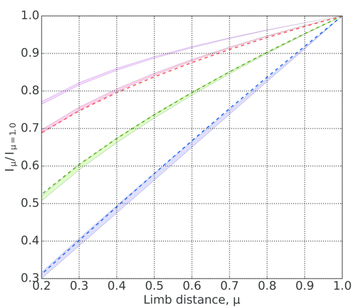

- *golden age of fluxtube modeling = hole in surface*
  - Zwaan – Spruit: idealized magnetostatic fluxtubes
  - Stenflo – Solanki – Keller: unresolved FTS polarimetry
  - Steiner – Keller – Carlsson: realistic MHD simulations
- *bright-point enhancements = hole deepening*
  - CH G-band, CN 3883 band: dissociaton
  - Fe I line gaps: ionization
  - Balmer line wings: small collision broadening
  - Mn I line cores: large hyperfine broadening
- *dark age of 1D irradiance modeling = down the rabbit hole*
  - "chromospheric cloud" ⇒ "photosphere heating"
  - FALP > FALC fudge ⇒ SATIRE (ADS N39 H13)
  - 1600 Å – 1700 Å [SST/CHROMIS Ca II K wing scans]
- *coming age of simulation irradiance modeling ⇒ of age*
  - ∼ 1D ⇒ 3D abundances ("pre/post Asplund")
  - first step: MURaM with LTE
  - to do: 3D(t) MHD with NLTE, line haze, H NSE?

SOLAR SPECTRUM FORMATION: EXAMPLES

Robert J. Rutten
https://webspace.science.uu.nl/~rutte101

REVERSED GRANULATION OBSERVATION & SIMULATION

Leenaarts & Wedemeyer-Böhm 2005A&A...431..687L

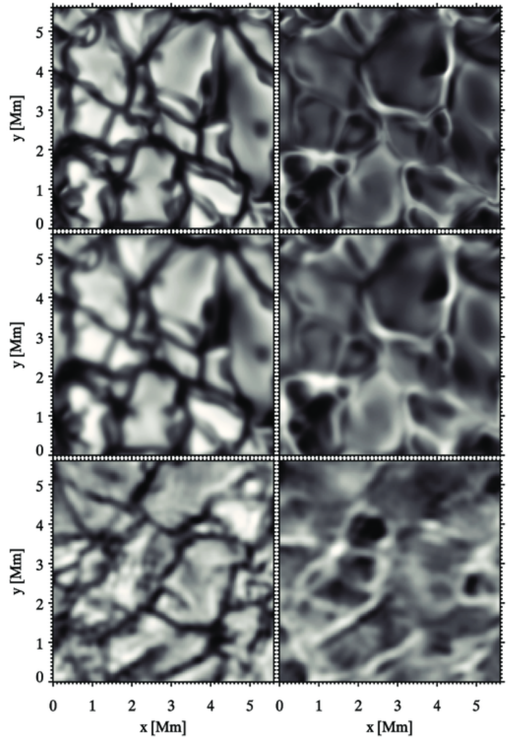

- observation simular to simulation so phenomenon "explained"
- no magnetism since pure hydro simulation (CO^5BOLD)
- internal gravity waves?

OBSERVATION & SIMULATION OF Na I D_1, Mg I b_2, Ca II 8542 Å

Rutten et al. *2011A&A...531A..17R*

- SST images blue wing - core - red wing 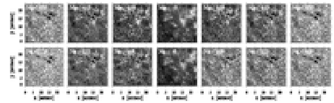
- atlas profiles 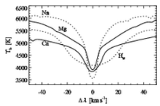

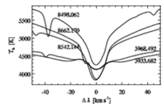

- FALC formation 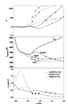
- Dopplergram comparisons 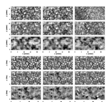
- profile comparisons 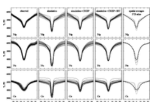

upshot

- simulation $\approx$ observation but computed Ca II 8542 Å is much too narrow
- difference in showing reversed granulation is set by reversed intensity–Dopplershift correlation sampled differently by different inner-wing steepness
- Na I D_1 Dopplergrams are upper-photosphere kilogauss magnetograms

SOLAR SPECTRUM FORMATION: EXAMPLES

Robert J. Rutten
https://webspace.science.uu.nl/~rutte101

thin: cloud modeling corona chromosphere Rydberg per ALMA?

thick: UV line flip VAL3C temperature VAL3C spectrum Kurucz stars

photospheric lines: inversions bright points reversed granulation Na I D1 MGs limb emission lines

continua from VAL3C: Avrett models versus 3D MHD VAL3C continua VALII budget hydrogen budget all

lines from ALC7: model optical spectrum ultraviolet depletion hydrogen strong lines plot formats pops plot BSJ plot profile plot Mg I 4571 Fe I 6302 Mg I b_2 Na I D_1 Ba II 4554 Ca II 8542 Å Ca II K Mg II k Lyα Hα Hβ He I 584 He I 10830 canonical Hα Na I D_1–Mg I b_2 Lyα–Hα Hα–Ca II 8542 Å Ca II K–Mg II k versus FCHHT-B ALC7–FALC FALC–FALP ALC7–FALP

detour lines: pumping suction

Oslo-simulated dynamic atmosphere: 1D RADYN 3D Bifrost Bifrost line synthesis

LA-conjectured PSBE atmosphere: non-E Hα aureole boosting Hα extinction CE–SB EBs spicules-II contrail ALMA non-E chromosphere?

IRIS diagnostics: overview diagnostics

Na I D_1 IN A MAGNETIC CONCENTRATION

Leenaarts et al. 2010ApJ...709.1362L

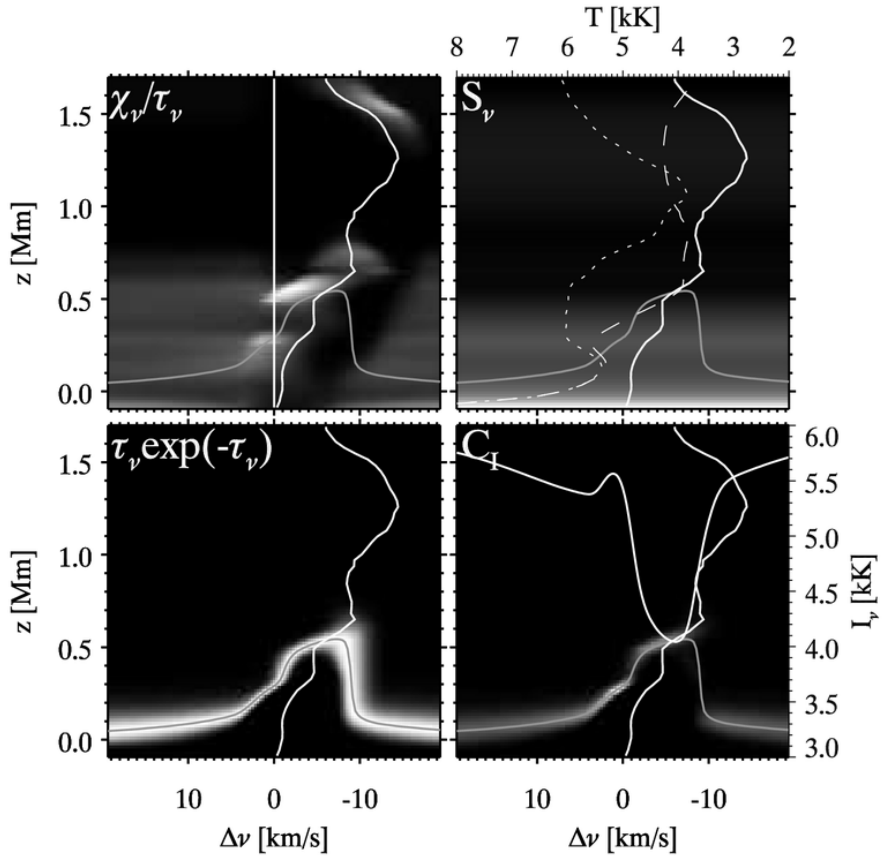

FORMATION BREAKDOWNS Na I D_1 & Ca II 8542 Å

Leenaarts et al. *2010ApJ...709.1362L*

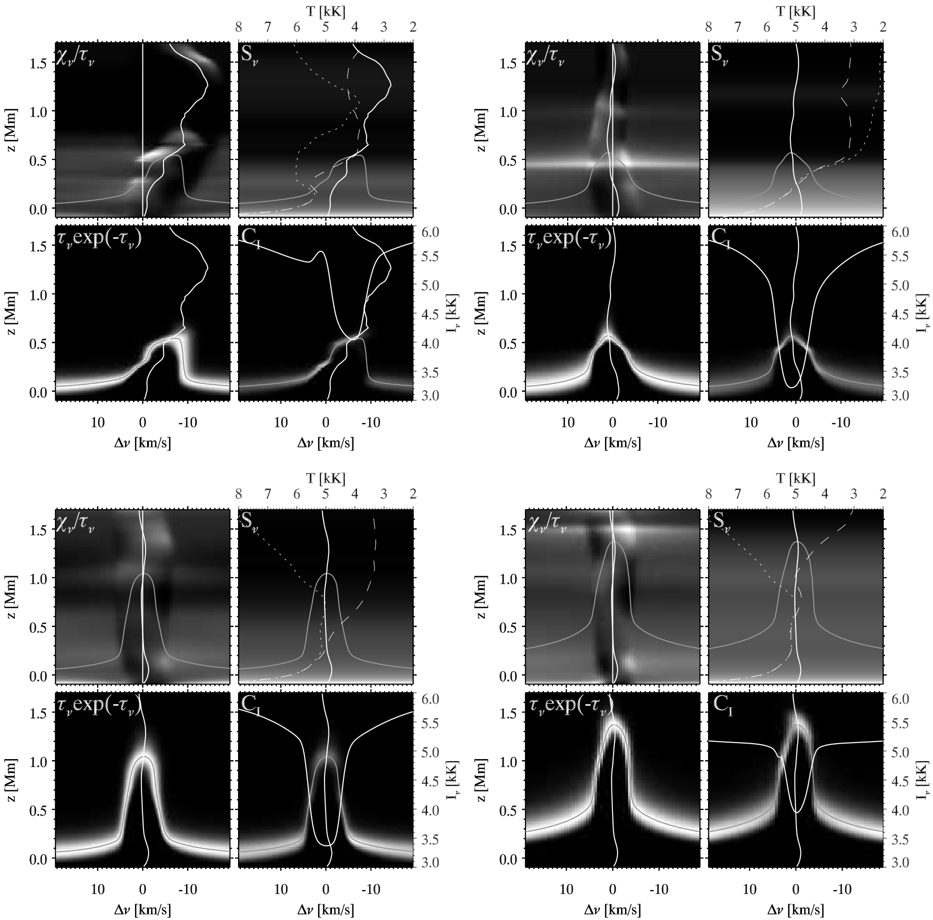

start

index

STAGGER/MULTI3D Na I D_1 DOPPLERGRAMS AS UNSIGNED MAGNETOGRAMS

Rutten et al. 2011A&A...531A..17R

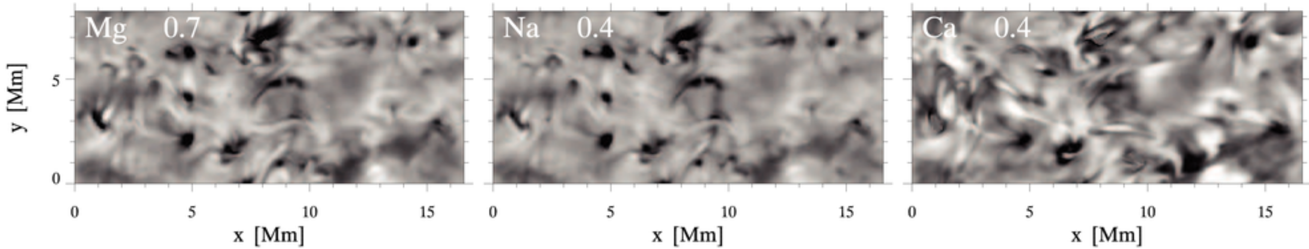

Fig. 16. Dopplergrams from the simulation as in the bottom row of Figure 7 but closer to line center and with only CRISP spectral smearing, no spatial PSF smearing.

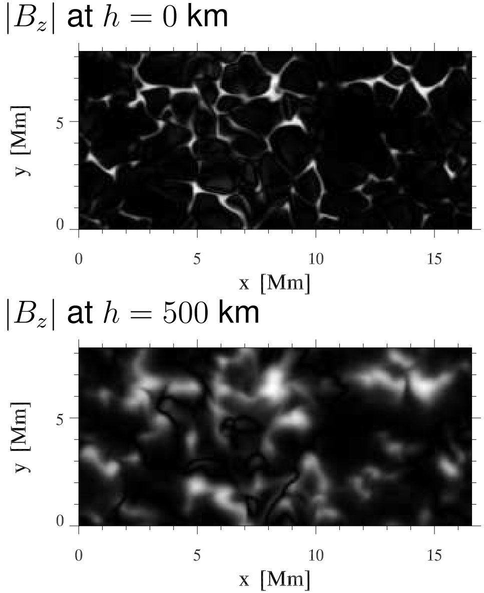

A corollary is that searches for global g-modes and so-called "chromosphere seismology" using full-disk resonance-cell sampling of the Na line as with GOLF-NG (e.g., Turck-Chièze et al. 2006; Salabert et al. 2009) will suffer noise from reversed granulation just as classical helioseismology suffers noise from granulation. Magnetic concentrations contribute much noise (literally) by their shocks. GOLF-NG's 15 passbands, spread over $\Delta\lambda = \pm 9$ km s^{-1}, have $FWHM = 30$ mÅ, half CRISP's passband in this line and clearly narrow enough. Interpretation of such multi-passband oscillation sampling that relies on one-dimensional height-of-formation interpretation, for example to diagnose upward propagation from inward phase difference, is likely to fail since the clapotispheric signals are better described as clouds of varying opacity at varying height of which the varying Dopplershifts act as shutters obscuring the inner line wings.

SOLAR SPECTRUM FORMATION: EXAMPLES

Robert J. Rutten
https://webspace.science.uu.nl/~rutte101

thin: cloud modeling   corona   chromosphere   Rydberg per ALMA?

thick: UV line flip   VAL3C temperature   VAL3C spectrum   Kurucz stars

photospheric lines: inversions   bright points   reversed granulation   Na I D1 MGs   limb emission lines

continua from VAL3C: Avrett models   versus 3D MHD   VAL3C   continua   VALII   budget hydrogen   budget all

lines from ALC7: model   optical spectrum   ultraviolet depletion   hydrogen   strong lines   plot formats   pops plot   BSJ plot   profile plot   Mg I 4571   Fe I 6302   Mg I b_2 Na I D_1 Ba II 4554   Ca II 8542 Å   Ca II K   Mg II k   Lyα Hα Hβ He I 584   He I 10830   canonical Hα Na I D_1–Mg I b_2 Lyα–Hα Hα–Ca II 8542 Å   Ca II K–Mg II k   versus FCHHT-B   ALC7–FALC   FALC–FALP   ALC7–FALP

detour lines: pumping   suction

Oslo-simulated dynamic atmosphere: 1D RADYN   3D Bifrost   Bifrost line synthesis

LA-conjectured PSBE atmosphere: non-E Hα aureole boosting   Hα extinction   CE–SB   EBs   spicules-II   contrail   ALMA   non-E chromosphere?

IRIS diagnostics: overview   diagnostics

LIMB EMISSION LINES

- *tabulations*
  - Menzel, thesis 1930, Pubs. Lick Obs., Campbell eclipse spectra, ADS antiquities
  - Dunn et al. 1968ApJS...15..275D HAO eclipse spectra comprehensive plot
  - Pierce 1968ApJS...17....1P extreme limb spectra plate with Mg I 4571 Å
  - Rutten & Stencel 1980A&AS...39..415R limb emission lines in Ca II H & K wings
  - Rutten + XX: limb emission lines in Mg II h & k wings
- *rare earths*
  - Canfield 1971A&A....10...54C excerpt 1971A&A....10...64C excerpt
  - interlocking $\Rightarrow \eta > \varepsilon \Rightarrow S > B$ with much spatial smoothing
  - higher emission for larger quasi-continuous extinction (Ce II in H & K wings)
- *pumped ion lines*
  - Fe II 3969.4 Å between Ca II H and Hϵ: Cram et al. 1980ApJ...241..374C excerpt
  - subordinate lines sharing upper levels with strong UV lines
  - large sensitivity to deep temperature variations
- *strong lines with PRD wings*
  - Ba II 4554 Å: Rutten 1978SoPh...56..237R excerpt 1979ApJ...231..277R excerpt
  - others: Fe II, Ti II, . . .
- *LTE lines*
  - Mg I 4571 Å Rutten 1977SoPh...51....3R excerpt

SOLAR SPECTRUM FORMATION: EXAMPLES

Robert J. Rutten
https://webspace.science.uu.nl/~rutte101

thin: cloud modeling corona chromosphere Rydberg per ALMA?

thick: UV line flip VAL3C temperature VAL3C spectrum Kurucz stars

photospheric lines: inversions bright points reversed granulation Na I D1 MGs limb emission lines

continua from VAL3C: Avrett models versus 3D MHD VAL3C continua VALII budget hydrogen budget all

lines from ALC7: model optical spectrum ultraviolet depletion hydrogen strong lines plot formats pops plot BSJ plot profile plot Mg I 4571 Fe I 6302 Mg I b_2 Na I D_1 Ba II 4554 Ca II 8542 Å Ca II K Mg II k Lyα Hα Hβ He I 584 He I 10830 canonical Hα Na I D_1–Mg I b_2 Lyα–Hα Hα–Ca II 8542 Å Ca II K–Mg II k versus FCHHT-B ALC7–FALC FALC–FALP ALC7–FALP

detour lines: pumping suction

Oslo-simulated dynamic atmosphere: 1D RADYN 3D Bifrost Bifrost line synthesis

LA-conjectured PSBE atmosphere: non-E Hα aureole boosting Hα extinction CE–SB EBs spicules-II contrail ALMA non-E chromosphere?

IRIS diagnostics: overview diagnostics

AVRETT SOLAR-ANALOG STARS

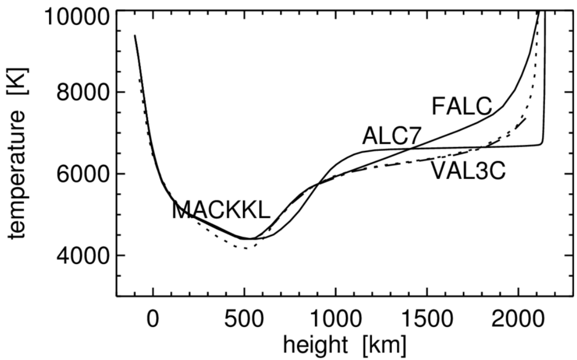

- VAL3C = Vernazza, Avrett, Loeser 1981ApJS...45..635V: best-fit to UV continua
- MACKKL = Maltby et al. 1986ApJ...306..284M: less steep upper photosphere
- FALC = Fontenla, Avrett, Loeser 1993ApJ...406..319F: ambipolar diffusion
- ALC7 = Avrett & Loeser 2008ApJS..175..229A: UV-line fit; update 2015ApJ...811...87A

[. . .] The results may be interpreted as holding for a computationally existing star called VALIII [. . .]. This star is remarkably like the Sun in its temporally and spatially averaged continuous spectral distribution, but in contrast to the Sun it does obey hydrostatic equilibrium and static plane-parallel geometry, and it contains only those atoms, ions and electrons that were specified in the Pandora code, fortunately with just the corresponding cross-sections. Its modeling is exact! The advantage of studying the star VALIII rather than the star Sol is that the physics of VALIII radiation is fully understandable. Also, it keeps adhering to these course notes ad infinitum while solar physics evolves to more complexity.

Rutten "Radiative Transfer in Stellar Amospheres"

OSLO SIMULATION VERSUS 1D STANDARD MODELS

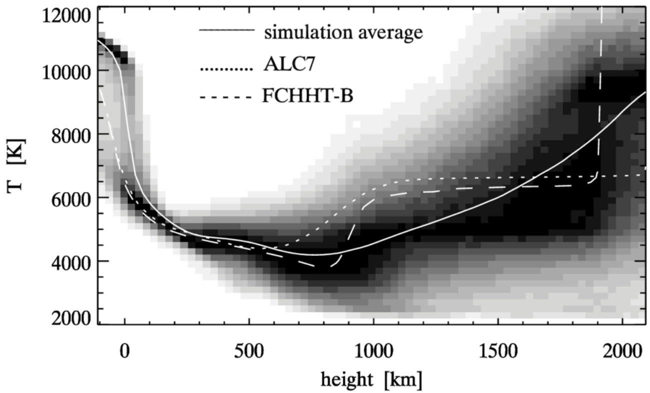

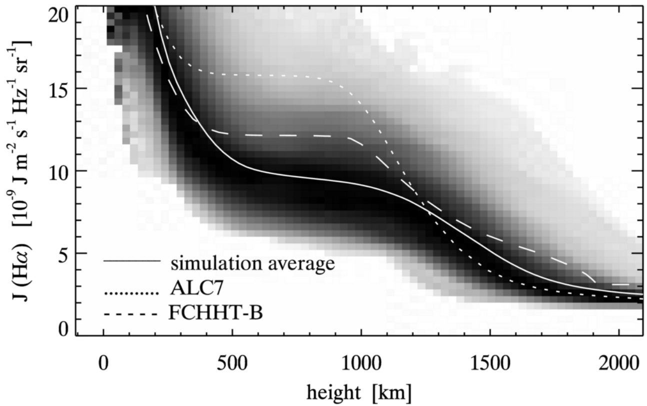

- simulation = state-of-the-art: 3D(t), $\vec{B}$, non-HE, SE populations but NE for H
  Leenaarts, Carlsson & Rouppe van der Voort *2012ApJ...749..136L*
- ALC7 = UV fit: 1D static, no $\vec{B}$, HE + microturbulence, SE populations
  Avrett & Loeser *2008ApJS..175..229A*
- FCHHT-B = UV fit: 1D static, no $\vec{B}$, HE + imposed acceleration, SE populations
  Fontenla, Curdt, Haberreiter, Harder & Tian *2009ApJ...707..482F*

The T and $J_\nu(\mathrm{H}\alpha)$ behavior seems arguably similar. However, the conceptual differences between plane-parallel static hydrostatic-equilibrium modeling and the 3D(t) MHD simulation are enormous (cf. Newtonian gravitation versus general relativity). The $T(h)$ stratifications in the simulation vary tremendously, with shocks propagating upwards and sideways and the increase to coronal temperature dancing up and down over a large height range.

VALIIIC MODEL

Vernazza, Avrett, Loeser *1981ApJS...45..635V*

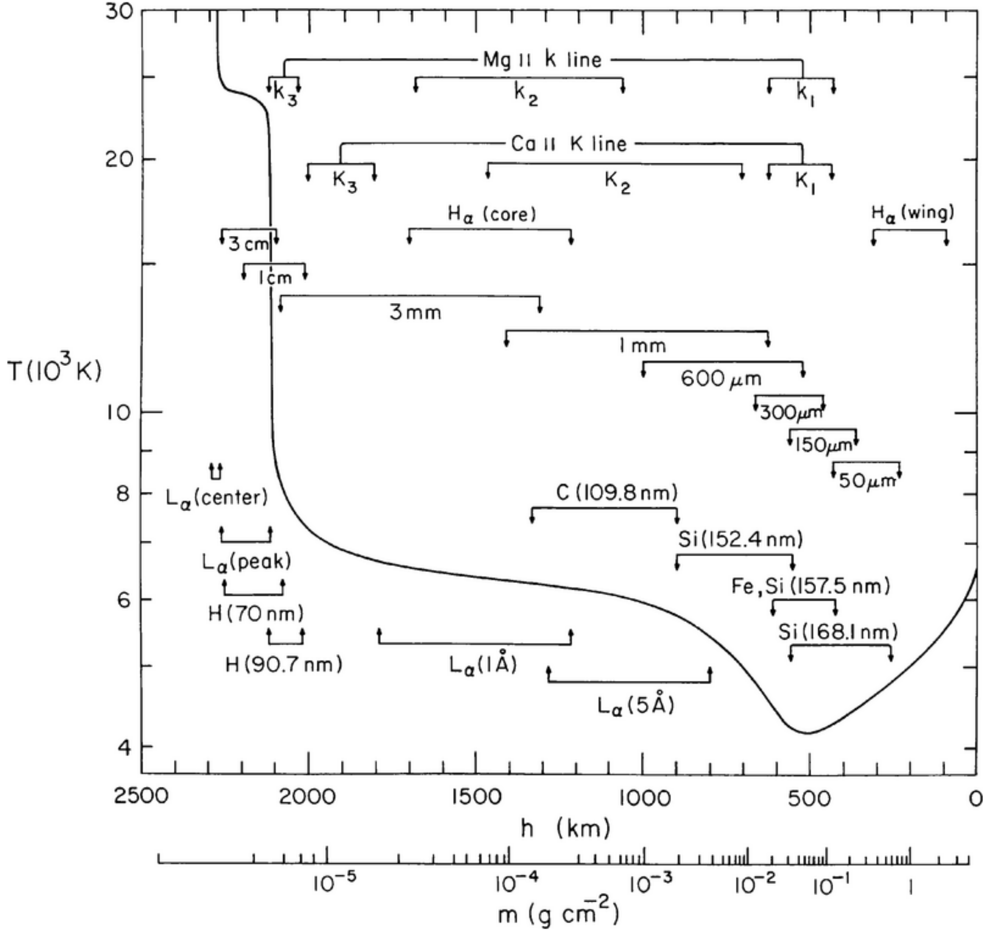

VALIIIC 500 nm FORMATION

$$I_\nu(0,1) = \int_0^\infty S_\nu \,\mathrm{e}^{-\tau_\nu}\,\mathrm{d}\tau_\nu = \int_0^\infty j_\nu \,\mathrm{e}^{-\tau_\nu}\,\mathrm{d}h \qquad \frac{\mathrm{d}I_\nu}{\mathrm{d}h} = j_\nu \,\mathrm{e}^{-\tau_\nu}$$

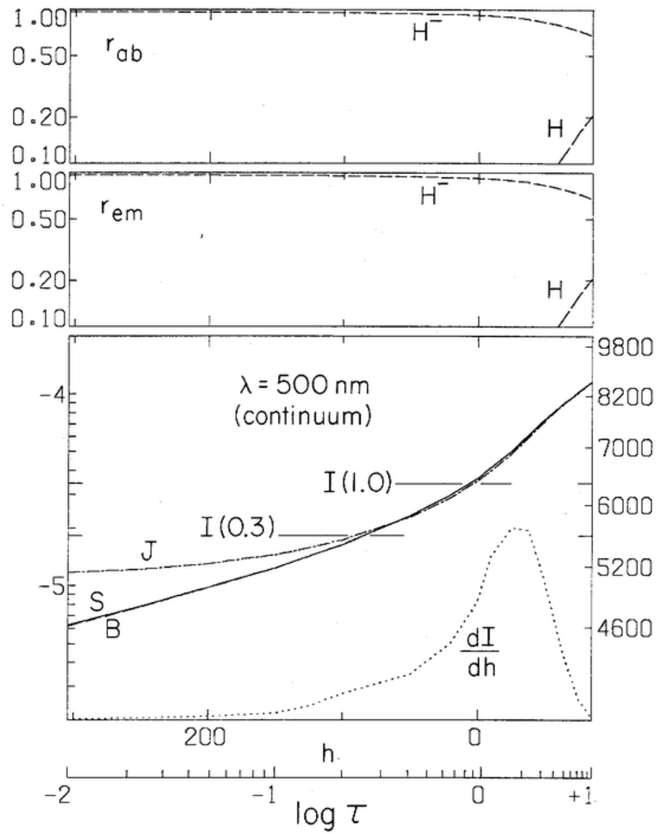

VAL3C CONTINUUM FORMATION

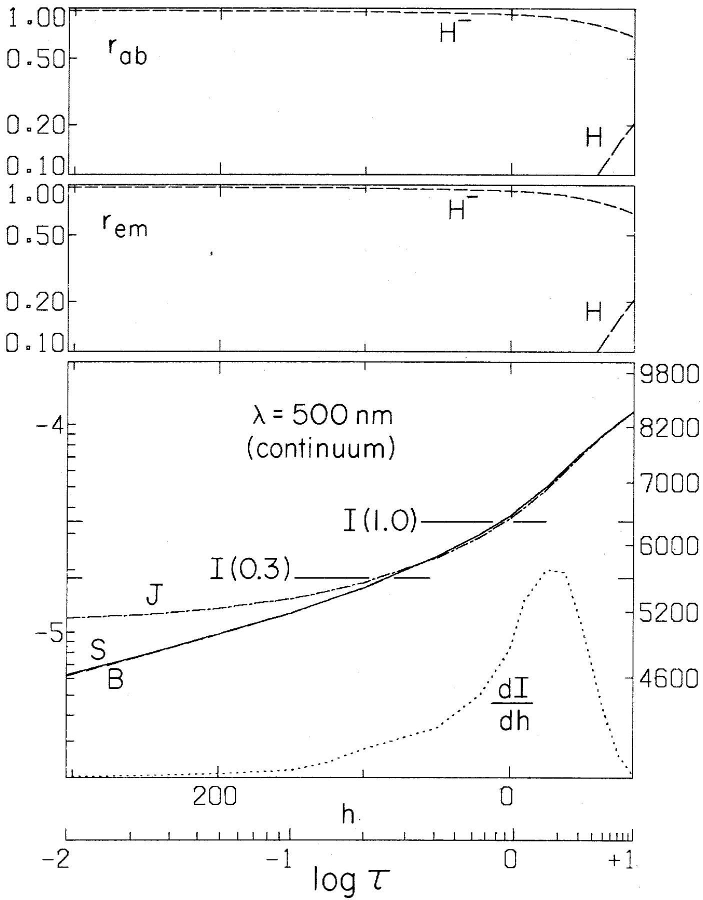

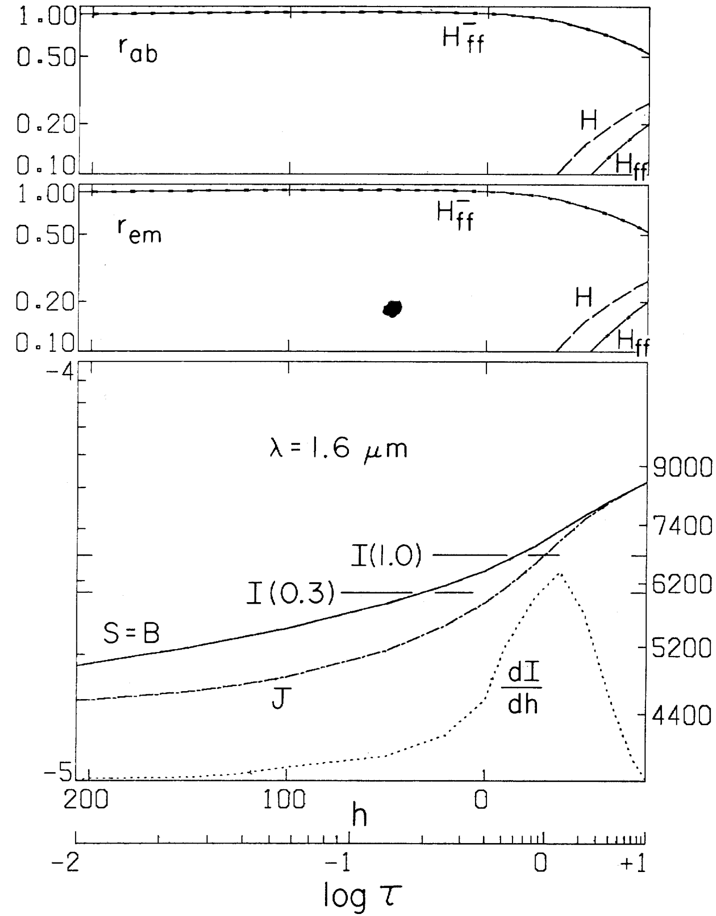

VAL3C CONTINUUM FORMATION

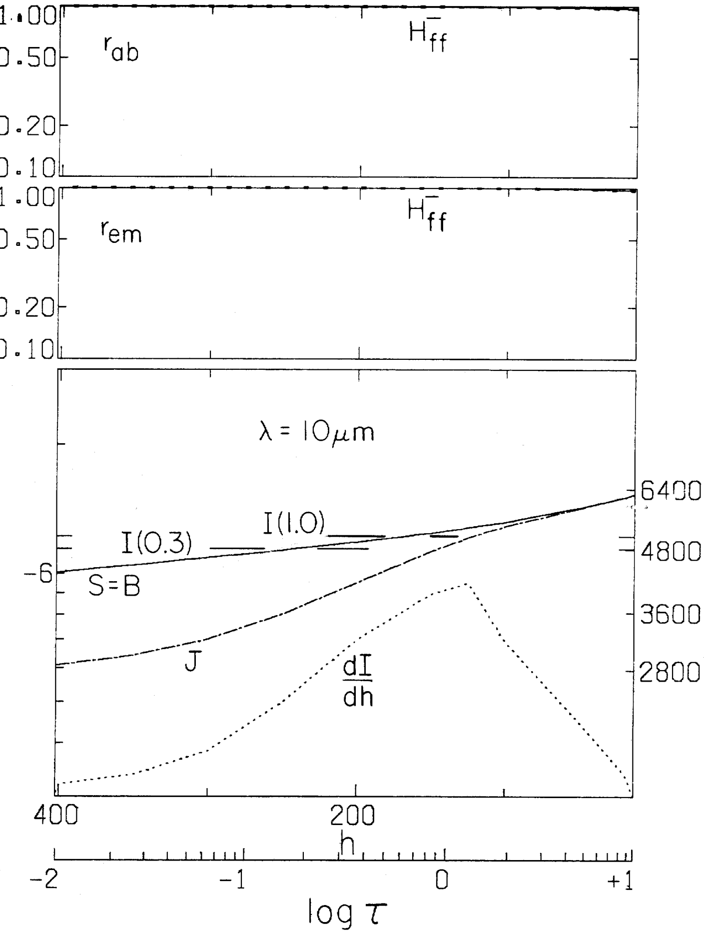

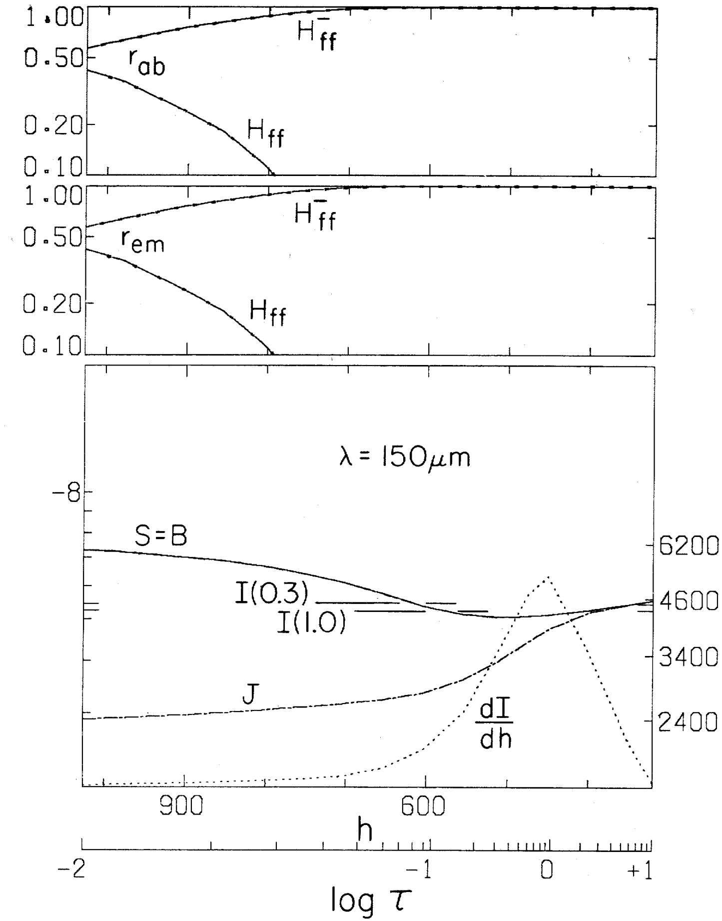

VAL3C CONTINUUM FORMATION

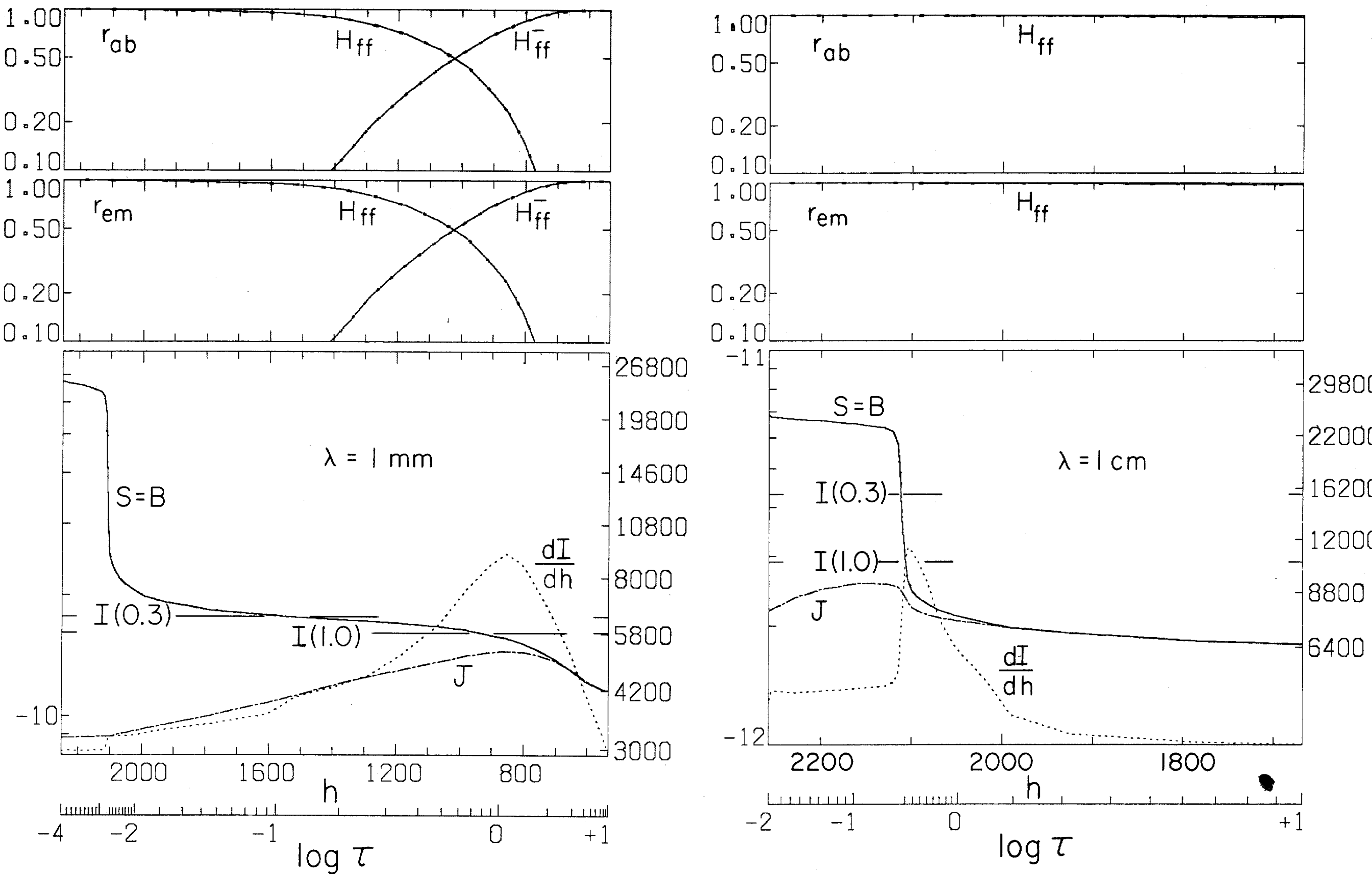

VAL3C CONTINUUM FORMATION

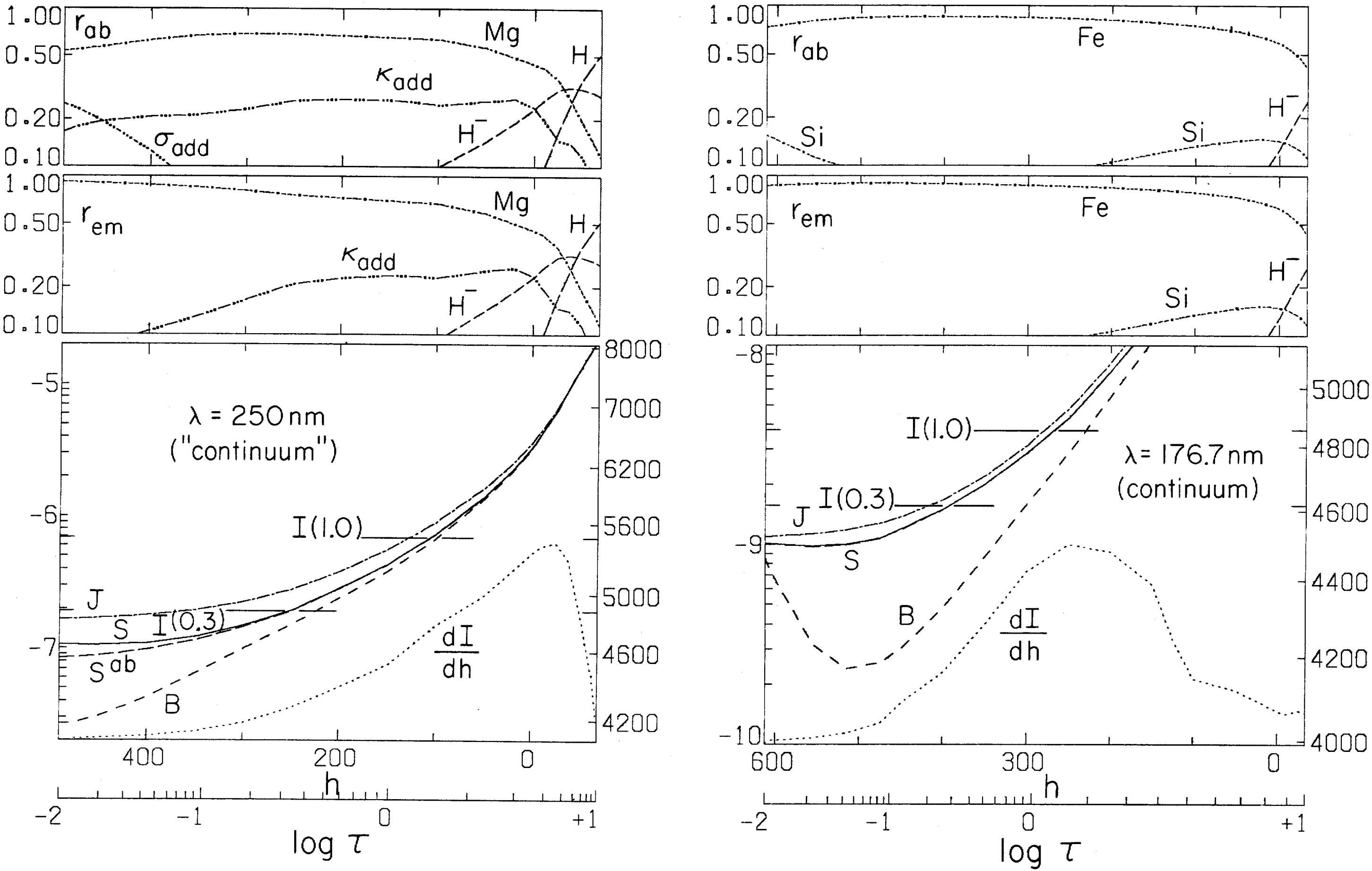

VAL3C CONTINUUM FORMATION

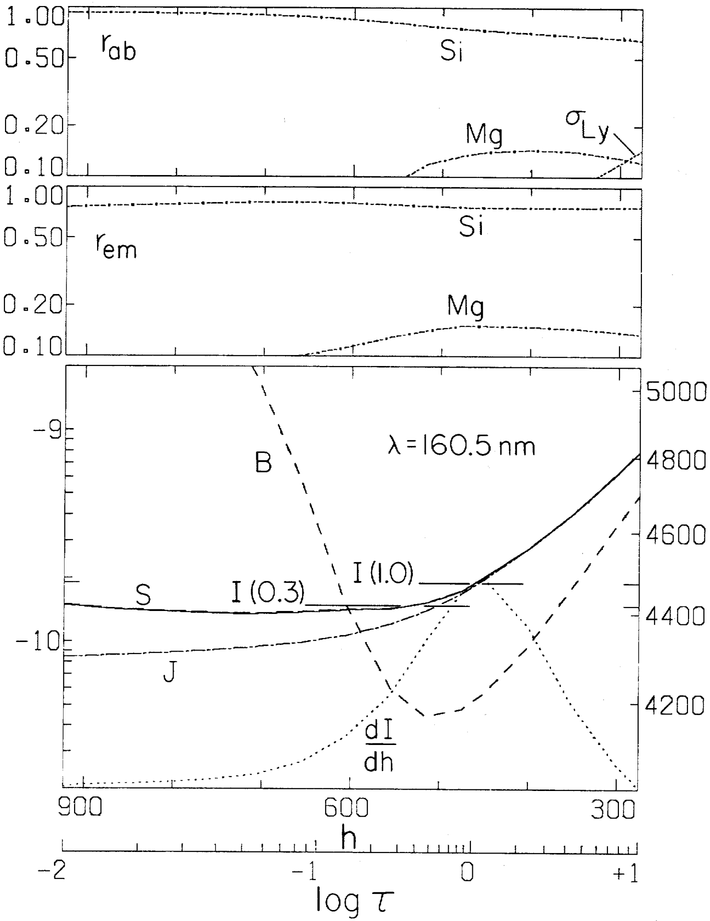

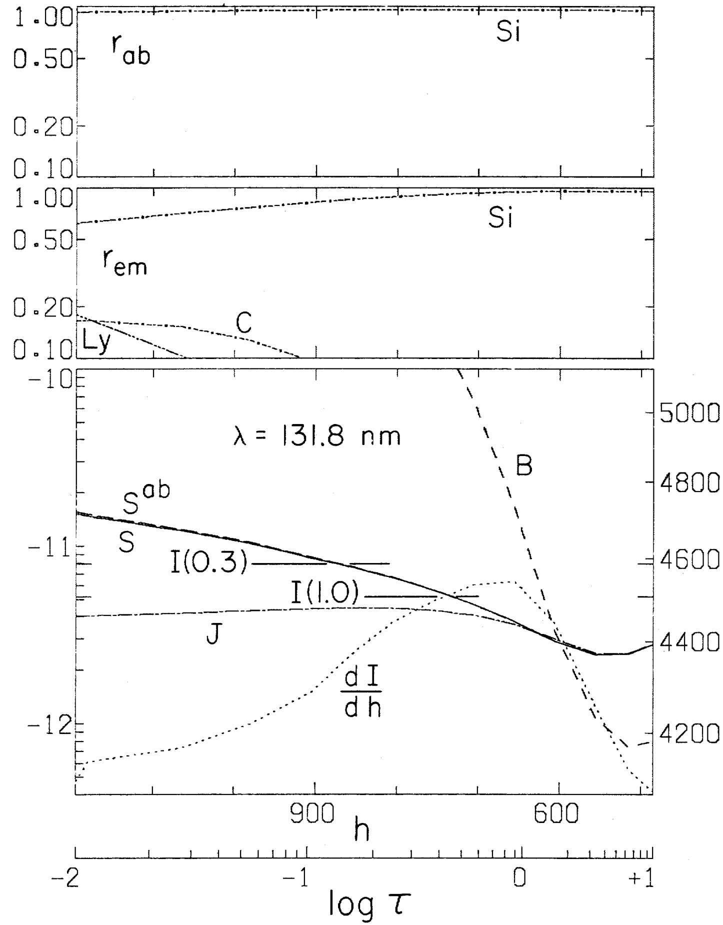

VAL3C CONTINUUM FORMATION

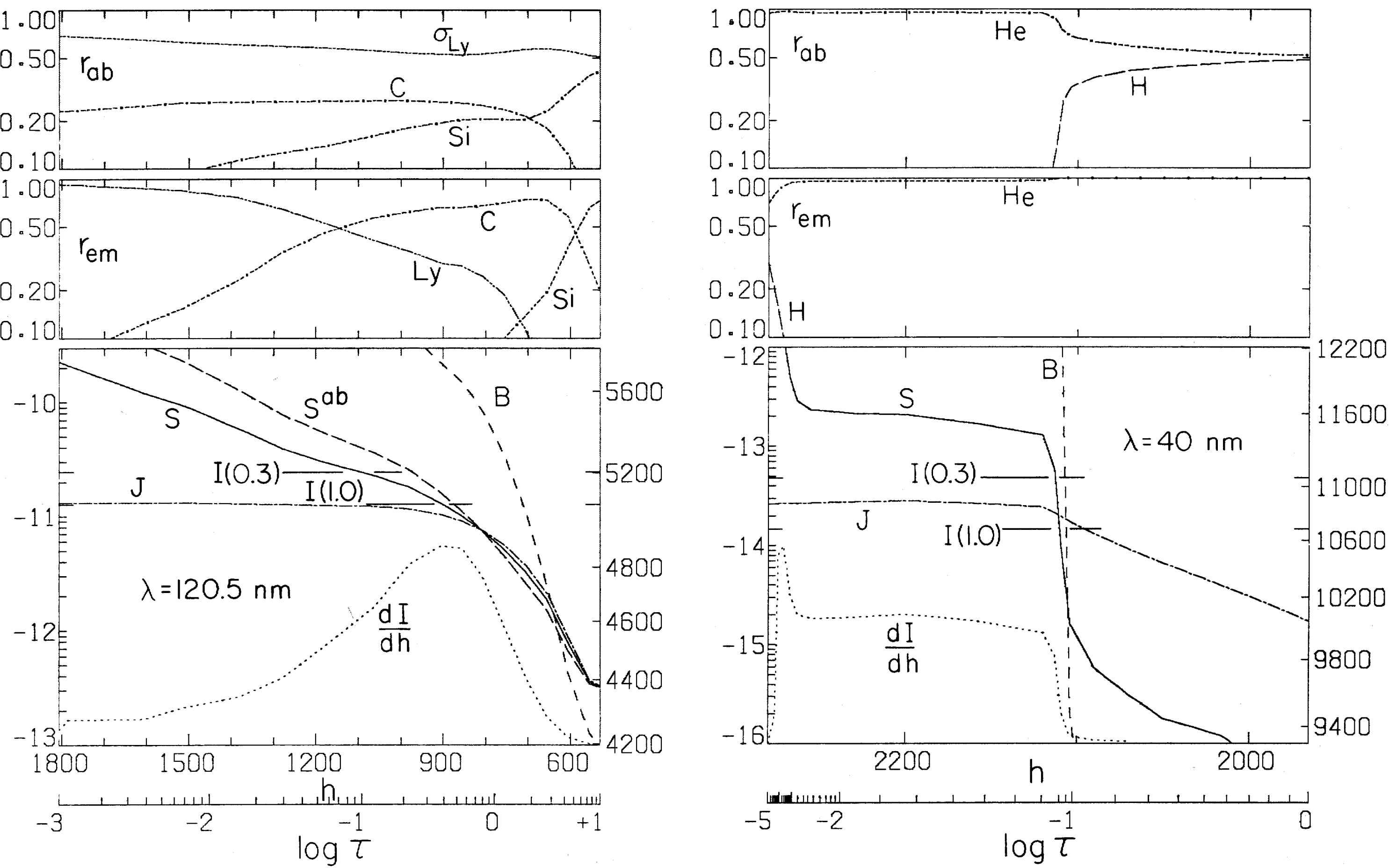

TEMPERATURE MINIMUM IN VALII

Vernazza, Avrett & Loeser 1976ApJS...30....1V (VALII)

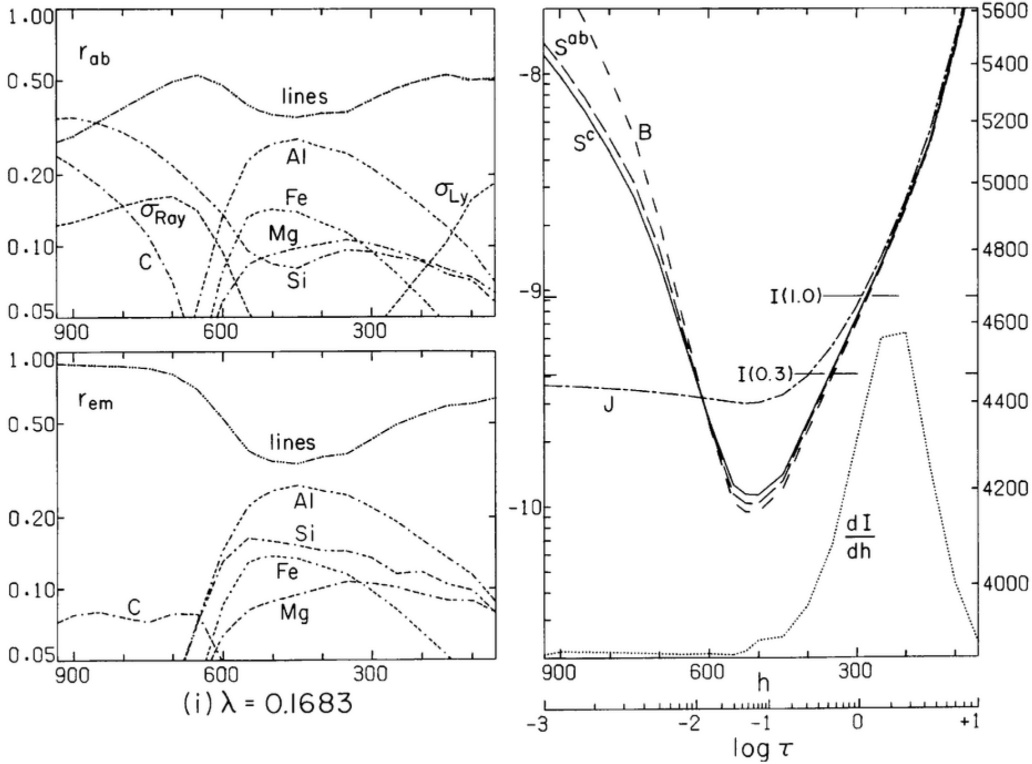

- oops: bf edges of electron-donor metals wrongly in LTE
- oops: too few line-haze lines and wrongly in LTE

VAL3C RADIATION BUDGET

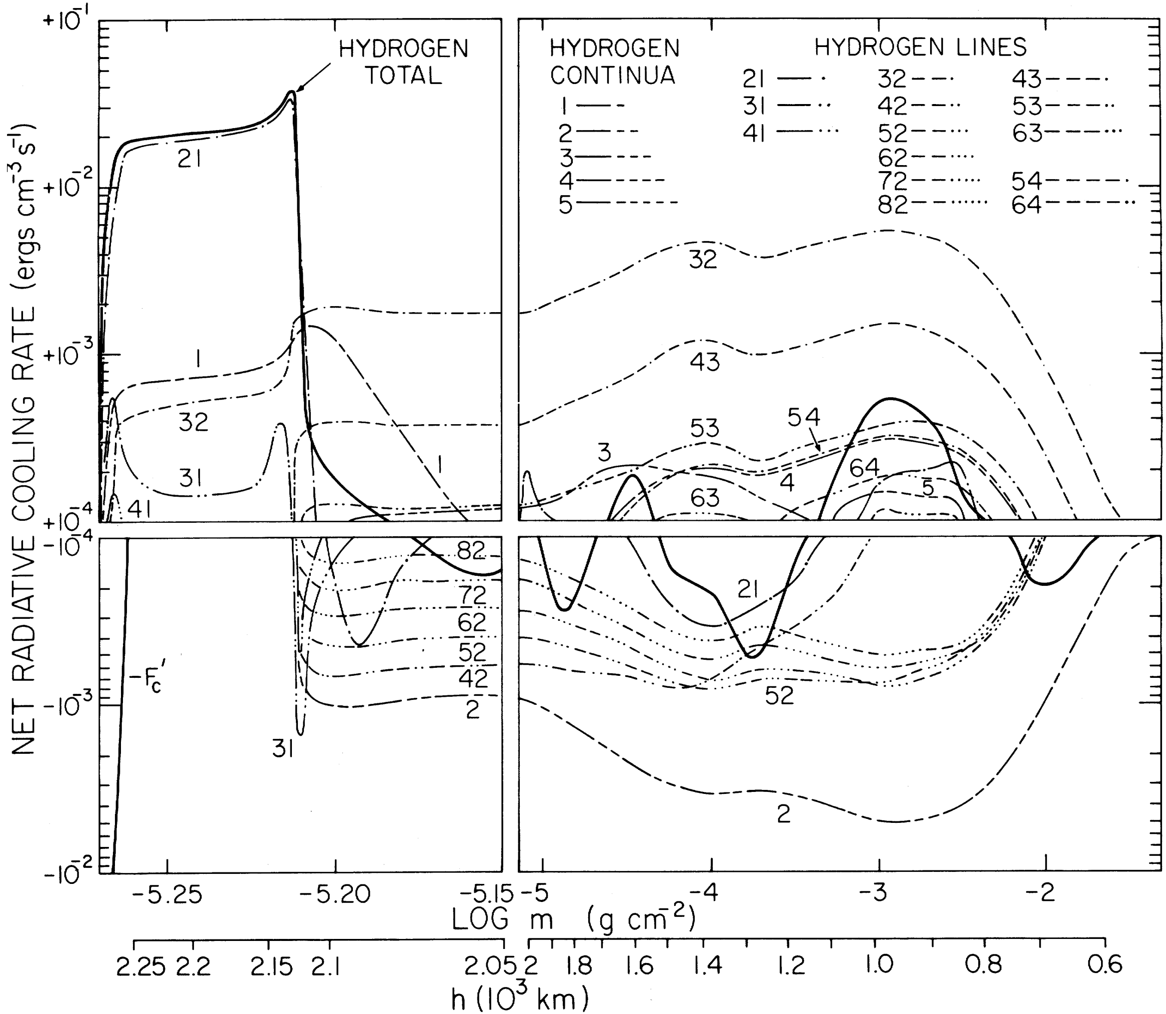

VAL3C RADIATION BUDGET

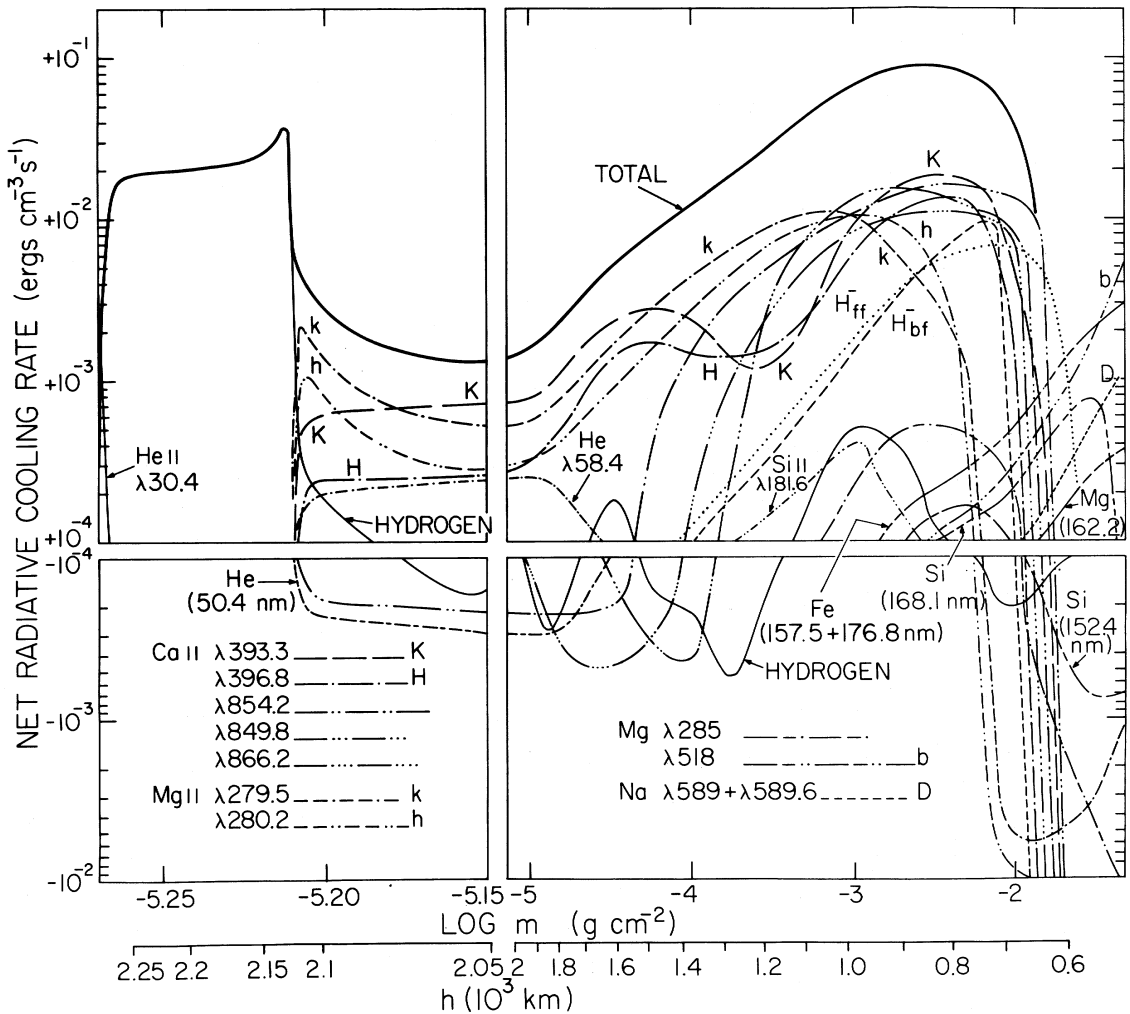

SOLAR SPECTRUM FORMATION: EXAMPLES

Robert J. Rutten
https://webspace.science.uu.nl/~rutte101

ALC7 ATMOSPHERE

Avrett & Loeser *2008ApJS..175..229A*

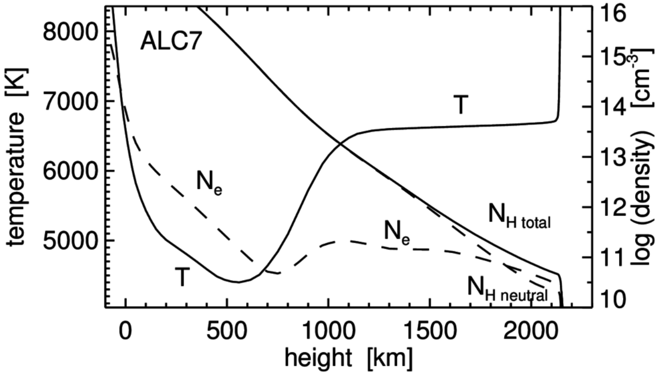

- unrealistic plane-parallel static computational star with solar-like average spectrum
  – exemplary in obeying all equations in my RT courses: understandable line formation
- best-fit temperature: near-RE in photosphere, shock-dominated in chromosphere
  – slope in upper photosphere depends on NLTE ultraviolet line haze
- total hydrogen density: exponential decay
  – turbulent presssure added to gain scale height and chromospheric extent
- low electron density in photosphere and temperature minimum
  – from ionization of donor-elements Si, Fe, Mg, Al with 10^{-4} relative abundance
- increasing hydrogen ionization across chromosphere
  – electron density reaches proton density at its top
- near-isothermal near-constant-N_e chromosphere
  – mimics Avrett's (1965) isothermal constant-ε two-level-atom scattering atmosphere

CRD RESONANT SCATTERING IN AN ISOTHERMAL ATMOSPHERE

RTSA figure 4.12; from Avrett 1965SAOSR.174..101A

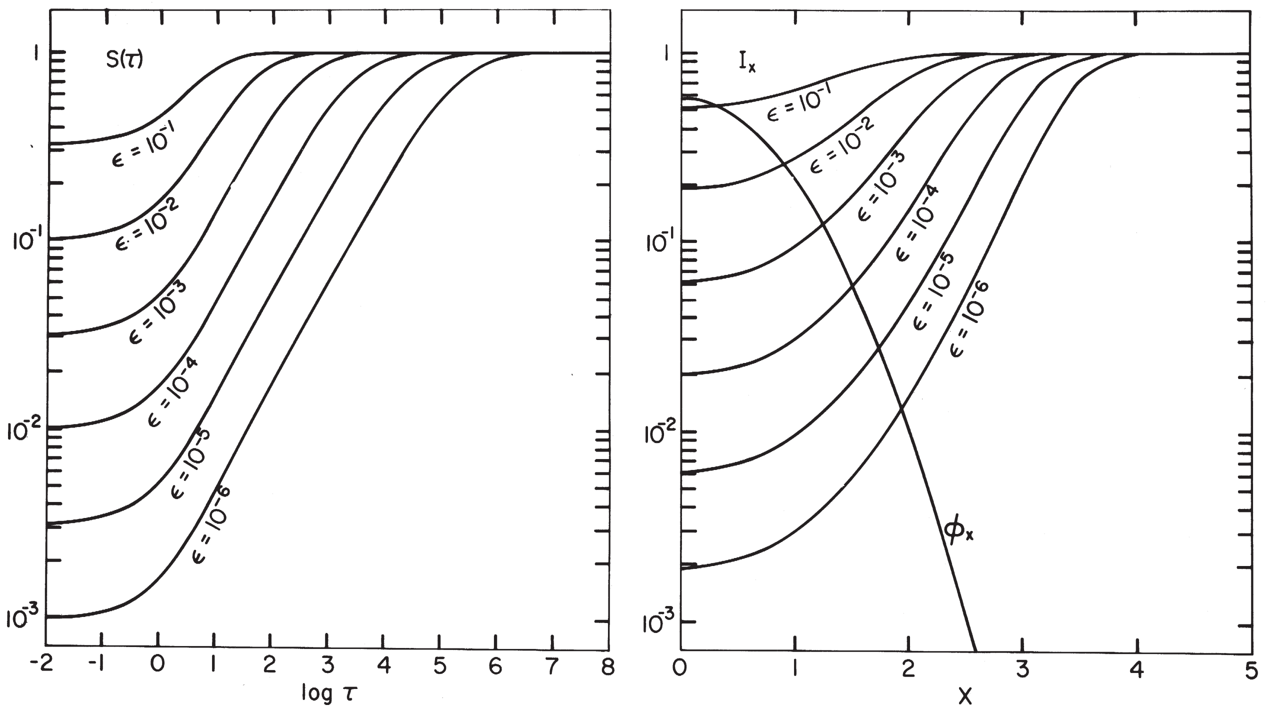

- left: S/B in a plane-parallel isothermal atmosphere with constant ε for complete redistribution. The curves illustrate the $\sqrt{\varepsilon}$ law and thermalization at $\Lambda \approx 1/\varepsilon$.
- right: corresponding emergent line profiles and Gaussian extinction profile shape ϕ (only the righthand halves; $x = \Delta\lambda/\Delta\lambda_{\mathrm{D}}$)

SOLAR OPTICAL VERSUS ALC7 OPTICAL – ON DISK AND OFF LIMB

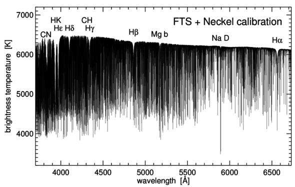

- *observed disk-center spectrum*
  - Na I D lines darkest from scattering
  - H I Balmer lines widest from linear Stark + Holtsmark
  - Ca II H & K strongest from Saha-Boltzmann (“Cecilia Payne”)

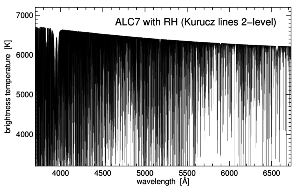

- *ALC7 disk-center spectrum per RH*
  - 1D-SE without granules, waves, shocks, fibrils, magnetism
  - chromospheric extent from imposed turbulent pressure
  - good reproduction, also ultraviolet (RH: not H, not Kurucz)

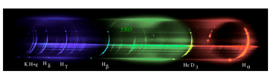

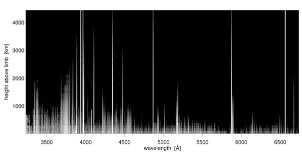

- *observed flash spectrum*
  - H I Balmer, Ca II H & K, He I $\equiv$ Lockyer’s “chromosphere”
  - Janssen/Lockyer discovery of He I D_3
  - made up of spicules

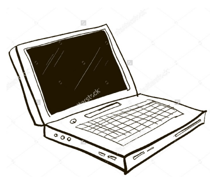

- *ALC7 flash spectrum per RH*
  - too small extent
  - cannot explain H I Balmer, let be He I D_3
  - no spicules

ULTRAVIOLET DEPLETION IN THE ALC7 ATMOSPHERE

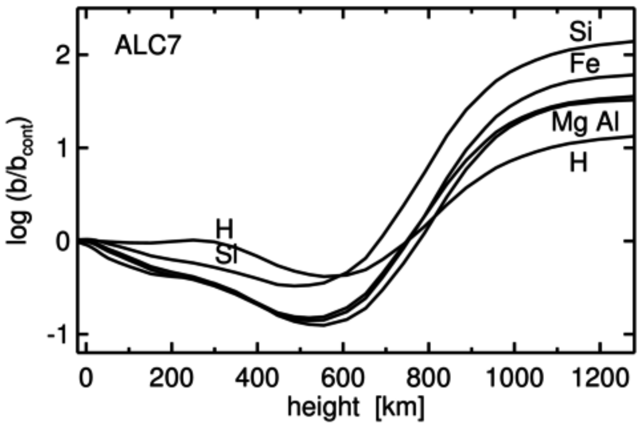

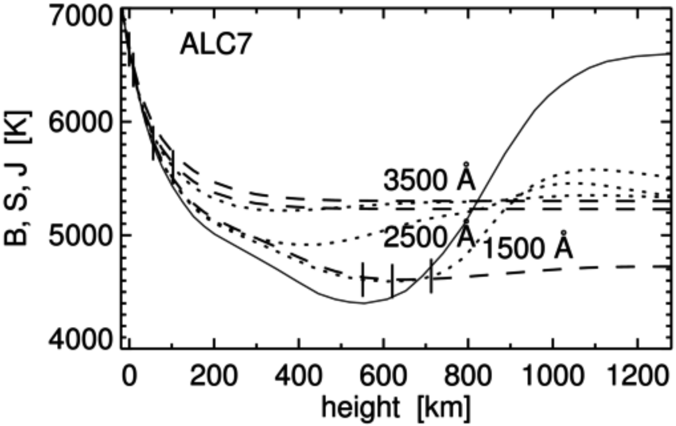

minority atoms: photospheric extinction depletion by ultraviolet bound-free scattering

- ultraviolet bound-free edges produce scattering continua
- $J > B$ from:
  - $T(h)$ gradient defined by radiative equilibrium for the optical
  - $B(h)$ steeper in the ultraviolet due to Wien nonlinearity
  - Λ operator gives $J > S$ for steep $S(\tau)$
  - deep escape from small H I bf extinction
- $b_1/b_{\rm cont}$ for electron donors Mg I, Fe I, Si I and Al I imply b_1 population depletion across photosphere because $b_{\rm cont} \approx 1$
- their photospheric lines have increasing extinction deficits compared to LTE
- $b_2/b_{\rm cont}$ for H I shows similar behavior for the top of the hydrogen atom starting at $n=2$

HYDROGEN LINES IN THE ALC7 ATMOSPHERE

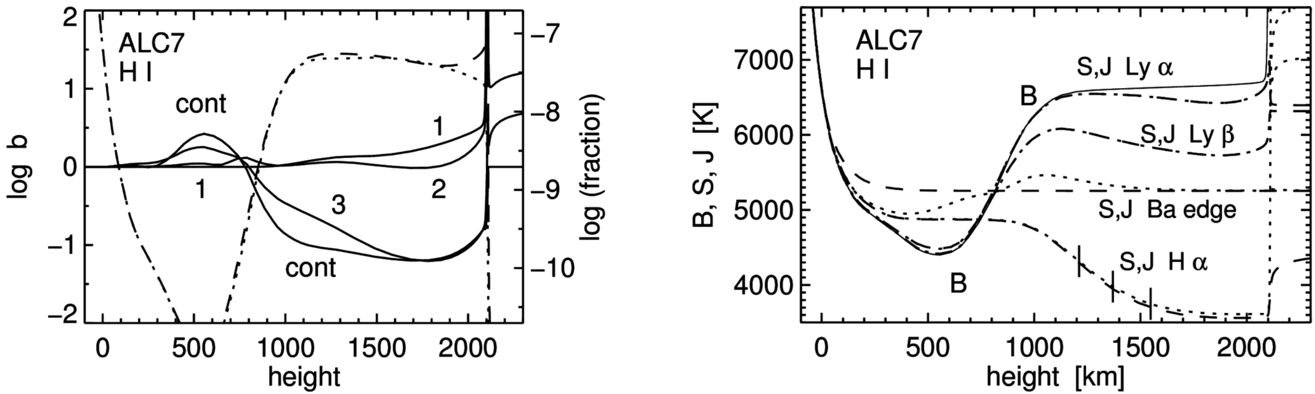

Hα: chromosphere is back-scattering attenuator for radiation from deep photosphere; outward S decline as in isothermal constant-ε two-level-atom atmosphere

Lyα: tremendous scattering with $S_{\rm Ly\,\alpha} \approx J_{\rm Ly\,\alpha}$ but local thermalization with $J_{\rm Ly\,\alpha} \approx B_{\rm Ly\,\alpha}$ from short photon mean free paths (S dotted, J dashed; dot-dashed = identity)

Lyβ: scattering as Lyα, shares photon losses in Hα (Hα ticks $\tau = 3, 1, 0.3$) (same $S/B \approx b_3/b_l$ since $b_2 \approx b_1$ but offsets differ in temperature representation)

$n=1$: Saha-Boltzmann $b_1 \approx 1$ population because hydrogen is neutral (except in transition region at right)

$n=2$: Saha-Boltzmann $b_2 \approx 1$ population from Lyα thermalization (dotted fraction curve = $n_2^{\rm LTE}/N_{\rm Htot}$ $\approx$ dashed curve = actual $n_2/N_{\rm Htot}$)

ionization: $b_{\rm cont}/b_2$ defined by SE balancing of $B(T_{\rm rad}^{\rm Bacont})/B(T_{\rm e})$ ionization driving and cascade recombination with high-n line photon losses. The H I top ($n \geq 2$) represents a 3.4 eV alkali atom with ground-state population set by Lyα.

STRONG LINES IN ALC7

Avrett & Loeser *2008ApJS..175..229A* *Rutten* *2016A&A...590A.124R*

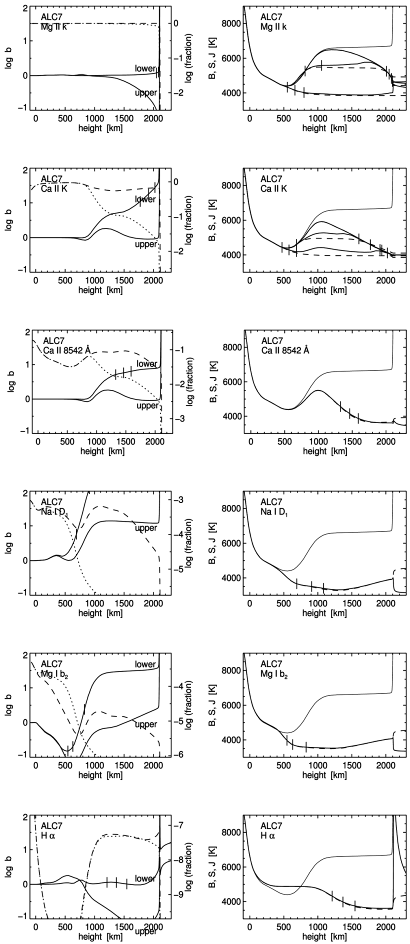

- *Mg II k*
  - extinction LTE, source function 2-level scattering
  - high peaks, low PRD dips, low wings
- *Ca II K*
  - lower abundance and ionization, underionization
  - small peaks and PRD dips
- *Ca II 8542*
  - as Ca II K with Boltzmann lowering and sensitivity
  - similar source function sampling as Hα
- *Na I D*$_1$
  - photospheric scattering, suction and underionization
  - no sensitivity to temperature rise
- *Mg I b*$_2$
  - as Na I D$_1$ but photospheric overionization
  - no sensitivity to temperature rise
- *H*α
  - chromospheric scattering of photospheric photons
  - chromospheric extinction LTE from Lyα box-up

LINES FROM THE ALC7 CHROMOSPHERE: PLOT FORMATS (Na I D_1)

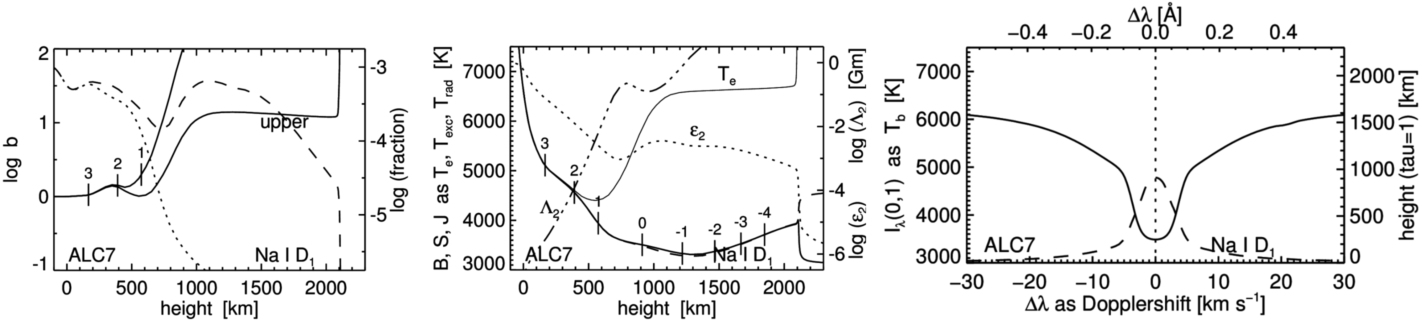

$b_i \equiv n_i/n_i^{\rm LTE}$ $\alpha^l \approx b_l\,\alpha^{\rm LTE}$ $S^l \approx (b_u/b_l)B$ $S^l \approx (1-\varepsilon_2)\,J + \varepsilon_2\,B$ $\Lambda_2 \approx \sqrt{\pi}/(\alpha_0\,\varepsilon_2)$ $I(0) \approx S[\tau=1]$

- *first plot: populations*
  - solid: population departure coefficients. Always unity in the deep photosphere. Divergence with increasing $b_u < b_l$ shows resonance scattering. Steep b_l rise due to radiative overionization of this minority species (Na I). $\log\tau$ ticks on b_l curve are for line center.
  - dashed: fractional population $n_l/N_{\rm element}$ in NLTE. Scale at right. Na I is minority species.
  - dotted: fractional population $n_l/N_{\rm element}$ per Saha-Boltzmann. Difference with the NLTE curve corresponds to departure of b_l from unity.

- *second plot: line source function*
  - solid thin, thick, dashed: B, S, J as formal temperatures (for common scale with other lines). $\log\tau$ ticks are for line center.
  - dotted: ε for the Doppler core in 2-level approximation. Scale to the right.
  - dot-dashed: thermalization length in Gm. $\Lambda_2=-6$ means thermalization of S to B within a homogeneous slab of 1 km. The Λ mark is near core thermalization depth.

- *third plot: emergent profile*
  - solid: emergent profile as brightness temperature
  - dashed: $\tau_\lambda=1$ height scale at right
  - dotted, vertical: wavelength sampling(s) for second plot

start index

LINES FROM THE ALC7 ATMOSPHERE: POPULATIONS PLOT (Na I D_1)

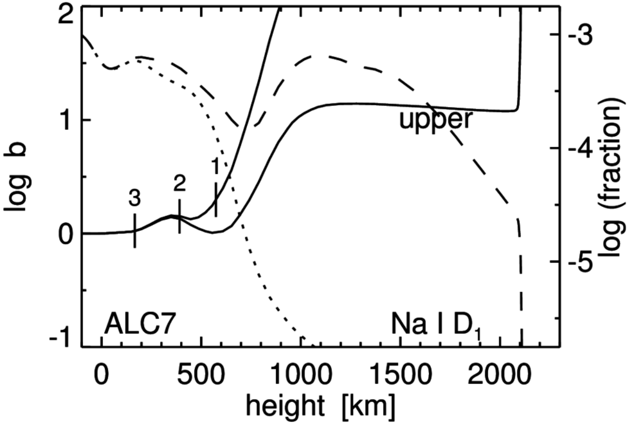

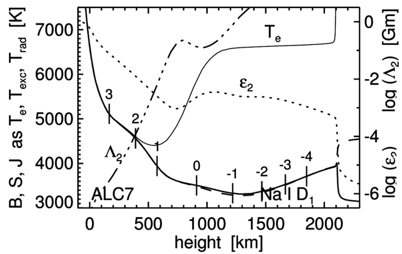

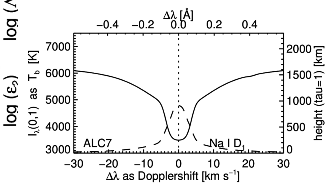

$b_i \equiv n_i/n_i^{\rm LTE}$ $\quad \alpha^l \approx b_l\, \alpha^{\rm LTE}$ $\quad S^l \approx (b_u/b_l)B$ $\quad \varepsilon \approx \varepsilon_2 = \alpha^{\rm a}/(\alpha^{\rm s}+\alpha^{\rm a})$ $\quad S^l \approx (1-\varepsilon_2)\,\overline{J} + \varepsilon_2\, B$

- *solid*: population departure coefficients for Na I D_1. Unity in deep photosphere from large collision frequency at high density, with $\varepsilon \approx 1$ ($B\,S\,J$ plot). Increasing $b_u < b_l$ divergence = $S^l < B$ divergence ($B\,S\,J$ plot) from $\sqrt{\varepsilon}$-law resonance scattering. Small initial hump in upper photosphere from photon suction (replenishment from ion reservoir) by scattering-out Na I D photons. Steep b_l rise above 700 km from ultraviolet underionization ($1-c$ edge at 2412 Å, typical for minority neutrals). The $\log\tau$ ticks on the b_l curve are for line center.
- *dotted*: fractional population $n_l^{\rm LTE}/N_{\rm elem}$ per Saha-Boltzmann. Scale at right. Na I is a minority species. Initial decrease from increasing ionization at decreasing $N_{\rm e}$, slight hump from less ionization at lower temperature, steep decline at increasing T and decreasing $N_{\rm e}$ (Saha).
- *dashed*: fractional population $n_l/N_{\rm elem}$ in NLTE. Line-center optical depth $\tau_\lambda = -\int(\alpha^l+\alpha^c)\,{\rm d}h$ has $\alpha^l >> \alpha^c$ and $\alpha^l_\lambda \sim n_l = (n_l/N_{\rm elem})A_{\rm elem}N_{\rm Htot}$. Divergence from LTE curve corresponds to departure of b_l from unity. The steep b_l increase compensates the steep $n_l^{\rm LTE}$ decrease.

LINES FROM THE ALC7 ATMOSPHERE: B S J PLOT (Na I D$_1$)

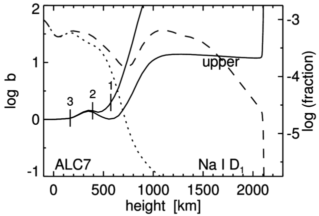

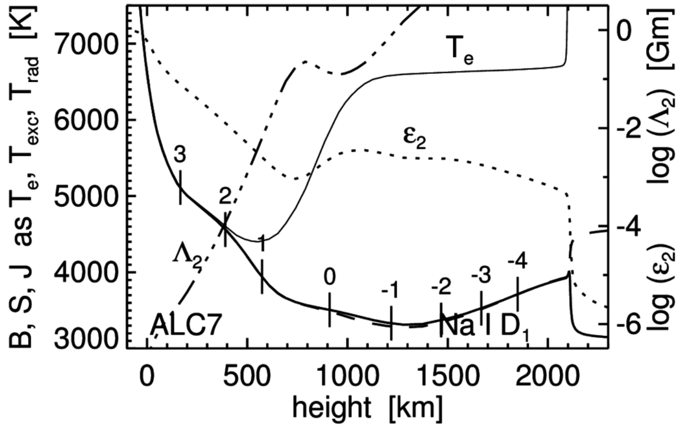

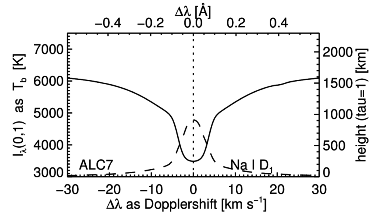

$S^l \approx (b_u/b_l)B$ $\quad\varepsilon \approx \varepsilon_2 \equiv \alpha^{\rm a}/(\alpha^{\rm s}+\alpha^{\rm a})$ $\quad S^l \approx (1-\varepsilon_2)\,\overline{J} + \varepsilon_2\,B$ $\quad\Lambda_2 \approx \sqrt{\pi}/(\alpha_0\,\varepsilon_2)$

- *thin solid*: B_{λ_0} as temperature $T_{\rm e}$ to remove Planck function variation with wavelength for comparison with other lines. The ALC7 atmosphere has a near-isothermal chromosphere.
- *thick solid*: Na I D$_1$ S^l as formal excitation temperature $T_{\rm exc}$. The $B > S$ divergence corresponds to the $b_l > b_u$ divergence in the populations plot, but not equally in their plotted logarithms due to the B and S conversions to formal temperature. The $\log\tau$ ticks are for line center. This scattering line does not sense the ALC7 chromosphere in S^l.
- *dashed*: profile-averaged angle-averaged intensity $\overline{J}$ as formal radiation temperature $T_{\rm rad}$.
- *dotted*: 2-level photon destruction probability ε_2 for the Doppler core. Scale to the right. Follows N_e, so fairly constant over 1000–2000 km from increasing hydrogen ionization.
- *dot-dashed*: 2-level thermalization length Λ_2 for the Doppler core in gigameter. Scale to the right. Example: $\Lambda_2 = -6$ implies thermalization of S to B at the center of a 2-km thick feature. The curve label is placed near the line-core thermalization height in the mid photosphere.

LINES FROM THE ALC7 ATMOSPHERE: PROFILE PLOT (Na I D_1)

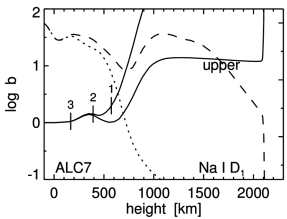

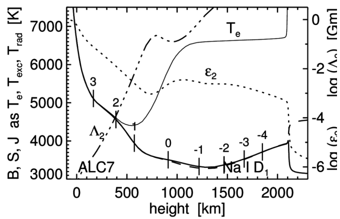

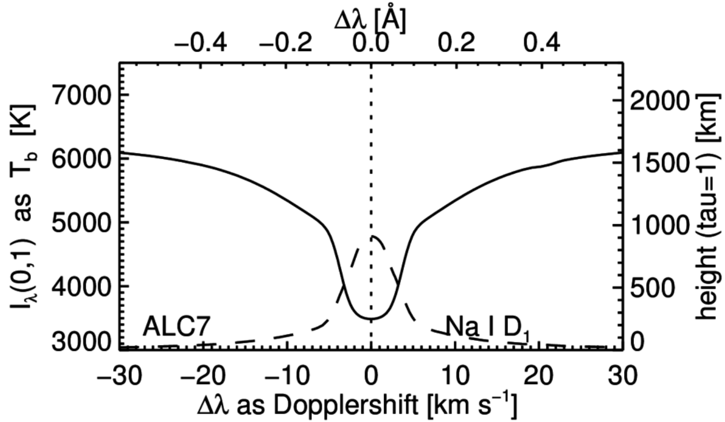

$$\alpha^l_\lambda \sim b_l\,(n^{\rm LTE}_l/N_{\rm elem})A_{\rm elem}N_{\rm Htot}\,\varphi(\lambda-\lambda_0) \qquad \tau_\lambda = -\int(\alpha^l+\alpha^c)\,{\rm d}h \qquad I_\lambda(0)\approx S^{\rm total}_\lambda[\tau_\lambda=1]$$

- *solid*: emergent intensity in the radial direction, represented as formal brightness temperature for comparison with other lines and the Eddington-Barbier estimate (BSJ plot, temperature axes match in the coming line-formation displays). Similarly, the bottom scale for wavelength separation from line center is in km s^{-1} for comparison with other lines. Wavelength separations in Å along the top.
- *dashed*: $\tau_\lambda = 1$ height, scale at right.
- *dotted, vertical*: sampling wavelength(s) for S and J in the BSJ plot. Only one for CRD lines (as Na I D_1) with frequency-independent line source functions (and $\overline{J}$ in the BSJ plot).
- one might overplot an observed solar disk-center profile, but this is misleading because even a perfect match does not imply that the ALC7 model is correct. ALC7 is an idealized didactic star not like the Sun with an easier-to-understand solar-lookalike spectrum.

Mg I 4571 Å FROM THE ALC7 ATMOSPHERE

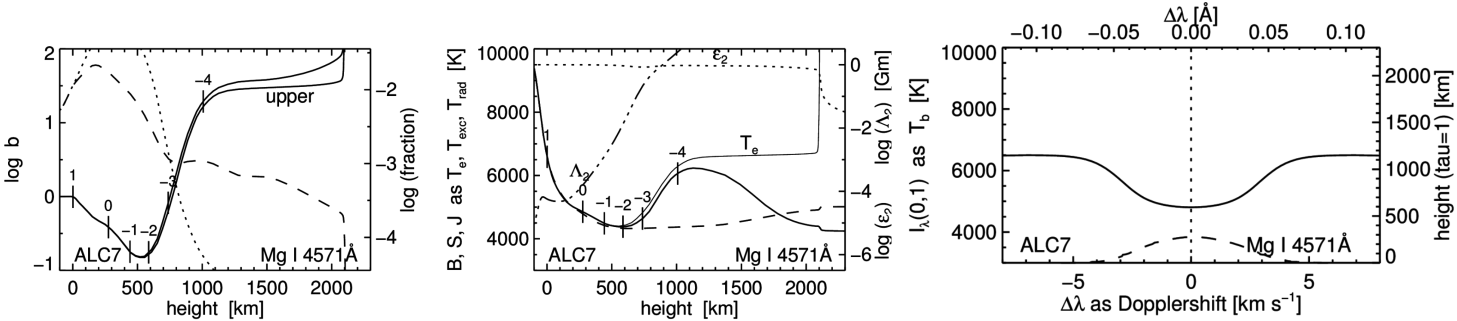

unique photospheric line with LTE source function

- extinction severely out of LTE. Deep b_l dip across the ALC7 photosphere from overionization by deeply escaping bound-free scattering ultraviolet radiation, including edges of Mg I itself at 2512 and 1621 Å. Corresponding steep b_l rise above 700 km from ultraviolet underionization where the temperature increases in excess of the ultraviolet radiation temperature.

- this pattern is common to all lines of minority neutrals with ultraviolet ionization wavelenghs, including the electron donors (Mg I, Fe I, Si I, Al I).

- source function unusually close to LTE because this is a “forbidden” intersystem line with small $A_{ul} = 2.7\,10^2\,\mathrm{s}^{-1}$, dominated by collisions $(\varepsilon \approx 1)$ with $b_u \approx b_l,\ S^l \approx B$ to large heights.

- yet fairly strong because its lower level is the Mg I ground state

- usefulness: photospheric thermometer but requires ultraviolet NLTE for optical depth

Fe I 6301.5 Å FROM THE ALC7 ATMOSPHERE

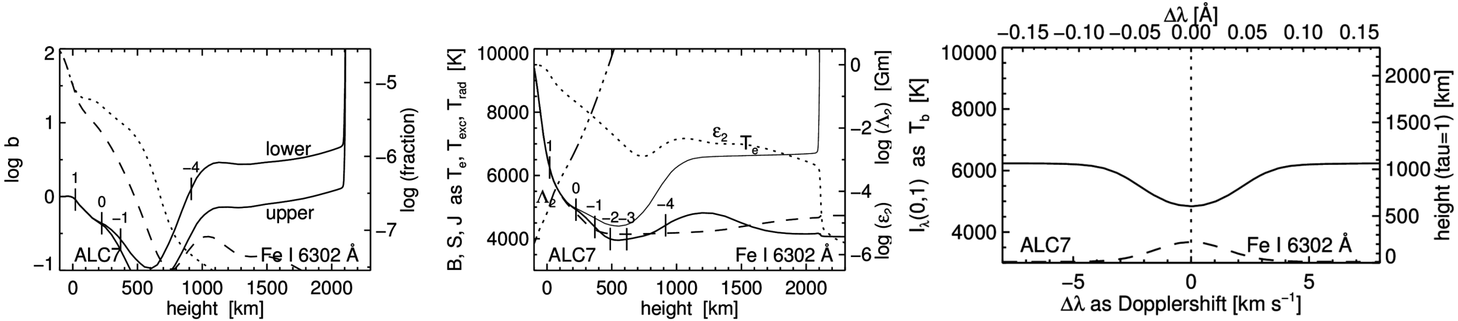

standard polarimetry line

- severe extinction NLTE across the photosphere due to ultraviolet bound-free scattering overionization and affecting the tau scaling (b_l curve)
- minor S^l NLTE from resonance scattering in the upper photosphere ($S < B$ split)
- "inversion" codes (numerical best-fit iteration) sometimes include S^l NLTE but usually not extinction NLTE, ignoring that bound-free scattering with $S^{\rm UV} \approx \overline{J}^{\rm UV}$ depends on 3D temperature gradients in deeper layers and makes b_l (hence n^l and α^l) non-local both in space and wavelength
- problem: the enormous density of NLTE lines ("haze") in the ultraviolet affecting $J^{\rm UV}$
- usefulness: differential line-pair polarimetry with its twin Fe I 6302.5 Å

Mg I b_2 5173 Å FROM THE ALC7 ATMOSPHERE

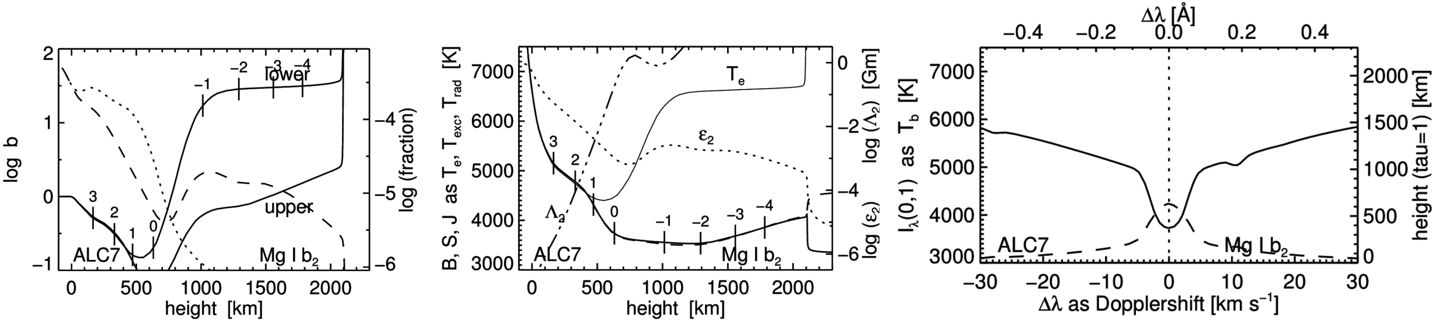

diagnostic of upper photosphere

- large NLTE n_l depletion from ultraviolet bound-free scattering across the photosphere
- large NLTE b_l increase from ultraviolet scattering offsets Saha decline in chromosphere
- CRD scattering source function with $\varepsilon \approx 10^{-3}$
- similar to Na I D_1
- usefulness: as Na I D_1 but wider core = less asymmetry from reversed granulation

Na I D_1 5896 Å FROM THE ALC7 ATMOSPHERE

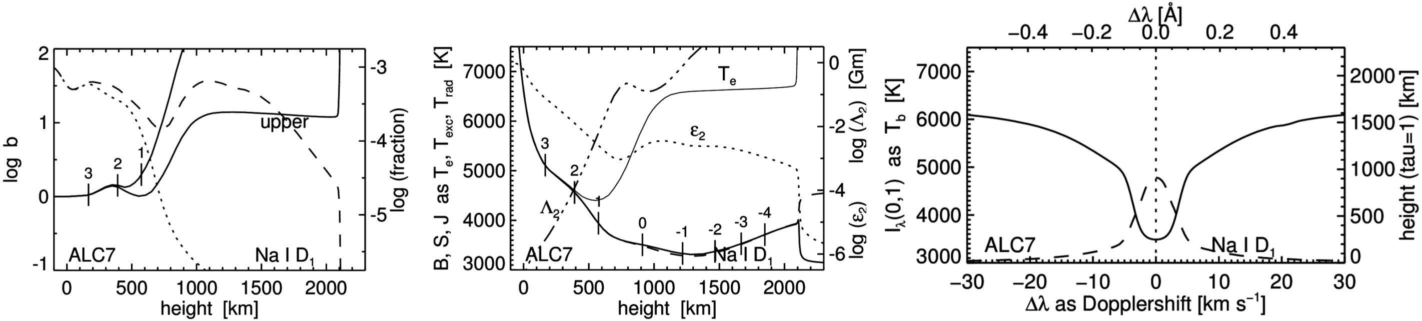

Na I D lines: darkest lines in optical spectrum = textbook example of two-level scattering

- photon suction offsets ultraviolet overionization across the photosphere
- ultraviolet underionization offsets Saha depletion above 700 km
- 2-level CRD scattering with $\varepsilon \approx 10^{-3}$ and $S \approx \overline{J} << B$ in the ALC7 chromosphere
- thermalization in mid photosphere: core intensity does not sense ALC7 chromosphere, observed photons are created near the thermalization depth (height of Λ_2 label), observed intensity variation preferentially encodes temperature variation there
- last scattering near $\tau = 1$: Doppler and Stokes inner-wing encoding occurs around 500 km
- usefulness: sharp Na I D Dopplergrams indicate deeply-located shocks in fluxtubes

Ba II 4554 Å FROM THE ALC7 ATMOSPHERE

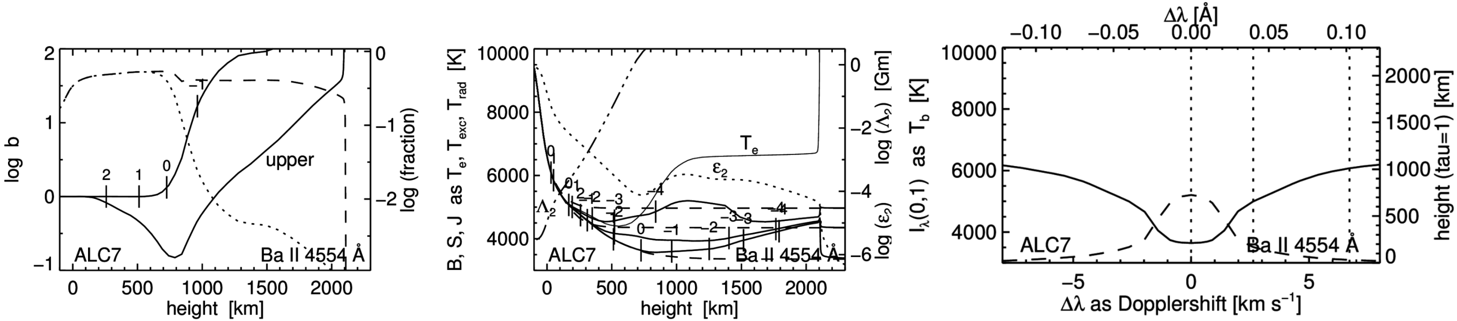

weakest PRD line, best veloctiy diagnostic, good Hanle diagnostic

- extinction LTE up to line-core formation height thanks to photon losses offsetting overionization (edge at 1240 Å outside Lyα)
- steep b_l increase above 800 km from underionization offsets Saha depletion
- resonance line with Grotrian diagram similar to Ca II K. PRD scattering source function with $\varepsilon \approx 10^{-4}$, therefore different monochromatic S_λ and J_λ curves for line center, inner wings, outer wings
- S^l split in upper photosphere produces emission wings at the limb (my 1976 eclipse-expedition PhD thesis)
- usefulness: non-thermal Doppler sensitivity from large mass ($\sqrt{m_{\rm Ba}/m_{\rm H}} = 11.7$)
  intricate near-limb Hanle profile from hyperfine structure

Ca II 8542 Å FROM THE ALC7 ATMOSPHERE

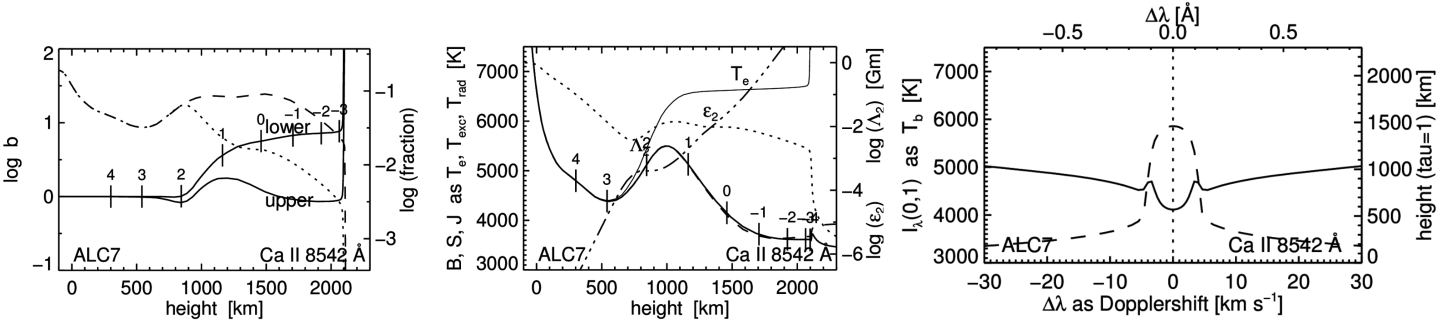

cleanest chromospheric diagnostic in the near infared

- extinction: b_l boost from its own photon losses compensates Saha depletion
- CRD scattering source function with $\varepsilon \approx 10^{-2}$
- core formation spans lower ALC7 chromosphere
- best optical line for chromospheric magnetometry
- usefulness: at longer wavelengths more diffraction but less seeing $\Rightarrow$ prime DKIST line

Ca II K 3934 Å FROM THE ALC7 ATMOSPHERE

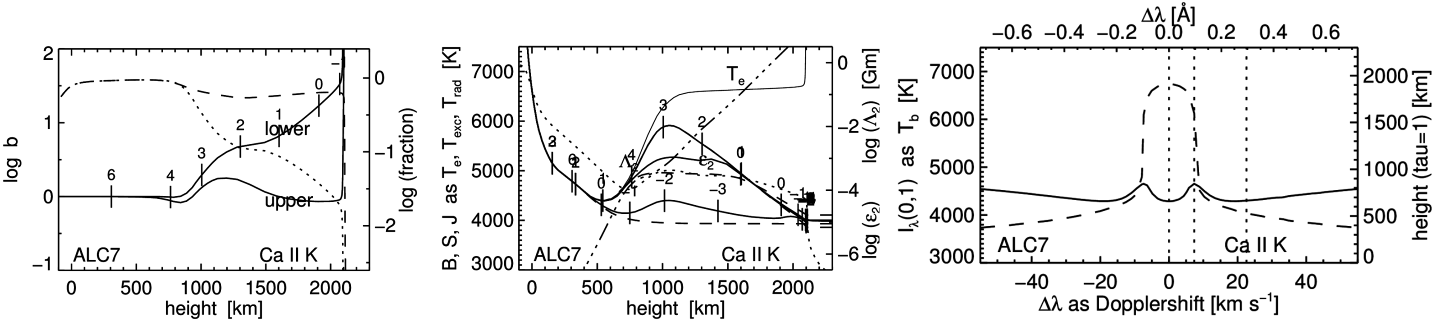

largest extinction in the optical spectrum

- extinction: successive b_l boosts from photon losses in infrared triplet and H&K compensates Saha depletion
- PRD scattering source function with $\varepsilon \approx 10^{-4}$ (split between profile center, peaks, dips)
- core formation spans the ALC7 chromosphere
- narrowness of the Doppler core upsets filter imaging so far
- Sunrise-2/SuFi best so far; high hopes for SST/CHROMIS
- usefulness: best optical chromosphere diagnostic but challenging (bandwidth, S/N)

Mg II k 2796 Å IN THE ALC7 CHROMOSPHERE

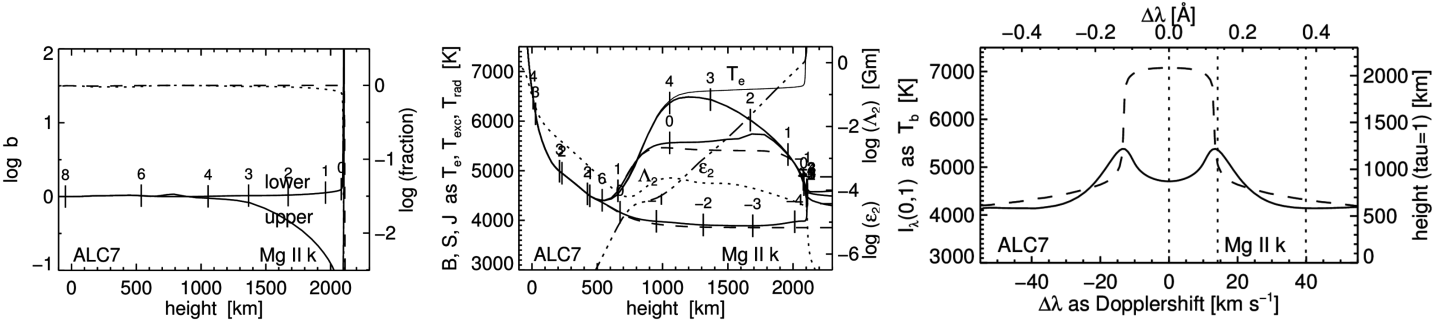

cleanest PRD line and yet larger extincton than Ca II K

- LTE lower-level population and extinction because all Mg sits in the Mg II ground state
- PRD scattering source function with $\varepsilon \approx 10^{-4}$ (split between profile center, peaks, dips)
- textbook scattering decline
- similar to Ca II K but with 18× larger abundance and with much darker wings
- usefulness: key diagnostic but requires space platform
  slitless imaging spectrometry very difficult
  combine with “triplet” doublet between h & k (recombination indicator)

Lyα 1216 Å IN THE ALC7 CHROMOSPHERE

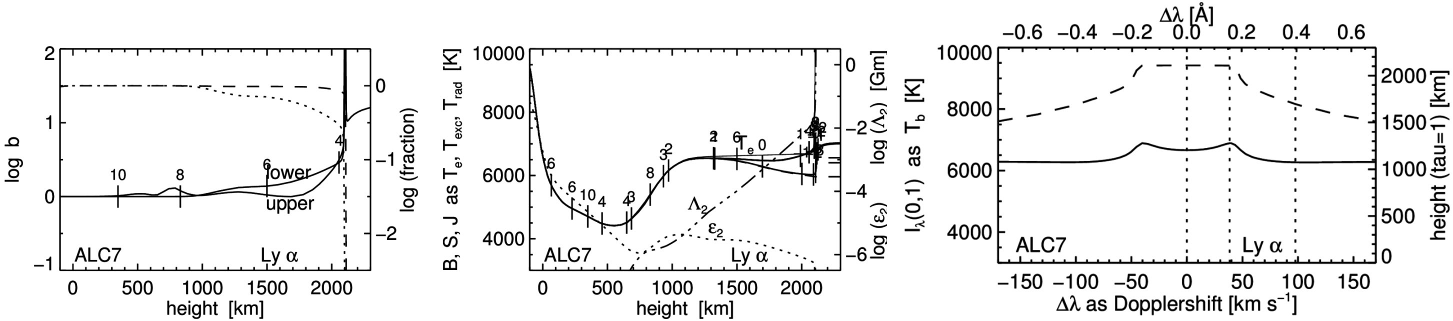

champion: largest extinction and most scattering of all lines

- lower-level population fraction ≈ 1: all hydrogen in ground state
- overpopulation of the ground state towards the transition region from photon losses in wings with slight scattering drops $S \approx J < B$
- enormous line-center extinction across the ALC7 chromosphere
- PRD scattering source function with $\varepsilon \approx 10^{-6}$ (split between profile center, peaks, dips)
- Λ goes from $\propto 1/\varepsilon$ towards $\propto 1/\varepsilon^2$ with density from Stark wing development (not shown)
- radiation lock-in from large extinction produces radiative balance $n_u(A_{ul} + B_{ul}\overline{J}) = n_l B_{lu}\overline{J}$
- local thermalization from small Λ produces $\overline{S} \approx B$ throughout ALC7 chromosphere; $b_u \approx b_l \approx 1$ implies LTE extinction for Hα where it escapes
- usefulness: premier diagnostic but needs space; slitless imaging spectrometry difficult

Hα 6563 Å FROM THE ALC7 ATMOSPHERE

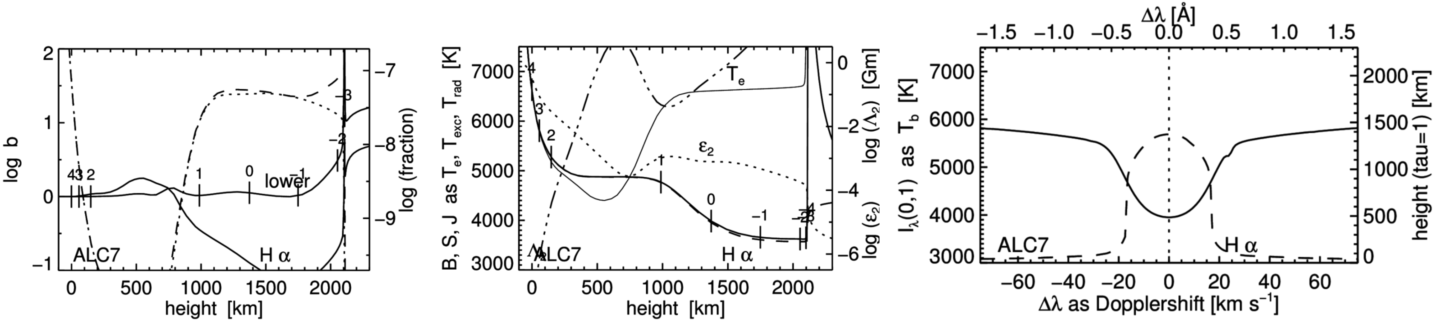

Hα: extraordinary from high excitation energy, huge element abundance, on top of Lyα

- lower-level fractional population varies $10^{-10} - 10^{-7}$ due to 10 eV in Boltzmann
- extinction coefficient near-LTE up to 2000 km by Lyα thermalization
- S^l $\approx$ two-level scattering below transition region (not "photoelectric") just like Ca II 8542 Å
- upper photosphere transparent: core shows fibrils, wings show granules
- Eddington-Barbier tau $=$ 1 in chromosphere, but photon creation in deep photosphere
- large J across T-min from backscattering: ALC7 chromosphere $\approx$ scattering attenuator
- wide line core from small atomic mass in Doppler broadening $\sim \sqrt{2kT/m_{\rm H} + v^2_{\rm micro}}$
- extended wings from linear Stark effect in deep photosphere (Holtsmark distribution)
- usefulness: prominences, flares, Ellermans, dynamic fibrils, spicules-II, . . . = non-E

Hβ 4861 Å FROM THE ALC7 ATMOSPHERE

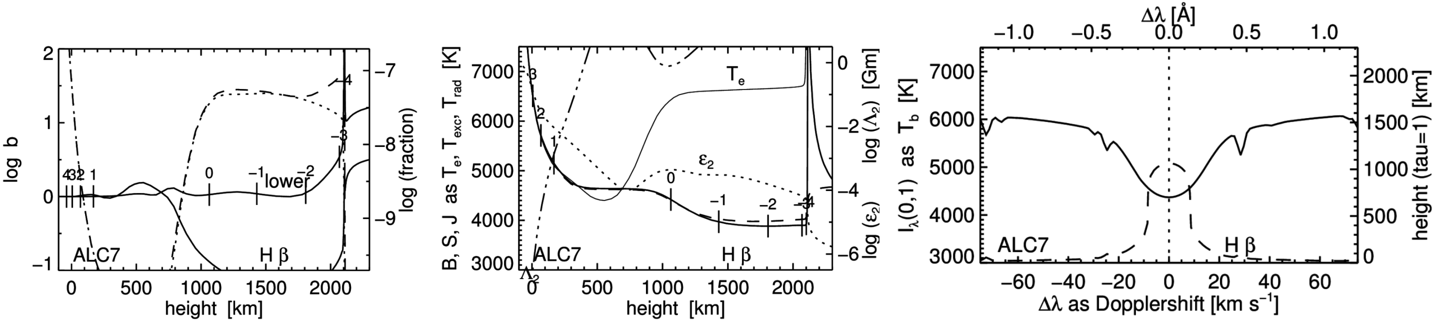

Hβ: analogon to Hα at 5.4$\times$ smaller oscillator strength and in the blue

- same large Boltzmann sensitivity and Lyα lower-level control as Hα
- in comparison with Hα (blink with previous):
  – same b_l, steeper b_u decay
  – similar scattering
  – less steep S^l decay from shorter wavelength
  – smaller chromosphere thickness from smaller gf
  – narrower core and $\tau = 1$ peak
- RH-computed profile has less deep wings then observed atlas profile (not shown) because RH does not use the Holtsmark distribution for linear Stark broadening by charged particles (less steep wing drop than Voigt function)
- usefulness: differences against Hα

He I 584 Å IN THE ALC7 CHROMOSPHERE

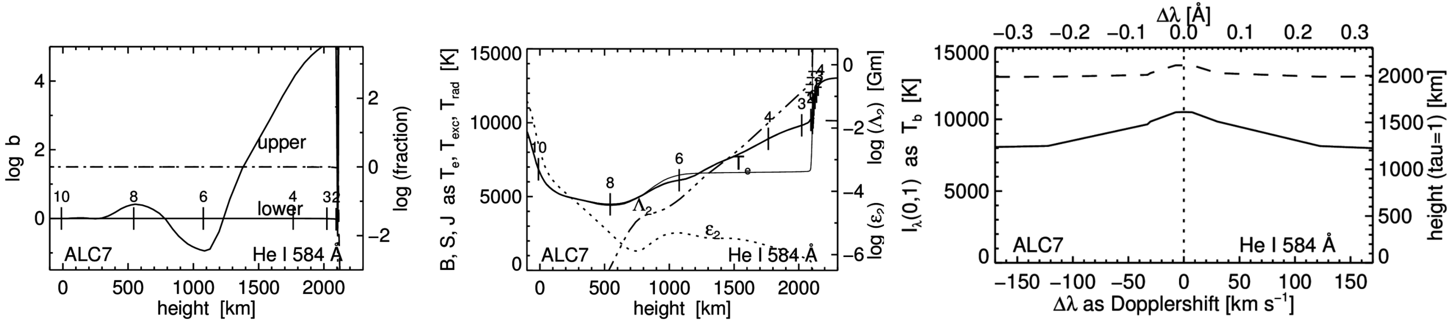

backradiator into chromosphere

- lower-level population fraction ≈ 1: all helium in He I ground state
- $b_1 = 1$ up to coronal rise
- PRD neglected here but not much difference
- detailed radiative balance $S \approx \overline{J}$
- much radiation from coronal rise down into chromosphere due to fairly large Λ, resulting in b_u increase to very large values
- radiation lock-in to $S \approx B$ only below 1000 km

He I 10830 Å IN THE ALC7 CHROMOSPHERE

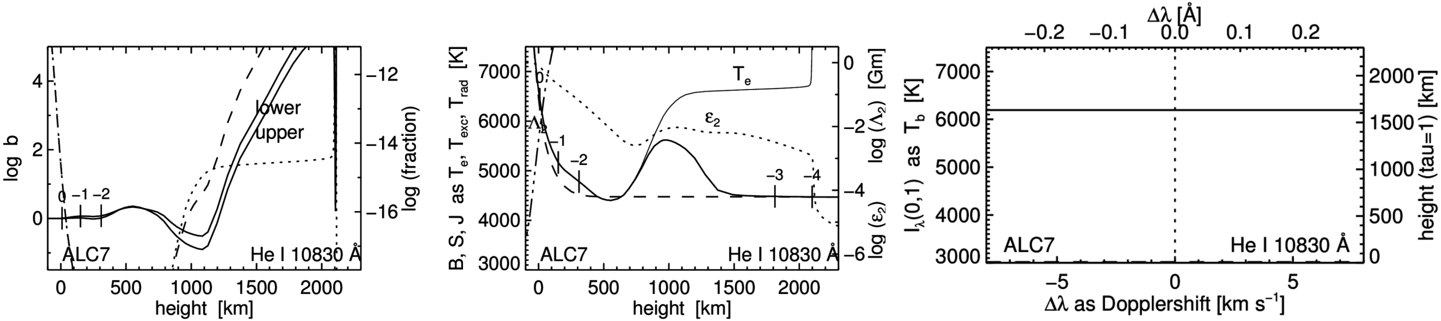

not of interest in ALC7

- high-excitation line supposedly obtaining visibility from coronal irradiation – not in ALC7
- minute fractional population from large Boltzmann factor
- upper-level b_1 set by He I 584 Å plus collisional coupling 2p^{3}P – 2p^{1}P with large He I 584 Å down-radiation from transition region into chromosphere
- total source function $\approx$ LTE H$^-$ source function until Thomson scattering takes over
- nothing in the ALC7 spectrum

CANONICAL CHROMOSPHERIC LINE FORMATION

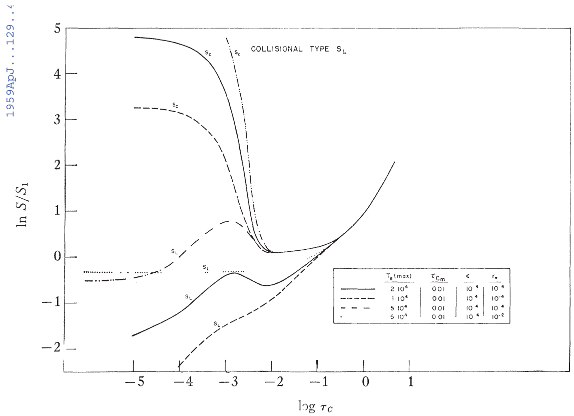

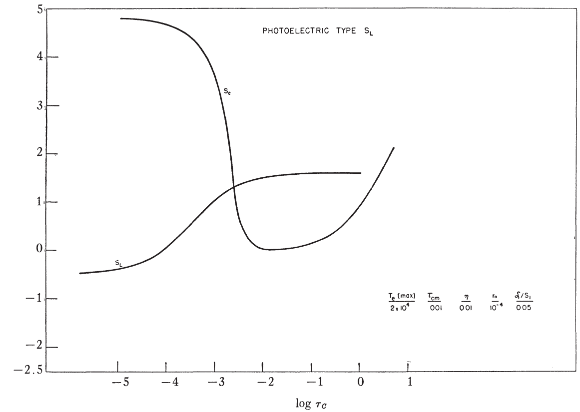

- CRD line source function including detour paths:

$$S^l_{\nu_0} = \frac{\overline{J}_{\nu_0} + \varepsilon'_{\nu_0} B_{\nu_0}(T) + \eta'_{\nu_0} B_{\nu_0}(T_\mathrm{d})}{1 + \varepsilon'_{\nu_0} + \eta'_{\nu_0}}$$
$$= (1 - \varepsilon_{\nu_0} - \eta_{\nu_0})\,\overline{J}_{\nu_0} + \varepsilon_{\nu_0} B_{\nu_0}(T) + \eta_{\nu_0} B_{\nu_0}(T_\mathrm{d})$$

- ε = upper-lower collisional destruction fraction of total extinction
  η = detour-path extinction fraction of total extinction
  ε', η' = idem as ratio to scattering extinction
  $\overline{J}$ = profile-averaged angle-averaged intensity
  T_d = formal detour excitation temperature: $(g_u\, D_{ul})/(g_l\, D_{lu}) \equiv \exp(h\nu_0/kT_\mathrm{d})$

- line source function split (Thomas 1957ApJ...125..260T):
  "collision type" (H & K) or "photoelectric type" (Hα, Balmer continuum feeding)

Hα SOURCE FUNCTION IN THE ALC7 CHROMOSPHERE

after Rutten & Uitenbroek 2012A&A...540A..86R

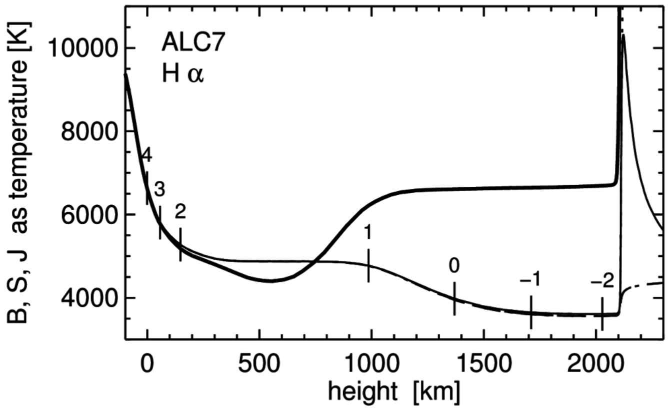

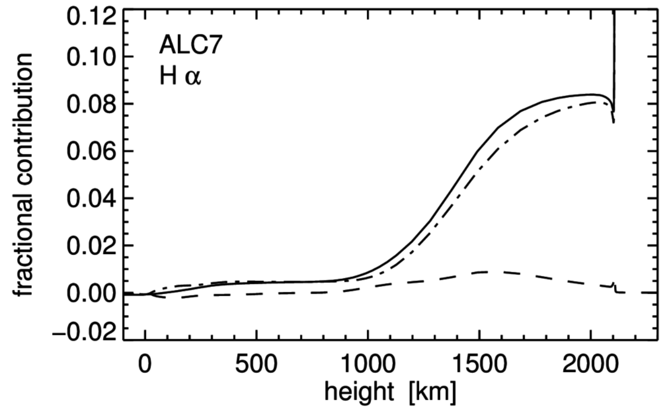

- $S^l_{\nu_0} = (1-\varepsilon_{\nu_0}-\eta_{\nu_0})\,\overline{J}_{\nu_0} + \varepsilon_{\nu_0} B_{\nu_0}(T) + \eta_{\nu_0} B_{\nu_0}(T_\mathrm{d}) = \overline{J}_{\nu_0} + \varepsilon_{\nu_0}[B_{\nu_0}(T) - \overline{J}_{\nu_0}] + \eta_{\nu_0}[B_{\nu_0}(T_\mathrm{d}) - \overline{J}_{\nu_0}]$

  The detour part $\eta_{\nu_0}[B_{\nu_0}(T_\mathrm{d}) - \overline{J}_{\nu_0}]/S^l_{\nu_0}$ exceeds the collision part $\varepsilon_{\nu_0}[B_{\nu_0}(T) - \overline{J}_{\nu_0}]/S^l_{\nu_0}$. However, their sum $[S^l_{\nu_0} - \overline{J}_{\nu_0}]/S^l_{\nu_0}$ (solid) reaches only a few percent so $S^l_{\nu_0} \approx \overline{J}_{\nu_0}$. Across the ALC7 chromosphere Hα is a scattering line, not "photoelectrically controlled".

- The Hα core is dominated by resonance scattering with a formation gap below the chromosphere filled by backscattered radiation. The ALC7 chromosphere acts as scattering attenuator building up its own irradiation. Most emerging photons are created in the deep photosphere where $\varepsilon_{\nu_0} \approx 1$ and $\overline{J}_{\nu_0} \approx B_{\nu_0}(T)$. The granulation pattern has larger contrast than the fibril pattern but is washed out in the scattering across the gap.

- The ALC7 Hα core formation is well described by the Eddington-Barbier approximation for an irradiated finite isothermal scattering atmosphere.

HYDROGEN IN THE ALC7 and FCHHT-B PLANE-PARALLEL STARS

ALC7: *2008ApJS..175..229A* *FCHHT-B:* *2009ApJ...707..482F* *discussion:* *2017IAUS..327....1R*

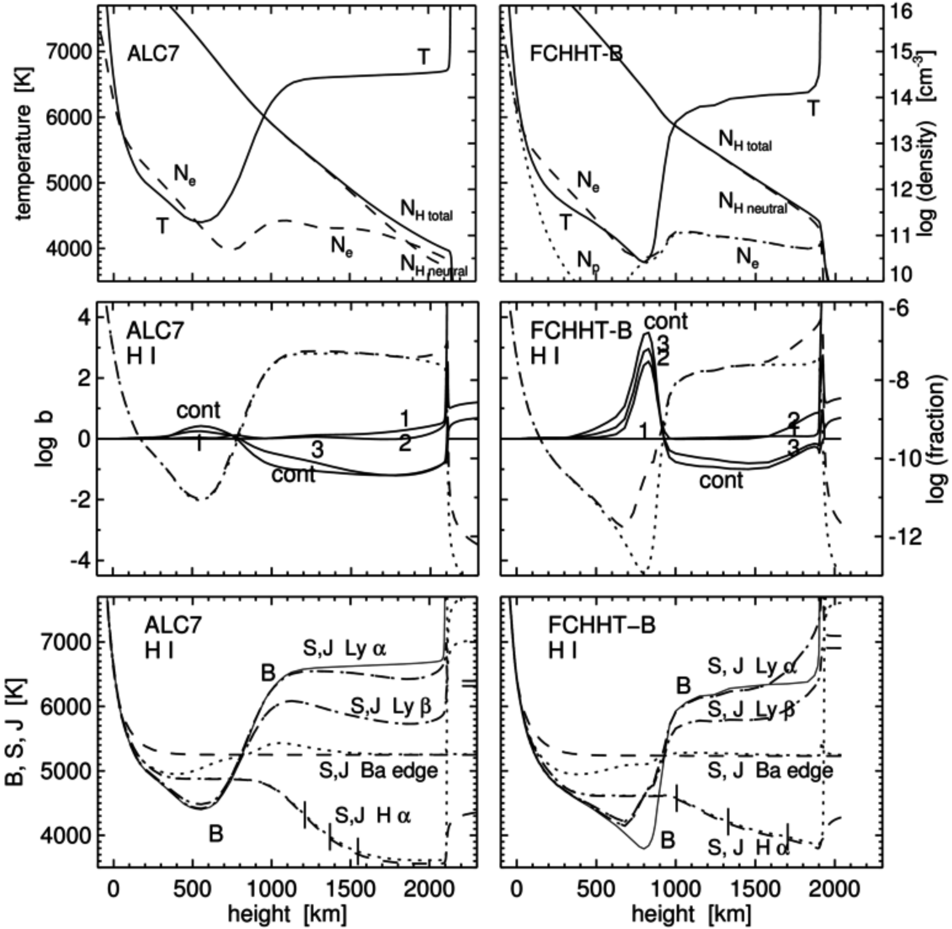

start *index*

Na I D_1 AND Mg I b_2

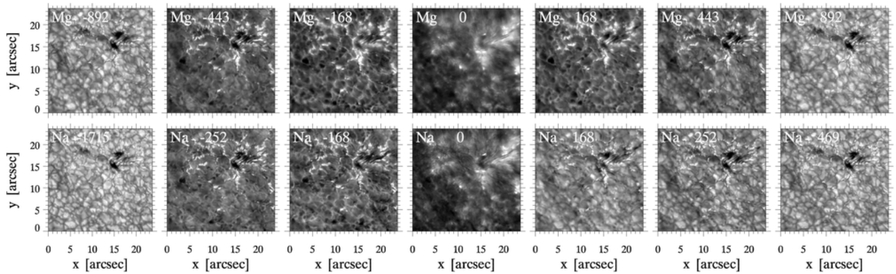

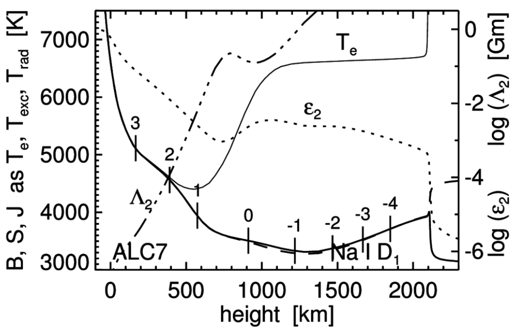

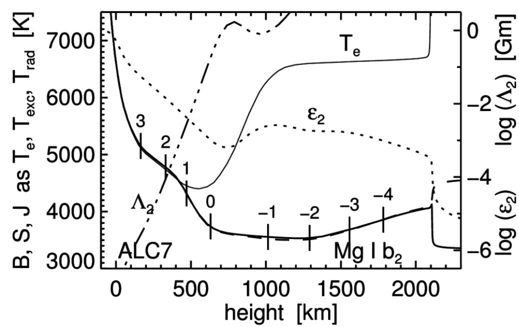

- similar NLTE formation $=$ heavy two-level scattering
- core intensities do not sense ALC7 chromosphere
- narrow Na I D_1 flanks reverse reversed granulation
- minority stages: recombination $\propto N_e$ senses non-E Lyα settling and scattering
- SST: Dopplergrams $\approx$ unsigned fluxtube magnetograms (Na I D_1 formation) non-E enhanced in cooling recombining downflows? (SE $=$ Bifrost snapshot OK)

Lyα and Hα

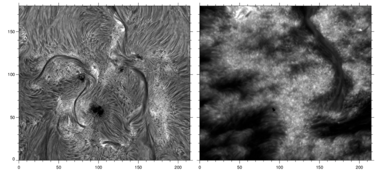

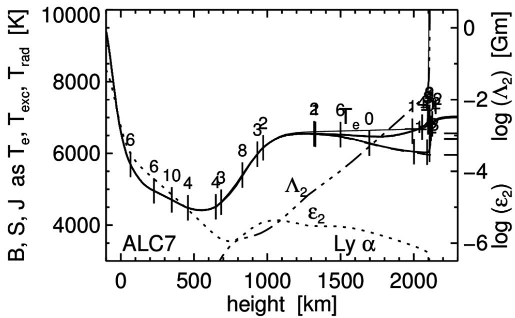

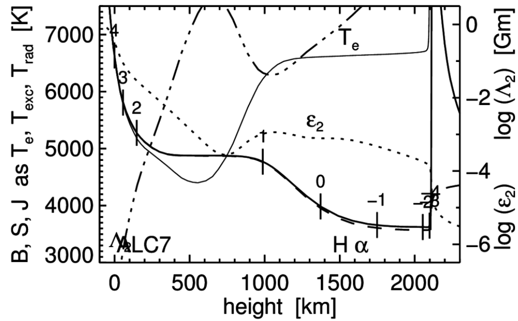

- both: heavy NLTE scatterers with $S \approx J$
- Lyα: boxed-in by enormous extinction $\Rightarrow$ radiative detailed balance: $S = J$
  in shocks ($\approx$ ALC7 chromosphere) collisional thermalization: $b_2 \approx b_1$
  in cool gas surrounding hot structures $b_2 \gg 1$ from Lyα surround scattering
  in post-hot cool gas slow $S \approx J$ thermalization with $b_2 \gg 1$: S^l memory of hot past
- Hα: photons created in granulation
  scatter 3D across upper-photosphere opacity gap and through chromosphere
  in shocks etc. Boltzmann extinction $b_2 \approx b_1$
  in post-hot cool gas $b_2 \gg 1$: extinction memory of hot past
- Lyα scene: heating events bright down-throat, cooling contrails dark from scattering?
  Hα scene: RBE/RRE heating events, cooling contrails dark from non-E opacity?

Hα and Ca II 8542 Å

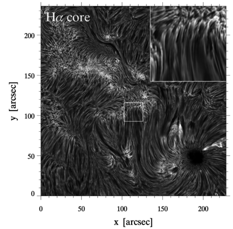

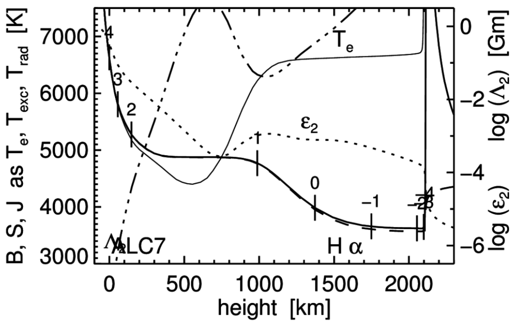

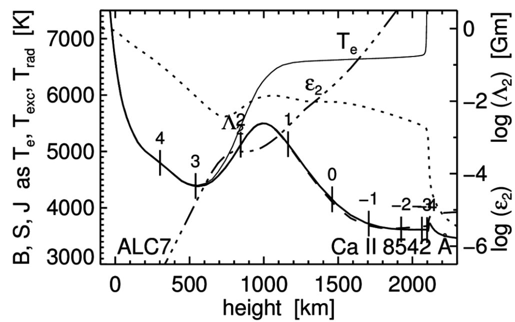

- both: heavy NLTE scatterers with $S \approx J$ sampled at similar $\tau = 1$ heights
- both: Saha-Boltzmann or larger extinction in shocks and ALC7
- core widths: both decrease away from network $=$ decreasing temperature
- Hα fibrils extend further, contradicting Saha-Boltzmann extinction sensitivities
- fibril opacity in Ca II 8542 Å instantenous, in Hα post-hot non-E?

Ca II K and Mg II k

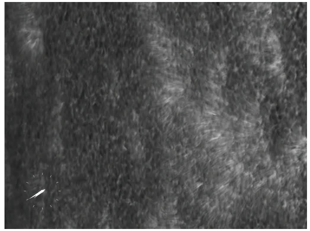

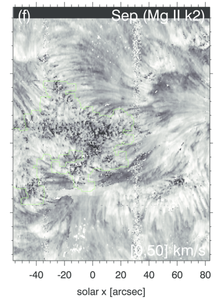

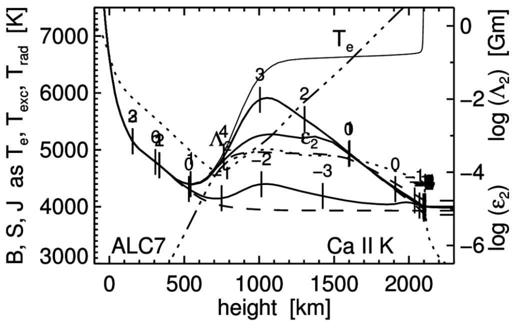

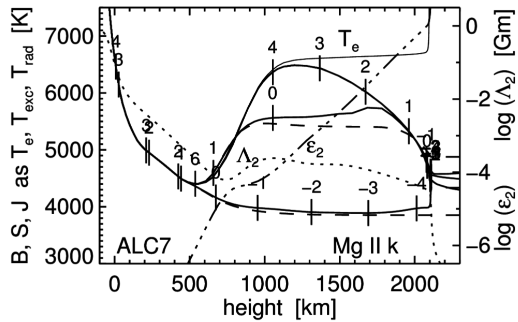

- both: heavy NLTE scatterers with PRD source function splits
- both: near-Saha-Boltzmann extinction everywhere; abundance ratio 18
- both: absence of non-E sensitivities $=$ instantaneous chromosphere
- both: slender fibrils emanating from network, in Ca II H & K better at narrower bandwidth, in Mg II k best in k_2 peak separation
- slender fibrils $=$ propagating heating events?

ALC7 ATMOSPHERE VERSUS FALC ATMOSPHERE

Avrett & Loeser *2008ApJS..175..229A* *Fontenla, Avrett & Loeser* *1993ApJ...406..319F*

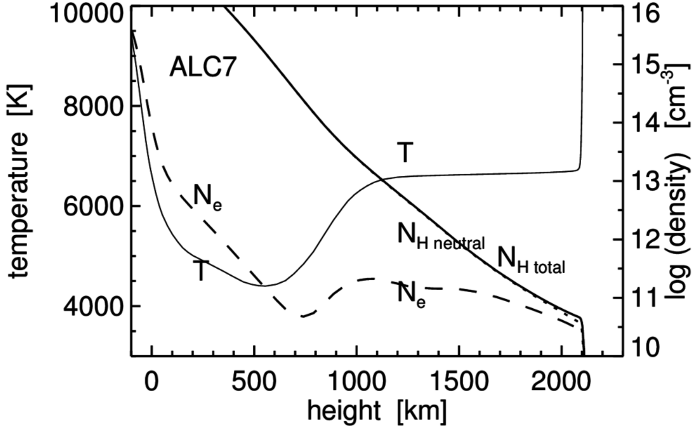

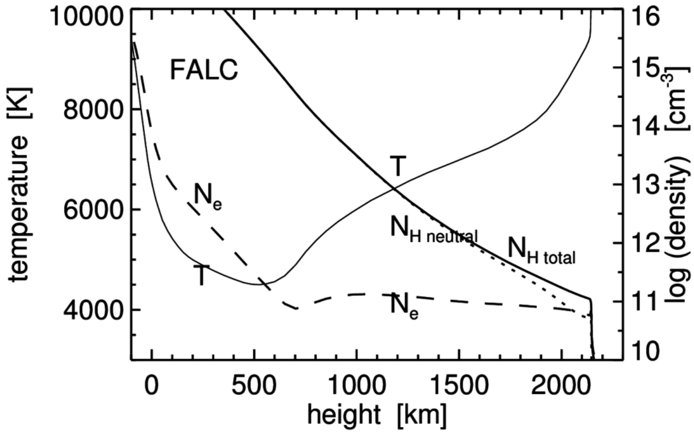

Mg I 4571 Fe I 6302 Mg I b_2 Na I D_1 Ba II 4554 Ca II 8542 Ca II K Mg II k Lyα Hα Hβ He I 584

start *index*

Mg I 4571 Å IN ALC7 AND FALC

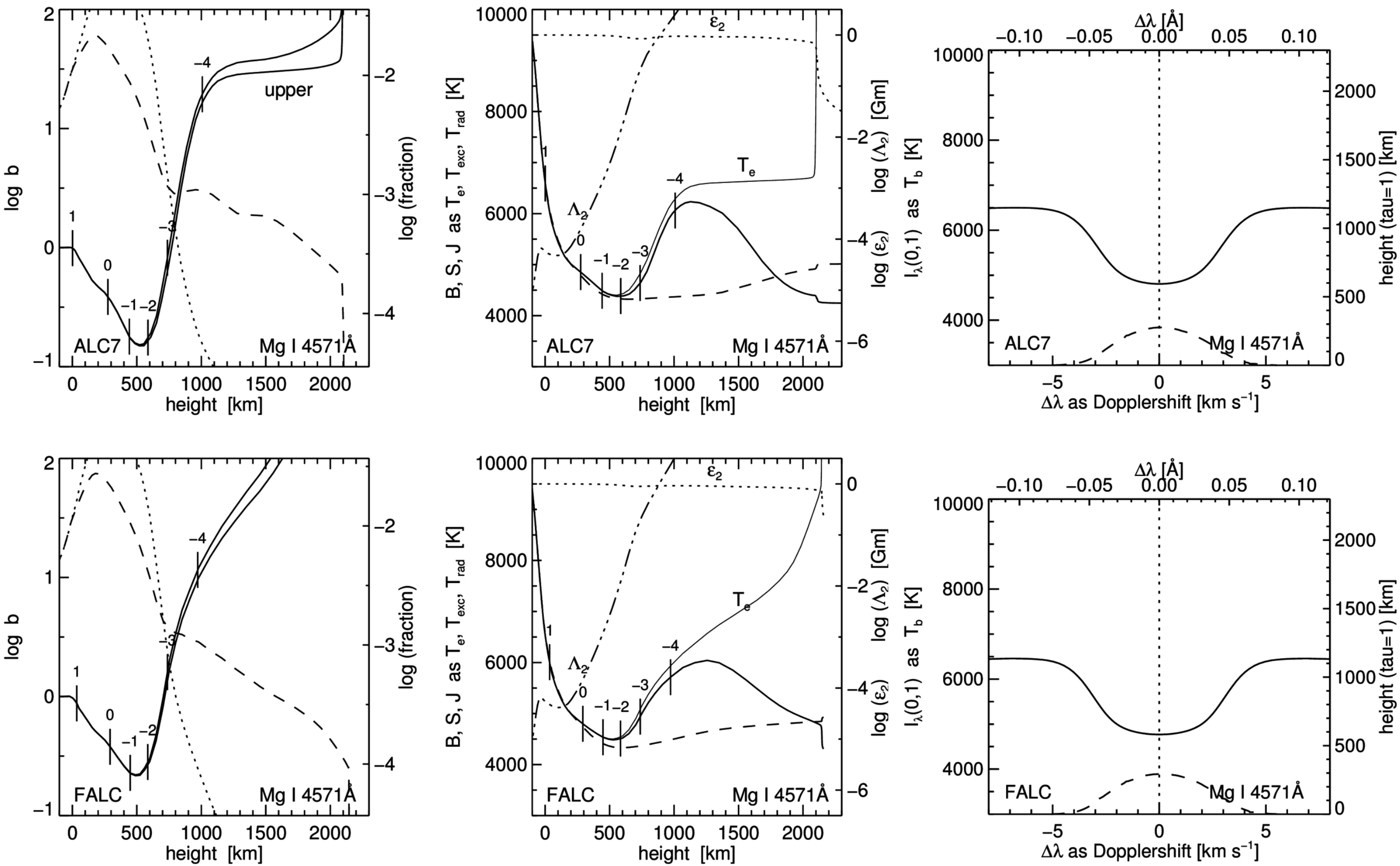

unique photospheric line with LTE source function

start
index

Fe I 6301.5 Å IN ALC7 AND FALC

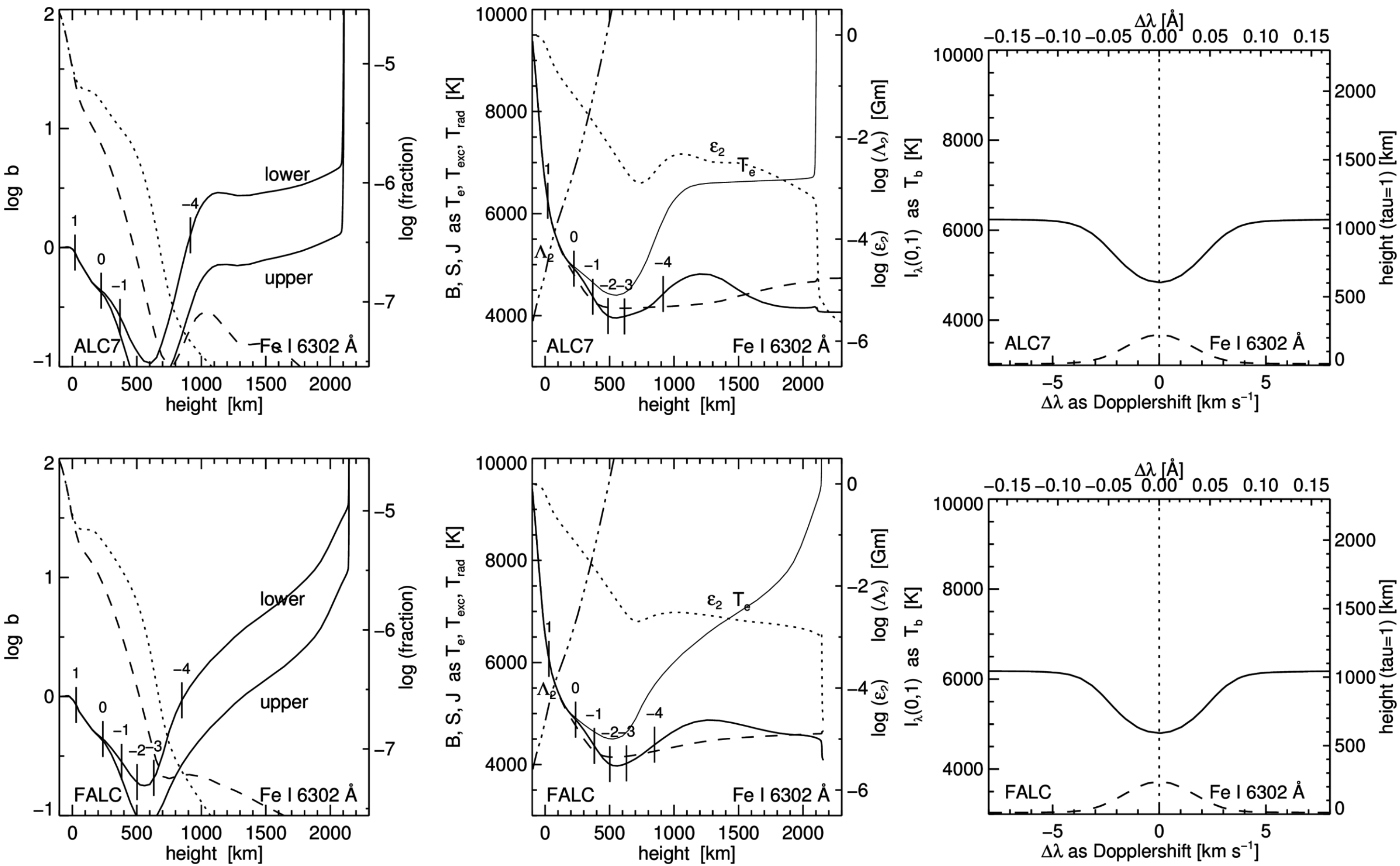

standard polarimetry line

start

index

Mg I b_2 5173 Å IN ALC7 AND FALC

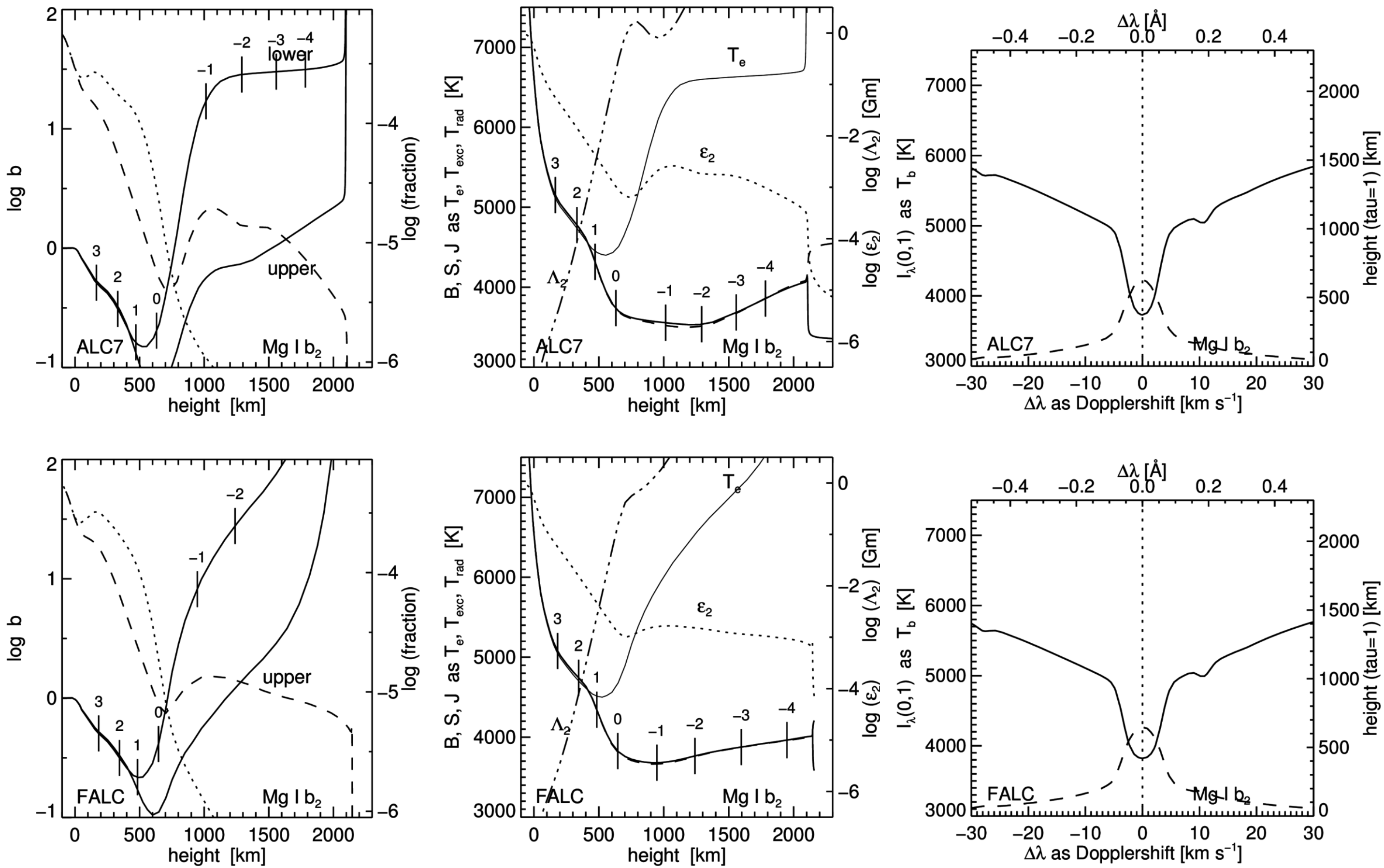

diagnostic of upper photosphere

Na I D_1 5896 Å IN ALC7 AND FALC

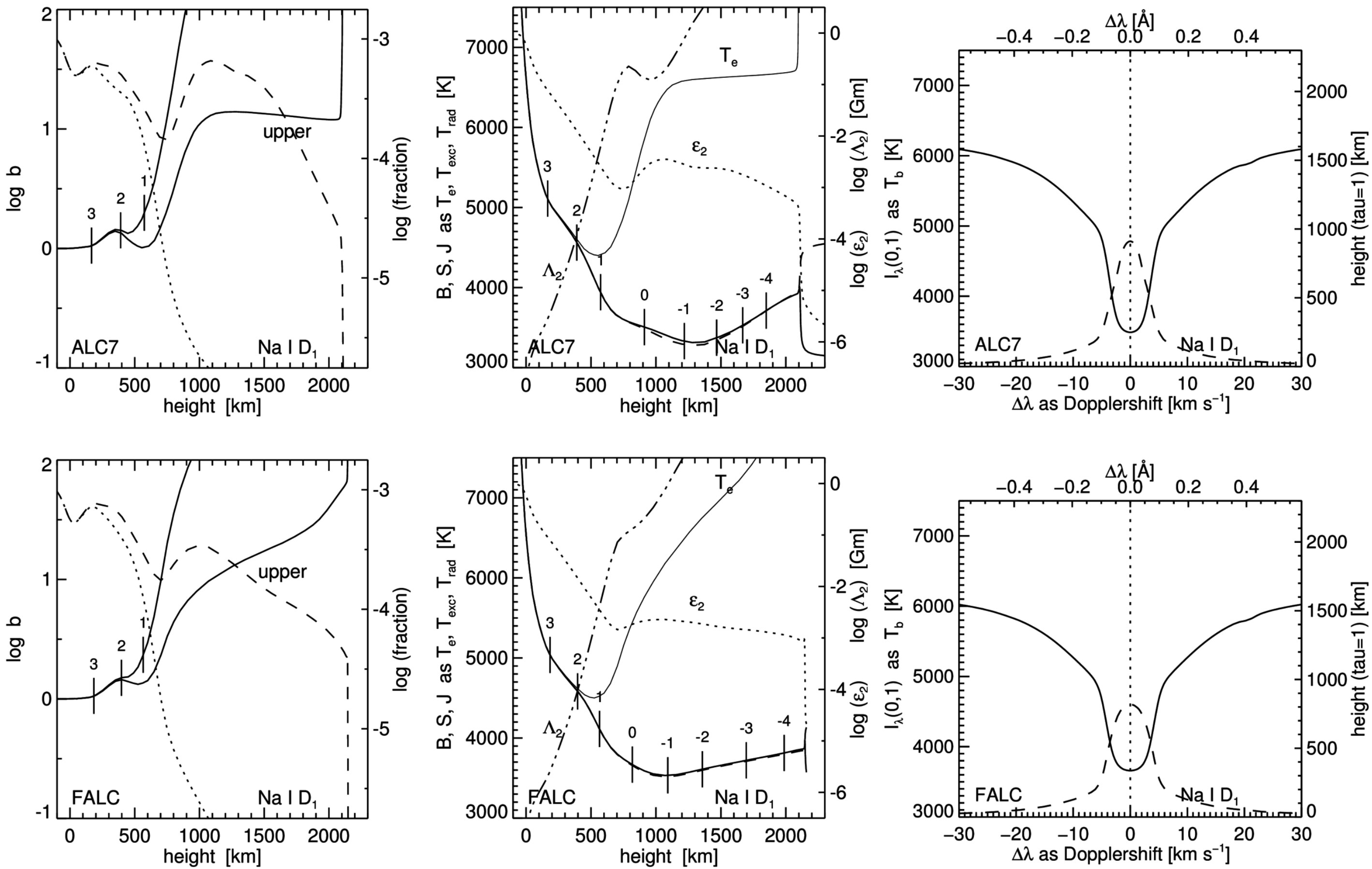

Na I D_1: darkest solar line in optical spectrum = textbook example of two-level scattering

start
index

Ba II 4554 Å IN ALC7 AND FALC

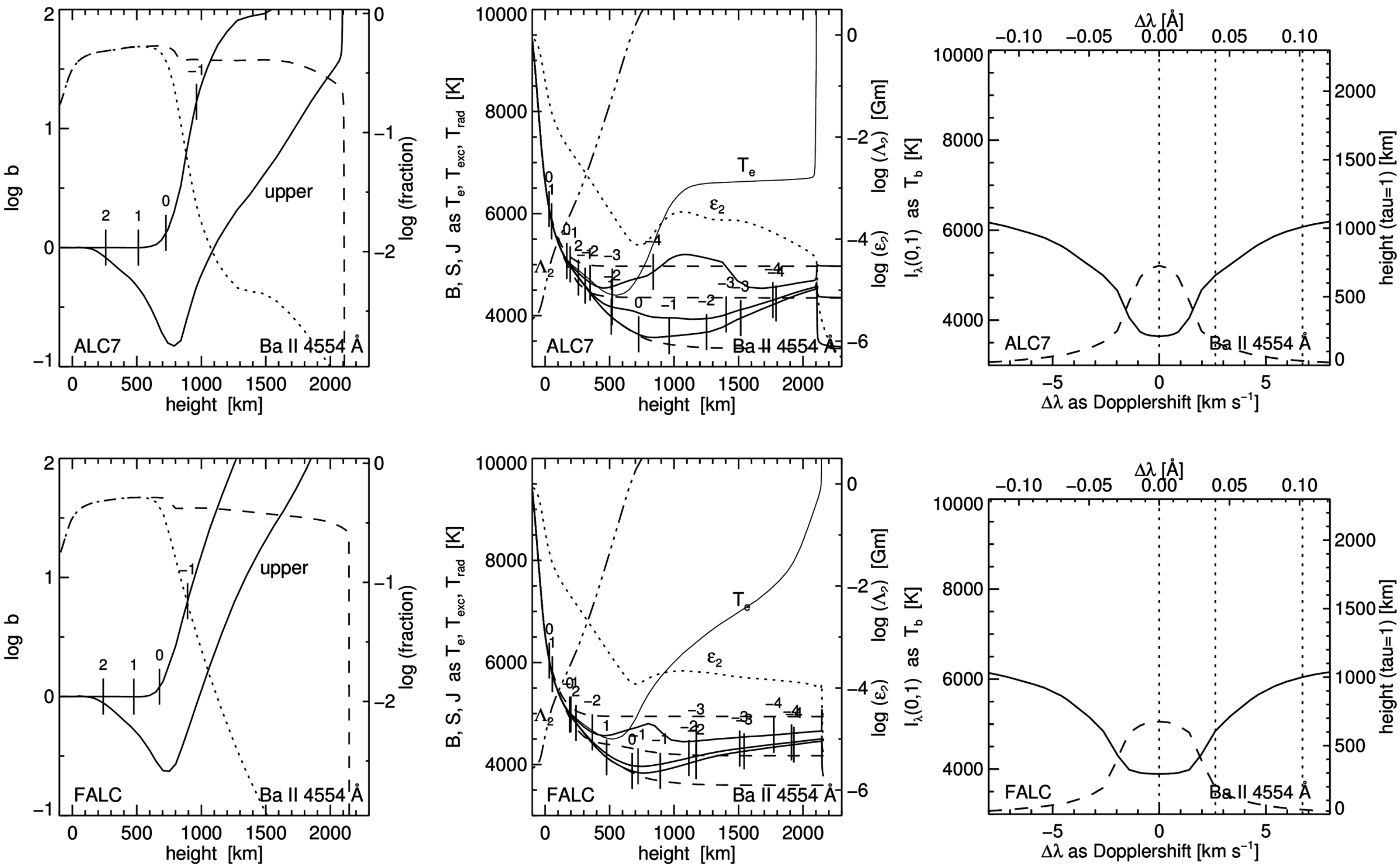

weakest PRD line, best veloctiy diagnostic, good Hanle diagnostic

Ca II 8542 Å IN ALC7 AND FALC

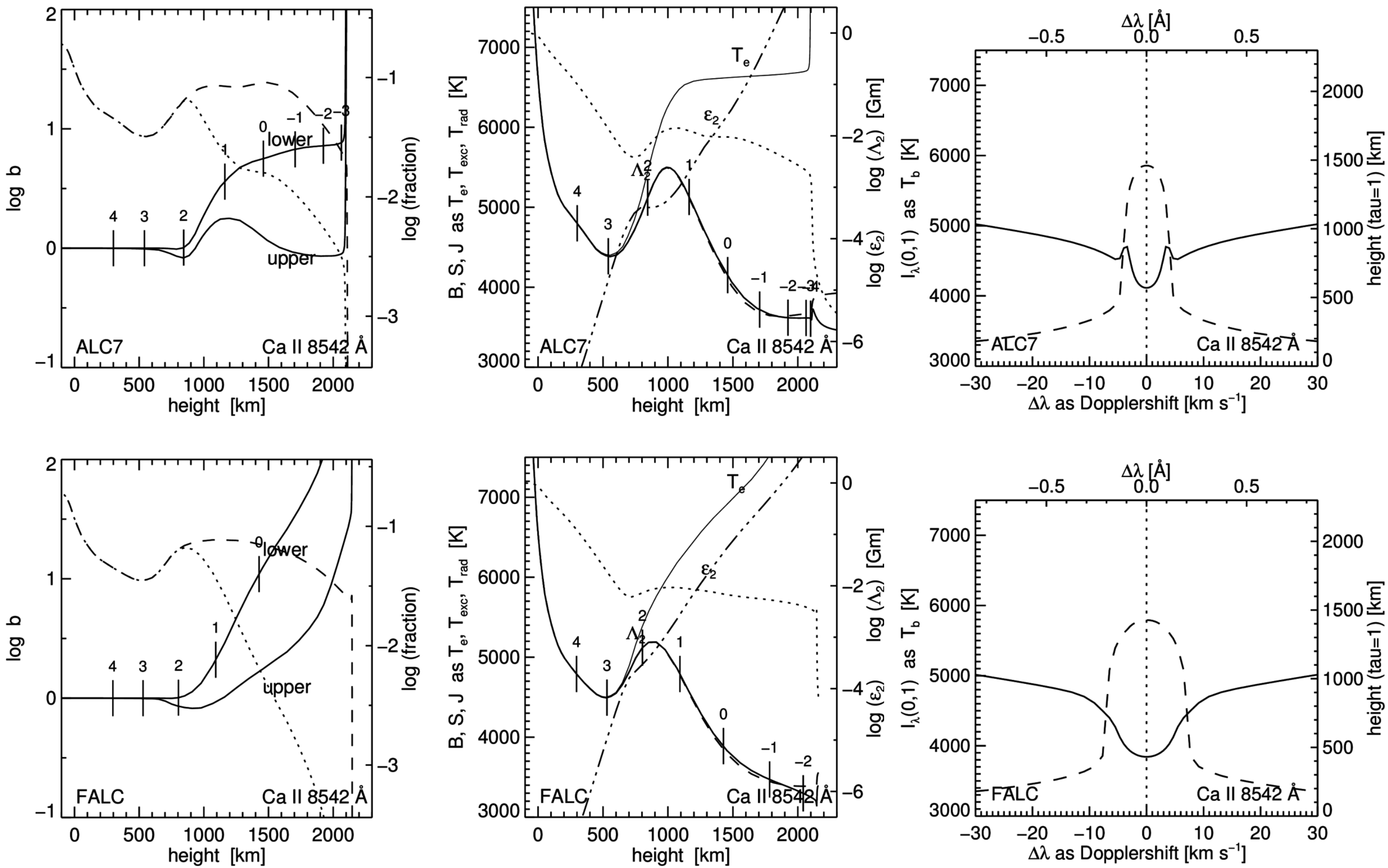

cleanest chromospheric diagnostic in the near infared

start

index

Ca II K 3934 Å IN ALC7 AND FALC

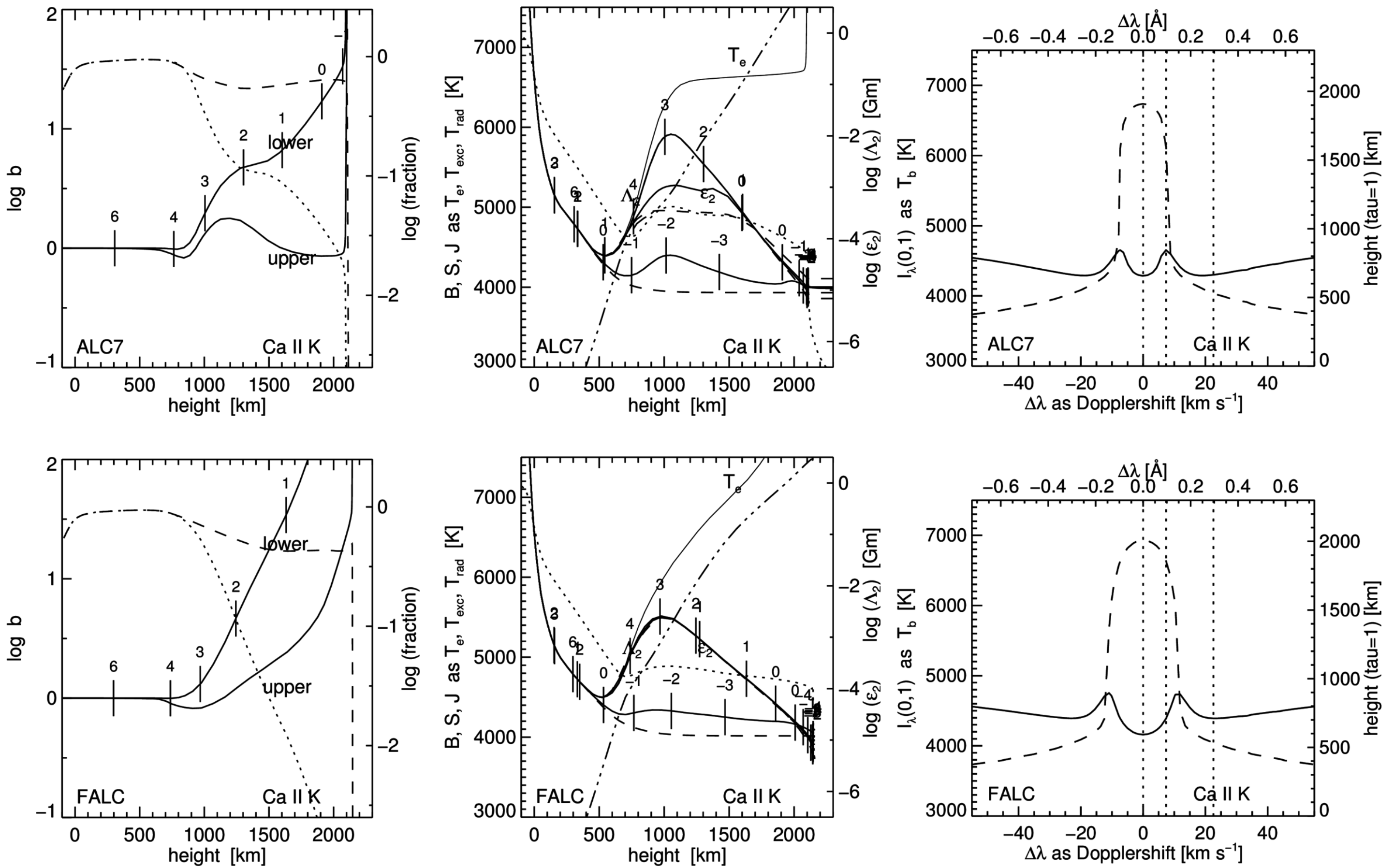

largest extinction in the optical spectrum

Mg II k 2796 Å IN ALC7 AND FALC

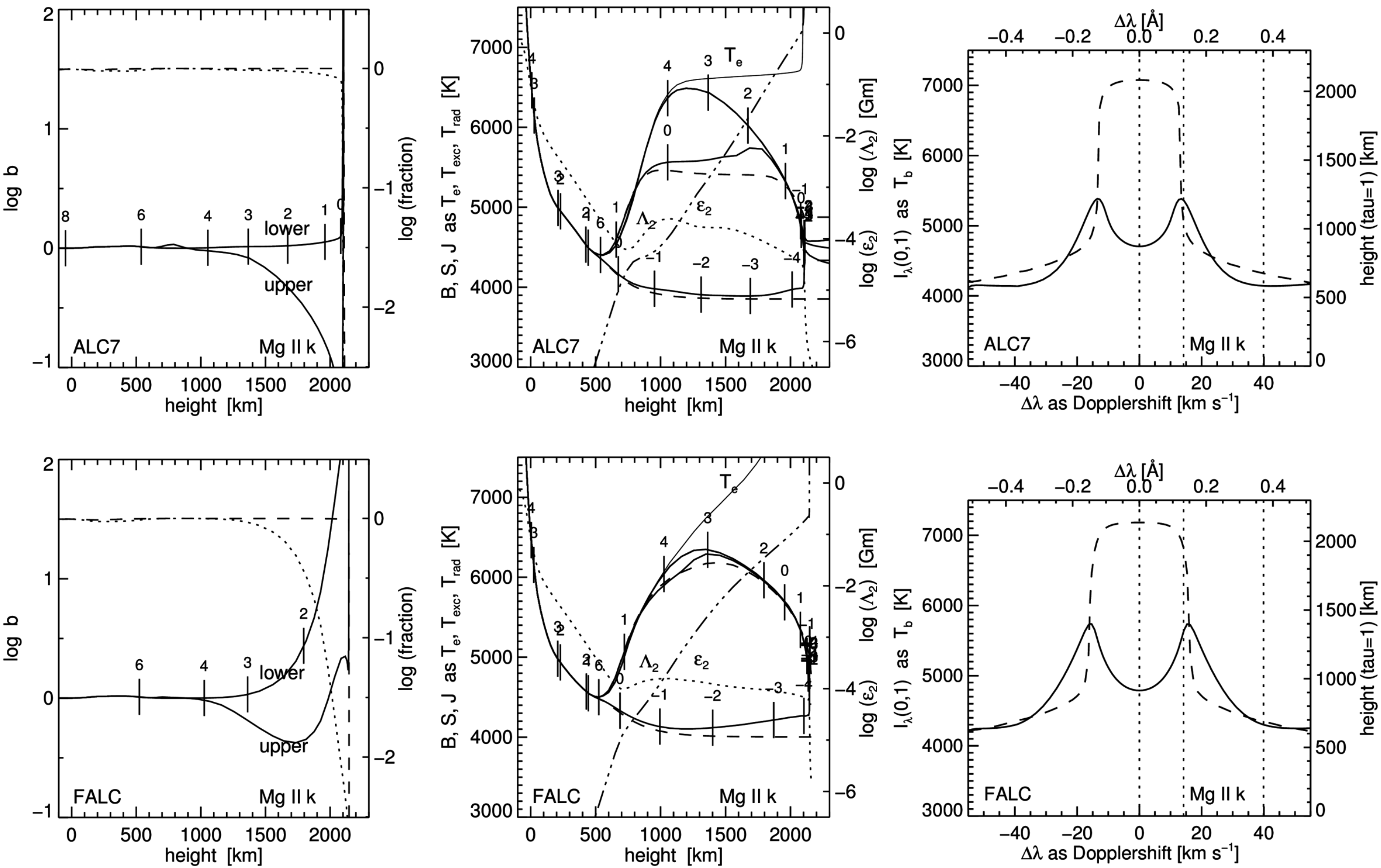

cleanest PRD line and yet larger extincton than Ca II K

Lyα 1216 Å IN ALC7 AND FALC

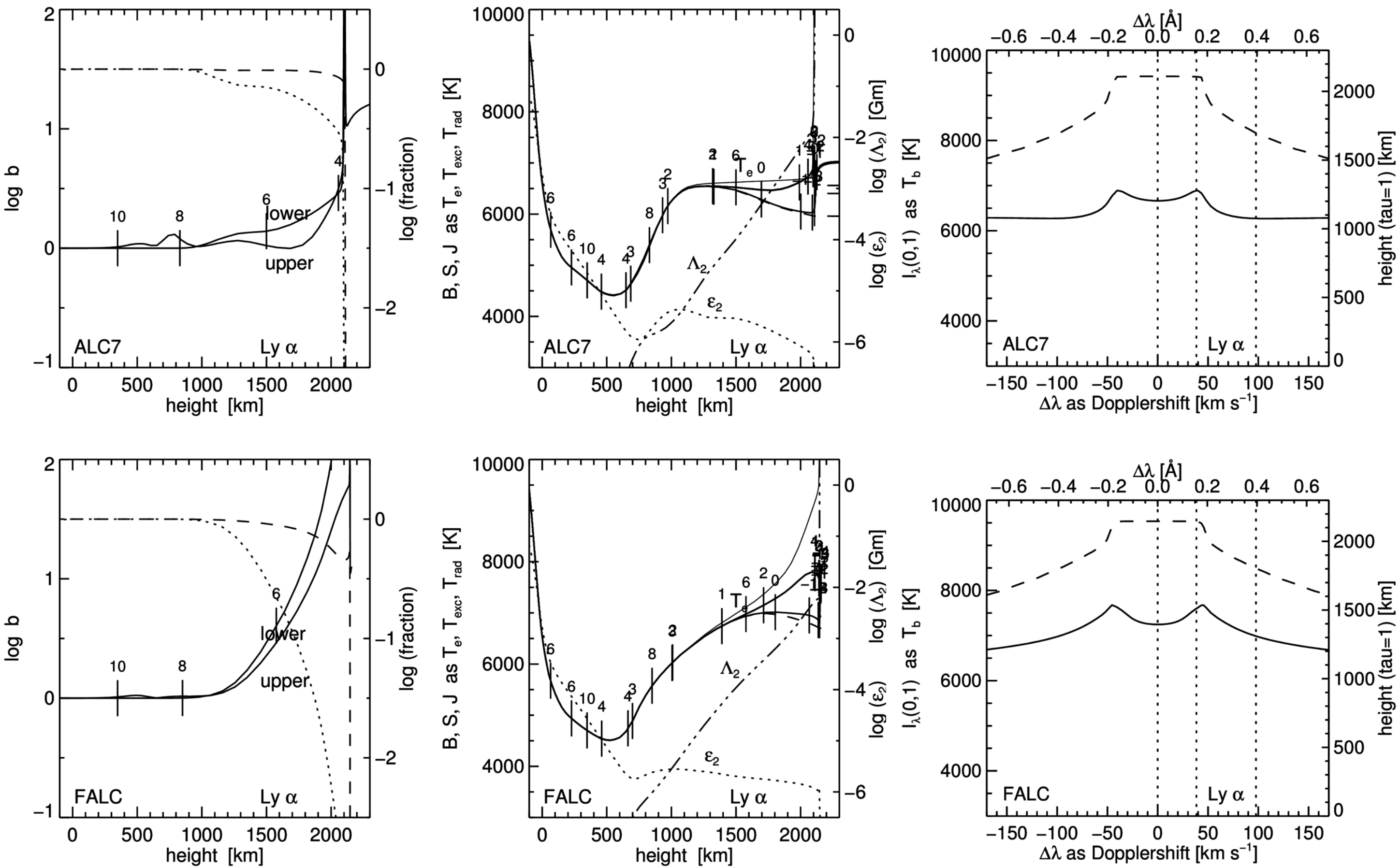

champion: largest extinction and most scattering of all lines

Hα 6563 Å IN ALC7 AND FALC

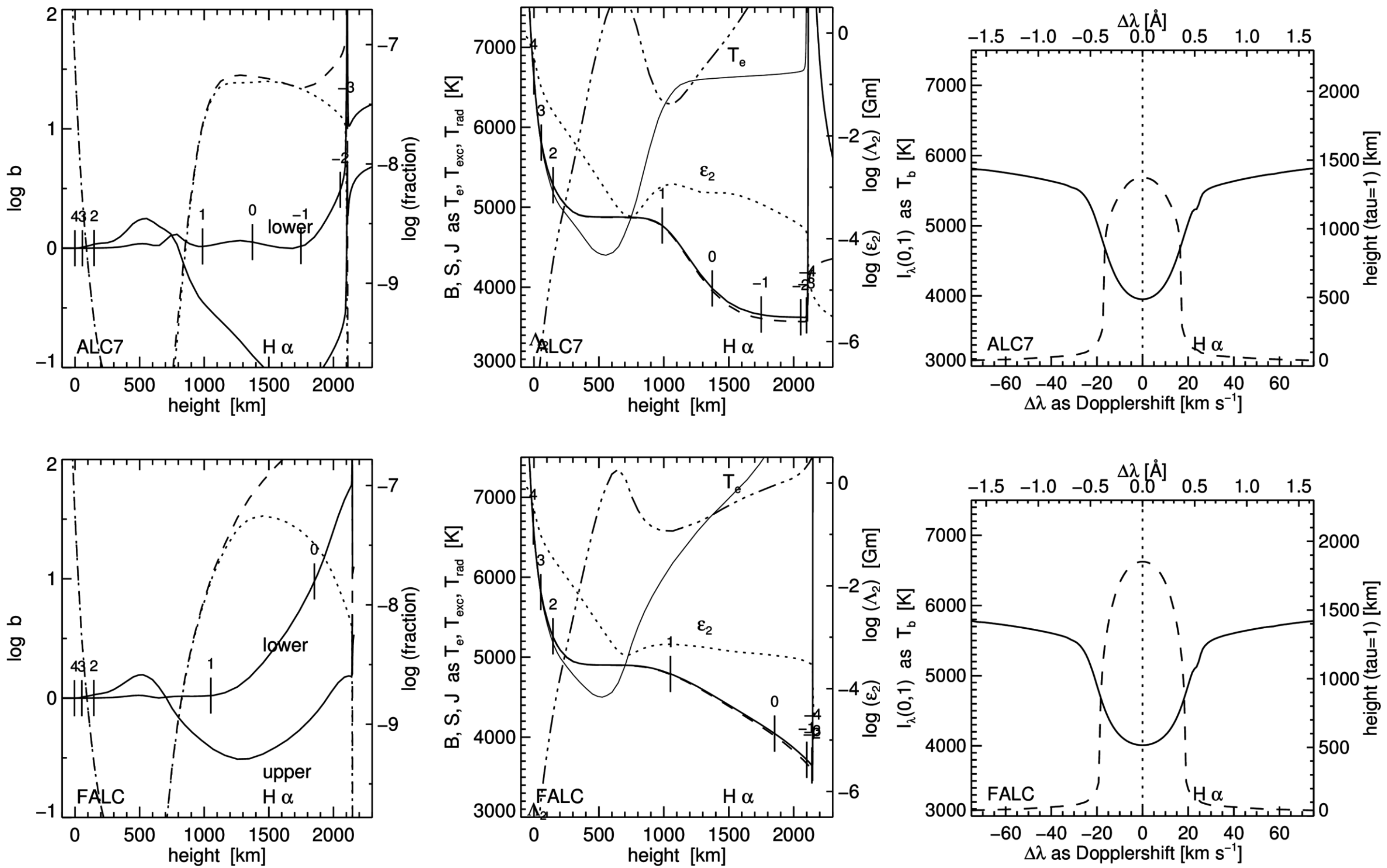

Hα: extraordinary from high excitation energy, huge element abundance, on top of Lyα

Hβ 4861 Å IN ALC7 AND FALC

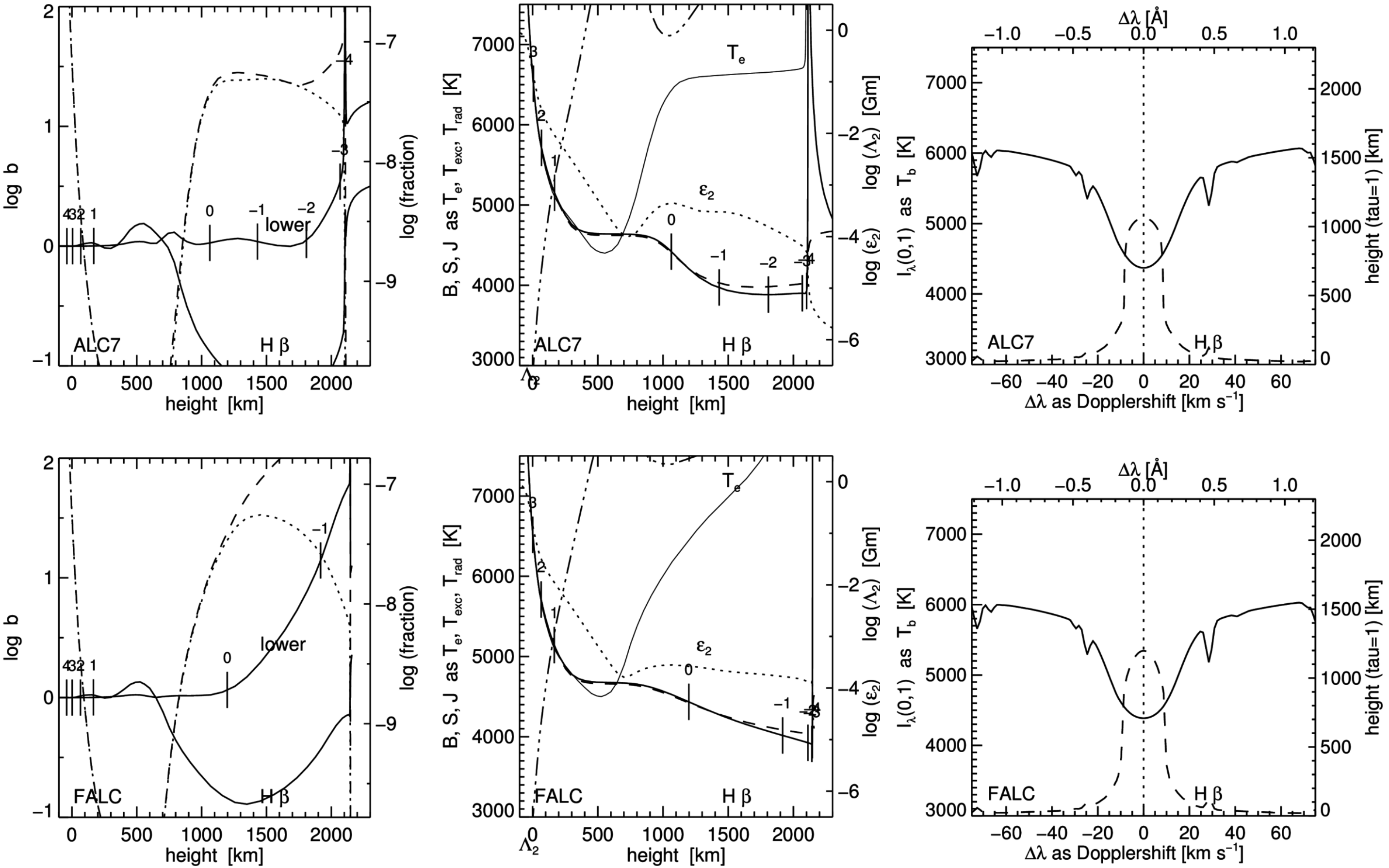

Hβ: analogon to Hα at 5.4$\times$ smaller oscillator strength and in the blue

start
index

He I 584 Å IN ALC7 AND FALC

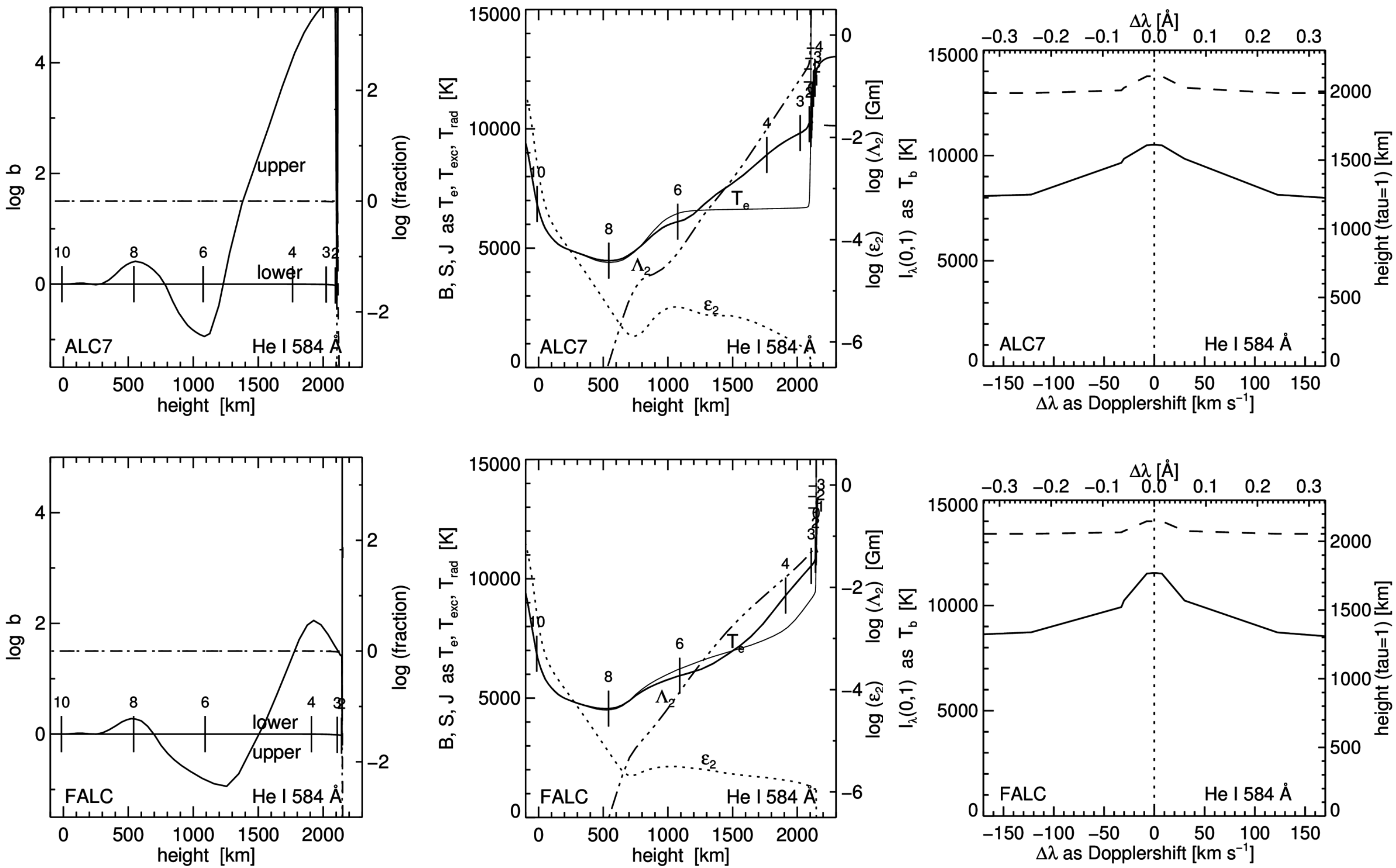

backradiator into chromosphere

FALC ATMOSPHERE VERSUS FALP ATMOSPHERE

Fontenla, Avrett & Loeser *1993ApJ...406..319F*

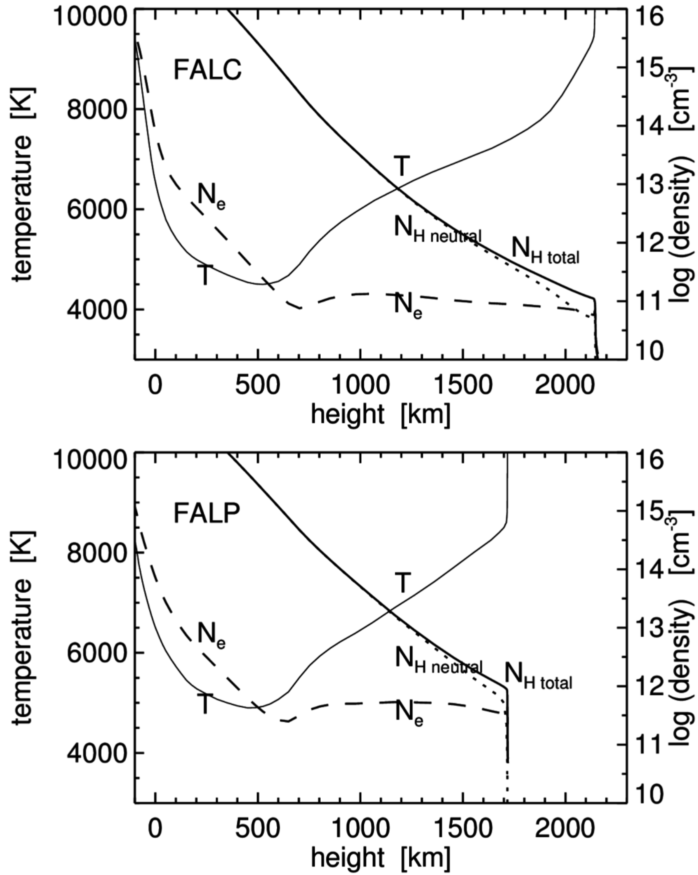

Mg I 4571 Fe I 6302 Mg I b$_2$ Na I D$_1$ Ba II 4554 Ca II 8542 Ca II K Mg II k Lyα Hα Hβ He I 584

start *index*

Mg I 4571 Å IN FALC AND FALP

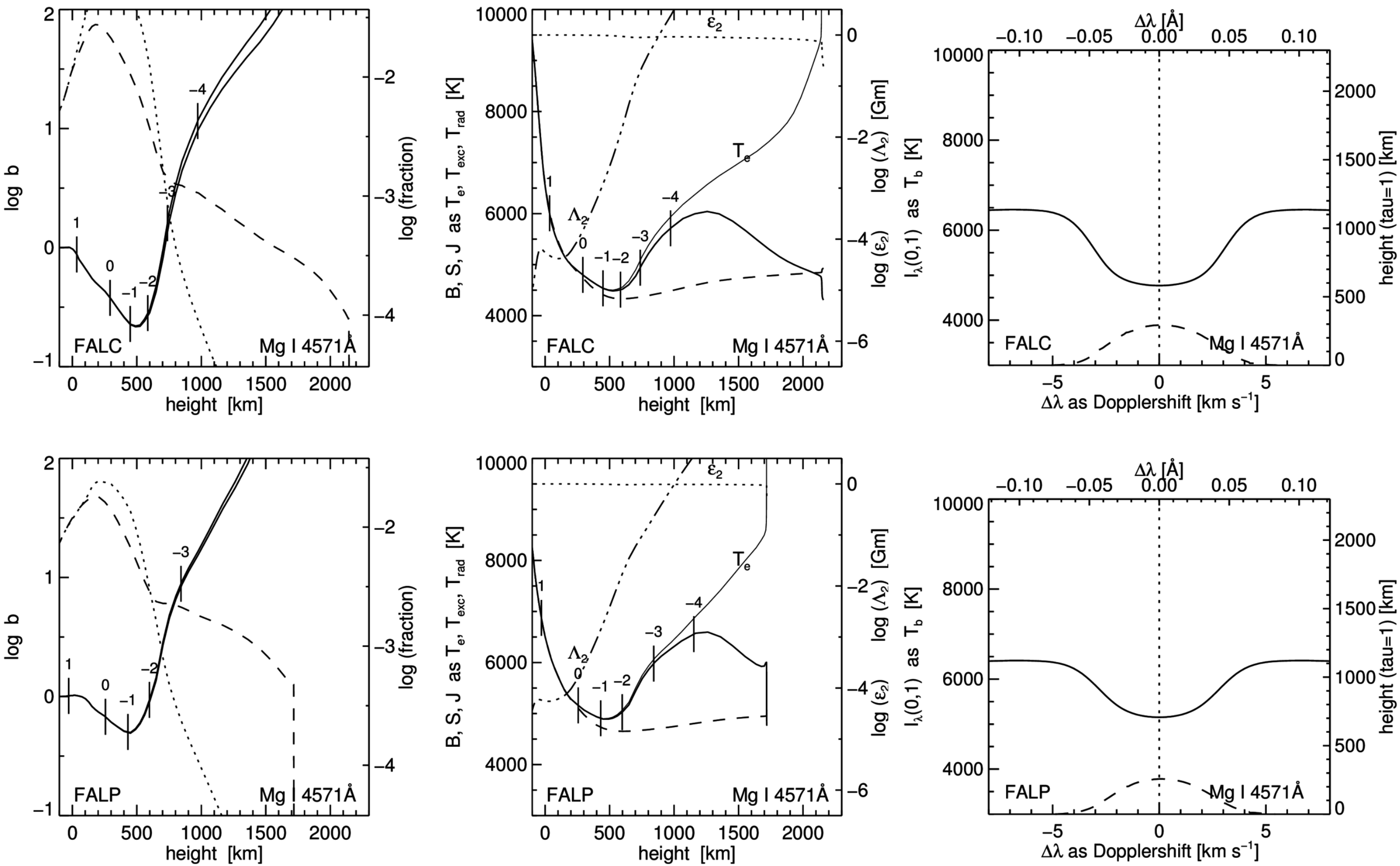

unique photospheric line with LTE source function

start

index

Fe I 6301.5 Å IN FALC AND FALP

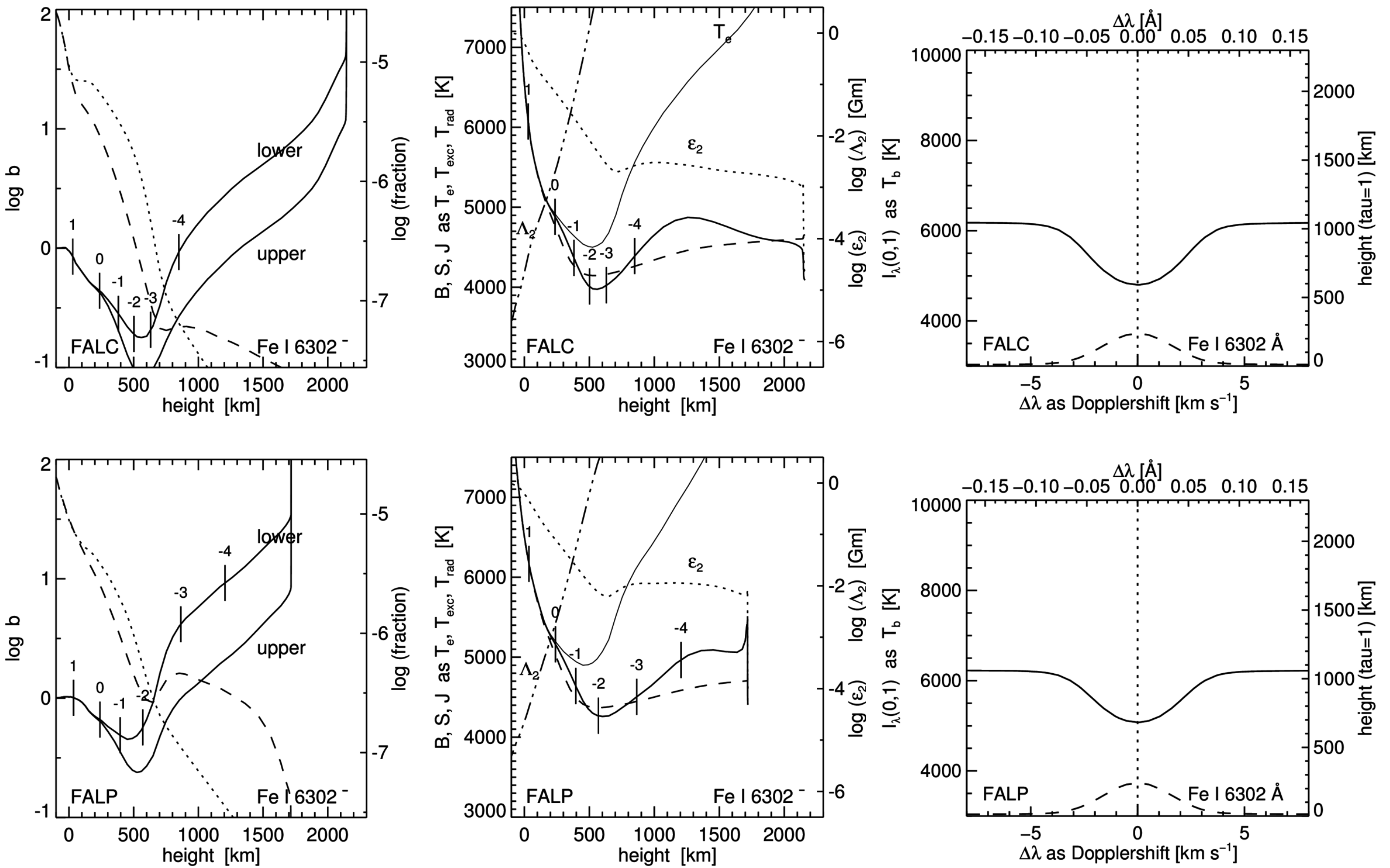

standard polarimetry line

start

index

Mg I b_2 5173 Å IN FALC AND FALP

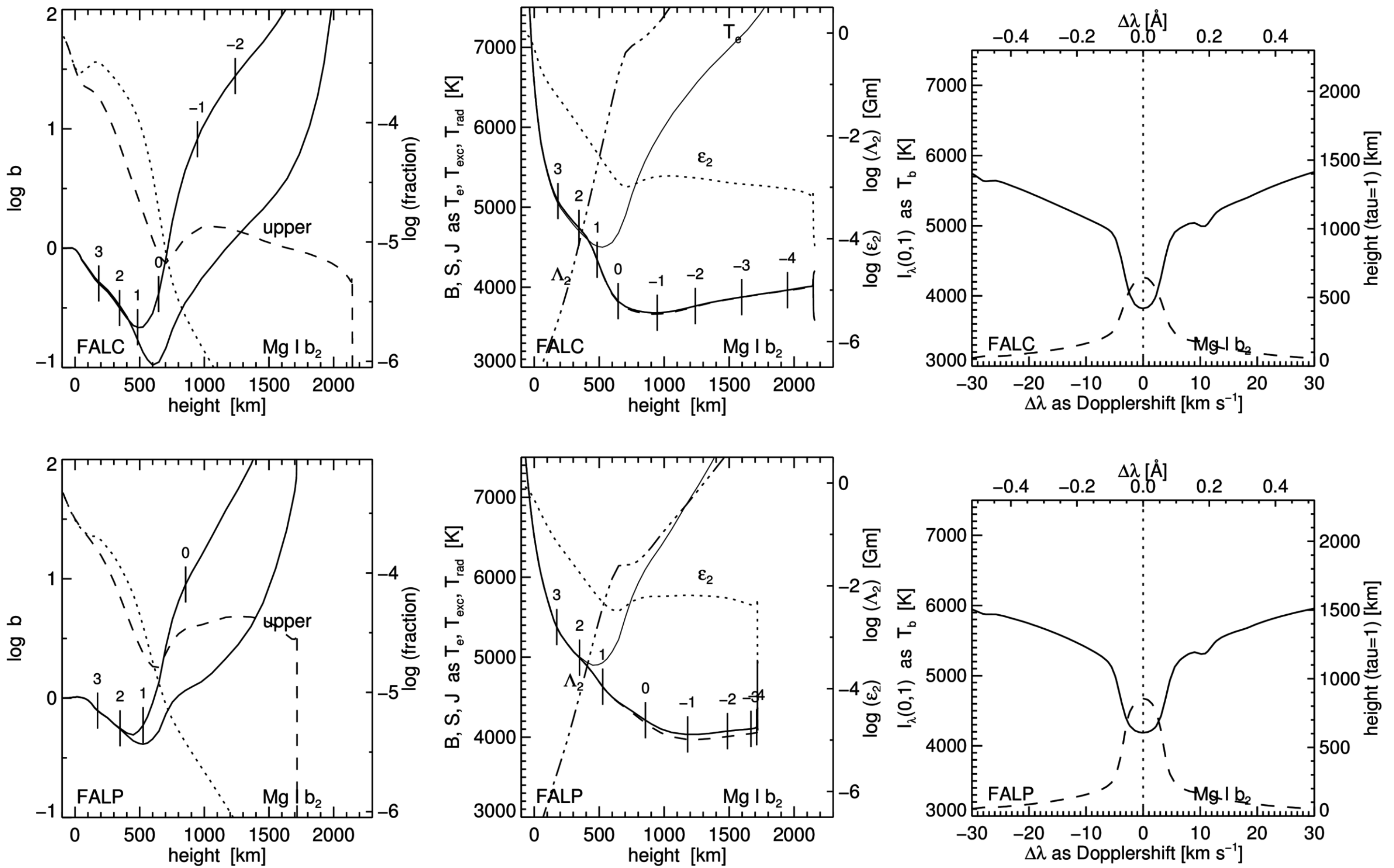

diagnostic of upper photosphere

Na I D_1 5896 Å IN FALC AND FALP

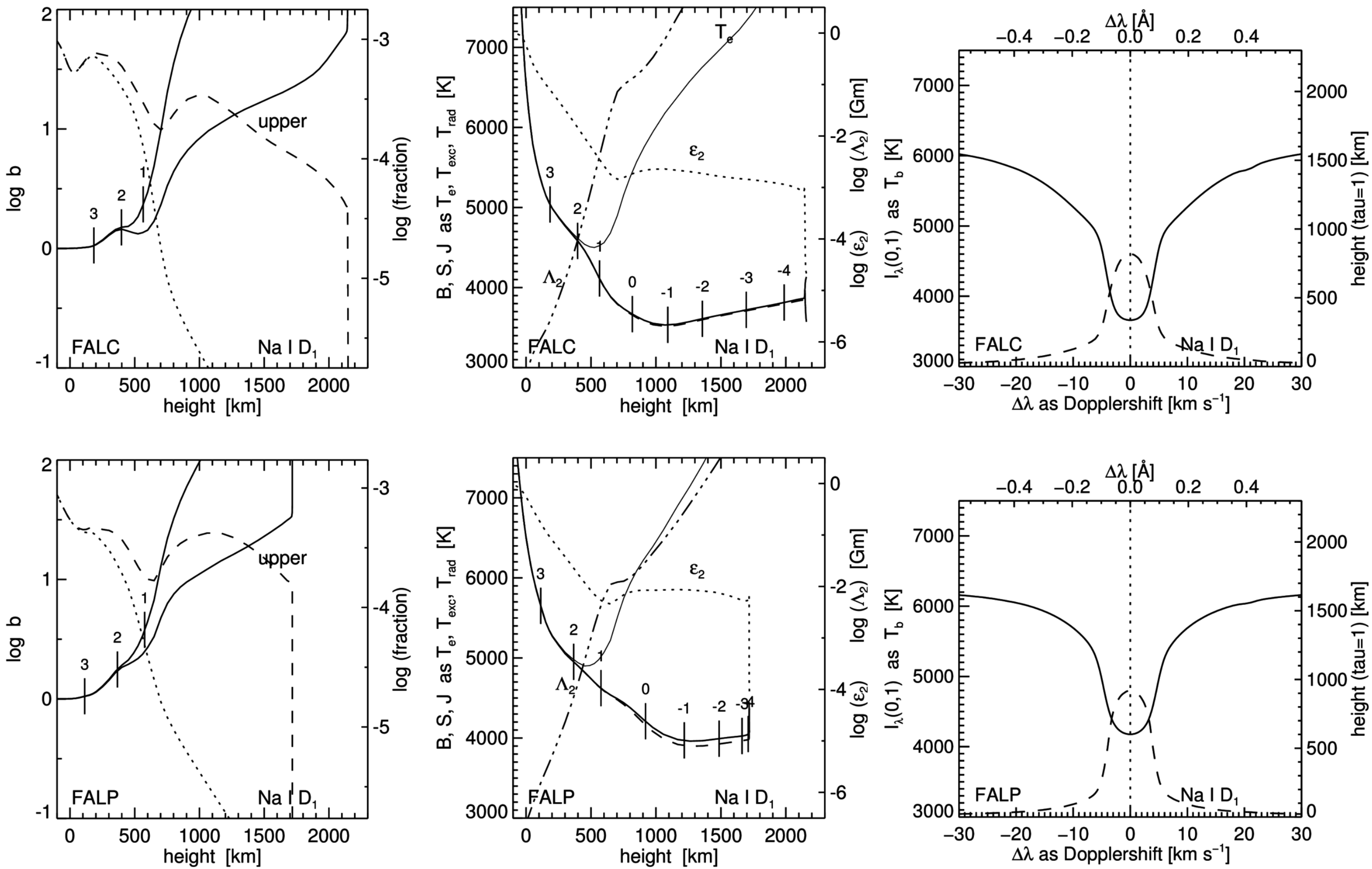

Na I D_1: darkest solar line in optical spectrum = textbook example of two-level scattering

Ba II 4554 Å IN FALC AND FALP

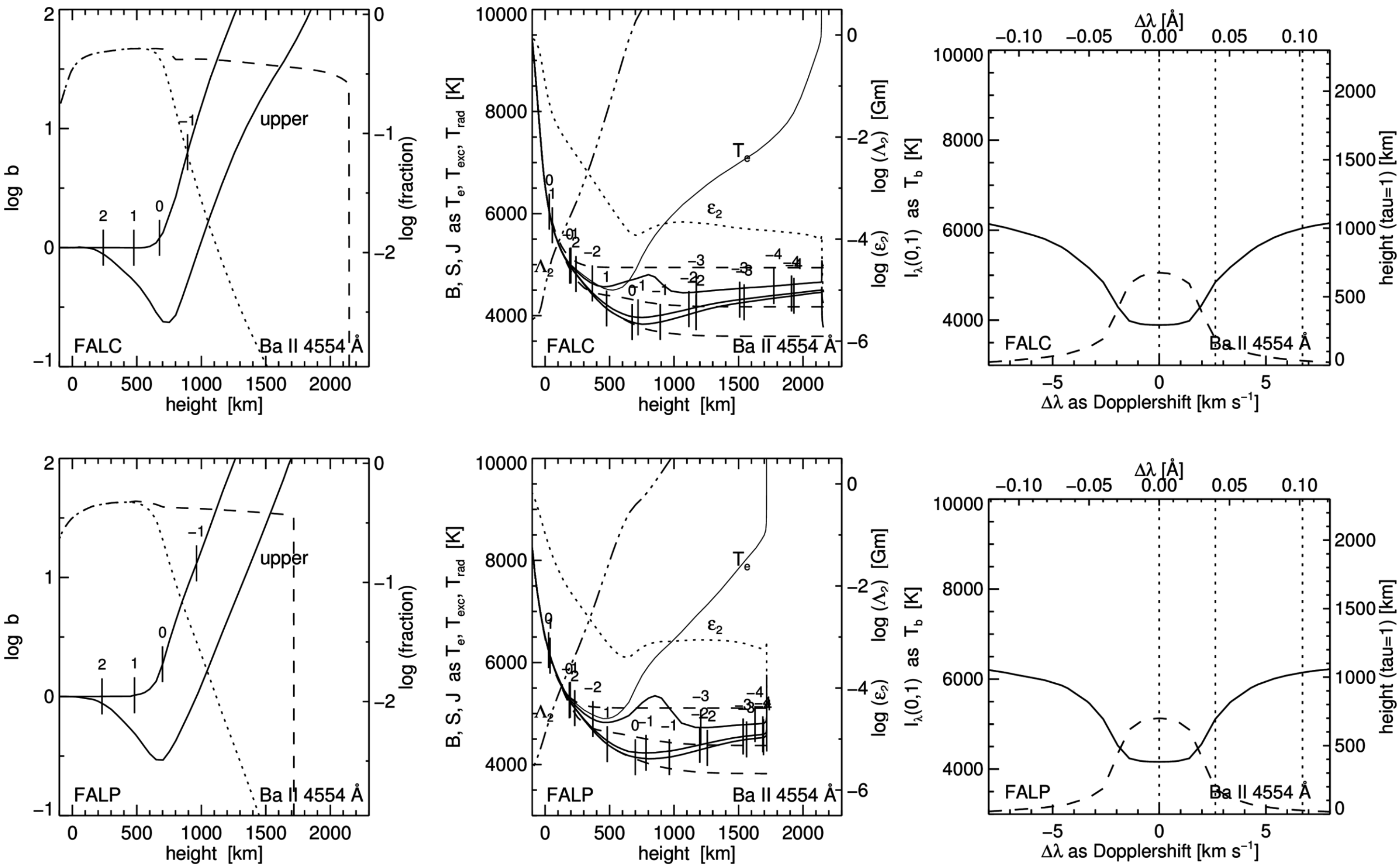

weakest PRD line, best veloctiy diagnostic, good Hanle diagnostic

Ca II 8542 Å IN FALC AND FALP

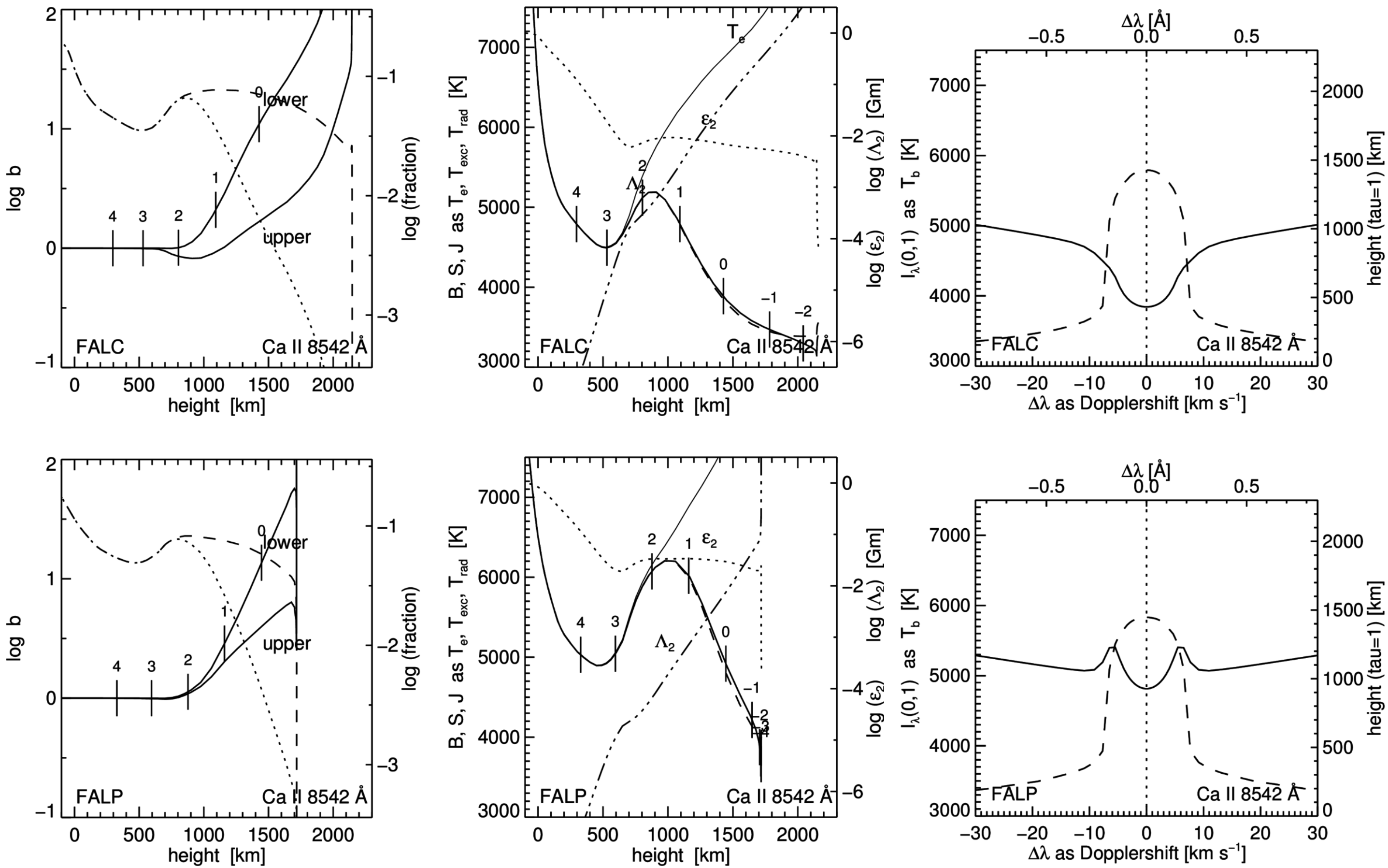

cleanest chromospheric diagnostic in the near infared

Ca II K 3934 Å IN FALC AND FALP

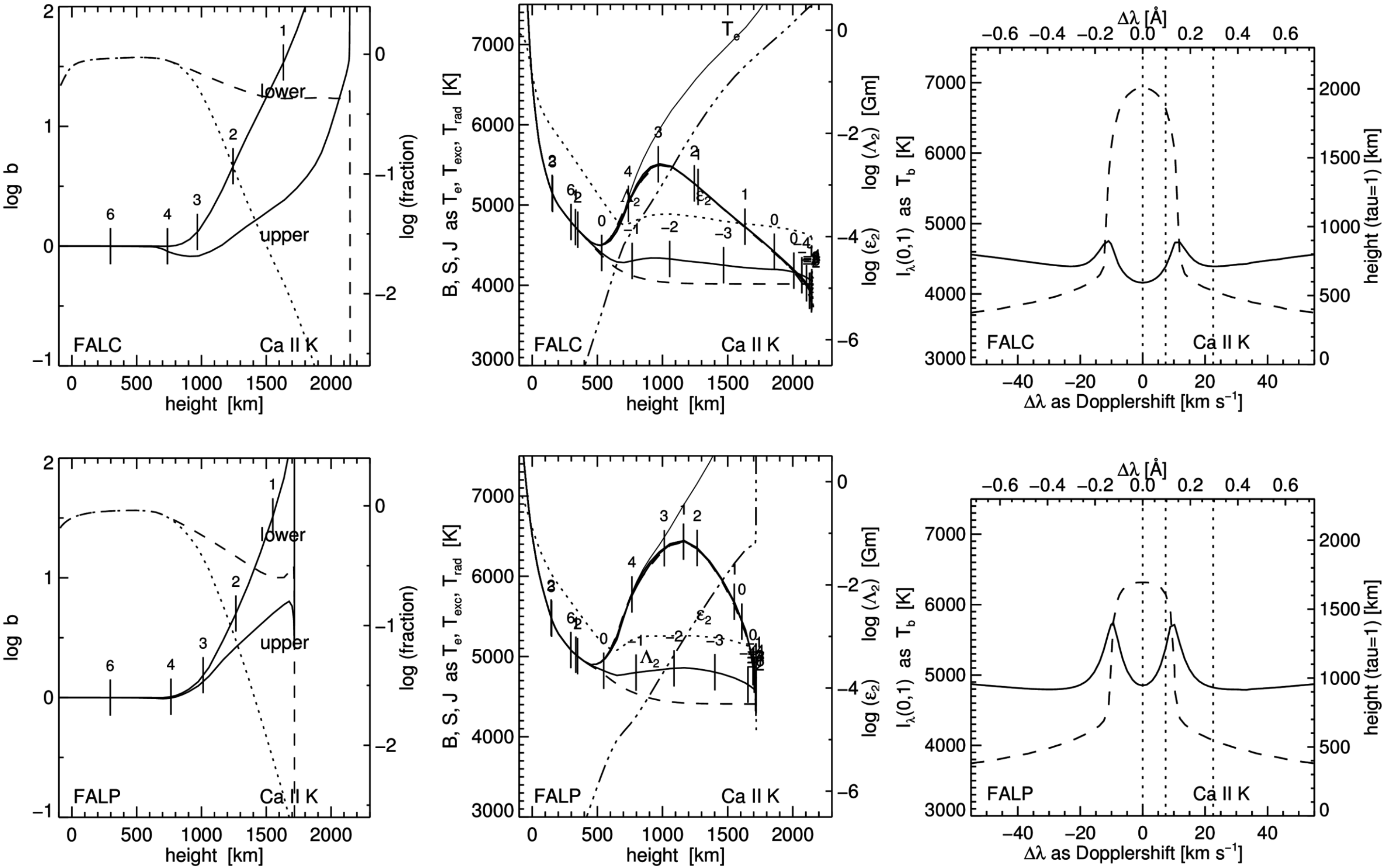

largest extinction in the optical spectrum

start

index

Mg II k 2796 Å IN FALC AND FALP

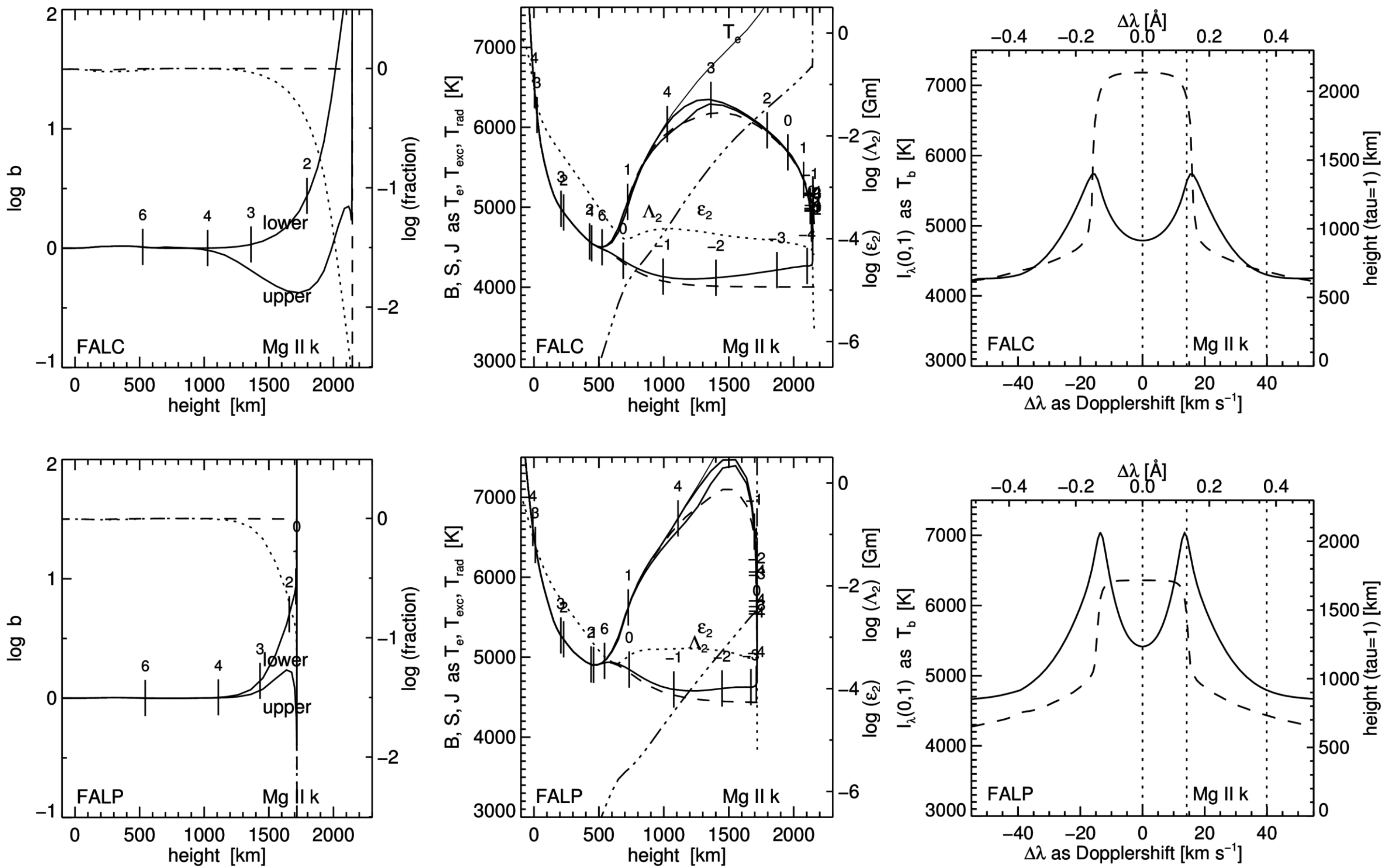

cleanest PRD line and yet larger extincton than Ca II K

Lyα 1216 Å IN FALC AND FALP

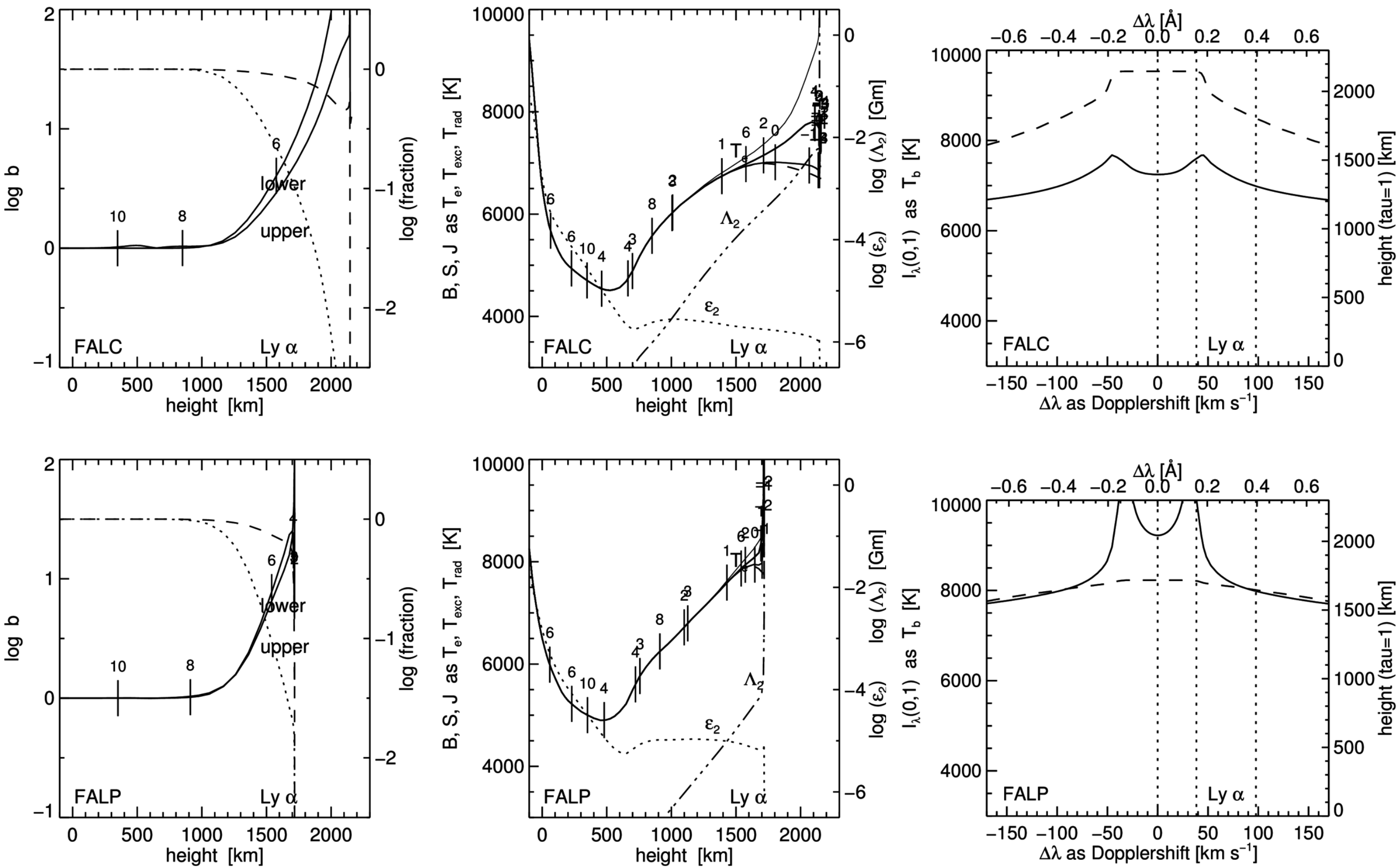

champion: largest extinction and most scattering of all lines

Hα 6563 Å IN FALC AND FALP

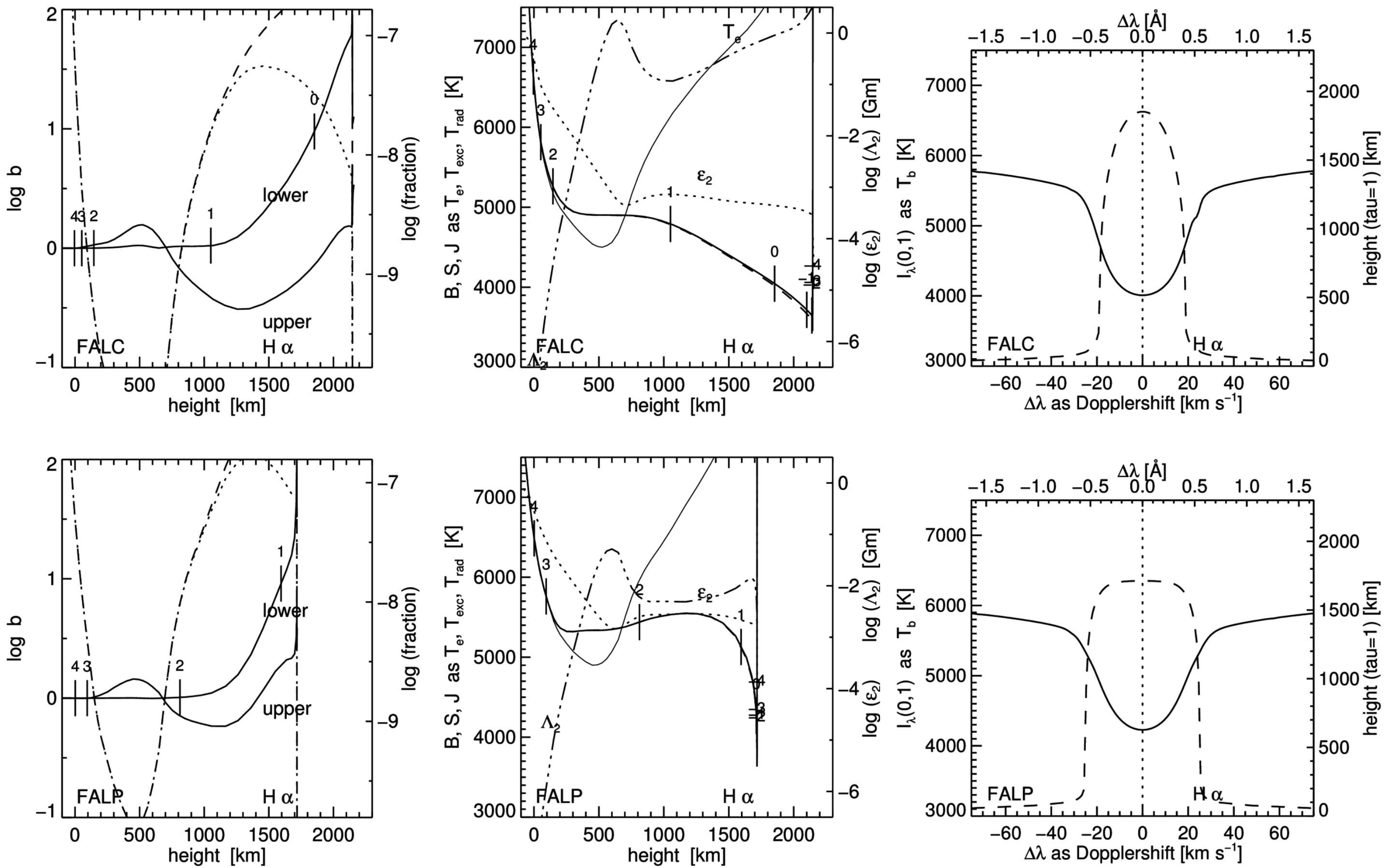

Hα: extraordinary from high excitation energy, huge element abundance, on top of Lyα

Hβ 4861 Å IN FALC AND FALP

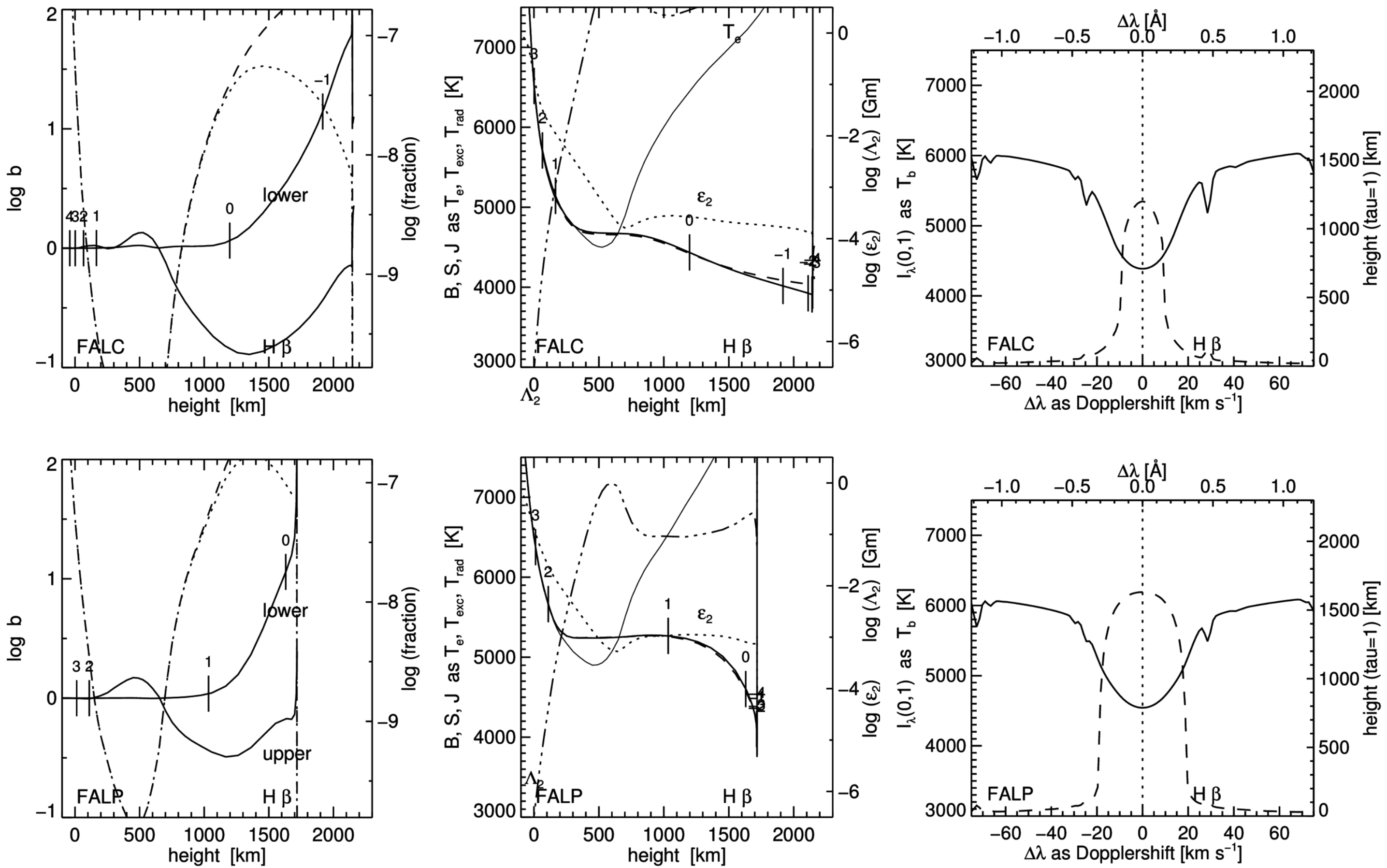

Hβ: analogon to Hα at 5.4$\times$ smaller oscillator strength and in the blue

He I 584 Å IN FALC AND FALP

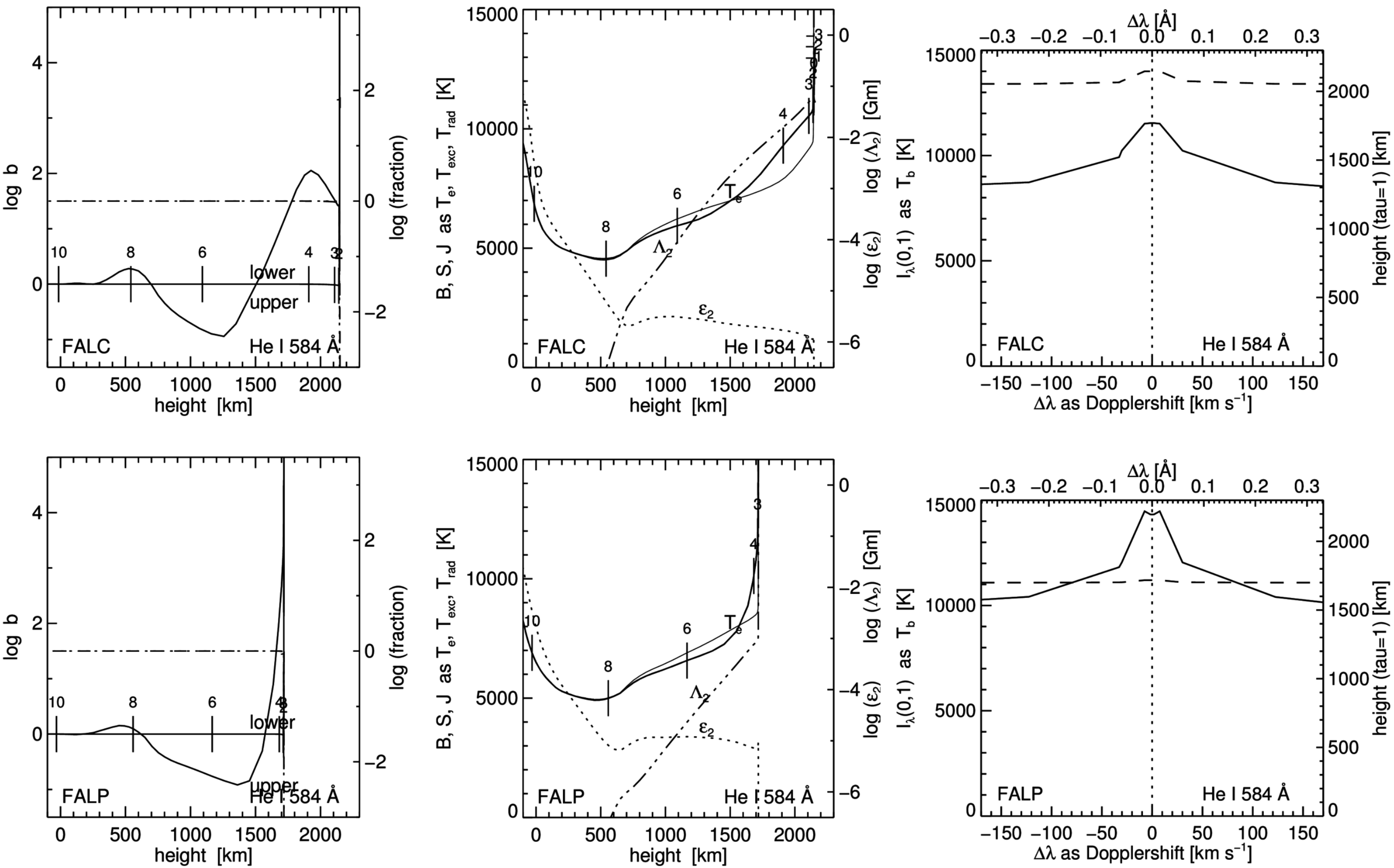

backradiator into chromosphere

ALC7 ATMOSPHERE VERSUS FALP ATMOSPHERE

Avrett & Loeser 2008ApJS..175..229A   *Fontenla, Avrett & Loeser* 1993ApJ...406..319F

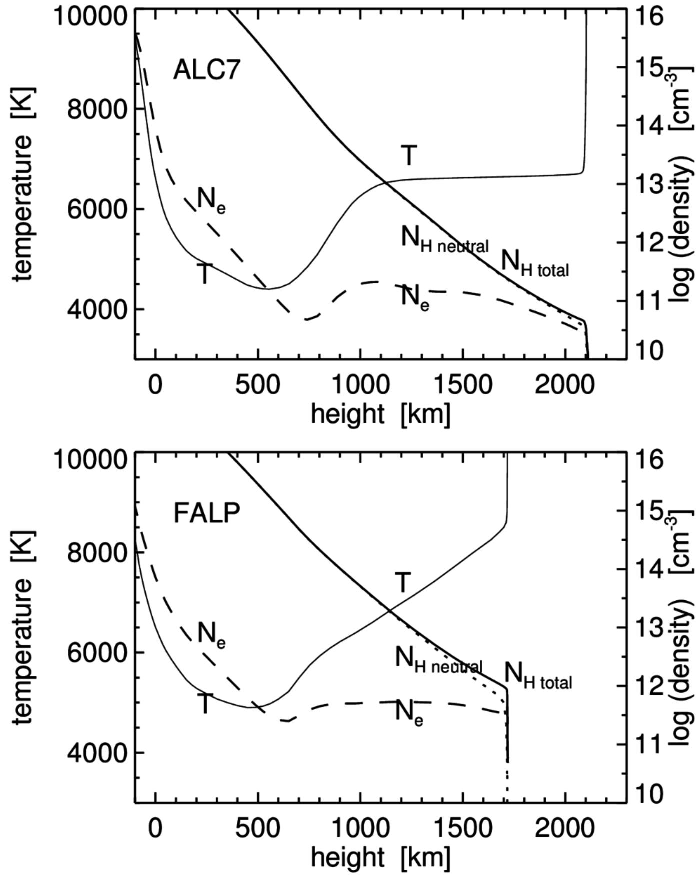

Mg I 4571   Fe I 6302   Mg I b_2 Na I D_1 Ba II 4554   Ca II 8542   Ca II K   Mg II k   Lyα Hα Hβ He I 584

start   *index*

Mg I 4571 Å IN ALC7 AND FALP

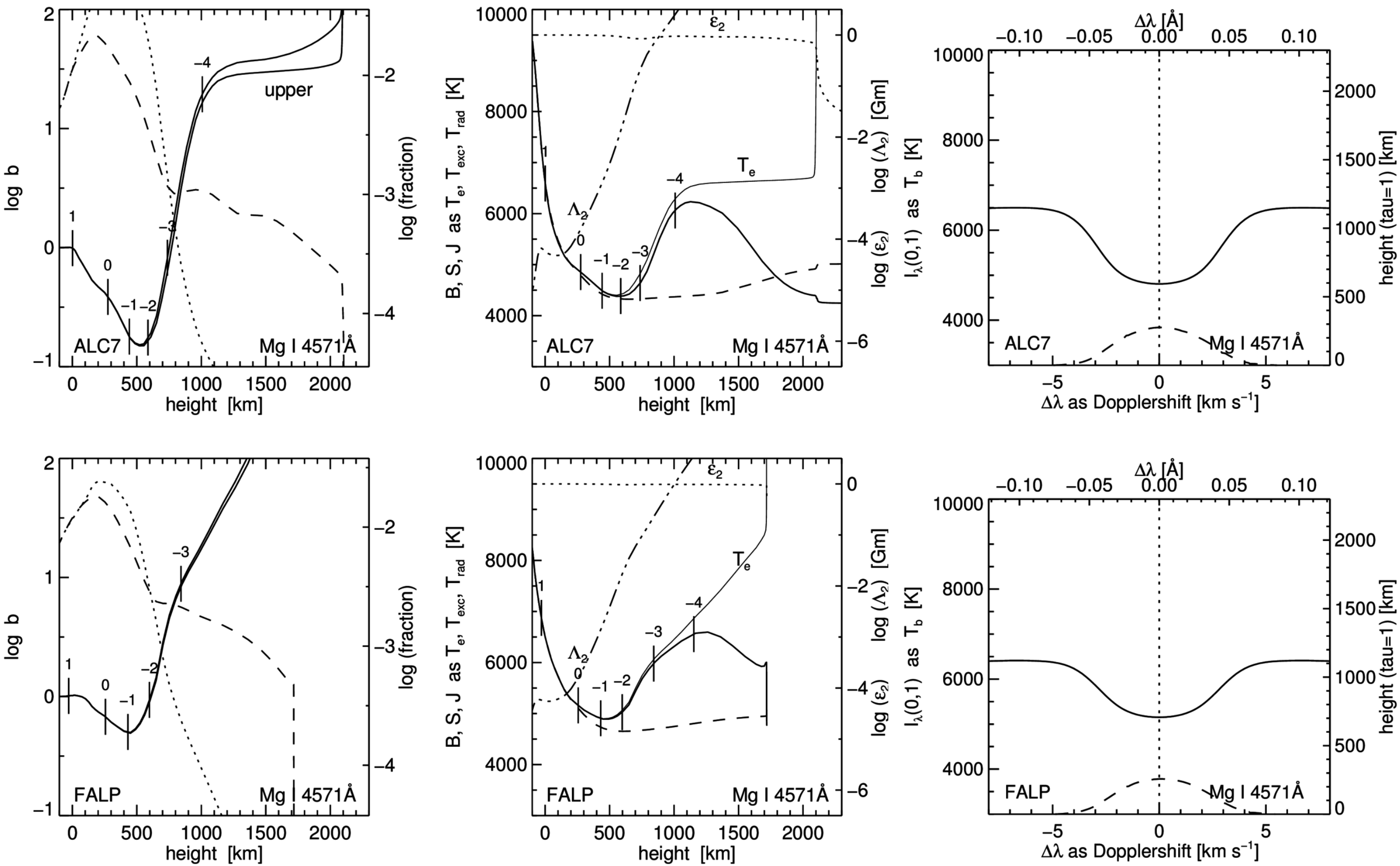

unique photospheric line with LTE source function

Fe I 6301.5 Å IN ALC7 AND FALP

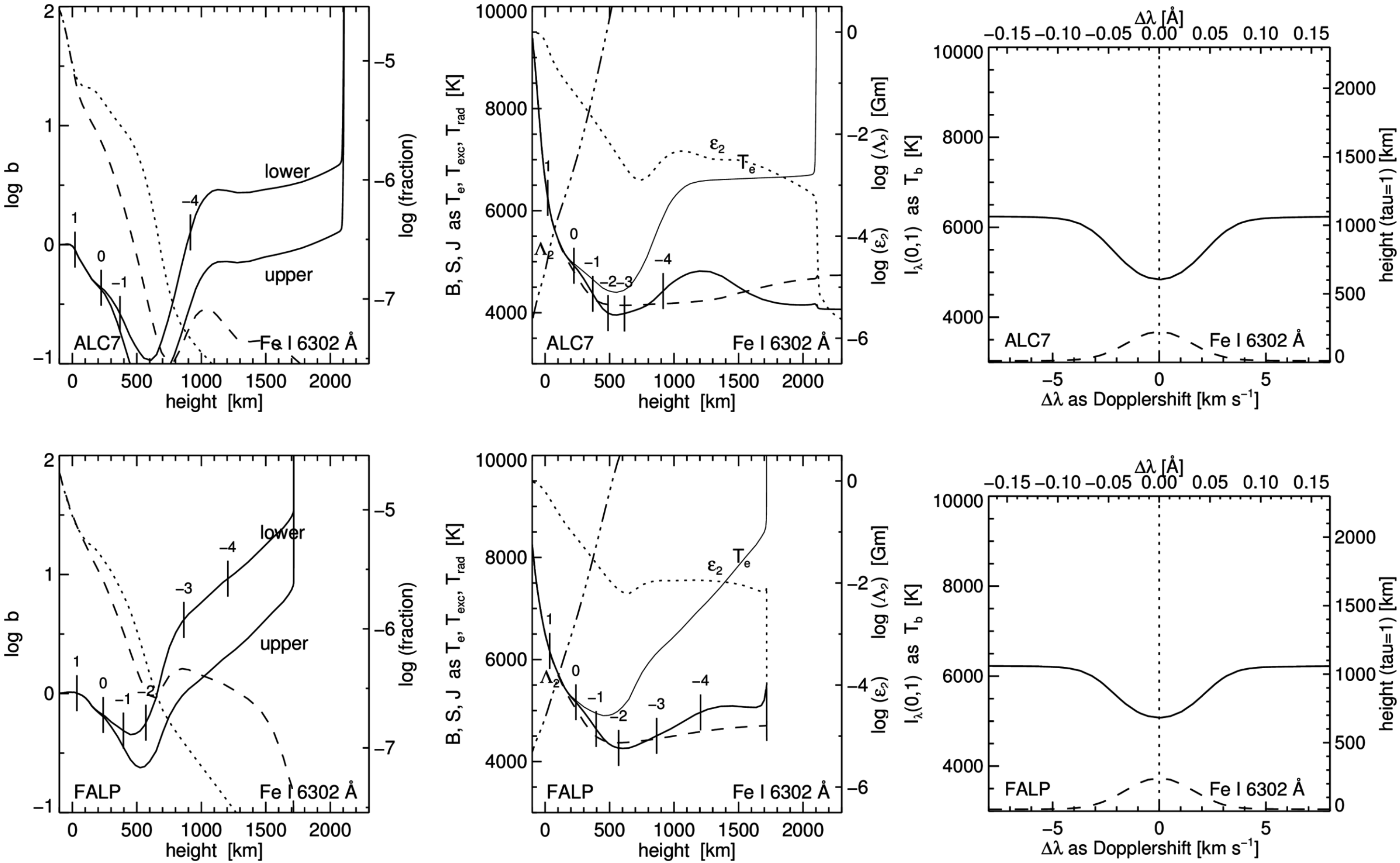

standard polarimetry line

Mg I b_2 5173 Å IN ALC7 AND FALP

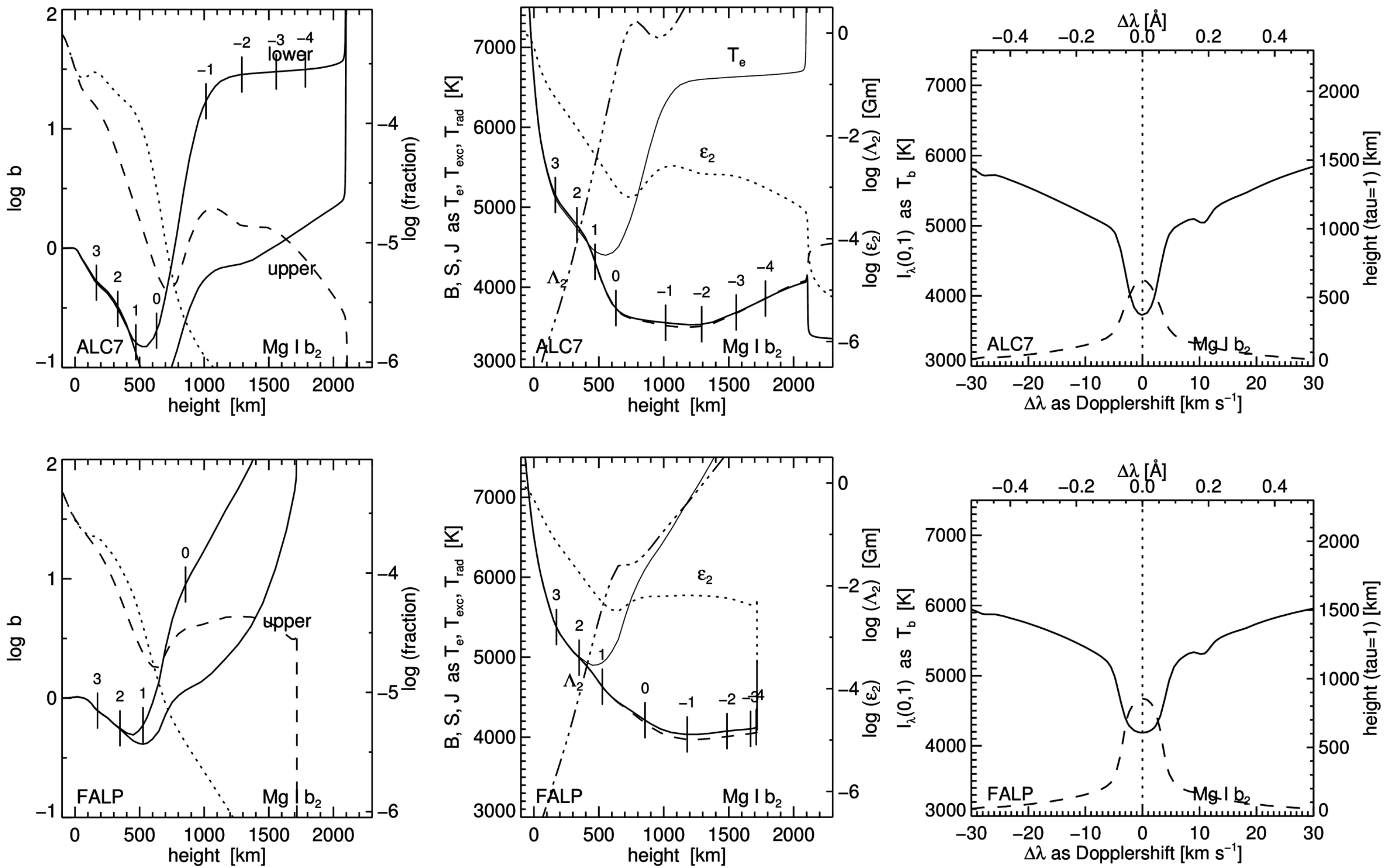

diagnostic of upper photosphere

start

index

Na I D_1 5896 Å IN ALC7 AND FALP

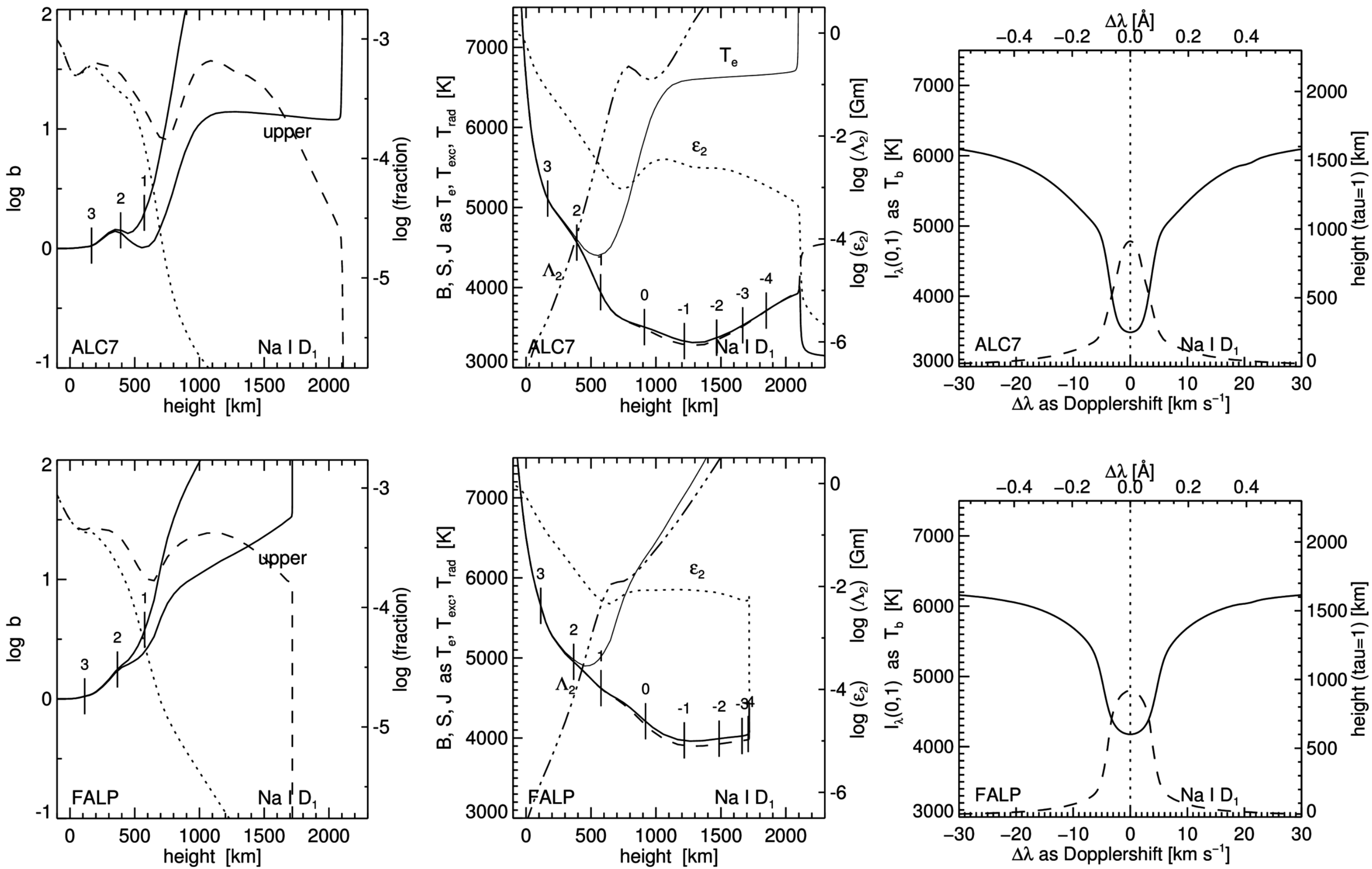

Na I D_1: darkest solar line in optical spectrum = textbook example of two-level scattering

Ba II 4554 Å IN ALC7 AND FALP

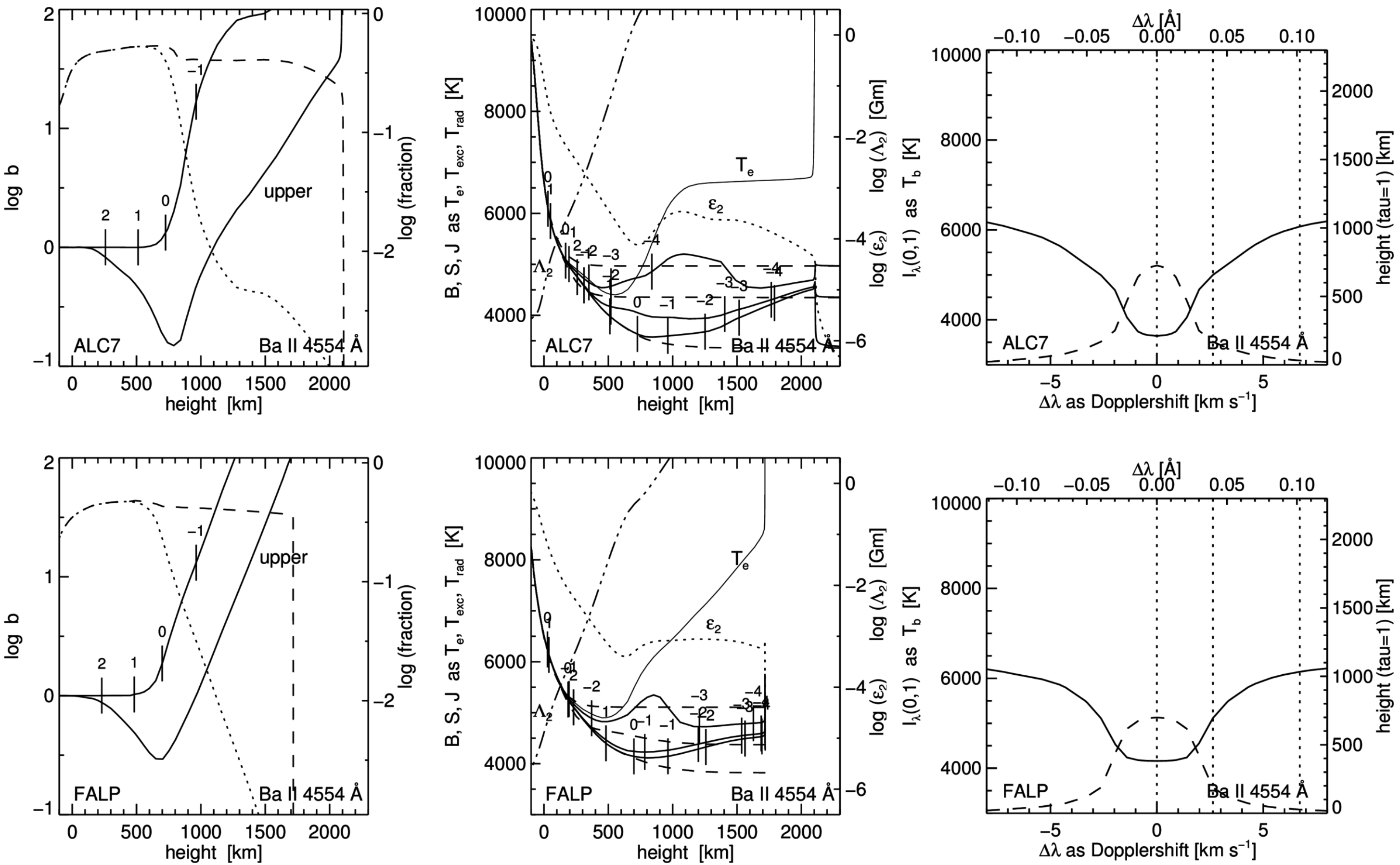

weakest PRD line, best velocity diagnostic, good Hanle diagnostic

start
index

Ca II 8542 Å IN ALC7 AND FALP

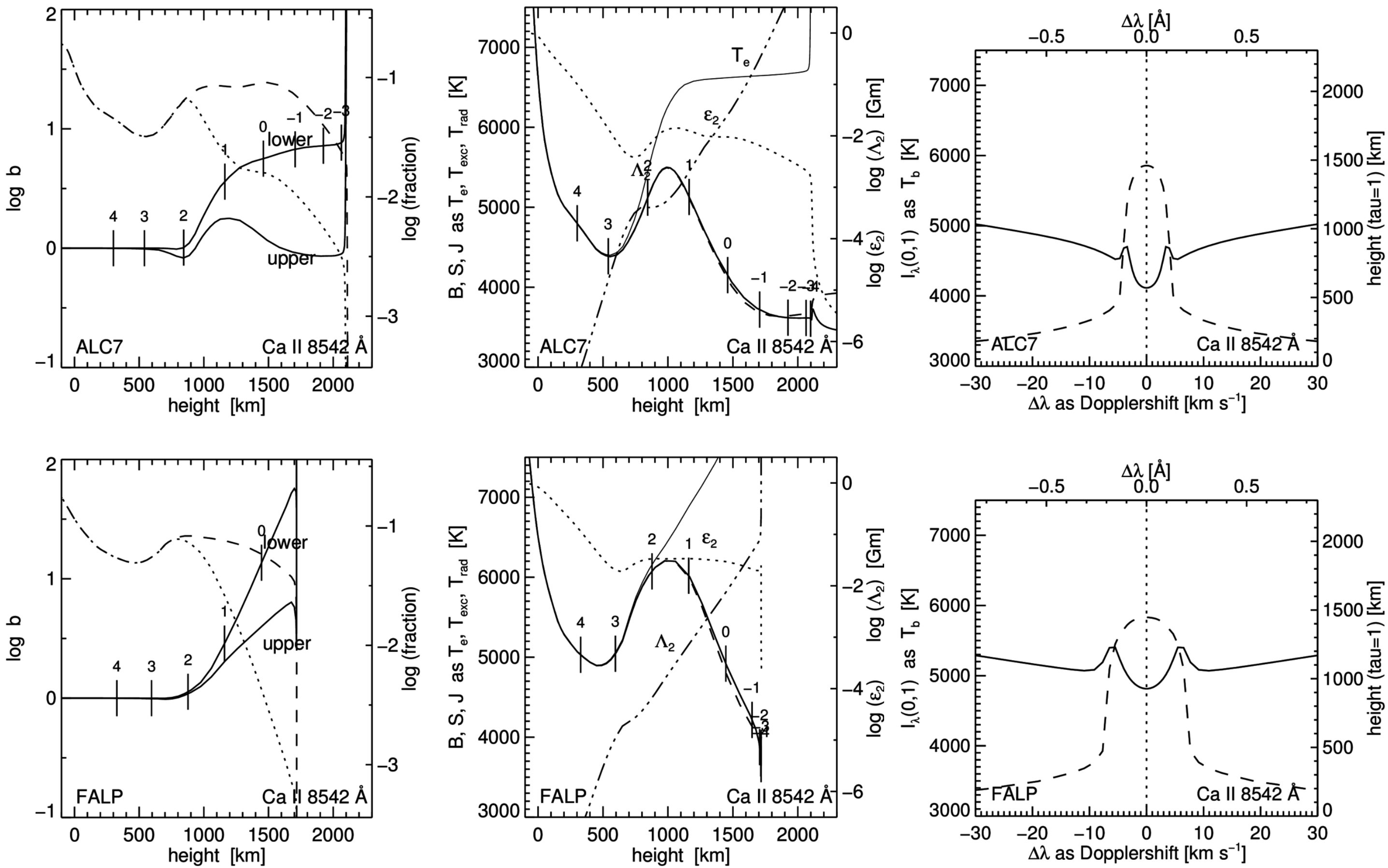

cleanest chromospheric diagnostic in the near infared

start *index*

Ca II K 3934 Å IN ALC7 AND FALP

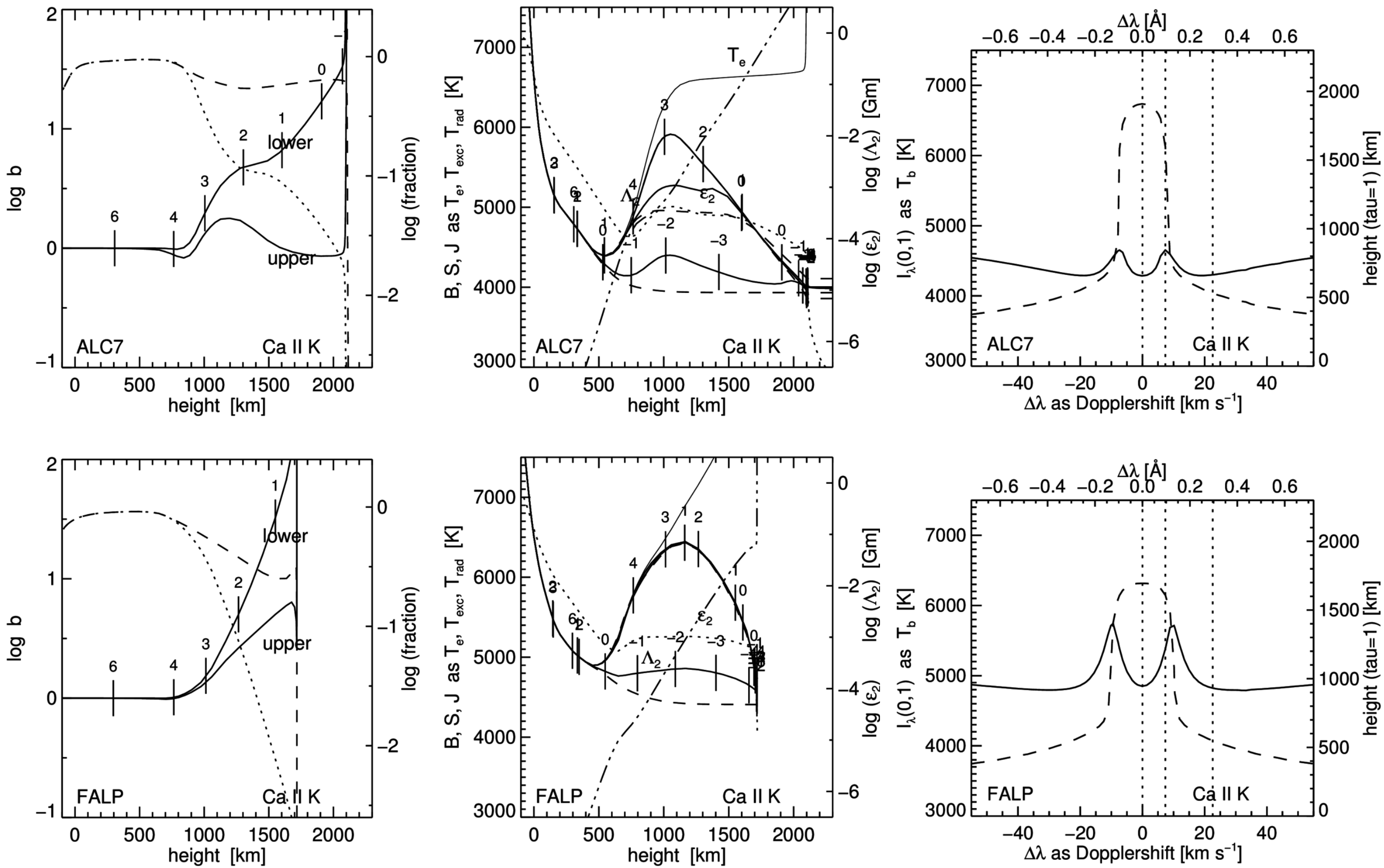

largest extinction in the optical spectrum

Mg II k 2796 Å IN ALC7 AND FALP

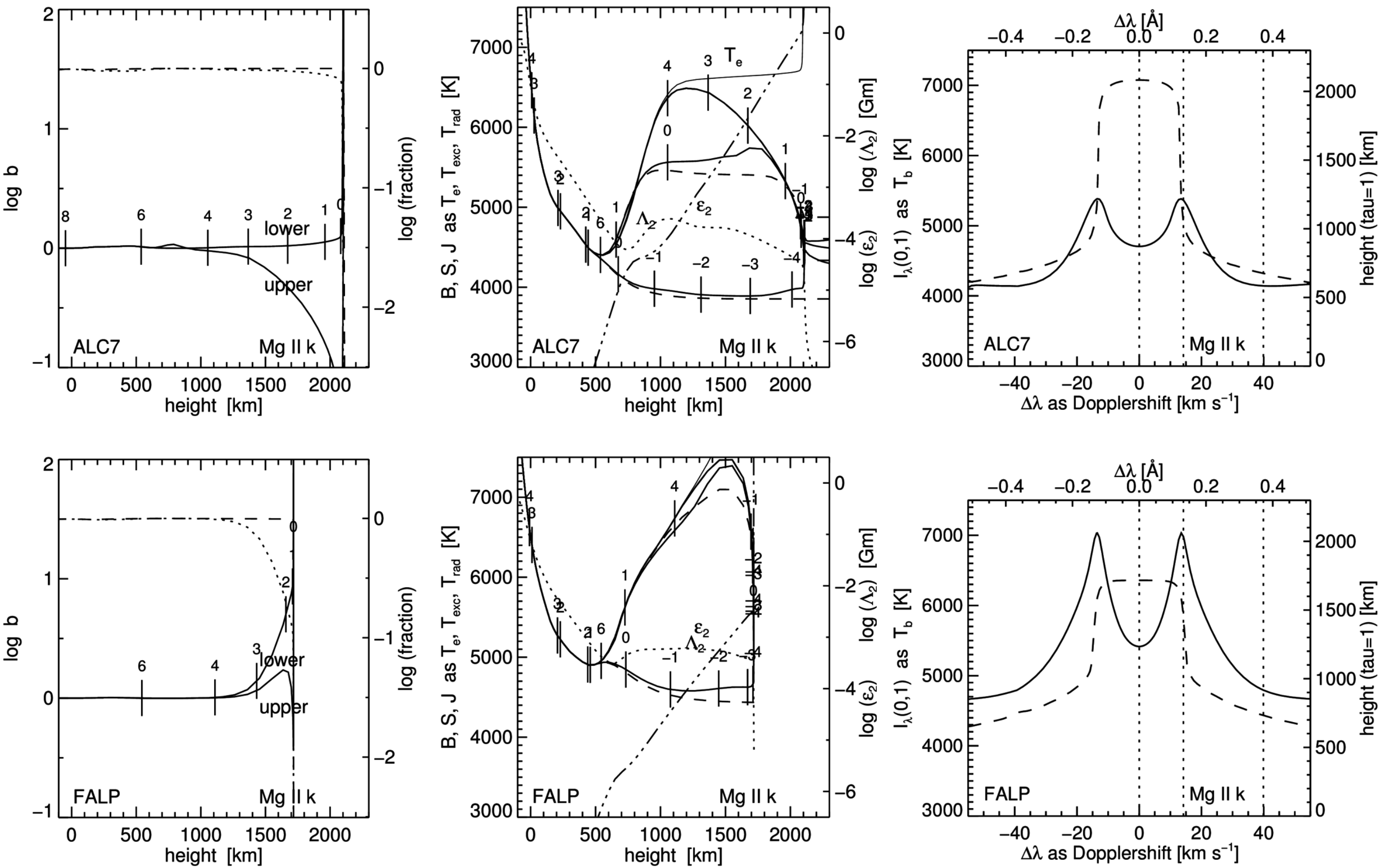

cleanest PRD line and yet larger extincton than Ca II K

start
index

Lyα 1216 Å IN ALC7 AND FALP

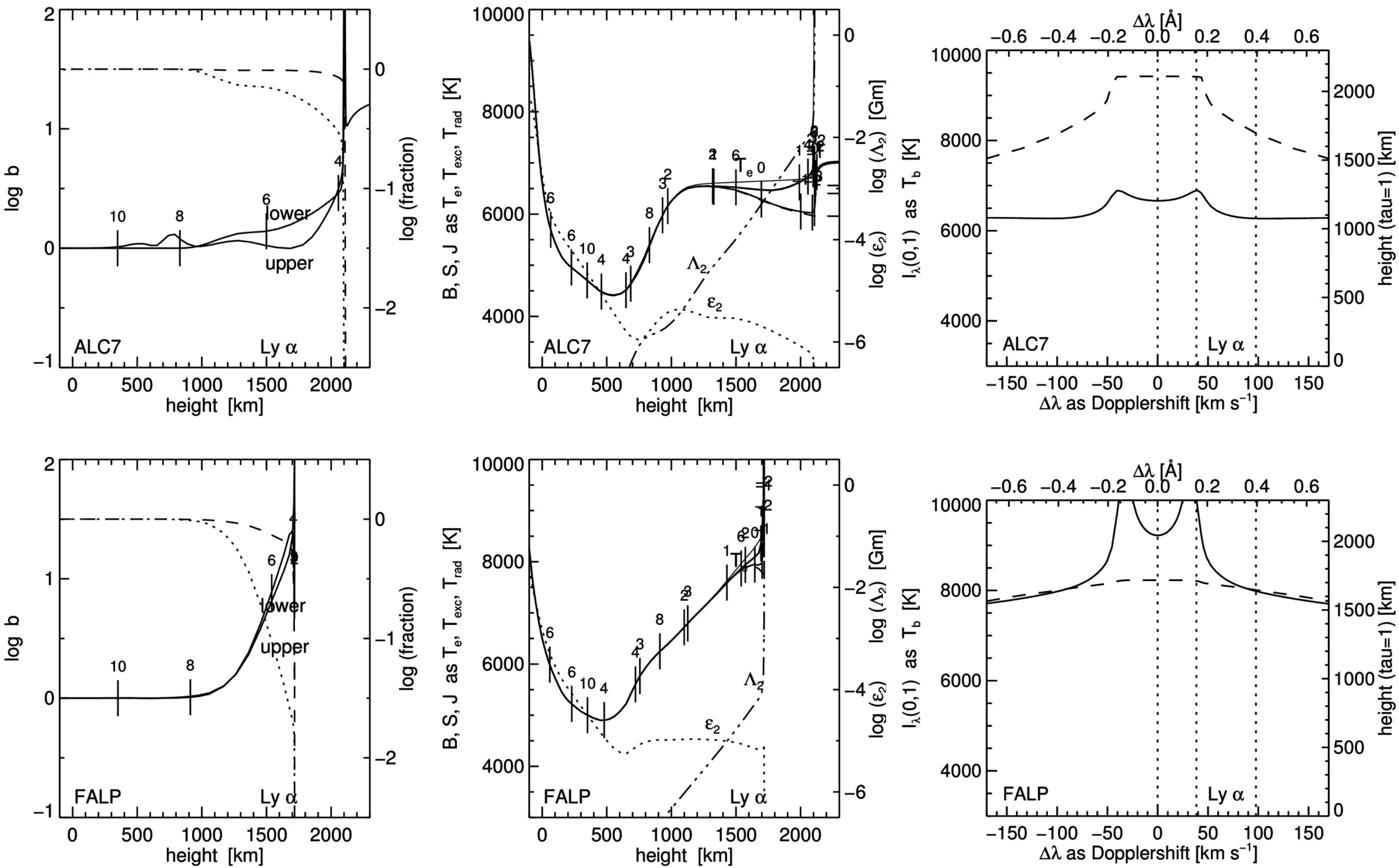

champion: largest extinction and most scattering of all lines

start
index

Hα 6563 Å IN ALC7 AND FALP

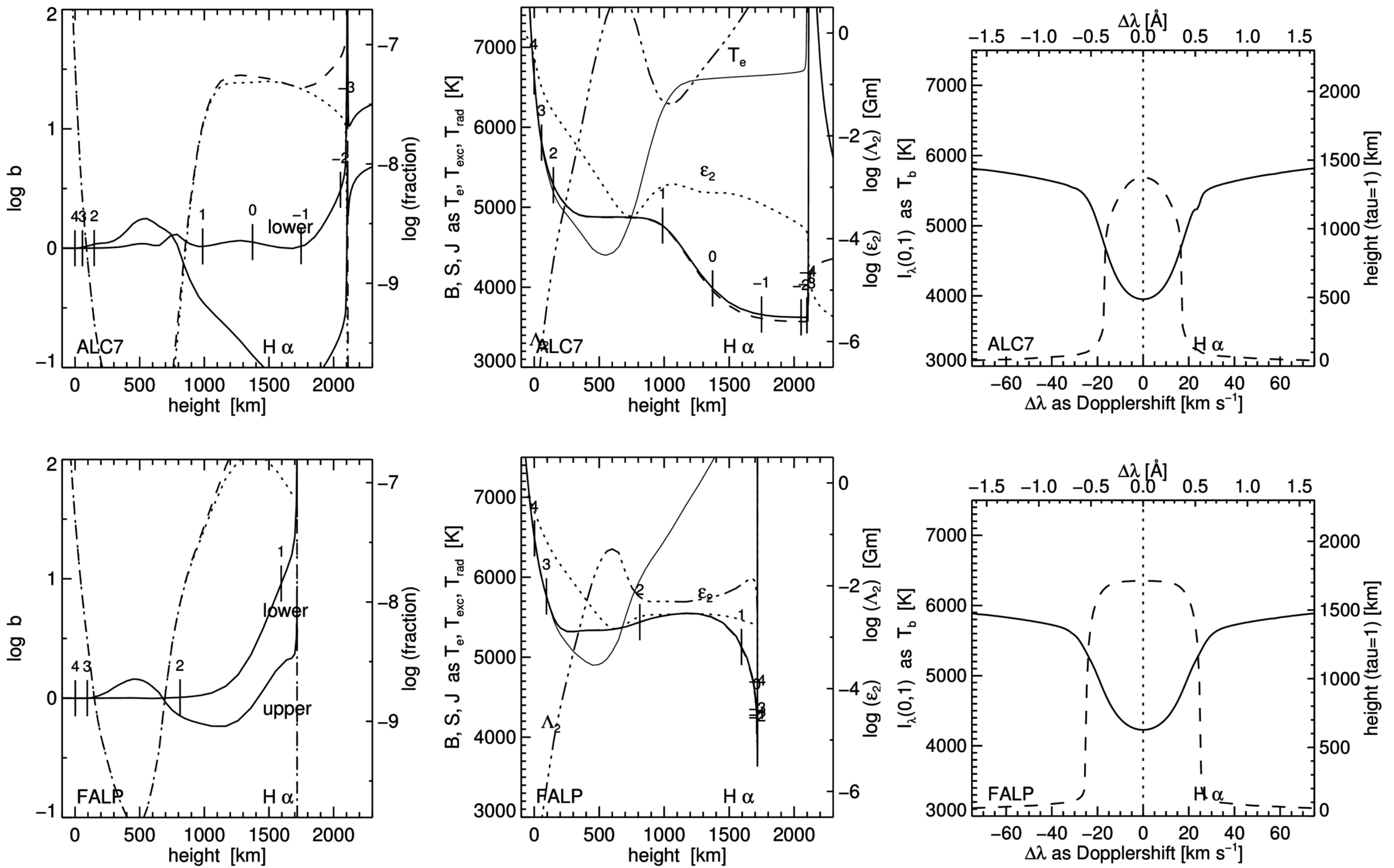

Hα: extraordinary from high excitation energy, huge element abundance, on top of Lyα

Hβ 4861 Å IN ALC7 AND FALP

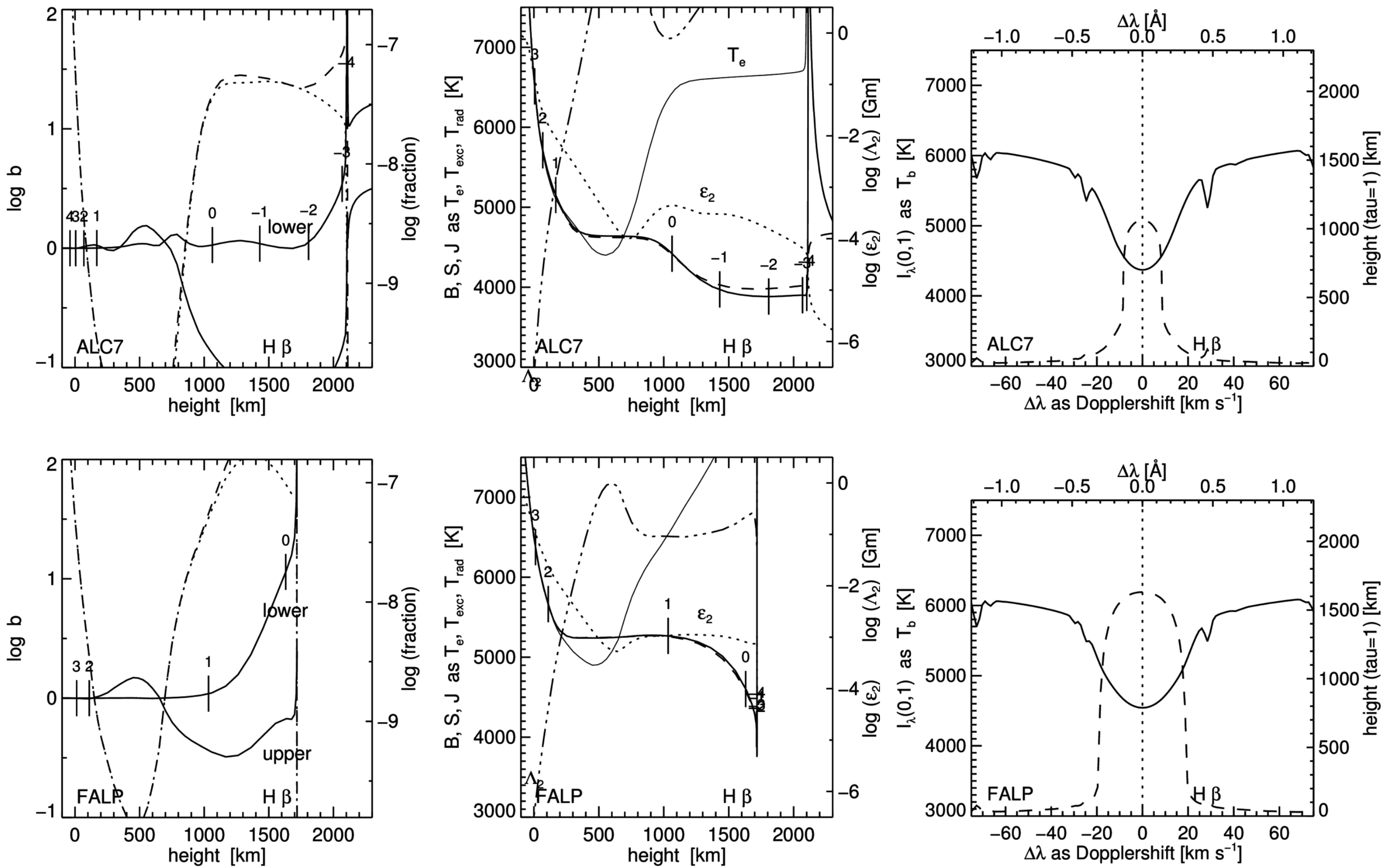

Hβ: analogon to Hα at 5.4× smaller oscillator strength and in the blue

He I 584 Å IN ALC7 AND FALP

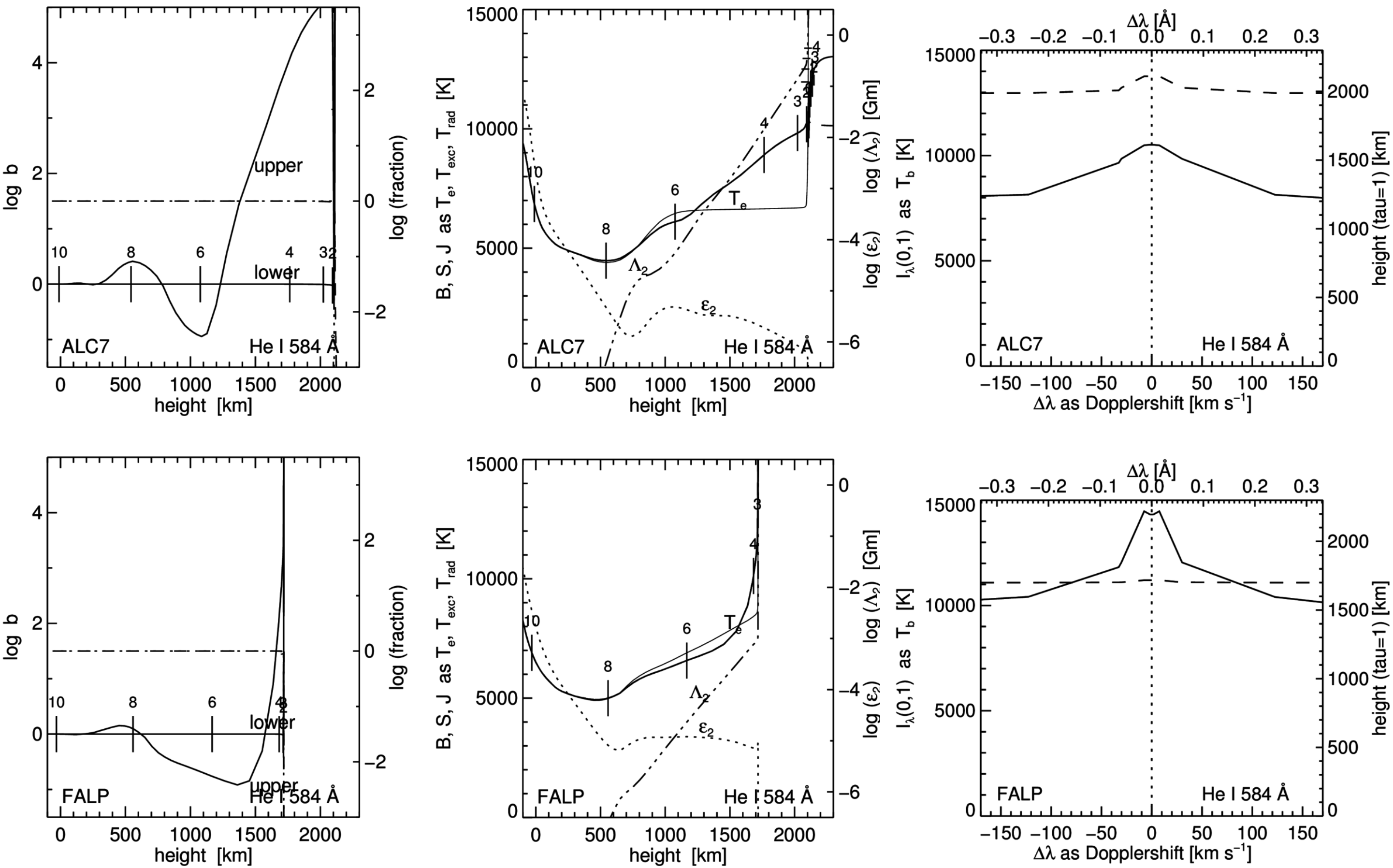

backradiator into chromosphere

start
index

SOLAR SPECTRUM FORMATION: EXAMPLES

Robert J. Rutten
https://webspace.science.uu.nl/~rutte101

Ring Nebula – M57 – NGC 6720

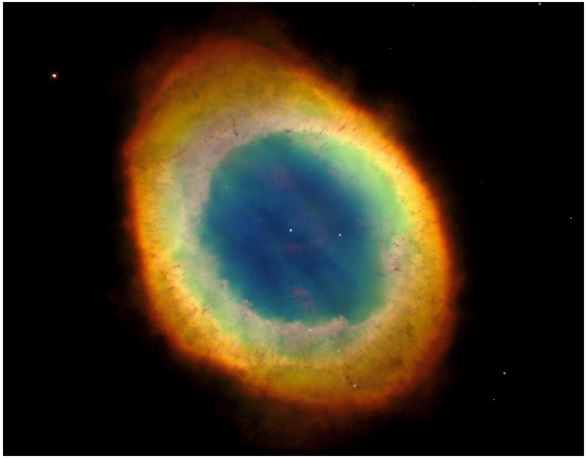

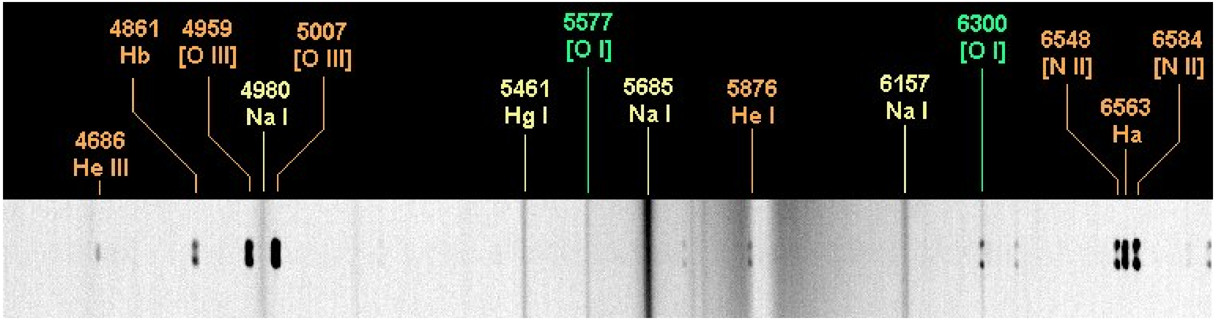

Rydberg solution for coronium and nebulium

Thesis Henrik Hartman, Lund 2003

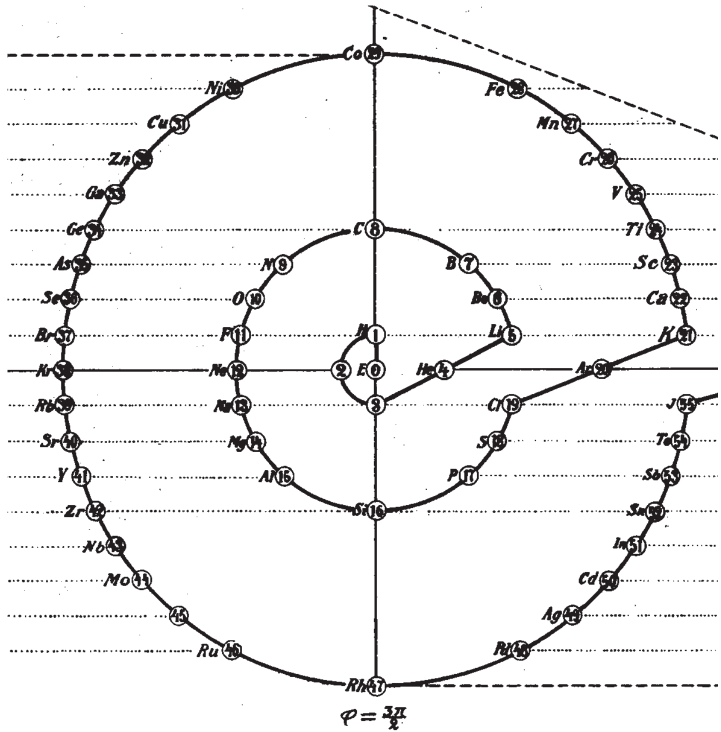

Figure 2.1: Rydberg's periodic table of the elements. In the center is the electron and between hydrogen (1) and helium (4) there are two holes (2 and 3) in which Rydberg placed two elements called Coronium and Nebulium (Rydberg 1913).

Zanstra mechanism

Osterbrock: *In 1922 Russell, the very perceptive American astrophysicist, deduced on the basis of these observational results that the mechanism by which the gas in nebulae is excited to emit its line spectrum is radiation from the hot star or stars involved in a nebula. He suggested the radiation might be electromagnetic (light, visual and ultraviolet) or corpuscles (fast particles)*

Osterbrock re Herman Zanstra: *he considered only the hydrogen Balmer lines, Hα, Hβ, Hγ, for they and a few He I lines had been identified in gaseous nebulae, but the origin of the rest of the observed nebular emission lines was still a mystery. Zanstra knew that these H I lines could be excited by absorption of ultraviolet continuum radiation in the higher-energy Lyman lines Lyβ, Lγ, Lyδ, which, absorbed by neutral H atoms in its ground state with principal quantum number n = 1, excite them to levels with n $\geq$ 3, leading to emission of the Balmer series. (The excitations to n = 2 lead only to scattering of Lyα.) The hotter a star is, the stronger its ultraviolet continuum.*

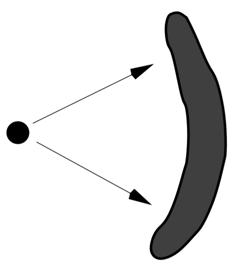

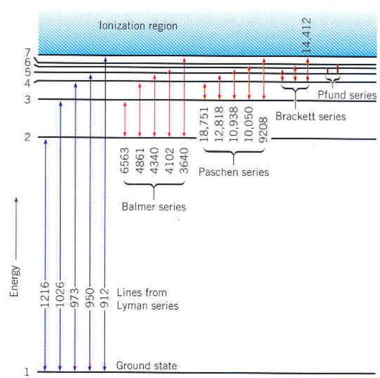

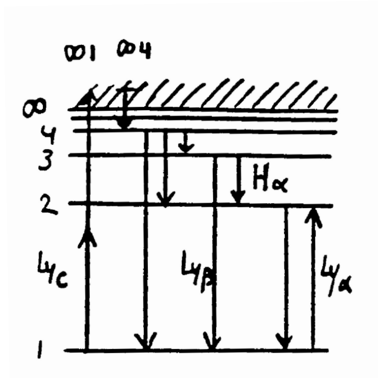

THE ASTROPHYSICAL JOURNAL

AN INTERNATIONAL REVIEW OF SPECTROSCOPY AND ASTRONOMICAL PHYSICS

VOLUME LXVII JANUARY 1928 NUMBER 1

THE ORIGIN OF THE NEBULAR LINES AND THE STRUCTURE OF THE PLANETARY NEBULAE

By I. S. BOWEN

ABSTRACT

Identification of nebular lines.—Eight of the strongest nebular lines are classified as due to electron jumps from metastable states in N_{II}, O_{II} and O_{III}. Several of the weaker lines are identified with recently discovered lines in the spectrum of highly ionized oxygen and nitrogen.

Behavior of lines in nebulae.—The lines thus identified are shown to behave in various nebulae in a way consistent with the foregoing classifications. A similar study of the few lines yet unknown makes it possible to estimate the stage of ionization from which they arise.

Structure of the planetary nebulae.—On the basis of the foregoing identifications, the relative sizes and intensities of the monochromatic images of the planetary nebulae are explained by an extension and modification of the ideas developed by Zanstra for hydrogen in the diffuse nebulae.

Bowen line pumping

Thesis Henrik Hartman, Lund 2003

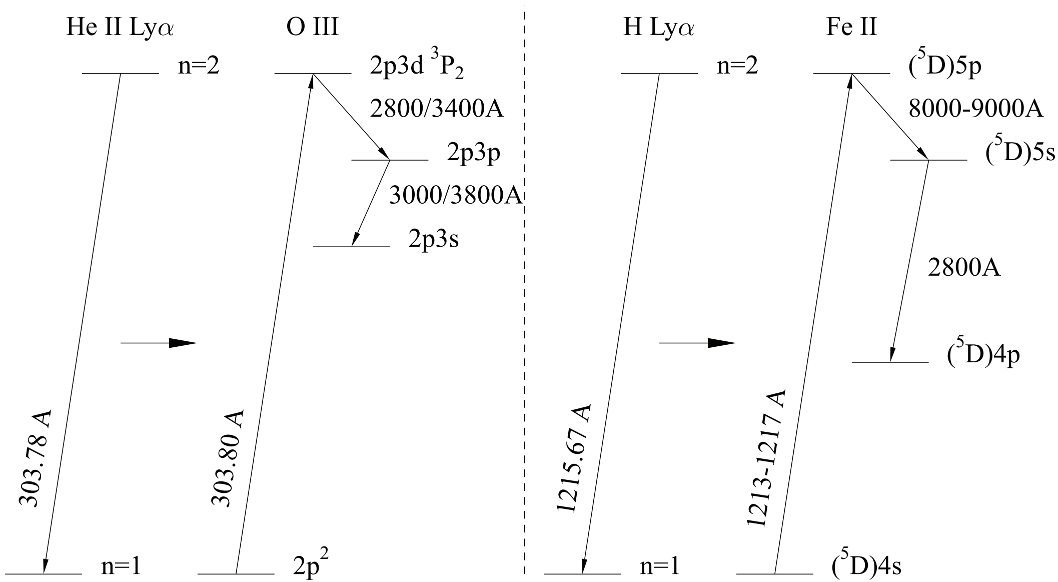

Figure 4.1: Principle for the Bowen mechanism in O III and a similar fluorescence case in Fe II.

Pumped Fe II lines from symbiotic Mira RR Tel

Thesis Henrik Hartman, Lund 2003

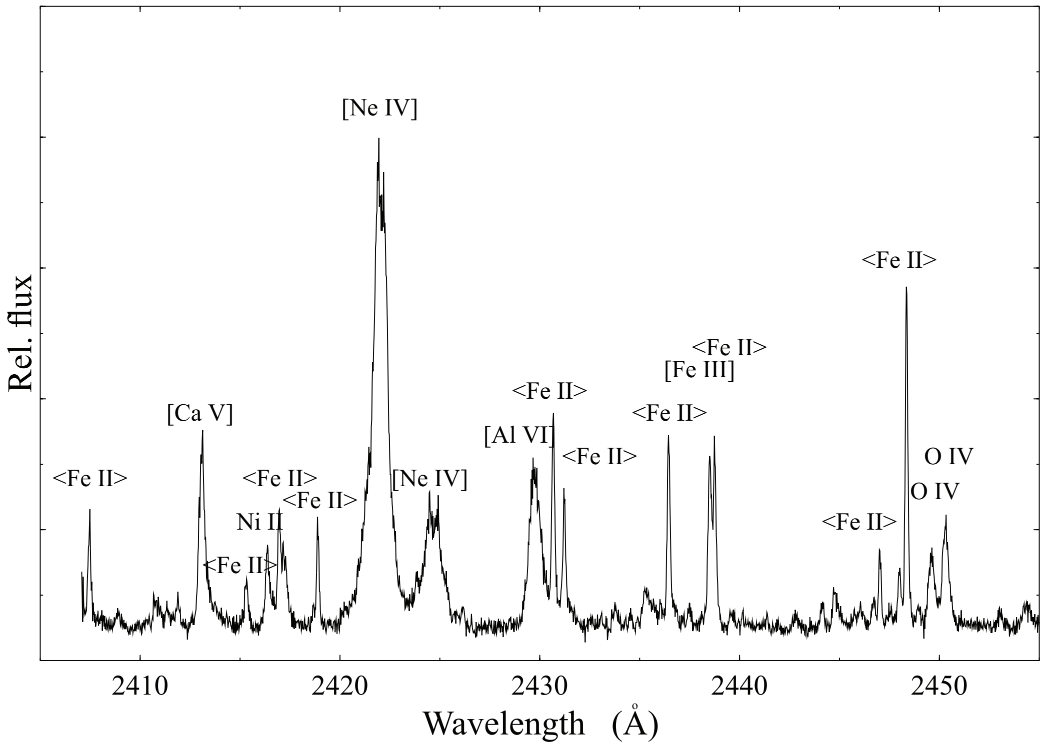

Figure 4.2: Part of the ultraviolet spectrum of RR Tel showing numerous fluorescent <Fe II> and high ionization lines.

SOLAR SPECTRUM FORMATION: EXAMPLES

Robert J. Rutten
https://webspace.science.uu.nl/~rutte101

thin: cloud modeling corona chromosphere Rydberg per ALMA?

thick: UV line flip VAL3C temperature VAL3C spectrum Kurucz stars

photospheric lines: inversions bright points reversed granulation Na I D1 MGs limb emission lines

continua from VAL3C: Avrett models versus 3D MHD VAL3C continua VALII budget hydrogen budget all

lines from ALC7: model optical spectrum ultraviolet depletion hydrogen strong lines plot formats pops plot BSJ plot profile plot Mg I 4571 Fe I 6302 Mg I b_2 Na I D_1 Ba II 4554 Ca II 8542 Å Ca II K Mg II k Lyα Hα Hβ He I 584 He I 10830 canonical Hα Na I D_1–Mg I b_2 Lyα–Hα Hα–Ca II 8542 Å Ca II K–Mg II k versus FCHHT-B ALC7–FALC FALC–FALP ALC7–FALP

detour lines: pumping suction

Oslo-simulated dynamic atmosphere: 1D RADYN 3D Bifrost Bifrost line synthesis

LA-conjectured PSBE atmosphere: non-E Hα aureole boosting Hα extinction CE–SB EBs spicules-II contrail ALMA non-E chromosphere?

IRIS diagnostics: overview diagnostics

PHOTON SUCTION IN ALKALI ATOMS

Bruls, Rutten, Shchukina 1992A&A...265..237B

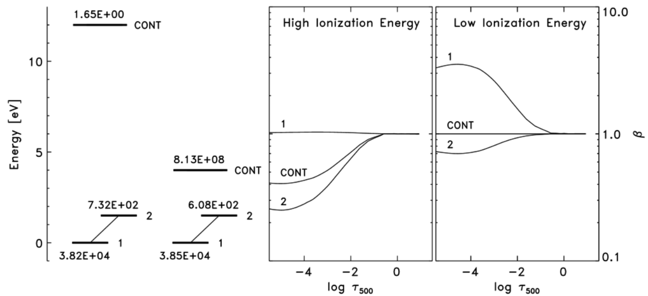

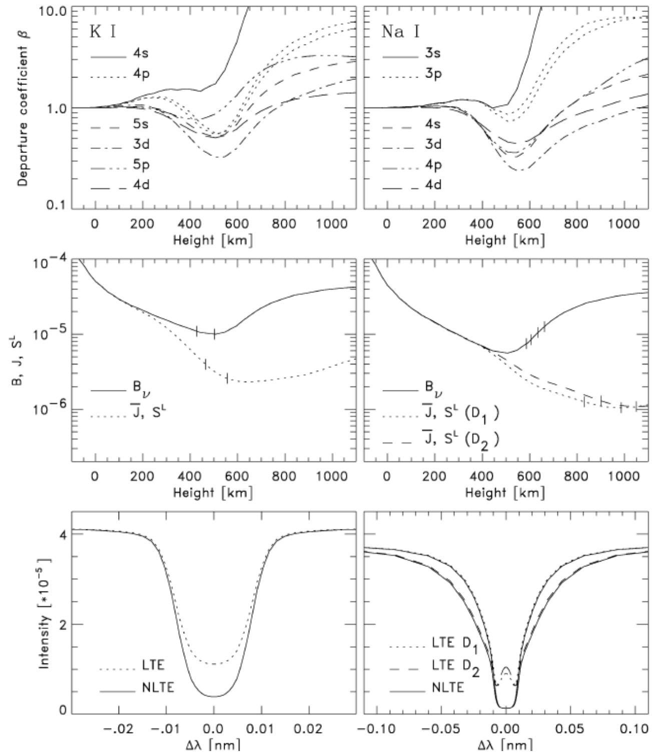

- minority atom: continuum = reservoir
- line photon losses drive replenishment recombination flow
- ground state gets overpopulated to reach photoionization balancing

Mg I EMISSION FEATURES AT 12 MICRON

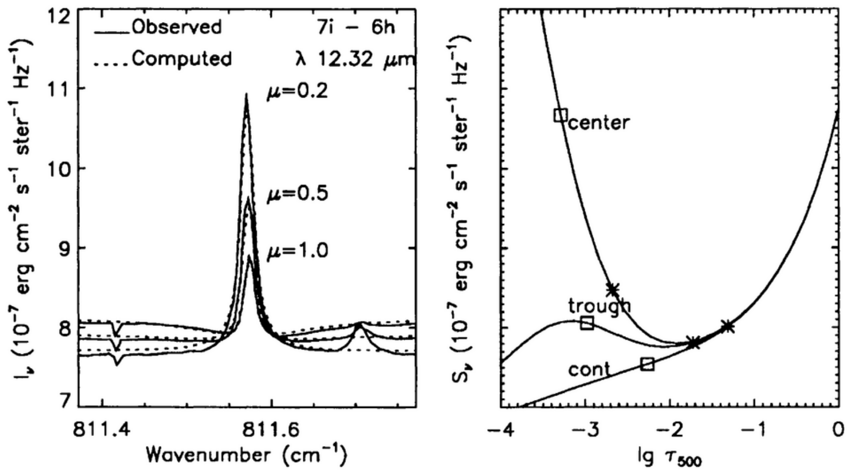

- *discovery*
  - Brault & Testerman 1980: McMath FTS, unpublished
  - Murcray, Murcray & Murcray 1981: South Pole FTS, handmasked
  - Brault & Noyes 1983ApJ...269L..61B: McMath FTS data
  - Chang & Noyes 1983ApJ...275L..11C: identification
- *explanation (Carlsson, Rutten, Shchukina 1992A&A...253..567)*
  - upper-level overpopulation toward laser rise
  - bound-bound suction and bound-free pumping
  - collisionally dominated recombination cascade

12 MICRON EMISSION FEATURES

Carlsson, Rutten & Shchukina 1992A&A...253..567C, Rutten & Carlsson 1994IAUS..154..309R

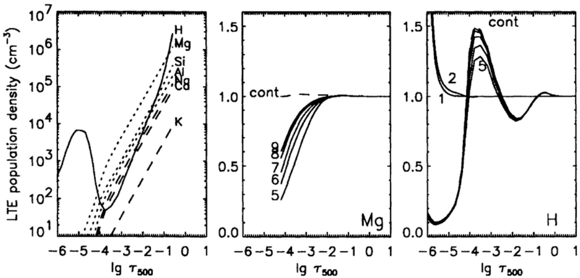

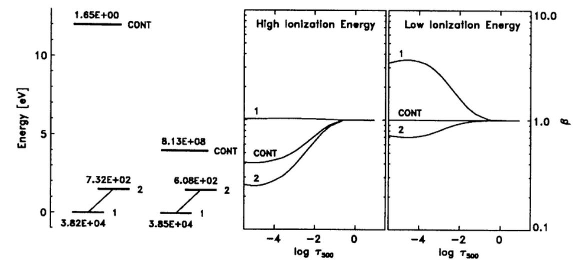

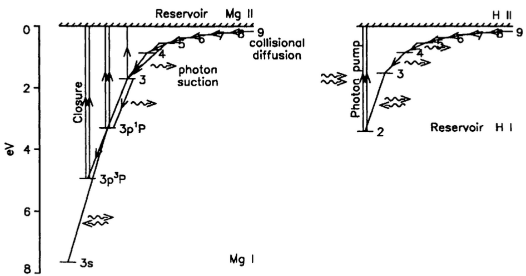

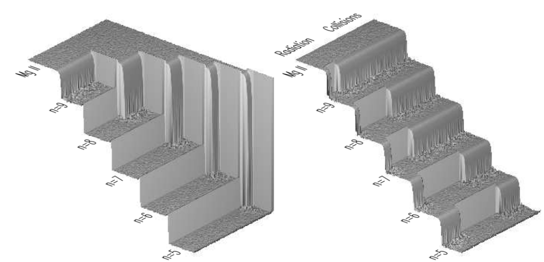

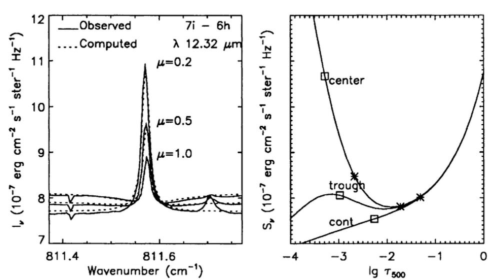

THE SIMPLEST HYDROGEN PROBLEM

Auer & Mihalas *1969ApJ...156..157A* *1969ApJ...156..681A*

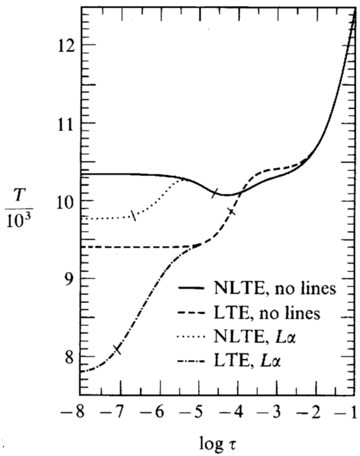

- *simple*
  - plane-parallel HE + RE
  - 2-level + continuum + CRD
- *straightforward*
  - Lyα photon-loss cooling
  - Balmer continuum heating
- *intricate*
  - Hα photon-loss cooling
  - Hα photon-loss heating

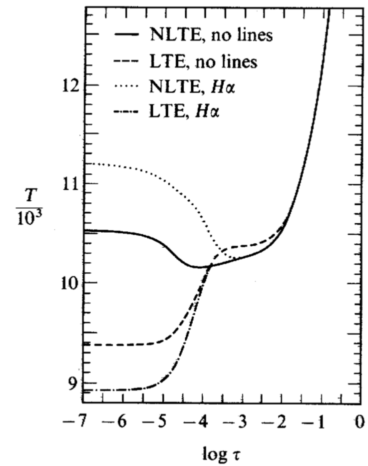

- work through final problem in RTSA course notes
  (only 5 pages of questions + 3 pages of footnotesize answers)
- explain every curve in every graph of Wiersma et al. 2003ASPC..288..130W

SOLAR SPECTRUM FORMATION: EXAMPLES

Robert J. Rutten
https://webspace.science.uu.nl/~rutte101

INTERNETWORK H_{2V} GRAINS = ACOUSTIC SHOCKS

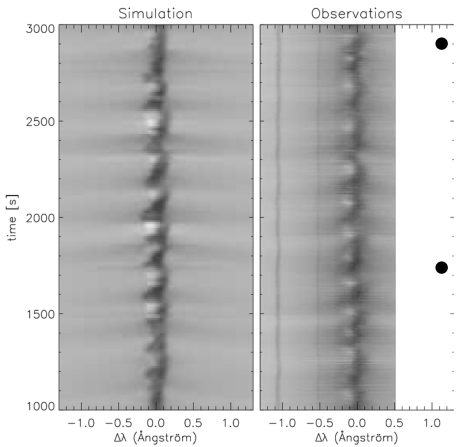

- *Ca II K_{2V} grains (Rutten & Uitenbroek 1991SoPh..134...15R)*
  - extended and confused literature (600 references)
  - most likely non-magnetic phenomenon
  - most likely acoustic shocks
  - wave interference reminiscent of "clapotis"
- *observation (Lites, Rutten & Kalkofen 1993ApJ...414..345L)*
  - sawtooth line-center shift
  - triangular whiskers
  - H_{2V} grains
- *simulation (Carlsson & Stein 1997ApJ...481..500C)*
  - 1D radiation hydrodynamics
  - subsurface piston derived from Fe I Doppler
  - emulation of observer's diagnostics
- *analysis*
  - source function breakdown
  - dynamical chromosphere

CLAPOTISPHERE

Rutten 1995soho....1..151R “The internetwork chromosphere is inherently a clapotisphere”

“The extensive literature on the Ca II K_{2V} grains and related cell-interior phenomena leads us to the conclusion that bright cell grains are of hydrodynamical origin, due to oscillations that are present all over the solar surface but which produce grains only at places and moments set by pattern interference between the velocity oscillations in the K_3 layer and the evanescent wave trains of the p-mode oscillation deeper down. They remind us of what is called “clapotis” on sea charts for areas where wave interference produces waterspouts on the ocean (Dowd 1981).”

Rutten & Uitenbroek 1991SoPh..134...15R

“When the crests of such waves coincide, their amplitudes combine, creating huge standing waves, much steeper than traveling waves. This phenomenon is called “clapotis”. Off the northern tip of New Zealand, where major wave patterns collide in deep water, clapotis is regularly seen. The pinnacling waves formed here have so much vertical power that they can throw a laden kayak clear out of the water.”

Dowd 1981 (not on ADS)

SHOCK GRAIN DIAGNOSIS

Carlsson & Stein *1997ApJ...481..500C*

$$I_\nu(0) = \int_0^\infty S_\nu \ \mathrm{e}^{-\tau_\nu} \ \mathrm{d}\tau_\nu = \int_0^\infty S_\nu \ \tau_\nu \ \mathrm{e}^{-\tau_\nu} \ \frac{\mathrm{d}\ln\tau_\nu}{\mathrm{d}z} \ \mathrm{d}z$$

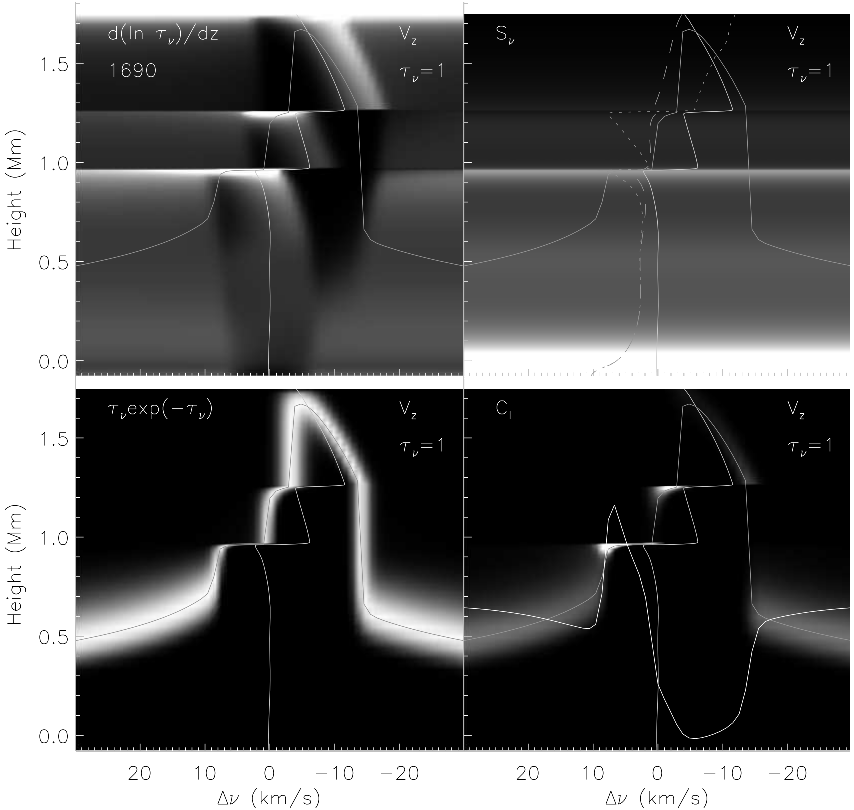

SHOCK-RIDDEN COOL LOWER CHROMOSPHERE

Carlsson & Stein *1995ApJ...440L..29C*

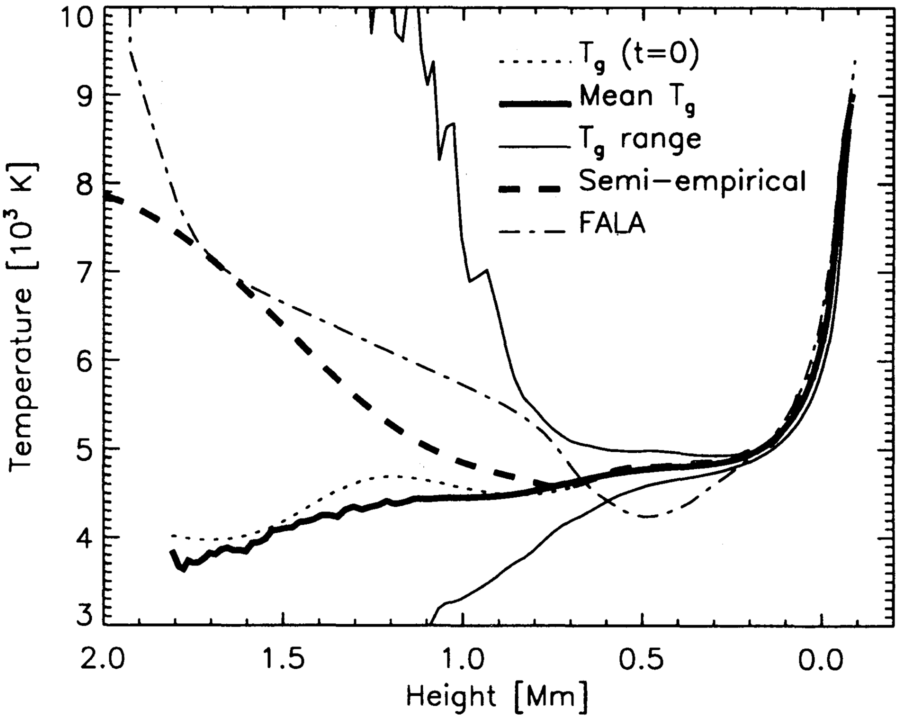

- mean T(h) (thick solid) remains close to RE starting model (dotted)
- bandwidth of T fluctuations (thin solid borders) very large above 1000 km
- a fit of the mean ultraviolet intensities needs a temperature rise (dashed)

SOLAR SPECTRUM FORMATION: EXAMPLES

Robert J. Rutten
https://webspace.science.uu.nl/~rutte101

BIFROST SOLAR-ANALOG STAR

- *Bifrost: a Modular Python/C++ Framework for Development of High-Throughput Data Analysis Pipelines* 2017AAS...22923605C
- *Vertical crustal motion observed in the BIFROST project* 2003JGeo...35..425S
- *BIFROST project: 3-D crustal deformation rates derived from GPS confirm post-glacial rebound in Fennoscandia* 2001EP&S...53..703S
- *"SP.ACE" 2013-2015: ASGARD Balloon and BIFROST Parabolic Flights: Latest Developments in Hands-On Space Education Projects for Secondary School Students* 2015ESASP.730..635D
- *BIFROST: conference hotel in Iceland* (not on ADS)
- Bifrost: computational star in Carlssonscandia, remarkably like the Sun in its spectral characteristics and likewise non-plane-parallel, inconstant, and inconsistent, with the virtue of showing much spatio-temporal fine structure similar to solar fine structure:
  - granules and intergranules
  - acoustic box modes similar to solar p-mode interference patterns
  - non-diagnosed internal gravity waves
  - clapotispheric internetwork shocks
  - magnetic network concentrations
  - dynamic fibrils
  - Ellerman reconnection bursts

  but lacking: spicules-II, long fibrils, k_2 - h_2 peak separation, Si IV in UV bursts, more?
- Bifrost analogs in chromosphere-formation stage: CO5BOLD MURaM Mancha

BIFROST

- *heritage*
  - Nordlund & Stein 3D HD ⇒ granulation
  - Carlsson & Stein 1D HD RADYN ⇒ Ca II H_{2V} shocks
  - Nordlund et al. 2D MHD Stagger ⇒ MCs, internetwork
- *code*
  - Gudiksen et al. 2011A&A...531A.154G Bifrost description
  - Carlsson & Leenaarts 2012A&A...539A..39C cooling + heating approximations
  - Leenaarts et al. 2012A&A...543A.109L fast angle-dependent PRD
  - Martínez-Sykora et al. 2012ApJ...753..161M ambipolar diffusion
  - Pereira et al. 2013A&A...554A.118P 3D simulation better than standard 1D models
  - Olluri et al. 2013AJ....145...72O non-E 3D solver
  - Golding et al. 2014ApJ...784...30G non-E He ionization
  - Carlsson et al. 2016A&A...585A...4C publicly available snapshot
  - Sukhorukov & Leenaarts 2016A&A...597A..46S PRD in 3D simulations
  - Martínez-Sykora et al. 2017ApJ...847...36M 2D (“2.5D”) ion-neutral
  - Leenaarts 2018arXiv180506666L tracer particles ⇒ Lagrangian flow lines
- *warnings*
  - if no Lyα RT no $N_{\rm e}$ boosting from Lyα surround scattering around hot structures
  - 3D RT may be needed (MULTI3D of Leenaarts & Carlsson 2009ASPC..415...87L) beyond columnwise (RH1.5D of Pereira & Uitenbroek 2015A&A...574A...3P)
  - non-E RT may be needed beyond snapshot-wise SE (especially H, He)

BIFROST ANALYSES 1

Hayek et al. 2010A&A...517A..49H solar-type stars

Martínez-Sykora et al. 2011ApJ...732...84M EUV line asymmetries

Leenaarts et al. 2012ApJ...749..136L 3D Hα formation

Stepán et al. 2012ApJ...758L..43S Lyα Hanle

de la Cruz Rodriguez et al. 2012A&A...543A..34D Ca II 8542 Å inversion test

Olluri et al. 2013ApJ...767...43O non-E in O IV ratios

Martínez-Sykora et al. 2013ApJ...771...66M Ca II and Hα from a spicule-II

Leenaarts et al. 2013ApJ...772...89L Mg II h & k for IRIS I

Leenaarts et al. 2013ApJ...772...90L Mg II h & k for IRIS II

Pereira et al. 2013ApJ...778..143 Mg II h & k for IRIS

Hansteen & Archontis 2014ApJ...788L...2A reconnecting strong-field simulation

Olluri et al. 2015ApJ...802....5O optically thin emission lines

Leenaarts et al. 2015ApJ...802..136L Hα fibrils versus field

Stepán et al. 2015ApJ...803...65S scattering polarization Lyα

Pereira et al. 2015ApJ...806...14P MgII triplet formation

Carlsson et al. 2015ApJ...809L..30C Mg II k from plage

Hansteen et al. 2015ApJ...811..106H heating from footpoint braiding

Rathore et al. 2015ApJ...811...81R IRIS C II formation

Guerreiro et al. 2015ApJ...813...61G quiet-Sun heating events

BIFROST ANALYSES 2

Martínez-Sykora et al. 2016ApJ...817...46M non-E Si IV/O IV ratios

Golding et al. 2016ApJ...817..125G non-E He ionization

Nóbrega-Siverio et al. 2016ApJ...822...18N 2D (Hα) surges

Kato et al. 2016ApJ...827....7K waves from magnetic pumping

de la Cruz Rodriguez et al. 2016ApJ...830L..30D Mg II h & k + Mg II triplet inversions

Schmit+DePontieu 2016ApJ...831..158S IRIS Si IV QS internetwork versus IRIS

Leenaarts et al. 2016A&A...594A.104L spatial structure in He I 10830

Schmit & De Pontieu 2016ApJ...831..158S TR emission from internetwork

Martínez-Sykora et al. 2016ApJ...831L...1M 2.5D ambipolar misalignment fibrils-field

Fleischman et al. 2017ApJ...839...30F try NLFFF on Bifrost snapshot

Golding et al. 2017A&A...597A.102G He resonance lines

Kanella & Gudiksen 2017A&A...603A..83K detect reconnection sites and current sheets

Guerreiro et al. 2017A&A...603A.103G small-scale heating events

Martínez-Sykora et al. 2017Sci...356.1269M spicules from ambipolar diffusion

Hansteen et al. 2017ApJ...839...22H generation of bombs and nano/micro-flares

Nóbrega-Siverio et al. 2017ApJ...850..153N 2D non-E Si IV surges

Rouppe van der Voort et al. 2017ApJ...851L...6R plasmoids in UV-burst reconnection

BIFROST ANALYSES 3

Bjørgen et al. 2018A&A...611A..62B Ca II H & K insufficient peak separation

Liu et al. 2018arXiv180402931L automatic swirl detection

Nóbrega-Siverio et al. 2018ApJ...858....8N 2D non-E Si IV, O IVsurges

Martínez-Sykora et al. 2018arXiv180506475M ion-neutral 2D: spicules-II

RECENT DEVELOPMENTS IN PRD LINE SYNTHESIS

- *RH code: Uitenbroek 2001ApJ...557..389U*
  - Rybicky & Hummer: not $\mathbf{\Lambda}(S)$ but $\mathbf{\Psi}(j)$ iteration; preconditioning
  - overlappping lines
  - 1D, 2D, 3D, spherical versions
- *RH 1.5D: Pereira & Uitenbroek 2015A&A...574A...3P*
  - 1.5D $=$ column-by-column
  - massively parallel
  - also molecular lines (but Kurucz lines in LTE)
- *angle-dependent redistribution: Leenaarts et al. 2012A&A...543A.109L*
  - good summary PRD theory and equations
  - non-stationary atmosphere requires angle-dependent PRD
  - hybrid approximation: transform to gas parcel frame, assume angle-averaged PRD ($\approx$ angle dependent from deep isotropy), transform back
- *towards Bifrost PRD: Sukhorukov & Leenaarts 2017A&A...597A..46S*
  - hybrid approximation for small memory
  - linear frequency interpolation for speed
  - 252$\times$252$\times$496 grid, 1024 CPUs: 2 days for Mg II k $\approx$ doable
- *next: 3D PRD with multigrid (Bjørgen & Leenaarts 2017A&A...599A.118B)*

NON-EQUILIBRIUM HYDROGEN IONIZATION IN 1D SHOCKS

Carlsson & Stein *2002ApJ...572..626C*

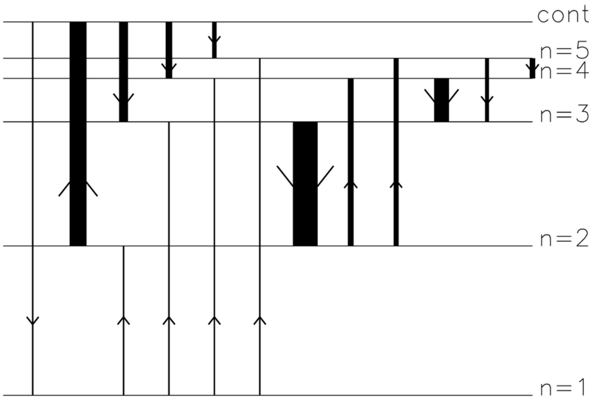

atom top ∼ 3.4 eV alkali: NLTE-SE ionization loop
– driven by photon pumping Balmer continuum, scattering from deep, ≈5300 K, smooth
– closure by photon losses in n_α lines

atom bottom actually up to 10 eV: non-E Lyα
– tremendous scatttering from small ε
– tremendous opacity from huge H abundance
– small structures already detailed radiative balance
– non-E: fast settling at high T, slow at low T

- RADYN code: 1D(t) hydrodynamics, time-dependent, NLTE radiation, simple PRD
- observed subphotosphere piston drives acoustic waves up that shock near $h = 1000$ km
- Lyα scatters in radiative balance and controls $n = 2$. Within shocks $S \approx J$ saturates to B from radiation lock-in (increased ε from partial hydrogen ionization) so that $b_2 \approx 1$
- collisional Lyα balancing has Boltzmann temperature sensitivity: fast (seconds) in hot gas, slow (minutes) in cool gas, resulting in retardation: post-shock cooling gas maintains the high n_2 shock value at increasing b_2 during minutes, up to huge overpopulation ($b_2 \approx 10^{10}$)
- ionization from $n = 2$: instantaneous statistical-equilibrium balance driven by Balmer continuum $J \neq B$ and closed by cascade recombination, with $b_{\rm cont}/b_2 \approx 10^{-1}$ in hot and $\approx 10^{+3}$ in cool gas, the latter adding to much larger retarded b_2
- between shocks hydrogen remains hugely overionized versus SE and LTE predictions

DETAILED BALANCING

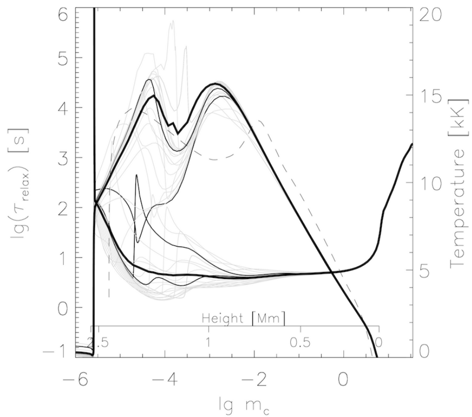

Hydrogen ionization/recombination relaxation timescale throughout the solar-like shocked Radyn atmosphere. The timescale for settling to equilibrium at the local temperature is very long, 15–150 min, in the chromosphere but much shorter, only seconds, in shocks in which hydrogen partially ionizes.
Carlsson & Stein 2002ApJ...572..626C

net radiative and collisional downward rates (Wien approximation)

$$n_u R_{ul} - n_l R_{lu} \approx \frac{4\pi}{h\nu_0}\, n_l^{\rm LTE}\, b_u\, \sigma^l_{\nu_0} \left(B_{\nu_0} - \frac{b_l}{b_u} \overline{J}_{\nu_0} \right) \qquad \text{zero for } S = \overline{J}, \text{ no heating/cooling}$$

$$n_u C_{ul} - n_l C_{lu} = n_l C_{lu} \left(\frac{b_u}{b_l} - 1 \right) = b_u n_l^{\rm LTE} C_{lu} \left(1 - \frac{b_l}{b_u} \right) \qquad \text{zero for } b_u = b_l, \text{ LTE } S^l$$

dipole approximation for atom collisions with electrons (Van Regemorter 1962)

$$C_{ul} \approx 2.16 \left(\frac{E_{ul}}{kT} \right)^{-1.68} T^{-3/2} \frac{g_l}{g_u}\, N_{\rm e}\, f$$

Einstein relation

$$C_{lu} = C_{ul} \frac{g_l}{g_u}\, {\rm e}^{-E_{ul}/kT}$$

C_{ul} is not very temperature sensitive (any collider will do); C_{lu} has Boltzmann sensitivity

NON-E HYDROGEN IONIZATION IN 2D MHD SHOCKS

Leenaarts et al. *2007A&A...473..625L*

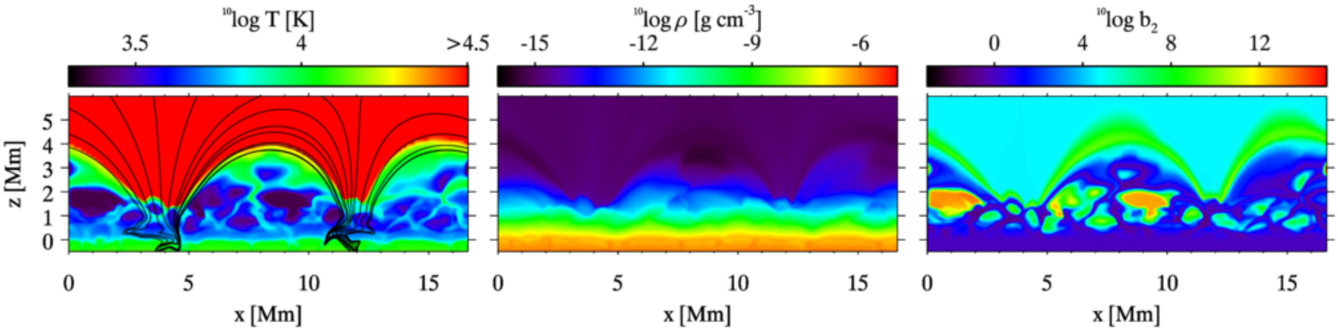

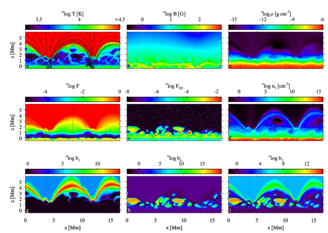

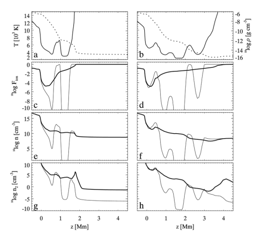

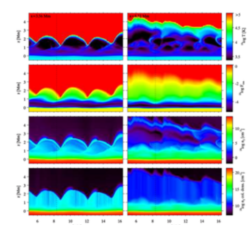

- in shocks Lyα has $S\!\approx\!B$ from high T (fast balancing) and N_e (10% H ionization)
- retarded collisional balancing in Lyα: n_2 hangs near high shock value $n_2 \approx n_2^{\rm LTE}$
- gigantic post-shock $n\!=\!2$ overpopulations versus LTE (“S-B underestimates”)
- yet larger post-shock overionization from hydrogen-top Balmer balancing
- no Lyman RT: green arches artifacts, no lateral $N_{\rm e}$ boost from Lyα scattering

Hα IN BIFROST

1D plane-parallel SE: Rutten & Uitenbroek 2012A&A...540A..86R

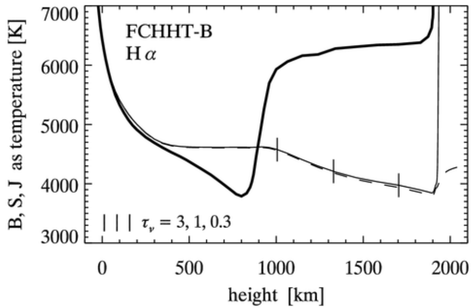

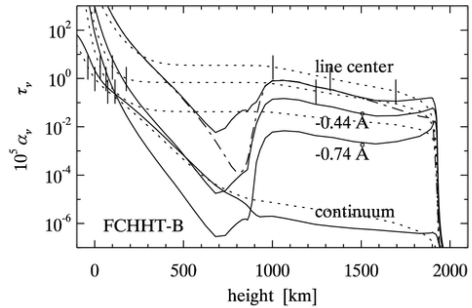

3D non-E MHD: Leenaarts et al. 2012ApJ...749..136L

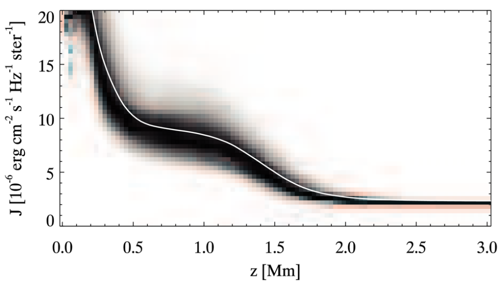

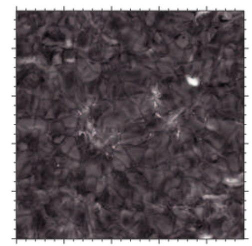

- Hα is a pure scattering line with $S \approx J$ and a deep opacity dip in the upper photosphere
- 3D scattering across the opacity gap enhances fibril visibility
- core darkness measures density, core width measures temperature
- caveats: Bifrost snapshot, no non-E RT, lacking spicules-II, long fibrils

OSLO SIMULATION VERSUS 1D STANDARD MODELS

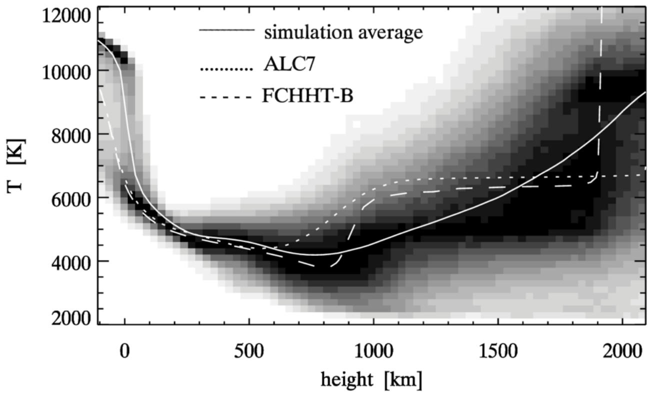

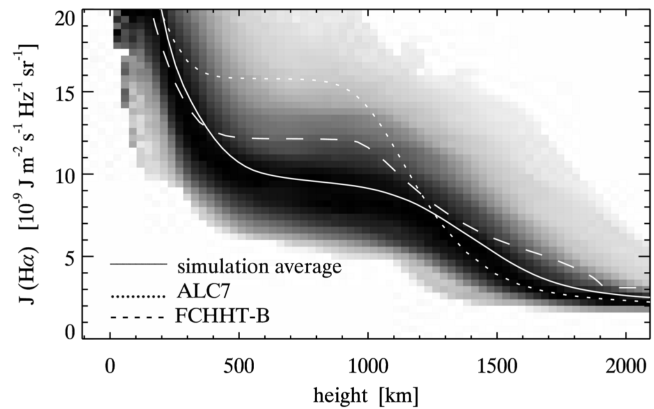

- simulation = state-of-the-art: 3D(t), $\vec{B}$, non-HE, SE populations but NE for H
  Leenaarts, Carlsson & Rouppe van der Voort 2012ApJ...749..136L
- ALC7 = UV fit: 1D static, no $\vec{B}$, HE + microturbulence, SE populations
  Avrett & Loeser 2008ApJS..175..229A
- FCHHT-B = UV fit: 1D static, no $\vec{B}$, HE + imposed acceleration, SE populations
  Fontenla, Curdt, Haberreiter, Harder & Tian 2009ApJ...707..482F

The T and $J_\nu(\mathrm{H}\alpha)$ behavior seems arguably similar. However, the conceptual differences between plane-parallel static hydrostatic-equilibrium modeling and the 3D(t) MHD simulation are enormous (cf. Newtonian gravitation versus general relativity). The $T(h)$ stratifications in the simulation vary tremendously, with shocks propagating upwards and sideways and the increase to coronal temperature dancing up and down over a large height range.

He I and He II

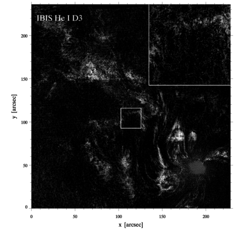

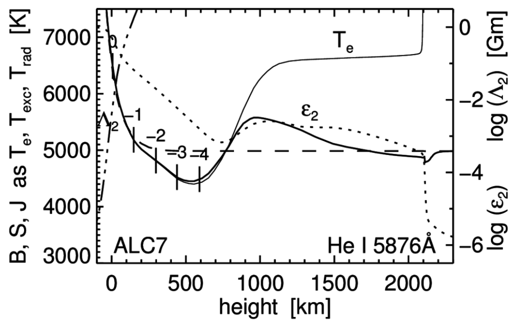

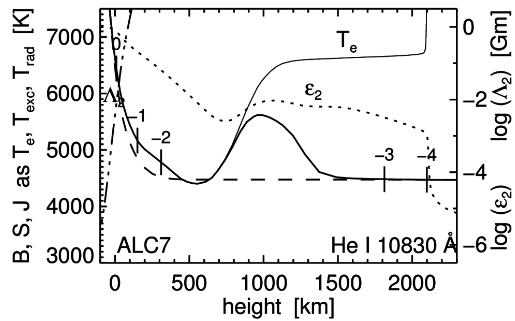

- optical He I lines: nothing in ALC7, nor in atlases, nor in Moore-Minnaert-Houtgast
- more complex non-E formation than H I: not only He I 584 acting as Lyα but ionization/recombination not limited to the atom top as for H I (smooth Balmer continuum driving from below) but sensing hot and structured irradiation from above
- see Bifrost He papers and more to come
- to-do for 2018 $=$ 150 years after Lockyer: explain He I D_3 in flash spectrum

  long dark Hα-like He II 304 fibrils also memorial-opacity contrails?

HYDROGEN AUREOLE BOOSTING IN COOL GAS BESIDE HOT GAS

Fontenla et al. 2009ApJ...707..482F *Rutten & Uitenbroek* 2012A&A...540A..86R *Rutten* 2016A&A...590A.124R

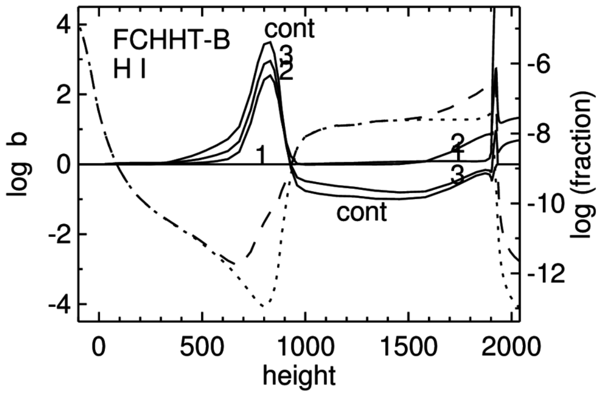

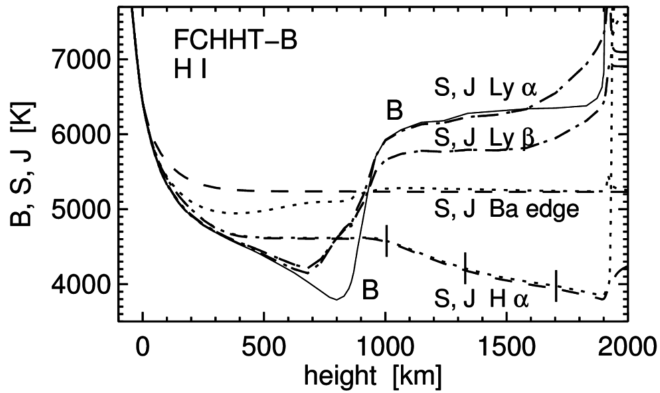

FCHHT-B: steep B rises to chromosphere and corona emulate adjacent cool and hot features

Lyα: scattering back-radiation boosts $S_{\mathrm{Ly}\,\alpha}{\approx}J_{\mathrm{Ly}\,\alpha}$ and Hα extinction $\propto b_2 \approx S_{\mathrm{Ly}\,\alpha}/B_{\mathrm{Ly}\,\alpha}$ towards hot-feature value (left: dotted $n_2^{\mathrm{LTE}}/N_{\mathrm{Htot}}$, dashed actual n_2/N_{Htot})

ionization: also b_2-boosted, with additional b_{cont}/b_2 offset defined by the Balmer continuum

Lyβ: b_3 between b_2 and b_{cont} and sharing Hα photon losses

Hα: the FCHHT-B chromosphere is a back-scattering attenuator just as in the ALC7 atmosphere. The b_2 peak from Lyα irradiation does not affect Hα because even with this boost the Hα extinction in the temperature miminum remains negligible.

A hot feature embedded in cooler gas has a similar Lyα scattering aureole enhancing H ionization and Hα extinction around it. A temporary hot disturbance leaves such spread-out boost behind (a wake when moving).

Hα EXTINCTION RECIPE

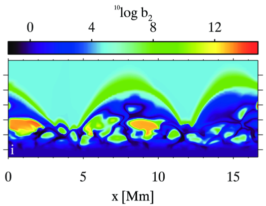

- *retarded Lyα balancing: extinction memory of hot moments*
  - $n_2 \approx n_2^{\rm LTE}$ in hot shocks from fast Lyα balancing and increased ε
  - n_2 decays slowly, tracking high shock values
  - gigantic b_2 in post-shock cooling clouds until next shock

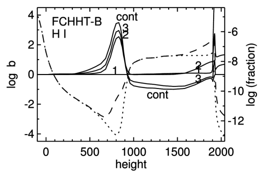

- *Lyα scattering: aureole boosting*
  - Lyα scattering defines $S_{\rm Ly} \approx J_{\rm Ly}$ with radiative balance
  - hot features in cool gas have Lyα scattering aureoles
  - H I top ($n \geq 2$ including $n_{\rm ion}$) boosted in aureoles

- *Hα extinction recipe*
  - find hottest instance nearby ($\sim$300 km) and in recent past ($\sim$minutes)
  - compute Saha-Boltzmann fractional n = 2 population then and there
  - use this extinction value in cooler gas around it and afterwards
  - small hot features leave wider Hα marks (as the grin of the Cheshire cat)
  - fast small hot features leave wider Hα trails (as contrails from jet engines)

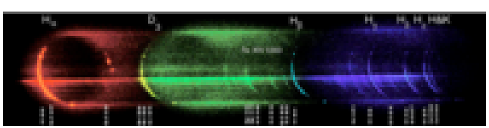
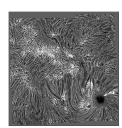
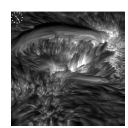
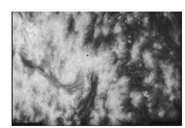
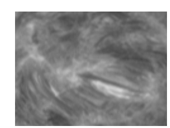

SAHA-BOLTZMANN FOR CHROMOSPHERIC LINES

Rutten 2016A&A...590A.124R

Bachelor exercise "Cecilia Payne": compute N_e and κ^LTE for given $N_\mathrm{H\_total}$

"I taught making Saha-Boltzmann graphs to hundreds of students at Utrecht and elsewhere with a lab exercise "Cecilia Payne" (available on my website). It uses a fictitious and unpronounceable didactic element called "Schadeenium" after Utrecht astrophysicist Aert Schadee (1936–1999), who invented it for teaching in the 1970s."

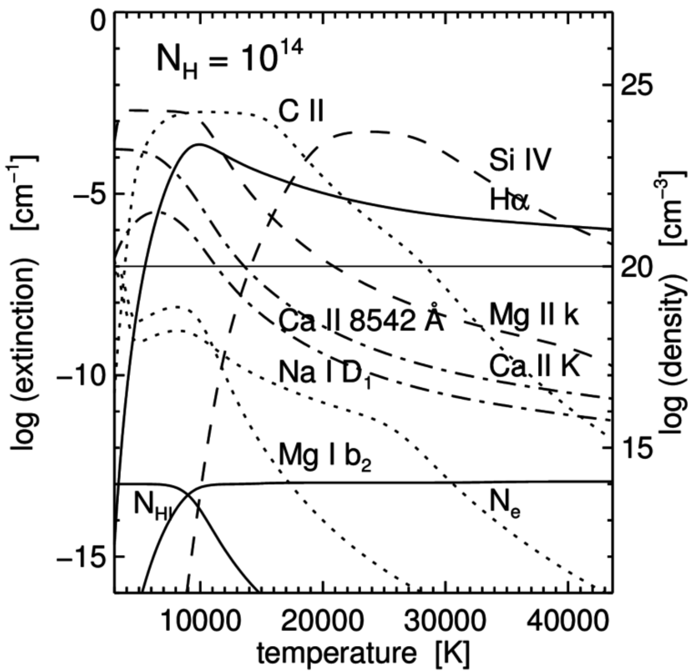

CORONAL EQUILIBRIUM VERSUS SAHA-BOLTZMANN IONIZATION

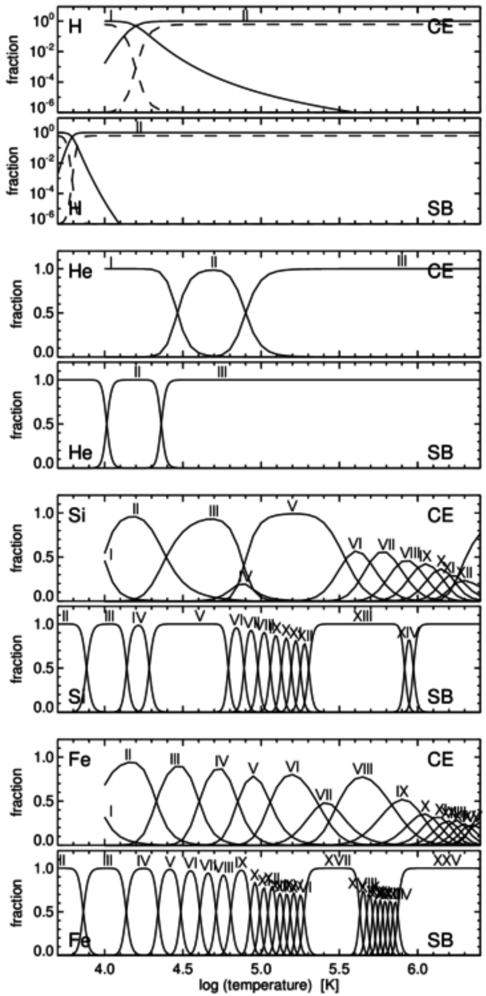

Rutten + Rouppe van der Voort *2017A&A...597A.138R*
"Carole Jordan versus Cecilia Payne"

- *CE*
  - up: collisional excitation/ionization
  - down: radiative deexcitation/recombination
  - NB: dielectronic recombination
- *SB*
  - up: collisional excitation/ionization
  - down: collisional deexcitation/recombination
- $N_\mathrm{e} = 10^{14}$ (other densities)
  - SB: N_e affects ionization, not excitation
  - CE: N_e affects excitation, not ionization
  - smaller N_e: SB peaks steepen and shift left
- *hydrogen*
  - long H I tail from no H III (log scales)
  - still competitive at $10^{-5} \approx$ others
- *Mg III, C V, Si V, Si XIII, Fe XVII, Fe XXV*
  - wide hump from closed shell (atom configs)
  - extra recombination radiation into previous ion

ELLERMAN BURSTS OVERVIEW

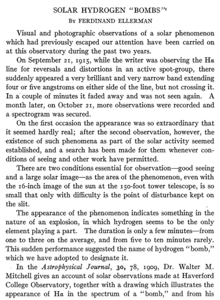

SOLAR HYDROGEN "BOMBS"[1]

By FERDINAND ELLERMAN

Visual and photographic observations of a solar phenomenon which had previously escaped our attention have been carried on at this observatory during the past two years.

On September 21, 1915, while the writer was observing the Hα line for reversals and distortions in an active spot-group, there suddenly appeared a very brilliant and very narrow band extending four or five angstroms on either side of the line, but not crossing it. In a couple of minutes it faded away and was not seen again. A month later, on October 21, more observations were recorded and a spectrogram was secured.

On the first occasion the appearance was so extraordinary that it seemed hardly real; after the second observation, however, the existence of such phenomena as part of the solar activity seemed established, and a search has been made for them whenever conditions of seeing and other work have permitted.

There are two conditions essential for observation—good seeing and a large solar image—as the area of the phenomenon, even with the 16-inch image of the sun at the 150-foot tower telescope, is so small that only with difficulty is the point of disturbance kept on the slit.

The appearance of the phenomenon indicates something in the nature of an explosion, in which hydrogen seems to be the only element playing a part. The duration is only a few minutes—from one to three on the average, and from five to ten minutes rarely. This sudden performance suggested the name of hydrogen "bomb," which we have adopted to designate it.

In the *Astrophysical Journal*, **30**, 78, 1909, Dr. Walter M. Mitchell gives an account of solar observations made at Haverford College Observatory, together with a drawing which illustrates the appearance of Hα in the spectrum of a "bomb," and from his

- Mount Wilson: solar hydrogen bombs
  Ellerman *1917ApJ....46..298E* ADS citation history (100=100?)
  - sudden brightenings in Hα wings
  - not in line core, only in Balmer and Ca II lines
  - between spots in complex emerging active regions

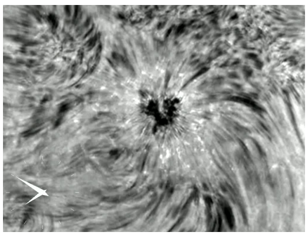

- DOT: pseudo Ellerman bombs
  Leenaarts et al. *2006A&A...449.1209L* *2006A&A...452L..15L*
  Rutten et al. *2013JPhCS.440a2007R*
  - magnetic concentrations in sunspot moat
  - Spruit hole radiation plus small collisional damping
  - Hα blue-wing BPs better than G-band BPs

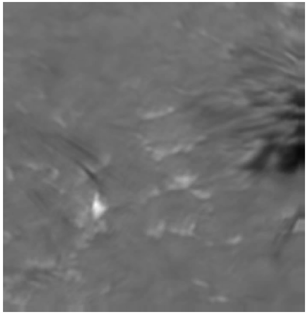

- SST: true Ellerman bombs
  Watanabe et al. *2011ApJ...736...71W*
  - photospheric jets in rapid succession along network
  - shielded in Hα core by overlying fibrils
  - photospheric strong-field reconnection?
- interpretation: *reconnection per cartoon*

ELLERMAN BOMB VISIBILITIES

Rutten *2016A&A...590A.124R*

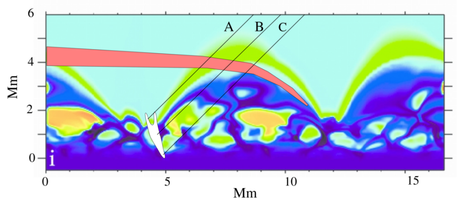

- *observations*
  - Ellerman bomb: Hα moustaches below core fibrils [example] [movie]
  - also bright but different in Ca II 8542 Å [example]
  - also bright but diffuse in AIA 1700 and 1600 Å [example]
  - not in optical continuum nor Fe I, Na I D, Mg I b lines [example]
  - also bright in IRIS C II and Si IV lines [example]
  - hot FAF-like aftermaths with cool blends [example] [EBs vs FAFs]
- *visibility recipes*
  - Balmer in hot and dense onsets: Saha-Boltzmann extinction
  - cooling aftermaths: long Balmer memory of large onset extinction
  - Hα wings: electron broadening (Stark + Holtsmark)
  - transition-region lines: at large $N_{\rm e}$ extinction closer to SB then CE
  - "cool" blends: surrounding cool clapotisphere in slanted viewing (above)
  - diffuse bright feet in 1700 Å: surround irradiation by EB + bound-free scattering

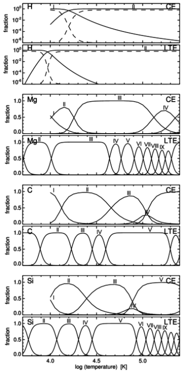

ELLERMAN BOMBS PER LTE

Rutten *2016A&A...590A.124R*

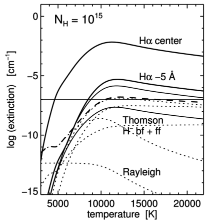

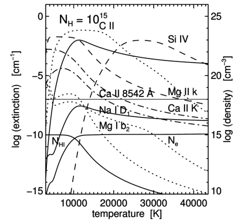

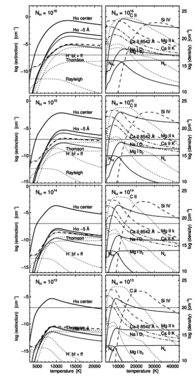

- *Hα*
  - extraordinary hot-gas opacity (large abundance, large excitation energy, no HIII)
  - extraordinary wide wings at large H ionization (Stark + Holtsmark)
  - extraordinary memory for hot past
- *ultraviolet Balmer continuuum*
  - same hot-gas opacity and memory as Hα
  - fibrils transparent so no Stark moustaches needed
  - shielding by surrounding photosphere, but scatter-through in Mg I and Fe I edges
- *other lines*
  - Na I D and Mg I b absent above 10 000 K
  - Si IV absent below 20 000 K but may have hot-past memory in cooling gas
  - EB bottoms shielded by adjacent or overlying cooler gas, except Hα and Si IV

STRAWS / SPICULES-II / RBEs / RREs

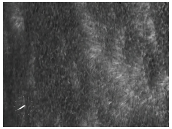

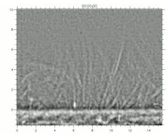

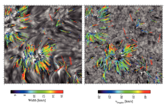

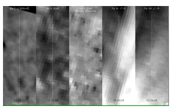

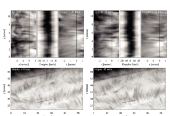

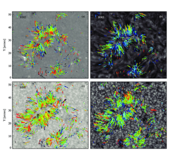

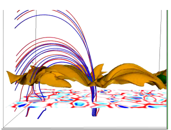

- *observations*
  - "straws", DOT Ca II H
    Rutten 2006ASPC..354..276R
  - "spicules-II", Hinode Ca II H
    De Pontieu et al. 2007Sci...318.1574D
  - "rapid blue excursions", SST Hα
    Rouppe van der Voort et al. 2009ApJ...705..272R
  - "coronal heating events", Hinode Hα + SDO EUV
    De Pontieu et al. 2011Sci...331...55D
  - "torsion-swaying jets", SST Hα + Ca II 8542 Å
    De Pontieu et al. 2012ApJ...752L..12D
  - "rapid red excursions", SST Hα
    Sekse et al. 2013ApJ...769...44S
- *simulation: Martínez-Sykora et al. 2011ApJ...736....9M*
  - feature called a spicule-II but questionable
  - no others in simulations so far
  - driver unknown (Pereira et al. 2012ApJ...759...18P)
- *upshot: ubiquitous small magnetic heating events possibly important in*
  - quiet-sun (also unipolar) coronal heating
  - fast solar wind driving
  - solar wind element segregation

LONG FIBRILS AS CONTRAILS

Rutten & Rouppe van der Voort *2017A&A...597A.138R*

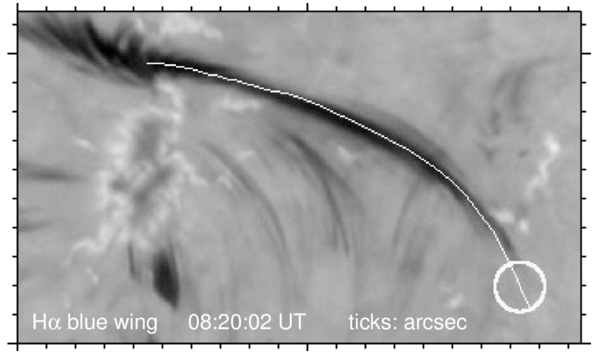

- Hα blue wing: fantail with slender extending dark thread $=$ wide blueshifted core
- visible in IRIS 1400 Å (Si IV), AIA 304, 171, 193 Å, not in Ca II 8542 Å $=$ hot
- three-four minutes later dark Hα core fibril $=$ non-E H recombination

- large non-E Hα opacity in cooling post-hot-disturbance gas
- fibril $\sim$ contrail: not representing cool present but much hotter precursor past
- line-tying by precursor H ionization: contrail maps preceding field topography

SAHA-BOLTZMANN HYDROGEN EXTINCTION AT ALMA WAVELENGTHS

Rutten *2017A&A...598A..89R* *2017IAUS..327....1R* *(tutorial)*

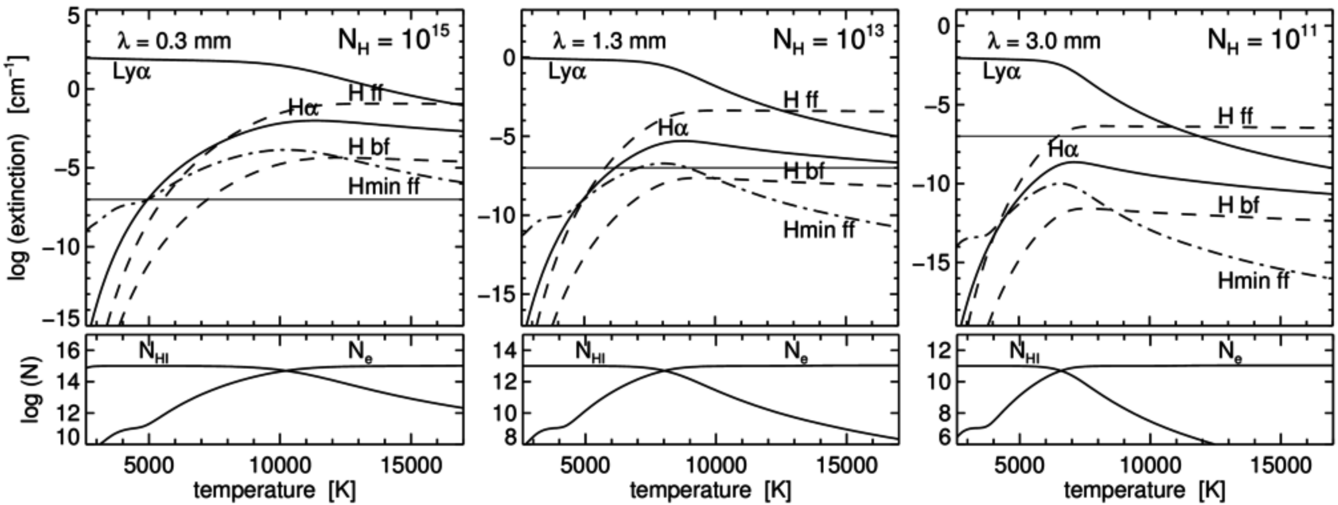

- LTE extinction: Lyα Hα H I continua H$^-$ ff continuum 8542 other lines
- Hα at high T: LTE extinction from $n_2 \approx n_2^{\rm LTE}$ enforced by enclosed Lyα
- H ionization: $n = 2$ population fixed by (actually non-E) Lyα; hydrogen top has additional NLTE-SE balancing between Balmer continum and Balmer lines
- Balmer continuum $T_{\rm rad} \approx$ 5250 K: overionization below, underionization above
  $\Rightarrow$ de-steepening of these LTE H ff Boltzmann increases around 5250 K pivot
- $\alpha_\nu^{\rm ff} \sim \lambda^2 N_{\rm e} N_{\rm ion}\, T^{-3/2}$ (RTSA Eq. 2.79) gives steep H ff increase between ALMA bands
- features with non-E post-hot Hα extinction have larger to very much larger H ff extinction

PREDICTIONS FOR SOLAR ALMA

2017A&A...598A..89R

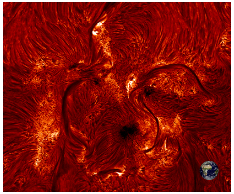

1. ALMA sun mostly covered by long fibrils (unlike simulated suns)
2. similar to Hα, good dark–dark correspondence, more opaque at longer ALMA wavelengths, less lateral contrast (no Dopplershifts)
3. temperatures: above 10 000 K in heating events propagating outward from activity, around 7000 K in initial fibrils, cooling down to 5000 K in long contrail fibrils (or less)
4. heating events best detectable with ALMA (if sufficient resolution)
5. if so, darker aureoles vanishing above 15 000 K (Lyα scattering)
6. small precursors produce 0.2–0.5 arcsec Hα and ALMA contrail widths (Lyα scattering)
7. precursors better field mappers than subsequent contrail fibrils (H ionization)
8. internetwork shocks only in quietest areas, with 4000 K cooling clouds (COmosphere)
9. no Ellerman bombs (hidden by fibrils)
10. flaring active-region fibrils poke through (@ measure reconnection temperature)
11. off-limb spicules-II more opaque than in Hα and Ca II H
12. coronal rain much more opaque than in Hα

SOLAR RYDBERG LINES WITH ALMA?

Rutten 2017IAUS..327....1R

- *"linear thermometer"*
  - H^- free-free + H I free-free: $S \equiv B$
  - thick feature: $T_\mathrm{b} = T(\tau_\nu = 1)$
  - thin feature: cloud contribution $\Delta T_\mathrm{b} = \tau T$
- *solar Rydberg lines so far*
  - in μm range Mg I stronger than H I
  - prediction H I α lines $n = 4 - 18$
  - H I 19α, 21α observed at limb
- *H I Rydberg lines with ALMA?*
  - candidate: H I 30α in Band 6 (1.3 mm)
  - much stronger than above predictions from large post-hot non-E extinction?
  - if so, unblendedly present since Mg I etc are not non-E boosted?
  - on disk as $T(\tau_\mu = 1)$ emission at steep $T(\tau)$ gradient
  - at limb as τT extension
  - Zeeman in I and Stokes: super-sensitive chromospheric magnetometer?

NON-EQUILIBRIUM CHROMOSPHERE

cromosphere potpourri

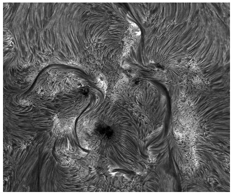

- *Hα chromosphere $=$ past defined by Lyα*
  - long fibrils $=$ post-hot cooling clouds
  - long-fibril contrast $=$ different histories and Dopplershifts
  - long-fibril widths $=$ Lyα scattering (0.2–0.5 arcsec)

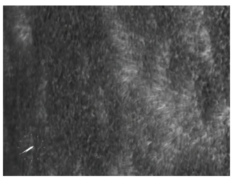

- *Ca II H & K chromosphere $=$ present defined by temperature*
  - thin fibrils $=$ horizontally launched heating events
  - thin-fibril widths $=$ heating-event widths + scattering halo
  - @ corresponding IRIS Si IV, AIA EUV, ALMA mm features?

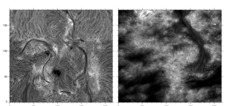

- *Hα versus Lyα $=$ past versus present*
  - Lyα grains $=$ heating events
  - Lyα short fribrils and comet heads $=$ initial tracks
  - @ Lyα, ALMA heating-event imaging spectroscoy?

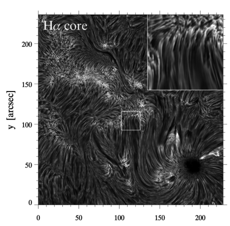

- *Hα versus Ca II 8542 Å versus He I D_3 versus He II 304 $=$ idem*
  - Ca II instantaneous $=$ short fibrils
  - He I $D_3 \sim$ He II 304 $=$ post-hot irradiated cooling gas?
  - @ time-delay image correlations

IRIS DIAGNOSTICS OVERVIEW

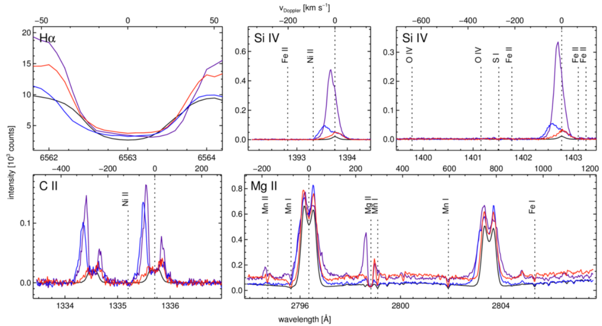

- *Si IV 1400 Å lines*
  - peak ratio 2: feature (not "lines") optically thin
  - if so: faithful Doppler mapping (e.g., EB bimodal jets)
  - gas temperature: 90 kK for CE, 20 kK for SB (ALMA at ratio $\Rightarrow 1$?)
- *Mg II h & k lines*
  - enormous SB opacity
  - strong PRD scatterers
  - SB opacity sampling classical chromosphere top to bottom
- *Mg II triplet lines*
  - bright suggests steep deep temperature rise
  - bright suggests (non-E?) recombination from wide Mg III reservoir
  - Mn I blend $=$ photospheric gas along line of sight

IRIS DIAGNOSTICS

- *Mg II h & k*
  - Leenaarts et al. 2013ApJ...772...89L
  - Leenaarts et al. 2013ApJ...772...90L
  - Pereira et al. 2013ApJ...778..143
  - Carlsson et al. 2015ApJ...809L..30C

- *other lines*
  - Mg II triplet Pereira et al. 2015ApJ...806...14P
  - C II doublet Rathore et al. 2015ApJ...811...80R
  - C II doublet Rathore et al. 2015ApJ...811...81R
  - C II doublet Rathore et al. 2015ApJ...814...70R
  - O I 1355.6 Å Lin et al. 2015ApJ...813...34L

SOLAR SPECTRUM FORMATION: EXAMPLES

Robert J. Rutten
https://webspace.science.uu.nl/~rutte101

thin: cloud modeling corona chromosphere Rydberg per ALMA?

thick: UV line flip VAL3C temperature VAL3C spectrum Kurucz stars

photospheric lines: inversions bright points reversed granulation Na I D1 MGs limb emission lines

continua from VAL3C: Avrett models versus 3D MHD VAL3C continua VALII budget hydrogen budget all

lines from ALC7: model optical spectrum ultraviolet depletion hydrogen strong lines plot formats pops plot BSJ plot profile plot Mg I 4571 Fe I 6302 Mg I b_2 Na I D_1 Ba II 4554 Ca II 8542 Å Ca II K Mg II k Lyα Hα Hβ He I 584 He I 10830 canonical Hα Na I D_1–Mg I b_2 Lyα–Hα Hα–Ca II 8542 Å Ca II K–Mg II k versus FCHHT-B ALC7–FALC FALC–FALP ALC7–FALP

detour lines: pumping suction

Oslo-simulated dynamic atmosphere: 1D RADYN 3D Bifrost Bifrost line synthesis

LA-conjectured PSBE atmosphere: non-E Hα aureole boosting Hα extinction CE–SB EBs spicules-II contrail ALMA non-E chromosphere?

IRIS diagnostics: overview diagnostics

1

SOLAR SPECTRUM FORMATION: EXAMPLES

Robert J. Rutten

https://webspace.science.uu.nl/~rutte101

thin: cloud modeling corona chromosphere Rydberg per ALMA?

thick: UV line flip VAL3C temperature VAL3C spectrum Kurucz stars

photospheric lines: inversions bright points reversed granulation Na I D1 MGs limb emission lines

continua from VAL3C: Avrett models versus 3D MHD VAL3C continua VALII budget hydrogen budget all

lines from ALC7: model optical spectrum ultraviolet depletion hydrogen strong lines plot formats pops plot BSJ plot profile plot Mg I 4571 Fe I 6302 Mg I b_2 Na I D_1 Ba II 4554 Ca II 8542 Å Ca II K Mg II k Lyα Hα Hβ He I 584 He I 10830 canonical Hα Na I D_1–Mg I b_2 Lyα–Hα Hα–Ca II 8542 Å Ca II K–Mg II k versus FCHHT-B ALC7–FALC FALC–FALP ALC7–FALP

detour lines: pumping suction

Oslo-simulated dynamic atmosphere: 1D RADYN 3D Bifrost Bifrost line synthesis

LA-conjectured PSBE atmosphere: non-E Hα aureole boosting Hα extinction CE–SB EBs spicules-II contrail ALMA non-E chromosphere?

IRIS diagnostics: overview diagnostics

start index

2

CLOUD MODELING

review: Tziotziou 2007ASPC..368..217T

Formal solution for line of sight (LOS) through irradiated cloud

$$I_\nu = I_\nu(0)\,e^{-\tau_\nu^c} + \int_0^{\tau_\nu^c} S_\nu(t_\nu)\,e^{-(\tau_\nu - t_\nu)}\,dt_\nu$$

Homogeneous cloud, Gaussian broadening, parameters $I_0(\Delta\lambda)$, S, τ_0, LOS v

$$I(\Delta\lambda) = I_0(\Delta\lambda)\,e^{-\tau(\Delta\lambda)} + S\left(1 - e^{-\tau(\Delta\lambda)}\right) \qquad \tau(\Delta\lambda) = \tau_0\,e^{-\left(\frac{\Delta\lambda - \lambda_0 v/c}{\Delta\lambda_D}\right)^2}$$

$$C(\Delta\lambda) \equiv \frac{I(\Delta\lambda) - I_0(\Delta\lambda)}{I_0(\Delta\lambda} = \left(\frac{S}{I_0(\Delta\lambda} - 1\right)\left(1 - e^{-\tau(\Delta\lambda)}\right)$$

Refinements: Voigt, τ-dependent S, wavelength-dependent S (for PRD with $S \approx S^l$)

Interpretation: $S \Rightarrow (T, \rho)$
- Beckers 1968SoPh....3..367B: Giovanelli NLTE hydrogen ionization tables
- Molowny-Horas et al. 1999A&A...345..618M: "inversion" from many model profiles

Problems: impinging profile, sideways irradiation, multi-thread

start index

3

Hα CLOUD MODELING

Rutten & Uitenbroek 2012A&A...540A..86R

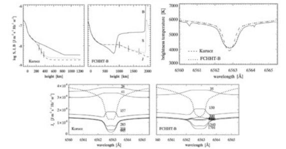

Ha-Ha formation: the Kurucz and FCHHT-B models both reproduce observed Hα

cloud modeling: $I_\nu = I_\nu(0)\,e^{-\tau_\nu^c} + \int_0^{\tau_\nu^c} S_\nu(t_\nu)\,e^{-(\tau_\nu - t_\nu)}\,dt_\nu$

new recipe: for the impinging profile $I_\nu(0)$ take the outward I_ν profile in a RE model at the depth τ_{ν_0} which equals the cloud thickness $\tau^c_{\nu_0}$ (dotted profiles)

start index

4

SOLAR SPECTRUM FORMATION: EXAMPLES

Robert J. Rutten

https://webspace.science.uu.nl/~rutte101

thin: cloud modeling corona chromosphere Rydberg per ALMA?

thick: UV line flip VAL3C temperature VAL3C spectrum Kurucz stars

photospheric lines: inversions bright points reversed granulation Na I D1 MGs limb emission lines

continua from VAL3C: Avrett models versus 3D MHD VAL3C continua VALII budget hydrogen budget all

lines from ALC7: model optical spectrum ultraviolet depletion hydrogen strong lines plot formats pops plot BSJ plot profile plot Mg I 4571 Fe I 6302 Mg I b_2 Na I D_1 Ba II 4554 Ca II 8542 Å Ca II K Mg II k Lyα Hα Hβ He I 584 He I 10830 canonical Hα Na I D_1–Mg I b_2 Lyα–Hα Hα–Ca II 8542 Å Ca II K–Mg II k versus FCHHT-B ALC7–FALC FALC–FALP ALC7–FALP

detour lines: pumping suction

Oslo-simulated dynamic atmosphere: 1D RADYN 3D Bifrost Bifrost line synthesis

LA-conjectured PSBE atmosphere: non-E Hα aureole boosting Hα extinction CE–SB EBs spicules-II contrail ALMA non-E chromosphere?

IRIS diagnostics: overview diagnostics

start index

5

SOLAR ECLIPSE VISIBILITY

P. den Hartog

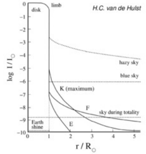

- dusty sky has 0.1 – 0.01% of the solar brighness ($10^{-3} - 10^{-4}$), brighter closer to Sun
- "coronal" blue sky (Rayleigh scattering) is one millionth (10^{-6}), even distribution across sky
- during totality the sky brightness is only one billionth (10^{-9}), less than the coronal brightness
- "K" = continuum component, "F" = Fraunhofer component, "E" = emission-line component
- earthshine (10^{-10}): new-moon brightness from full-earth-with-spot irradiation

start index

6

CORONAL WHITE LIGHT

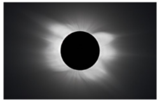

- Walter Grotrian (Potsdam, 1931)
  white ⇒ Thomson scattering of photospheric photons by free electrons
  weak ⇒ low electron density (electron cross-section only 10^{-25} cm^2)
  absence of photospheric Fraunhofer lines ⇒ washed out by large Dopplershifts
  required electron speeds 4000 km/s [⇒ if motions thermal: 1 million degrees !?]
- linear polarisation from right-angle scattering
- fine structure maps variatons in electron density dictated by magnetic fields
- the F component further out results from photon scattering by slower-moving interplanetary dust particles; its spectrum shows the photospheric Fraunhofer lines

Appreciate that during totality you are illuminated by normal photospheric light — but only a 10^{-7} fraction bounced around the moon, without Fraunhofer lines, and polarized too!

start index

7

WHITE LIGHT CORONA

M. Stix "The Sun", Section 9.1.3

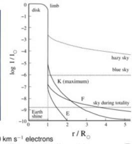

Grotrian (1931): Thomson scattering 8000 km s^{-1} electrons

$$\rho^2 = x^2 + y^2 \qquad I(x) = 2\int_0^\infty j(\rho)\,dy = 2\int_x^\infty \frac{\rho\, j(\rho)}{\sqrt{\rho^2 - x^2}}\,d\rho$$

N_e from inverse Abel transform = isotropically scattered irradiation

$$j(\rho) = -\frac{1}{\pi}\int_\rho^\infty \frac{dI/dx}{\sqrt{x^2 - \rho^2}}\,dx = \sigma_T\,N_e\,\frac{1}{4\pi}\int I_\odot(\theta)\,d\Omega$$

start index

8

"CORONIUM" LINES

M. Stix "The Sun", Section 9.1.3 *http://laserstars.org/spectra/Coronium.html*

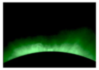

Grotrian (1939), Edlén (1942): forbidden lines high ionization stages (Stix Table 9.2 p. 398)

name	wavelength	identification	$\Delta\lambda_D$	$\overline{v}$	A_{ul}	previous ion	χ_{ion}
green line	530.29 nm	[Fe XIV]	0.051 nm	29 km/s	60 s^{-1}	Fe XIII	355 eV
yellow line	569.45	[Ca XV]	0.087	46	95	Ca XIV	820
red line	637.45	[Fe XI]	0.049	23	69	Fe X	235

Coronal sky at Dome C

start index

9

EUV CORONA

bf equilibria: collisional ionization = radiative recombination ⇒ only $f(T)$, not $f(N_e)$

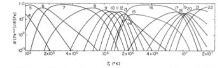

bb equilibria: collisional excitation = spontaneous deexcitation ⇒ $f(T, N_e)$

$$n_l C_{lu} = n_l N_e \int_{v_0}^\infty \sigma_{lu} f(v)\,v\,dv \approx n_u A_{ul} \qquad \sum h\nu \propto \int A_{elem} N_H N_e\,dz \approx \int N_e^2 \left(\frac{dT}{dz}\right)^{-1} dT \equiv EM$$

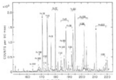

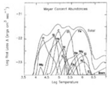

start index

10

BRIGHT AND DARK IN EUV IMAGES

Rutten 1999ASPC..184..181R

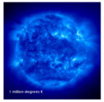

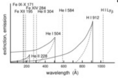

- *iron lines*
  - Fe IX/X 171 Å: about 1.0 MK
  - Fe XII 195 (AIA 193) Å: about 1.5 MK
  - Fe XIV 284 Å: about 2 MK
- *bright*
  - collision up, radiation down
  - thermal photon creation, NLTE equilibrium
  - one line: selected loops = special trees in forest
- *dark*
  - lack of emissivity ("volume blocking"??) or bound-free scattering
  - scattering: radiation up, re-radiation at bound-free threshold = black in narrow passband
  - scattering agents: H I, He I, He II

11

SOLAR SPECTRUM FORMATION: EXAMPLES

Robert J. Rutten
https://webspace.science.uu.nl/~rutte101

thin: cloud modeling corona chromosphere Rydberg per ALMA?

thick: UV line flip VAL3C temperature VAL3C spectrum Kurucz stars

photospheric lines: inversions bright points reversed granulation Na I D1 MGs limb emission lines

continua from VAL3C: Avrett models versus 3D MHD VAL3C continua VALII budget hydrogen budget all

lines from ALC7: model optical spectrum ultraviolet depletion hydrogen strong lines plot formats pops plot BSJ plot profile plot Mg I 4571 Fe I 6302 Mg I b_2 Na I D_1 Ba II 4554 Ca II 8542 Å Ca II K Mg II k Lyα Hα Hβ He I 584 He I 10830 canonical Hα Na I D_1–Mg I b_2 Lyα–Hα Hα–Ca II 8542 Å Ca II K–Mg II k versus FCHHT-B ALC7–FALC FALC–FALP ALC7–FALP

detour lines: pumping suction

Oslo-simulated dynamic atmosphere: 1D RADYN 3D Bifrost Bifrost line synthesis

LA-conjectured PSBE atmosphere: non-E Hα aureole boosting Hα extinction CE–SB EBs spicules-II contrail ALMA non-E chromosphere?

IRIS diagnostics: overview diagnostics

12

NORMAN LOCKYER

wikipedia

Sir Joseph Norman Lockyer, FRS (17 May 1836 – 16 August 1920), known simply as Norman Lockyer, was an English scientist and astronomer. Along with the French scientist Pierre Janssen he is credited with discovering the gas helium.

In 1885 he became the world's first professor of astronomical physics at the Royal College of Science, South Kensington, now part of Imperial College. At the college, the Solar Physics Observatory was built for him and here he directed research until 1913.

To facilitate the transmission of ideas between scientific disciplines, Lockyer established the general science journal Nature in 1869. He remained its editor until shortly before his death.

13

CHROMOSPHERE AND HELIUM NAMING

Abstract of Norman Lockyer's paper read Nov. 26, 1868; Procs. Royal Society of London, 17, 131

ADS 1868RSPS...17..131L courtesy Kevin Reardon 9 cites (7 RR)

Details are given of the observations made by the new instrument, which was received incomplete on the 16th of October. These observations include the discovery, and exact determination of the lines, of the prominence-spectrum on the 20th of October, and of the fact that the prominences are merely local aggregations of a gaseous medium which entirely envelopes the sun. The term *Chromosphere* is suggested for this envelope, in order to distinguish it from the cool absorbing atmosphere on the one hand, and from the white light-giving photosphere on the other. The possibility of variations in the thickness of this envelope is suggested, and the phenomena presented by the star in Corona are referred to.

Two of the lines correspond with Fraunhofer's C and F; another lies 8° or 9° (of Kirchhoff's scale) from D towards E. There is another bright line, which occasionally makes its appearance near C, but slightly less refrangible than that line. It is remarked that the line near D has no corresponding line ordinarily visible in the solar spectrum. The author has

Fraunhofer's "C" is Hα, "F" is Hβ. The non-Fraunhofer line near "D" (Na I D_1 + Na I D_2) for which Lockyer proposed a new element "helios" is He I D_3. The occasional "less refrangible" (redward) line near Hα is He I 6678 Å.

14

SOLAR FLASH SPECTRUM

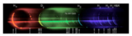

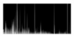

- *chromosphere naming = definition (Lockyer 1868 outside eclipse)*
  - strong: H I Balmer lines, He I D_3, Ca II H & K
  - weaker: Mg I b, Na I D, Sr II, Ba II
- *chromosphere research = flash spectrometry*
  - Menzel thesis = 1898–1908 Campbell 1930PLicO..17....1M (302 pp, on ADS)
  - Thomas & Athay book = 1952 HAO 1961psc..book.....A (422 pp, not on ADS)
  - Dunn et al. = 1962 HAO 1968ApJS...15..275D (275 pp, on ADS; RR digitized)
- *chromosphere = enigma*
  - flash spectrum ≠ reversed disk spectrum
  - both hot (He I D_3) and cool (Na I D_1 & D_2) lines
  - spatial extent exceeds radiative-equilibrum scale height

15

ECLIPSE WISDOM

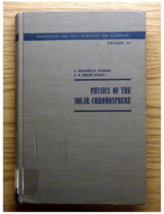

16

ANNOTATION IN SACRAMENTO PEAK OBSERVATORY LIBRARY COPY

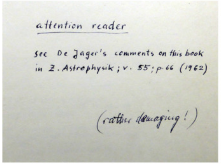

17

De Jager's review (1962ZA.....55...66T + 1962ZA.....55...70W)

Besprechungen

THOMAS, R. N., und R. G. ATHAY: *Physics of the Solar Chromosphere*. X + 422 Seiten. Interscience Publishers, Inc., New York 1961. Geb. $ 15.50.

Der Titel des Buches verspricht mehr, als der Inhalt gibt. Jeder, der schon einmal durch ein Hα-Filter oder durch ein Spektrohelioskop die bezaubernde Struktur der Chromosphärenoberfläche gesehen oder das Profil des Sonnenrandes beobachtet hat, wird — sobald er den Titel „Physik der Chromosphäre" hört — an eine Erklärung der Dynamik dieser Gasmassen denken. Er wird an Probleme der Schall-, Stoß- und Gravitationswellen und an die Dissipation von deren Energie denken. Vielleicht wird er sich fragen, was die Autoren von der Rolle halten, die Magnetfelder und magnetohydrodynamische Wellen spielen und in welchem Maße von ihnen die verschiedenen Strukturen der ruhigen bzw. gestörten Gebiete dieses merkwürdigen Teiles der Sonne bestimmt werden.

Von allem dem wird er aber in diesem Buche nichts finden: Die betreffenden Probleme werden kaum erwähnt, geschweige denn besprochen.

und so weiter... four pages more

Upshot: the book treats the derivation of a model atmosphere from the spectrograms taken by the 1952 HAO eclipse expedition but ignores the inhomogeneity and dynamics of the chromosphere such as sound, shock, gravity and MHD waves, as well as magnetic fields.

18

CHROMOSPHERE POTPOURRI

- *line formation theory*
  - flash spectrum @ Harvard, Boulder ⇒ Mihalas (1970, 1978): summary
  - static 1D "standard" models: VALIIIC more Avrett hydrogen exam
  - non-E: detailed balancing 1D Radyn 2D Stagger 3D Bifrost
- *chromosphere diagnostics*
  - Na I D_1+Mg I b_2 Lyα+Hα Hα+Ca II 8542 Å Ca II H & K+Mg II h & k Si IV mm He I+He II
- *chromospheric & coronal heating ingredients*
  - gravity waves
  - acoustic waves
  - Alfvénic waves
  - reconnection
- *fine structure*
  - sketched: Noyes 1979 Gabriel 1976 Rutten 1998 Wedemeyer 2016 Rutten 2016
  - observed and explained: Ca II grains dynamic fibrils
  - observed but not explained: straws/spicules-II/RBEs/RREs long Hα fibrils
  - fibril-field alignment for NLFFF: yes partly only at launch?

19

SOLAR SPECTRUM FORMATION: EXAMPLES

Robert J. Rutten

https://webspace.science.uu.nl/~rutte101

thin: cloud modeling corona chromosphere Rydberg per ALMA?

thick: UV line flip VAL3C temperature VAL3C spectrum Kurucz stars

photospheric lines: inversions bright points reversed granulation Na I D1 MGs limb emission lines

continua from VAL3C: Avrett models versus 3D MHD VAL3C continua VALII budget hydrogen budget all

lines from ALC7: model optical spectrum ultraviolet depletion hydrogen strong lines plot formats pops plot BSJ plot profile plot Mg I 4571 Fe I 6302 Mg I b_2 Na I D_1 Ba II 4554 Ca II 8542 Å Ca II K Mg II k Lyα Hα Hβ He I 584 He I 10830 canonical Hα Na I D_1–Mg I b_2 Lyα–Hα Hα–Ca II 8542 Å Ca II K–Mg II k versus FCHHT-B ALC7–FALC FALC–FALP ALC7–FALP

detour lines: pumping suction

Oslo-simulated dynamic atmosphere: 1D RADYN 3D Bifrost Bifrost line synthesis

LA-conjectured PSBE atmosphere: non-E Hα aureole boosting Hα extinction CE–SB EBs spicules-II contrail ALMA non-E chromosphere?

IRIS diagnostics: overview diagnostics

start index

20

SUMMARY 1D SCATTERING SOURCE FUNCTIONS

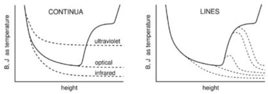

- *continua*
  - optical: $J \approx B$ for radiative equilibrium
  - ultraviolet: $S \approx J > B \rightarrow$ overionization of minority neutrals
  - infrared: $J < B$ but J doesn't matter since H^-_{ff} and H_{ff} have $S = B$
- *lines*
  - $dB/d\tau = dB/d(\tau^c + \tau^l)$ much less steep, so closer to isothermal $S \approx \sqrt{\varepsilon}\, B$
  - for stronger lines S sees more of the model chromosphere
  - PRD lines have frequency-dependent core-to-wing $S \approx J$ curves like these

start index

21

EXPLAIN EVERYTHING – INCLUDING SIMILARITIES AND DIFFERENCES

ALC7: *2008ApJS..175..229A* *FCHHT-B:* *2009ApJ...707..482F* *FALP:* *1993ApJ...406..319F*

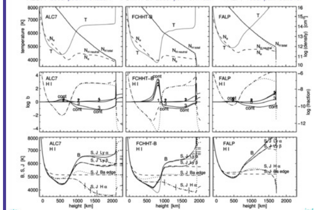

start index

22

DYNAMIC FIBRILS

Hα: *Hansteen et al.* *2006ApJ...647L..73H*, *De Pontieu et al.* *2007ApJ...655..624D* (plage)
Rouppe van der Voort & De la Cruz Rodiguez *2013ApJ...776...56R* (sunspots)
Ca II 8542: *Langangen et al.* *2008ApJ...673.1194L*
Lyα: *Koza et al.* *2009A&A...499..917K*
non-E 2D MHD simulation: *Leenaarts et al.* *2007A&A...473..625L*

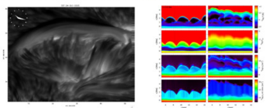

explanation: p-mode-driven 3–5 minute shock waves along inclined field as slanted wave guide with lowered cutoff frequency; fan pattern = surface network strings

Michalitsanos 1973SoPh...30...47M
Bel & Leroy 1977A&A....55..239B
Suematsu 1990LNP...367..211S
De Pontieu et al. *2004Natur.430..536D*

start index

23

CUT-OFF FREQUENCY LOWERING IN INCLINED FIELDS

1973SoPh...30...47M

THE FIVE-MINUTE PERIOD OSCILLATION IN MAGNETICALLY ACTIVE REGIONS

A. G. MICHALITSANOS* **

Institute of Astronomy, University of Cambridge, Cambridge, England

If we incline the magnetic field (with respect to g) through 45 degrees in Figure 1d, we note that in Region I, $\omega(k_x)$ is no longer asymptotic to ω_s as k_x tends to zero. Therefore, for an inclined magnetic field, magnetosonic waves may propagate vertically at frequencies $\omega < \omega_s$. If in Equation (3) we set $a=0$ and $k_x=0$, and let $b = -g\gamma/2V_s^2$ we will obtain the critical magnetosonic-gravity frequency ω_c, where

$$\omega_c^2 = \omega_s^2\left(\frac{1}{2} - \frac{1}{\gamma\beta}\right) + \omega_s^2\left[\left(\frac{1}{\gamma\beta} - \frac{1}{2}\right)^2 + \frac{2\cos^2\theta}{\gamma\beta}\right]^{1/2}, \qquad (4)$$

and $\theta = \arccos(B_z/B_0)$. Therefore, at levels where $\beta < 1$, the critical magnetosonic-gravity frequency is less than the critical sonic-gravity frequency ω_s when the field is inclined from the vertical.

start index

24

STRAWS / SPICULES-II / RBEs

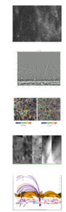

- *observations*
  - "straws", DOT Ca II H
    Rutten *2006ASPC..354..276R*
  - "spicules-II", SST Ca II H
    De Pontieu et al. *2007Sci...318.1574D*
  - on-disk visibility? DOT unpublished
  - "rapid blue excursions", SST Hα
    Rouppe van der Voort et al. *2009ApJ...705..272R*
  - "heating events", Hinode + SDO Hα + EUV
    De Pontieu et al. *2011Sci...331...55D*
- *simulation: Martínez-Sykora et al.* *2011ApJ...736....9M*
  - complex emergence, steep gradients, intense currents
  - spicular Joule heating (green), outflow (blue)
  - nearby coronal loop heating (red)
- *expectations*
  - quiet-sun (also unipolar) coronal heating
  - fast solar wind driving
  - solar wind element segregation

start index

25

DYNAMIC FIBRILS

Hα: *Hansteen et al.* *2006ApJ...647L..73H*, *De Pontieu et al.* *2007ApJ...655..624D* (plage)
Rouppe van der Voort & De la Cruz Rodiguez *2013ApJ...776...56R* (sunspots)
Ca II 8542: *Langangen et al.* *2008ApJ...673.1194L*
Lyα: *Koza et al.* *2009A&A...499..917K*
non-E 2D MHD simulation: *Leenaarts et al.* *2007A&A...473..625L*

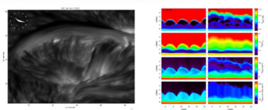

explanation: p-mode-driven 3–5 minute shock waves along inclined field as slanted wave guide with lowered cutoff frequency; fan pattern = surface network strings

Michalitsanos 1973SoPh...30...47M
Bel & Leroy 1977A&A....55..239B
Suematsu 1990LNP...367..211S
De Pontieu et al. *2004Natur.430..536D*

start index

26

FIBRIL–FIELD ALIGNMENT FOR NLFFF LOWER BOUNDARY

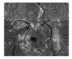

- *NLFFF tests with chromospheric boundary*
  - Na I D_1: Metcalf et al. 1995ApJ...439..474M 2005ApJ...623L..53M
  - Hα: Bobra & van Ballegooijen 2008ApJ...672.1209B Wiegelmann et al. 2008SoPh..247..249W
- *good alignment*
  - Aschwanden et al. 2016ApJ...826...61A
- *partial alignment*
  - de la Cruz Rodríguez & Socas-Navarro 2011A&A...527L...8D
  - Leenaarts et al. 2015ApJ...802..136L
  - Martínez-Sykora et al. 2016ApJ...831L...1M
  - Asensio Ramos et al. 2016arXiv161206088A
- non-E alignment only at H ionization in propagating heating events?

start index

27

Na I D_1 AND Mg I b_2

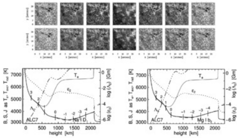

- similar NLTE formation = heavy two-level scattering
- core intensities do not sense ALC7 chromosphere
- narrow Na I D_1 flanks reverse reversed granulation
- non-E? minority stages: recombination $\propto N_e$ senses Lyα settling and scattering
- SST: Dopplergrams ≈ unsigned fluxtube magnetograms (Na I D_1 formation)
  non-E enhanced in cooling recombining downflows? (SE = Bifrost snapshot OK)

start index

Lyα and Hα

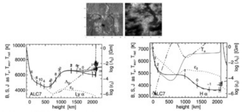

- both: heavy NLTE scatterers with $S \approx J$
- Lyα: boxed-in by enormous extinction ⇒ radiative detailed balance: $S = J$
  in shocks (≈ ALC7 chromosphere) collisional thermalization: $b_2 \approx b_1$
  in cool gas surroundng hot structures $b_2 \gg 1$ from Lyα surround scattering
  in post-hot cool gas slow $S \approx J$ thermalization with $b_2 \gg 1$: S^l memory of hot past
- Hα: photons created in granulation
  scatter 3D across upper-photosphere opacity gap and through chromosphere
  in shocks etc. Boltzmann extinction $b_2 \approx b_1$
  in post-hot cool gas $b_2 \gg 1$: extinction memory of hot past

Lyα scene: heating events bright down-throat, cooling contrails dark from scattering
Hα scene: RBE/RRE heating events, cooling contrails dark from non-E opacity

28 start index

Hα and Ca II 8542 Å

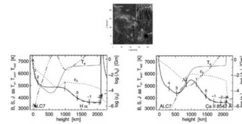

- both: heavy NLTE scatterers with $S \approx J$ sampled at similar $\tau = 1$ heights
- both: Saha-Boltzmann or larger extinction in shocks and ALC7
- core widths: both decrease away from network = decreasing temperature
- Hα fibrils extend further, contradicting Saha-Boltzmann extinction sensitivities

fibril opacity in Ca II 8542 Å instantenous, in Hα post-hot non-E?

29 start index

Ca II H & K and Mg II h & k

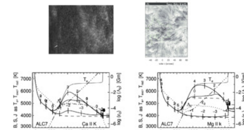

- both: heavy NLTE scatterers with PRD source function splits
- both: near-Saha-Boltzmann extinction everywhere; abundance ratio 18
- both: absence of non-E sensitivities = instantaneous chromosphere
- both: slender fibrils emanating from network, in Ca II H & K better at narrower bandwidth, in Mg II k best in k_3 peak separation

slender fibrils = propagating heating events?

30 start index

CLOSED AND OPEN QUIET-SUN INTERNETWORK IN Si IV

Peter et al. in preparation

- thin to thickish (ratio < 2) line formation
- Gaussian fits
- widths ≈ non-thermal widths

redshifted fibrils away from network ≈ recombining Hα contrails?

roundish coronal-hole blueshifts in network = down-throat heating events?

31 start index

SAHA-BOLTZMANN HYDROGEN EXTINCTION AT ALMA WAVELENGTHS

Rutten 2017A&A...598A..89R 2017IAUS..327....1R (tutorial)

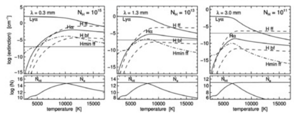

- LTE extinction: Lyα Hα H I continua H$^-$ ff continuum 8542 other lines
- Hα at high T: LTE extinction from $n_2 \approx n_2^{\rm LTE}$ enforced by enclosed Lyα
- H ionization: $n = 2$ population fixed by (actually non-E) Lyα; hydrogen top has additional NLTE-SE balancing between Balmer continum and Balmer lines
- Balmer continuum $T_{\rm rad} \approx$ 5250 K: overionization below, underionization above ⇒ de-steepening of these LTE H ff Boltzmann increases around 5250 K pivot
- $\alpha_\nu^{\rm ff} \sim \lambda^2 N_{\rm e} N_{\rm ion} T^{-3/2}$ (RTSA Eq. 2.79) gives steep H ff increase between ALMA bands
- features with non-E post-hot Hα extinction have larger to very much larger H ff extinction

32 start index

SOLAR RYDBERG LINES WITH ALMA?

Rutten 2017IAUS..327....1R

- *"linear thermometer"*
  - H$^-$ free-free + H I free-free: $S \equiv B$
  - thick feature: $T_{\rm b} = T(\tau_\nu = 1)$
  - thin feature: cloud contribution $\Delta T_{\rm b} = \tau T$
- *solar Rydberg lines so far*
  - in μm range Mg I stronger than H I
  - prediction H I α lines $n = 4 - 18$
  - H I 19α, 21α observed at limb
- *H I Rydberg lines with ALMA?*
  - candidate: H I 30α in Band 6 (1.3 mm)
  - much stronger than above predictions from large post-hot non-E extinction?
  - if so, unblendedly present since Mg I etc are not non-E boosted?
  - on disk as $T(\tau_\mu = 1)$ emission at steep $T(\tau)$ gradient
  - at limb as τT extension
  - Zeeman in I and Stokes: super-sensitive chromospheric magnetometer?

33 start index

SOLAR ULTRAVIOLET SPECTRUM

Scheffler & Elsässer, courtesy Karin Muglach

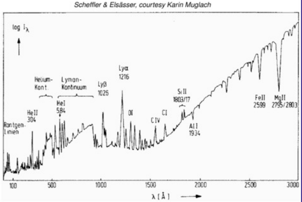

34 start index

VALIIIC MODEL

Vernazza, Avrett, Loeser 1981ApJS...45..635V

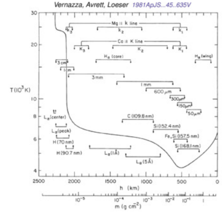

35 start index

VALIIIC SPECTRUM FORMATION

Avrett 1990IAUS..138....3A

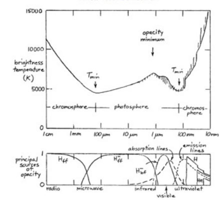

36 start index

37

KURUCZ STARS

Kurucz ATMOS program = *LTE–RE–HE* 1979ApJS...40....1K

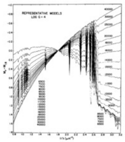

- color $M_V - M_{1.8}$
- $1/\lambda = 1.8\ \mu\mathrm{m}^{-1}$: $\lambda = 555$ nm = UBV color V
- Balmer edge at $1/\lambda = 2.74\ \mu\mathrm{m}^{-1}$
- Paschen edge at $1/\lambda = 1.22\ \mu\mathrm{m}^{-1}$

start index

38

SOLAR SPECTRUM FORMATION: EXAMPLES

Robert J. Rutten

https://webspace.science.uu.nl/~rutte101

thin: cloud modeling corona chromosphere Rydberg per ALMA?

thick: UV line flip VAL3C temperature VAL3C spectrum Kurucz stars

photospheric lines: inversions bright points reversed granulation Na I D1 MGs limb emission lines

continua from VAL3C: Avrett models versus 3D MHD VAL3C continua VALII budget hydrogen budget all

lines from ALC7: model optical spectrum ultraviolet depletion hydrogen strong lines plot formats pops plot BSJ plot profile plot Mg I 4571 Fe I 6302 Mg I b$_2$ Na I D$_1$ Ba II 4554 Ca II 8542 Å Ca II K Mg II k Lyα Hα Hβ He I 584 He I 10830 canonical Hα Na I D$_1$–Mg I b$_2$ Lyα–Hα Hα–Ca II 8542 Å Ca II K–Mg II k versus FCHHT-B ALC7–FALC FALC–FALP ALC7–FALP

detour lines: pumping suction

Oslo-simulated dynamic atmosphere: 1D RADYN 3D Bifrost Bifrost line synthesis

LA-conjectured PSBE atmosphere: non-E Hα aureole boosting Hα extinction CE–SB EBs spicules-II contrail ALMA non-E chromosphere?

IRIS diagnostics: overview diagnostics

start index

39

THE MOST SUCCESSFUL INVERSION EVER

Holweger 1967ZA.....65..365H (243 cites); Holweger & Müller 1974SoPh...39...19H (over 800 cites)

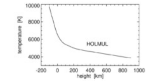

- PhD thesis: empirical LTE fit of the optical continuum and the depths of 900 lines
- very similar to subsequent "theoretical" radiative-equilibrium models
- HOLMUL = update (fitting Ba II lines) prefered in all pre-Asplund abundance determinations *because* it has no chromosphere – but also no granulation
- *"[...] Among the problems that need further study are deviations from LTE. Unfortunately, these are easily arising in the computer if important collisional processes are neglected, or if radiative rates are not realistic. In cool stars, collisional excitation by hydrogen atoms is generally neglected [...] However, in the Sun, hydrogen atoms outnumber the free electrons by a factor of 10000. The UV radiation field is complicated by a vast number of absorption lines ..."*

start index

40

NLTE MASKING

Rutten & Kostik 1982A&A...115..104R

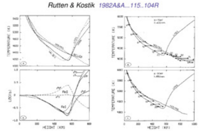

- VALIIIC ≈ LITES steeper decline than HOLMUL ≈ BELLEA
- ultraviolet bf scattering causes Fe I underopacities
- strong-line bb scattering causes Fe I source function deficits
- ultraviolet bb pumping causes Fe II source function excesses
- empirical LTE line depth fitting á la Holweger:
  - opacity-deficient Fe I cores suggest too small height
  - scattering Fe I cores suggest too low temperature
  - pumped Fe II cores suggest too high temperature

start index

41

MILNE-EDDINGTON APPROXIMATION IN A MURaM SIMULATION

Vitas et al. 2009A&A...499..301V

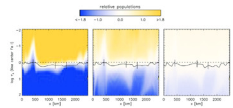

- representative weak Fe I line with excitation energy 0, 3, and 6 eV; transition probability scaled to obtain the same emergent line strength
- dotted curve: line-center $\tau = 1$ (normalization) solid curve: continuum $\tau = 1$. Its modulation represents line-core Doppler brightening. The line vanishes from ionization within a magnetic concentration at $x = 400$ km
- first panel: increasing Fe ionization and corresponding H$^-$ increase at larger depth cause very steep gradients in normalized populations $\sim \eta \equiv \alpha^l/\alpha^c$
- other panels: increasing compensation from Boltzmann excitation factor
- upshot: Milne-Eddington approximation better at higher excitation

start index

42

ULTRAVIOLET DEPLETION IN THE ALC7 ATMOSPHERE

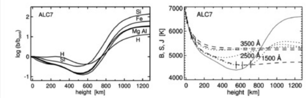

minority atoms: photospheric extinction depletion by ultraviolet bound-free scattering

- ultraviolet bound-free edges produce scattering continua
- $J > B$ from:
  - $T(h)$ gradient defined by radiative equilibrium for the optical
  - $B(h)$ steeper in the ultraviolet due to Wien nonlinearity
  - Λ operator gives $J > S$ for steep $S(\tau)$
  - deep escape from small H I bf extinction
- $b_l/b_{\rm ionz}$ for electron donors Mg I, Fe I, Si I and Al I imply b_l population depletion across photosphere because $b_{\rm ionz} \approx 1$
- their photospheric lines have increasing extinction deficits compared to LTE
- $b_2/b_{\rm ionz}$ for H I shows similar behavior for the top of the hydrogen atom starting at $n = 2$

start index

43

SOLAR SPECTRUM FORMATION: EXAMPLES

Robert J. Rutten

https://webspace.science.uu.nl/~rutte101

thin: cloud modeling corona chromosphere Rydberg per ALMA?

thick: UV line flip VAL3C temperature VAL3C spectrum Kurucz stars

photospheric lines: inversions bright points reversed granulation Na I D1 MGs limb emission lines

continua from VAL3C: Avrett models versus 3D MHD VAL3C continua VALII budget hydrogen budget all

lines from ALC7: model optical spectrum ultraviolet depletion hydrogen strong lines plot formats pops plot BSJ plot profile plot Mg I 4571 Fe I 6302 Mg I b$_2$ Na I D$_1$ Ba II 4554 Ca II 8542 Å Ca II K Mg II k Lyα Hα Hβ He I 584 He I 10830 canonical Hα Na I D$_1$–Mg I b$_2$ Lyα–Hα Hα–Ca II 8542 Å Ca II K–Mg II k versus FCHHT-B ALC7–FALC FALC–FALP ALC7–FALP

detour lines: pumping suction

Oslo-simulated dynamic atmosphere: 1D RADYN 3D Bifrost Bifrost line synthesis

LA-conjectured PSBE atmosphere: non-E Hα aureole boosting Hα extinction CE–SB EBs spicules-II contrail ALMA non-E chromosphere?

IRIS diagnostics: overview diagnostics

start index

44

FLUX TUBES

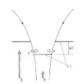

- *1970s: Utrecht fluxtube paradigm*
  - magnetostatic equilibrium: flaring
  - evacuation: Wilson depression
  - thin tube: hot walls bright, brighter limbwards

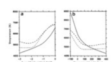

- *1980s: Zürich unsharp 1.5D models*
  - McMath-Pierce FTS Fe I & Fe II Stokes V
  - assume magnetostatic geometry
  - spatially-averaged LTE Stokes profile fitting
  - flatter-than-RE temperature gradient

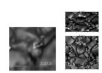

- *1990s+: sharp observations and simulations*
  - enhanced contrast in G band, strong-line wings
  - rapid morphology change, much vorticity
  - near-limb faculae: see-through into granules

start index

45

1970s magnetostatic fluxtubes

Kees Zwaan & Hans Rosenberg

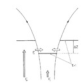

Zwaan 1978SoPh...60..213Z

Spruit 1976SoPh...50..269S

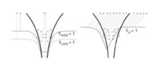

Rutten 1999ASPC..184..181

start index

46

MAGNETIC BRIGHT POINTS

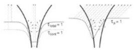

- *high-resolution observation*
  - Berger et al. 2004A&A...428..613B: G-band bright points as ribbons and flowers
- *high-resolution simulation*
  - Keller et al. 2004ApJ...607L..59K: continuum faculae simulation
  - Carlsson et al. 2004ApJ...610L.137C: G-band faculae simulation
- *bright points in Hα*
  - DOT Hα movie 2004-10-06
  - Leenaarts et al. 2006A&A...449.1209L: bright points in Hα
  - Leenaarts et al. 2006A&A...452L..15L: comparison of bright-point diagnostics
- *less bright points in "normal" lines*
  - Vitas et al. 2009A&A...499..301V: only Mn I lines are not mucked up by granulation

start index

47

MODELING NETWORK / PLAGE MAGNETISM FOR SPECTRAL IRRADIANCE

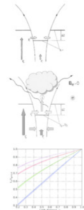

- *golden age of fluxtube modeling* = *hole in surface*
  - Zwaan – Spruit: idealized magnetostatic fluxtubes
  - Stenflo – Solanki – Keller: unresolved FTS polarimetry
  - Steiner – Keller – Carlsson: realistic MHD simulations
- *bright-point enhancements* = *hole deepening*
  - CH G-band, CN 3883 band: dissociaton
  - Fe I line gaps: ionization
  - Balmer line wings: small collision broadening
  - Mn I line cores: large hyperfine broadening
- *dark age of 1D irradiance modeling* = *down the rabbit hole*
  - "chromospheric cloud" ⇒ "photosphere heating"
  - FALP > FALC fudge ⇒ SATIRE (ADS N39 H13)
  - 1600 Å – 1700 Å [SST/CHROMIS Ca II K wing scans]
- *coming age of simulation irradiance modeling* ⇒ *of age*
  - ∼ 1D ⇒ 3D abundances ("pre/post Asplund")
  - first step: MURaM with LTE
  - to do: 3D(t) MHD with NLTE, line haze, H NSE?

start index

48

SOLAR SPECTRUM FORMATION: EXAMPLES

Robert J. Rutten
https://webspace.science.uu.nl/~rutte101

thin: cloud modeling corona chromosphere Rydberg per ALMA?

thick: UV line flip VAL3C temperature VAL3C spectrum Kurucz stars

photospheric lines: inversions bright points reversed granulation Na I D1 MGs limb emission lines

continua from VAL3C: Avrett models versus 3D MHD VAL3C continua VALII budget hydrogen budget all

lines from ALC7: model optical spectrum ultraviolet depletion hydrogen strong lines plot formats pops plot BSJ plot profile plot Mg I 4571 Fe I 6302 Mg I b$_2$ Na I D$_1$ Ba II 4554 Ca II 8542 Å Ca II K Mg II k Lyα Hα Hβ He I 584 He I 10830 canonical Hα Na I D$_1$–Mg I b$_2$ Lyα–Hα Hα–Ca II 8542 Å Ca II K–Mg II k versus FCHHT-B ALC7–FALC FALC–FALP ALC7–FALP

detour lines: pumping suction

Oslo-simulated dynamic atmosphere: 1D RADYN 3D Bifrost Bifrost line synthesis

LA-conjectured PSBE atmosphere: non-E Hα aureole boosting Hα extinction CE-SB EBs spicules-II contrail ALMA non-E chromosphere?

IRIS diagnostics: overview diagnostics

start index

49

REVERSED GRANULATION OBSERVATION & SIMULATION

Leenaarts & Wedemeyer-Böhm 2005A&A...431..687L

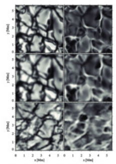

- observation simular to simulation so phenomenon "explained"
- no magnetism since pure hydro simulation (CO^{5}BOLD)
- internal gravity waves?

start index

50

OBSERVATION & SIMULATION OF Na I D$_1$, Mg I b$_2$, Ca II 8542 Å

Rutten et al. 2011A&A...531A..17R

- SST images blue wing - core - red wing 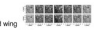
- atlas profiles 
- FALC formation 
- Dopplergram comparisons 
- profile comparisons 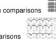

upshot
- simulation ≈ observation but computed Ca II 8542 Å is much too narrow
- difference in showing reversed granulation is set by reversed intensity–Dopplershift correlation sampled differently by different inner-wing steepness
- Na I D$_1$ Dopplergrams are upper-photosphere kilogauss magnetograms

start index

51

SOLAR SPECTRUM FORMATION: EXAMPLES

Robert J. Rutten
https://webspace.science.uu.nl/~rutte101

thin: cloud modeling corona chromosphere Rydberg per ALMA?

thick: UV line flip VAL3C temperature VAL3C spectrum Kurucz stars

photospheric lines: inversions bright points reversed granulation Na I D1 MGs limb emission lines

continua from VAL3C: Avrett models versus 3D MHD VAL3C continua VALII budget hydrogen budget all

lines from ALC7: model optical spectrum ultraviolet depletion hydrogen strong lines plot formats pops plot BSJ plot profile plot Mg I 4571 Fe I 6302 Mg I b$_2$ Na I D$_1$ Ba II 4554 Ca II 8542 Å Ca II K Mg II k Lyα Hα Hβ He I 584 He I 10830 canonical Hα Na I D$_1$–Mg I b$_2$ Lyα–Hα Hα–Ca II 8542 Å Ca II K–Mg II k versus FCHHT-B ALC7–FALC FALC–FALP ALC7–FALP

detour lines: pumping suction

Oslo-simulated dynamic atmosphere: 1D RADYN 3D Bifrost Bifrost line synthesis

LA-conjectured PSBE atmosphere: non-E Hα aureole boosting Hα extinction CE-SB EBs spicules-II contrail ALMA non-E chromosphere?

IRIS diagnostics: overview diagnostics

start index

52

Na I D$_1$ IN A MAGNETIC CONCENTRATION

Leenaarts et al. 2010ApJ...709.1362L

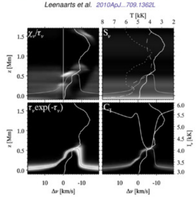

start index

53

FORMATION BREAKDOWNS Na I D$_1$ & Ca II 8542 Å

Leenaarts et al. 2010ApJ...709.1362L

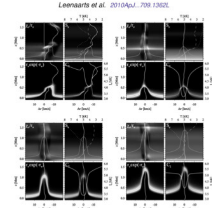

start index

54

STAGGER/MULTI3D Na I D$_1$ DOPPLERGRAMS AS UNSIGNED MAGNETOGRAMS

Rutten et al. 2011A&A...531A..17R

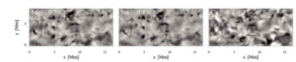

Fig. 16. Dopplergrams from the simulation as in the bottom row of Figure 7 but closer to line center and with only CRISP spectral smearing, no spatial PSF smearing.

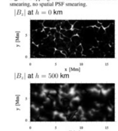

A corollary is that searches for global g-modes and so-called "chromosphere seismology" using full-disk resonance-cell sampling of the Na line as with GOLF-NG (e.g., Turck-Chièze et al. 2006; Salabert et al. 2009) will suffer noise from reversed granulation just as classical helioseismology suffers noise from granulation. Magnetic concentrations contribute much noise (literally) by their shocks. GOLF-NG's 15 passbands, spread over $\Delta\lambda = \pm 9$ km s^{-1}, have $FWHM$ = 30 mÅ, half CRISP's passband in this line and clearly narrow enough. Interpretation of such multi-passband oscillation sampling that relies on one-dimensional height-of-formation interpretation, for example to diagnose upward propagation from inward phase difference, is likely to fail since the clapotispheric signals are better described as clouds of varying opacity at varying height of which the varying Dopplershifts act as shutters obscuring the inner line wings.

start index

55

SOLAR SPECTRUM FORMATION: EXAMPLES

Robert J. Rutten
https://webspace.science.uu.nl/~rutte101

start index

56

LIMB EMISSION LINES

- *tabulations*
  - Menzel, thesis 1930, Pubs. Lick Obs., Campbell eclipse spectra, ADS antiquities
  - Dunn et al. 1968ApJS...15..275D HAO eclipse spectra comprehensive plot
  - Pierce 1968ApJS...17....1P extreme limb spectra plate with Mg I 4571 Å
  - Rutten & Stencel 1980A&AS...39..415R limb emission lines in Ca II H & K wings
  - Rutten + XX: limb emission lines in Mg II h & k wings
- *rare earths*
  - Canfield 1971A&A....10...54C excerpt 1971A&A....10...64C excerpt
  - interlocking $\Rightarrow \eta > \varepsilon \Rightarrow S > B$ with much spatial smoothing
  - higher emission for larger quasi-continuous extinction (Ce II in H & K wings)
- *pumped ion lines*
  - Fe II 3969.4 Å between Ca II H and Hϵ: Cram et al. 1980ApJ...241..374C excerpt
  - subordinate lines sharing upper levels with strong UV lines
  - large sensitivity to deep temperature variations
- *strong lines with PRD wings*
  - Ba II 4554 Å: Rutten 1978SoPh...56..237R excerpt 1979ApJ...231..277R excerpt
  - others: Fe II, Ti II, . . .
- *LTE lines*
  - Mg I 4571 Å Rutten 1977SoPh...51....3R excerpt

start index

57

SOLAR SPECTRUM FORMATION: EXAMPLES

Robert J. Rutten
https://webspace.science.uu.nl/~rutte101

thin: cloud modeling corona chromosphere Rydberg per ALMA?

thick: UV line flip VAL3C temperature VAL3C spectrum Kurucz stars

photospheric lines: inversions bright points reversed granulation Na I D1 MGs limb emission lines

continua from VAL3C: Avrett models versus 3D MHD VAL3C continua VALII budget hydrogen budget all

lines from ALC7: model optical spectrum ultraviolet depletion hydrogen strong lines plot formats pops plot BSJ plot profile plot Mg I 4571 Fe I 6302 Mg I b_2 Na I D_1 Ba II 4554 Ca II 8542 Å Ca II K Mg II k Lyα Hα Hβ He I 584 He I 10830 canonical Hα Na I D_1–Mg I b_2 Lyα–Hα Hα–Ca II 8542 Å Ca II K–Mg II k versus FCHHT-B ALC7–FALC FALC–FALP ALC7–FALP

detour lines: pumping suction

Oslo-simulated dynamic atmosphere: 1D RADYN 3D Bifrost Bifrost line synthesis

LA-conjectured PSBE atmosphere: non-E Hα aureole boosting Hα extinction CE–SB EBs spicules-II contrail ALMA non-E chromosphere?

IRIS diagnostics: overview diagnostics

start index

58

AVRETT SOLAR-ANALOG STARS

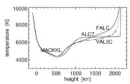

- VAL3C = Vernazza, Avrett, Loeser 1981ApJS...45..635V: best-fit to UV continua
- MACKKL = Maltby et al. 1986ApJ...306..284M: less steep upper photosphere
- FALC = Fontenla, Avrett, Loeser 1993ApJ...406..319F: ambipolar diffusion
- ALC7 = Avrett & Loeser 2008ApJS..175..229A: UV-line fit; update 2015ApJ...811...87A

[. . .] The results may be interpreted as holding for a computationally existing star called VALIII [. . .]. This star is remarkably like the Sun in its temporally and spatially averaged continuous spectral distribution, but in contrast to the Sun it does obey hydrostatic equilibrium and static plane-parallel geometry, and it contains only those atoms, ions and electrons that were specified in the Pandora code, fortunately with just the corresponding cross-sections. Its modeling is exact! The advantage of studying the star VALIII rather than the star Sol is that the physics of VALIII radiation is fully understandable. Also, it keeps adhering to these course notes ad infinitum while solar physics evolves to more complexity.

Rutten "Radiative Transfer in Stellar Amospheres"

start index

59

OSLO SIMULATION VERSUS 1D STANDARD MODELS

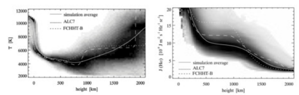

- simulation = state-of-the-art: 3D(t), $\vec{B}$, non-HE, SE populations but NE for H
  Leenaarts, Carlsson & Rouppe van der Voort 2012ApJ...749..136L
- ALC7 = UV fit: 1D static, no $\vec{B}$, HE + microturbulence, SE populations
  Avrett & Loeser 2008ApJS..175..229A
- FCHHT-B = UV fit: 1D static, no $\vec{B}$, HE + imposed acceleration, SE populations
  Fontenla, Curdt, Haberreiter, Harder & Tian 2009ApJ...707..482F

The T and $J_\nu(\mathrm{H}\alpha)$ behavior seems arguably similar. However, the conceptual differences between plane-parallel static hydrostatic-equilibrium modeling and the 3D(t) MHD simulation are enormous (cf. Newtonian gravitation versus general relativity). The $T(h)$ stratifications in the simulation vary tremendously, with shocks propagating upwards and sideways and the increase to coronal temperature dancing up and down over a large height range.

start index

60

VALIIIC MODEL

Vernazza, Avrett, Loeser 1981ApJS...45..635V

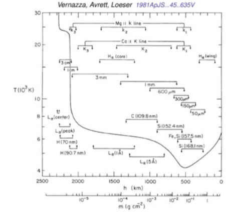

start index

61

VALIIIC 500 nm FORMATION

$$I_\nu(0,1) = \int_0^\infty S_\nu\, \mathrm{e}^{-\tau_\nu}\, \mathrm{d}\tau_\nu = \int_0^\infty j_\nu\, \mathrm{e}^{-\tau_\nu}\, \mathrm{d}h \qquad \frac{\mathrm{d}I_\nu}{\mathrm{d}h} = j_\nu\, \mathrm{e}^{-\tau_\nu}$$

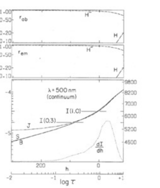

start index

62

VAL3C CONTINUUM FORMATION

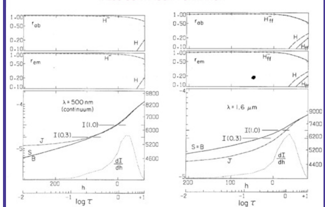

start index

63

VAL3C CONTINUUM FORMATION

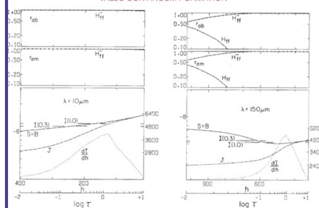

start index

64

VAL3C CONTINUUM FORMATION

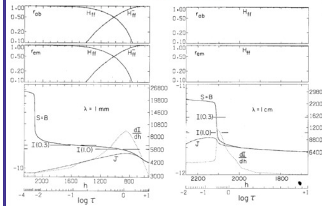

start index

65

VAL3C CONTINUUM FORMATION

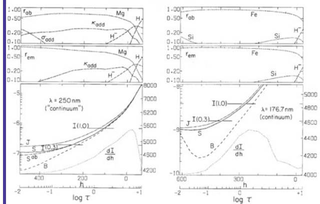

start index

66

VAL3C CONTINUUM FORMATION

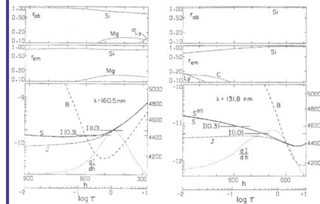

start index

67

VAL3C CONTINUUM FORMATION

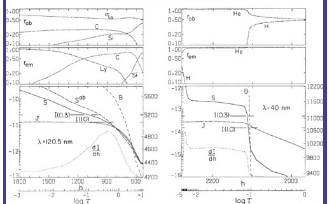

start index

68

TEMPERATURE MINIMUM IN VALII

Vernazza, Avrett & Loeser 1976ApJS...30....1V *(VALII)*

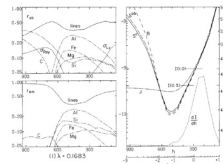

- oops: bf edges of electron-donor metals wrongly in LTE
- oops: too few line-haze lines and wrongly in LTE

start index

69

VAL3C RADIATION BUDGET

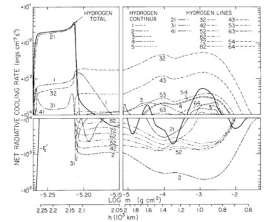

start index

70

VAL3C RADIATION BUDGET

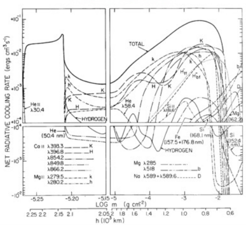

start index

71

SOLAR SPECTRUM FORMATION: EXAMPLES

Robert J. Rutten

https://webspace.science.uu.nl/~rutte101

thin: cloud modeling corona chromosphere Rydberg per ALMA?

thick: UV line flip VAL3C temperature VAL3C spectrum Kurucz stars

photospheric lines: inversions bright points reversed granulation Na I D1 MGs limb emission lines

continua from VAL3C: Avrett models versus 3D MHD VAL3C continua VALII budget hydrogen budget all

lines from ALC7: model optical spectrum ultraviolet depletion hydrogen strong lines plot formats pops plot BSJ plot profile plot Mg I 4571 Fe I 6302 Mg I b_2 Na I D_1 Ba II 4554 Ca II 8542 Å Ca II K Mg II k Lyα Hα Hβ He I 584 He I 10830 canonical Hα Na I D_1–Mg I b_2 Lyα–Hα Hα–Ca II 8542 Å Ca II K–Mg II k versus FCHHT-B ALC7–FALC FALC–FALP ALC7–FALP

detour lines: pumping suction

Oslo-simulated dynamic atmosphere: 1D RADYN 3D Bifrost Bifrost line synthesis

LA-conjectured PSBE atmosphere: non-E Hα aureole boosting Hα extinction CE–SB EBs spicules-II contrail ALMA non-E chromosphere?

IRIS diagnostics: overview diagnostics

start index

72

ALC7 ATMOSPHERE

Avrett & Loeser 2008ApJS..175..229A

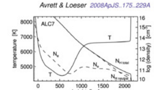

- unrealistic plane-parallel static computational star with solar-like average spectrum
  – exemplary in obeying all equations in my RT courses: understandable line formation
- best-fit temperature: near-RE in photosphere, shock-dominated in chromosphere
  – slope in upper photosphere depends on NLTE ultraviolet line haze
- total hydrogen density: exponential decay
  – turbulent presssure added to gain scale height and chromospheric extent
- low electron density in photosphere and temperature minimum
  – from ionization of donor-elements Si, Fe, Mg, Al with 10^{-4} relative abundance
- increasing hydrogen ionization across chromosphere
  – electron density reaches proton density at its top
- near-isothermal near-constant-N_e chromosphere
  – mimics Avrett's (1965) isothermal constant-ε two-level-atom scattering atmosphere

start index

73

CRD RESONANT SCATTERING IN AN ISOTHERMAL ATMOSPHERE

RTSA figure 4.12; from Avrett 1965SAOSR.174..101A

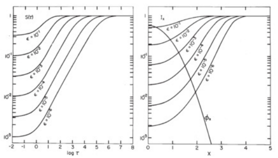

- left: S/B in a plane-parallel isothermal atmosphere with constant ε for complete redistribution. The curves illustrate the $\sqrt{\varepsilon}$ law and thermalization at $\Lambda \approx 1/\varepsilon$.
- right: corresponding emergent line profiles and Gaussian extinction profile shape ϕ (only the righthand halves; $x = \Delta\lambda/\Delta\lambda_D$)

start index

74

SOLAR OPTICAL VERSUS ALC7 OPTICAL – ON DISK AND OFF LIMB

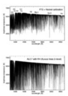

- *observed disk-center spectrum*
  - Na I D lines darkest from scattering
  - H I Balmer lines widest from linear Stark + Holtsmark
  - Ca II H & K strongest from Saha-Boltzmann ("Cecilia Payne")
- *ALC7 disk-center spectrum per RH*
  - 1D-SE without granules, waves, shocks, fibrils, magnetism
  - chromospheric extent from imposed turbulent pressure
  - good reproduction, also ultraviolet (RH: not H, not Kurucz)

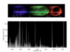

- *observed flash spectrum*
  - H I Balmer, Ca II H & K, He I ≡ Lockyer's "chromosphere"
  - Janssen/Lockyer discovery of He I D_3
  - made up of spicules

- *ALC7 flash spectrum per RH*
  - too small extent
  - cannot explain H I Balmer, let be He I D_3
  - no spicules

start index

75

ULTRAVIOLET DEPLETION IN THE ALC7 ATMOSPHERE

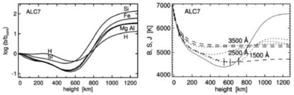

minority atoms: photospheric extinction depletion by ultraviolet bound-free scattering

- ultraviolet bound-free edges produce scattering continua
- $J > B$ from:
  - $T(h)$ gradient defined by radiative equilibrium for the optical
  - $B(h)$ steeper in the ultraviolet due to Wien nonlinearity
  - Λ operator gives $J > S$ for steep $S(\tau)$
  - deep escape from small H I bf extinction
- $b_1/b_{\rm cont}$ for electron donors Mg I, Fe I, Si I and Al I imply b_1 population depletion across photosphere because $b_{\rm cont} \approx 1$
- their photospheric lines have increasing extinction deficits compared to LTE
- $b_2/b_{\rm cont}$ for H I shows similar behavior for the top of the hydrogen atom starting at $n=2$

start index

76

HYDROGEN LINES IN THE ALC7 ATMOSPHERE

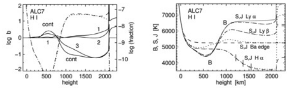

Hα: chromosphere is back-scattering attenuator for radiation from deep photosphere; outward S decline as in isothermal constant-ε two-level-atom atmosphere

Lyα: tremendous scattering with $S_{{\rm Ly}\,\alpha} \approx J_{{\rm Ly}\,\alpha}$ but local thermalization with $J_{{\rm Ly}\,\alpha} \approx B_{{\rm Ly}\,\alpha}$ from short photon mean free paths (S dotted, J dashed; dot-dashed = identity)

Lyβ: scattering as Lyα, shares photon losses in Hα (Hα ticks $\tau = 3, 1, 0.3$) (same $S/B \approx b_3/b_1$ since $b_2 \approx b_1$ but offsets differ in temperature representation)

$n=1$: Saha-Boltzmann $b_1 \approx 1$ population because hydrogen is neutral (except in transition region at right)

$n=2$: Saha-Boltzmann $b_2 \approx 1$ population from Lyα thermalization (dotted fraction curve = $n_2^{\rm LTE}/N_{\rm Htot}$ ≈ dashed curve = actual $n_2/N_{\rm Htot}$)

ionization: $b_{\rm cont}/b_2$ defined by SE balancing of $B(T_{\rm rad}^{\rm Bacont})/B(T_e)$ ionization driving and cascade recombination with high-n line photon losses. The H I top ($n \geq 2$) represents a 3.4 eV alkali atom with ground-state population set by Lyα.

start index

77

STRONG LINES IN ALC7

Avrett & Loeser *2008ApJS..175..229A* *Rutten* *2016A&A...590A.124R*

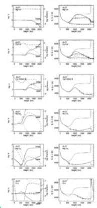

- *Mg II k*
  - extinction LTE, source function 2-level scattering
  - high peaks, low PRD dips, low wings
- *Ca II K*
  - lower abundance and ionization, underionization
  - small peaks and PRD dips
- *Ca II 8542*
  - as Ca II K with Boltzmann lowering and sensitivity
  - similar source function sampling as Hα
- *Na I D_1*
  - photospheric scattering, suction and underionization
  - no sensitivity to temperature rise
- *Mg I b_2*
  - as Na I D_1 but photospheric overionization
  - no sensitivity to temperature rise
- *Hα*
  - chromospheric scattering of photospheric photons
  - chromospheric extinction LTE from Lyα box-up

start index

78

LINES FROM THE ALC7 CHROMOSPHERE: PLOT FORMATS (Na I D_1)

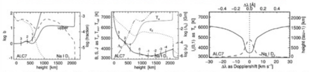

$b_i \equiv n_i/n_i^{\rm LTE}$ $\quad \alpha^l \approx b_l\,\alpha^{\rm LTE}$ $\quad S^l \approx (b_u/b_l)B$ $\quad S^l \approx (1-\varepsilon_2)\,J + \varepsilon_2\,B$ $\quad \Lambda_2 \approx \sqrt{\pi}/(\alpha_0\,\varepsilon_2)$ $\quad I(0) \approx S[\tau=1]$

- *first plot: populations*
  - solid: population departure coefficients. Always unity in the deep photosphere. Divergence with increasing $b_u < b_l$ shows resonance scattering. Steep b_l rise due to radiative overionization of this minority species (Na I). $\log\tau$ ticks on b_l curve are for line center.
  - dashed: fractional population $n_l/N_{\rm element}$ in NLTE. Scale at right. Na I is minority species.
  - dotted: fractional population $n_l/N_{\rm element}$ per Saha-Boltzmann. Difference with the NLTE curve corresponds to departure of b_l from unity.
- *second plot: line source function*
  - solid thin, thick, dashed: B, S, J as formal temperatures (for common scale with other lines). $\log\tau$ ticks are for line center.
  - dotted: ε for the Doppler core in 2-level approximation. Scale to the right.
  - dot-dashed: thermalization length in Gm. $\Lambda_2 = -6$ means thermalization of S to B within a homogeneous slab of 1 km. The Λ mark is near core thermalization depth.
- *third plot: emergent profile*
  - solid: emergent profile as brightness temperature
  - dashed: $\tau_\lambda = 1$ height scale at right
  - dotted, vertical: wavelength sampling(s) for second plot

start index

79

LINES FROM THE ALC7 ATMOSPHERE: POPULATIONS PLOT (Na I D_1)

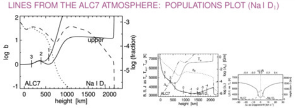

$b_i \equiv n_i/n_i^{\rm LTE}$ $\quad \alpha^l \approx b_l\,\alpha^{\rm LTE}$ $\quad S^l \approx (b_u/b_l)B$ $\quad \varepsilon \approx \varepsilon_2 = \alpha^a/(\alpha^s+\alpha^a)$ $\quad S^l \approx (1-\varepsilon_2)\,\overline{J} + \varepsilon_2\,B$

- *solid*: population departure coefficients for Na I D_1. Unity in deep photosphere from large collision frequency at high density, with $\varepsilon \approx 1$ ($B\,S\,J$ plot). Increasing $b_u < b_l$ divergence = $S^l < B$ divergence ($B\,S\,J$ plot) from $\sqrt{\varepsilon}$-law resonance scattering. Small initial hump in upper photosphere from photon suction (replenishment from ion reservoir) by scattering-out Na I D photons. Steep b_l rise above 700 km from ultraviolet underionization ($1-c$ edge at 2412 Å, typical for minority neutrals). The $\log\tau$ ticks on the b_l curve are for line center.
- *dotted*: fractional population $n_l^{\rm LTE}/N_{\rm elem}$ per Saha-Boltzmann. Scale at right. Na I is a minority species. Initial decrease from increasing ionization at decreasing N_e, slight hump from less ionization at lower temperature, steep decline at increasing T and decreasing N_e (Saha).
- *dashed*: fractional population $n_l/N_{\rm elem}$ in NLTE. Line-center optical depth $\tau_\lambda = -\int(\alpha^l+\alpha^c)\,{\rm d}h$ has $\alpha^l >> \alpha^c$ and $\alpha^l_\lambda \sim n_l = (n_l/N_{\rm elem})A_{\rm elem}N_{\rm Htot}$. Divergence from LTE curve corresponds to departure of b_l from unity. The steep b_l increase compensates the steep $n_l^{\rm LTE}$ decrease.

start index

80

LINES FROM THE ALC7 ATMOSPHERE: B S J PLOT (Na I D_1)

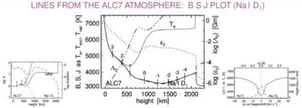

$S^l \approx (b_u/b_l)B$ $\quad \varepsilon \approx \varepsilon_2 \equiv \alpha^a/(\alpha^s+\alpha^a)$ $\quad S^l \approx (1-\varepsilon_2)\,\overline{J} + \varepsilon_2\,B$ $\quad \Lambda_2 \approx \sqrt{\pi}/(\alpha_0\,\varepsilon_2)$

- *thin solid*: B_{λ_0} as temperature T_e to remove Planck function variation with wavelength for comparison with other lines. The ALC7 atmosphere has a near-isothermal chromosphere.
- *thick solid*: Na I D_1 S^l as formal excitation temperature $T_{\rm exc}$. The $B > S$ divergence corresponds to the $b_l > b_u$ divergence in the populations plot, but not equally in their plotted logarithms due to the B and S conversions to formal temperature. The $\log\tau$ ticks are for line center. This scattering line does not sense the ALC7 chromosphere in S^l.
- *dashed*: profile-averaged angle-averaged intensity $\overline{J}$ as formal radiation temperature $T_{\rm rad}$.
- *dotted*: 2-level photon destruction probability ε_2 for the Doppler core. Scale to the right. Follows N_e, so fairly constant over 1000–2000 km from increasing hydrogen ionization.
- *dot-dashed*: 2-level thermalization length Λ_2 for the Doppler core in gigameter. Scale to the right. Example: $\Lambda_2 = -6$ implies thermalization of S to B at the center of a 2-km thick feature. The curve label is placed near the line-core thermalization height in the mid photosphere.

start index

81

LINES FROM THE ALC7 ATMOSPHERE: PROFILE PLOT (Na I D_1)

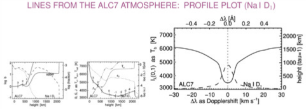

$\alpha^l_\lambda \sim b_l\,(n_l^{\rm LTE}/N_{\rm elem})A_{\rm elem}N_{\rm Htot}\,\varphi(\lambda-\lambda_0)$ $\quad \tau_\lambda = -\int(\alpha^l+\alpha^c)\,{\rm d}h$ $\quad I_\lambda(0) \approx S_\lambda^{\rm total}[\tau_\lambda=1]$

- *solid*: emergent intensity in the radial direction, represented as formal brightness temperature for comparison with other lines and the Eddington-Barbier estimate (BSJ plot, temperature axes match in the coming line-formation displays). Similarly, the bottom scale for wavelength separation from line center is in km s^{-1} for comparison with other lines. Wavelength separations in Å along the top.
- *dashed*: $\tau_\lambda = 1$ height, scale at right.
- *dotted, vertical*: sampling wavelength(s) for S and J in the BSJ plot. Only one for CRD lines (as Na I D_1) with frequency-independent line source functions (and $\overline{J}$ in the BSJ plot).
- one might overplot an observed solar disk-center profile, but this is misleading because even a perfect match does not imply that the ALC7 model is correct. ALC7 is an idealized didactic star not like the Sun with an easier-to-understand solar-lookalike spectrum.

start index

Mg I 4571 Å FROM THE ALC7 ATMOSPHERE

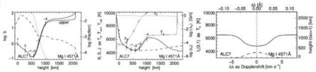

unique photospheric line with LTE source function

- extinction severely out of LTE. Deep b_l dip across the ALC7 photosphere from overionization by deeply escaping bound-free scattering ultraviolet radiation, including edges of Mg I itself at 2512 and 1621 Å. Corresponding steep b_l rise above 700 km from ultraviolet underionization where the temperature increases in excess of the ultraviolet radiation temperature.
- this pattern is common to all lines of minority neutrals with ultraviolet ionization wavelengths, including the electron donors (Mg I, Fe I, Si I, Al I).
- source function unusually close to LTE because this is a "forbidden" intersystem line with small $A_{ul} = 2.7\,10^2\,\mathrm{s}^{-1}$, dominated by collisions ($\varepsilon \approx 1$) with $b_u \approx b_l$, $S^l \approx B$ to large heights.
- yet fairly strong because its lower level is the Mg I ground state
- usefulness: photospheric thermometer but requires ultraviolet NLTE for optical depth

82

Fe I 6301.5 Å FROM THE ALC7 ATMOSPHERE

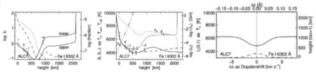

standard polarimetry line

- severe extinction NLTE across the photosphere due to ultraviolet bound-free scattering overionization and affecting the tau scaling (b_l curve)
- minor S^l NLTE from resonance scattering in the upper photosphere ($S < B$ split)
- "inversion" codes (numerical best-fit iteration) sometimes include S^l NLTE but usually not extinction NLTE, ignoring that bound-free scattering with $S^{\mathrm{UV}} \approx \overline{J}^{\mathrm{UV}}$ depends on 3D temperature gradients in deeper layers and makes b_l (hence n^l and α^l) non-local both in space and wavelength
- problem: the enormous density of NLTE lines ("haze") in the ultraviolet affecting J^{UV}
- usefulness: differential line-pair polarimetry with its twin Fe I 6302.5 Å

83

Mg I b_2 5173 Å FROM THE ALC7 ATMOSPHERE

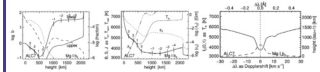

diagnostic of upper photosphere

- large NLTE n_l depletion from ultraviolet bound-free scattering across the photosphere
- large NLTE b_l increase from ultraviolet scattering offsets Saha decline in chromosphere
- CRD scattering source function with $\varepsilon \approx 10^{-3}$
- similar to Na I D_1
- usefulness: as Na I D_1 but wider core = less asymmetry from reversed granulation

84

Na I D_1 5896 Å FROM THE ALC7 ATMOSPHERE

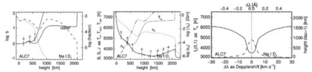

Na I D lines: darkest lines in optical spectrum = textbook example of two-level scattering

- photon suction offsets ultraviolet overionization across the photosphere
- ultraviolet underionization offsets Saha depletion above 700 km
- 2-level CRD scattering with $\varepsilon \approx 10^{-3}$ and $S \approx \overline{J} << B$ in the ALC7 chromosphere
- thermalization in mid photosphere: core intensity does not sense ALC7 chromosphere, observed photons are created near the thermalization depth (height of Λ_2 label), observed intensity variation preferentially encodes temperature variation there
- last scattering near $\tau = 1$: Doppler and Stokes inner-wing encoding occurs around 500 km
- usefulness: sharp Na I D Dopplergrams indicate deeply-located shocks in fluxtubes

85

Ba II 4554 Å FROM THE ALC7 ATMOSPHERE

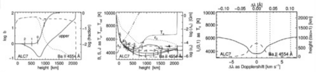

weakest PRD line, best velociy diagnostic, good Hanle diagnostic

- extinction LTE up to line-core formation height thanks to photon losses offsetting overionization (edge at 1240 Å outside Lyα)
- steep b_l increase above 800 km from underionization offsets Saha depletion
- resonance line with Grotrian diagram similar to Ca II K. PRD scattering source function with $\varepsilon \approx 10^{-4}$, therefore different monochromatic S_λ and J_λ curves for line center, inner wings, outer wings
- S^l split in upper photosphere produces emission wings at the limb (my 1976 eclipse-expedition PhD thesis)
- usefulness: non-thermal Doppler sensitivity from large mass ($\sqrt{m_{\mathrm{Ba}}/m_{\mathrm{H}}} = 11.7$)
  intricate near-limb Hanle profile from hyperfine structure

86

Ca II 8542 Å FROM THE ALC7 ATMOSPHERE

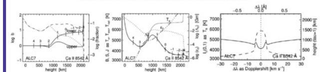

cleanest chromospheric diagnostic in the near infared

- extinction: b_l boost from its own photon losses compensates Saha depletion
- CRD scattering source function with $\varepsilon \approx 10^{-2}$
- core formation spans lower ALC7 chromosphere
- best optical line for chromospheric magnetometry
- usefulness: at longer wavelengths more diffraction but less seeing $\Rightarrow$ prime DKIST line

87

Ca II K 3934 Å FROM THE ALC7 ATMOSPHERE

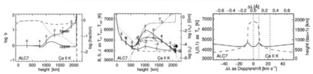

largest extinction in the optical spectrum

- extinction: successive b_l boosts from photon losses in infrared triplet and H&K compensates Saha depletion
- PRD scattering source function with $\varepsilon \approx 10^{-4}$ (split between profile center, peaks, dips)
- core formation spans the ALC7 chromosphere
- narrowness of the Doppler core upsets filter imaging so far
- Sunrise-2/SuFi best so far; high hopes for SST/CHROMIS
- usefulness: best optical chromosphere diagnostic but challenging (bandwidth, S/N)

88

Mg II k 2796 Å IN THE ALC7 CHROMOSPHERE

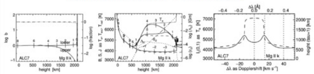

cleanest PRD line and yet larger extincton than Ca II K

- LTE lower-level population and extinction because all Mg sits in the Mg II ground state
- PRD scattering source function with $\varepsilon \approx 10^{-4}$ (split between profile center, peaks, dips)
- textbook scattering decline
- similar to Ca II K but with 18$\times$ larger abundance and with much darker wings
- usefulness: key diagnostic but requires space platform
  slitless imaging spectrometry very difficult
  combine with "triplet" doublet between h & k (recombination indicator)

89

Lyα 1216 Å IN THE ALC7 CHROMOSPHERE

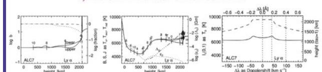

champion: largest extinction and most scattering of all lines

- lower-level population fraction ≈ 1: all hydrogen in ground state
- overpopulation of the ground state towards the transition region from photon losses in wings with slight scattering drops $S \approx J < B$
- enormous line-center extinction across the ALC7 chromosphere
- PRD scattering source function with $\varepsilon \approx 10^{-6}$ (split between profile center, peaks, dips)
- Λ goes from $\propto 1/\varepsilon$ towards $\propto 1/\varepsilon^2$ with density from Stark wing development (not shown)
- radiation lock-in from large extinction produces radiative balance $n_u(A_{ul} + B_{ul}\overline{J}) = n_l B_{lu}\overline{J}$
- local thermalization from small Λ produces $\overline{S} \approx B$ throughout ALC7 chromosphere;
  $b_u \approx b_l \approx 1$ implies LTE extinction for Hα where it escapes
- usefulness: premier diagnostic but needs space; slitless imaging spectrometry difficult

90

Hα 6563 Å FROM THE ALC7 ATMOSPHERE

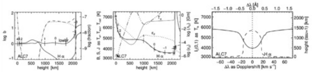

Hα: extraordinary from high excitation energy, huge element abundance, on top of Lyα

- lower-level fractional population varies $10^{-10}-10^{-7}$ due to 10 eV in Boltzmann
- extinction coefficient near-LTE up to 2000 km by Lyα thermalization
- $S^l \approx$ two-level scattering below transition region (not "photoelectric") just like Ca II 8542 Å
- upper photosphere transparent: core shows fibrils, wings show granules
- Eddington-Barbier tau $=$ 1 in chromosphere, but photon creation in deep photosphere
- large J across T-min from backscattering: ALC7 chromosphere ≈ scattering attenuator
- wide line core from small atomic mass in Doppler broadening $\sim \sqrt{2kT/m_{\rm H} + v^2_{\rm micro}}$
- extended wings from linear Stark effect in deep photosphere (Holtsmark distribution)
- usefulness: prominences, flares, Ellermans, dynamic fibrils, spicules-II, … = non-E

91

start index

Hβ 4861 Å FROM THE ALC7 ATMOSPHERE

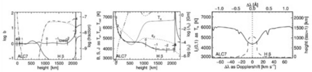

Hβ: analogon to Hα at 5.4× smaller oscillator strength and in the blue

- same large Boltzmann sensitivity and Lyα lower-level control as Hα
- in comparison with Hα (blink with previous):
  – same b_l, steeper b_u decay
  – similar scattering
  – less steep S^l decay from shorter wavelength
  – smaller chromosphere thickness from smaller gf
  – narrower core and $\tau=1$ peak
- RH-computed profile has less deep wings then observed atlas profile (not shown) because RH does not use the Holtsmark distribution for linear Stark broadening by charged particles (less steep wing drop than Voigt function)
- usefulness: differences against Hα

92

start index

He I 584 Å IN THE ALC7 CHROMOSPHERE

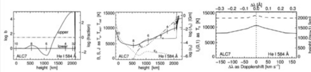

backradiator into chromosphere

- lower-level population fraction ≈ 1: all helium in He I ground state
- $b_1 = 1$ up to coronal rise
- PRD neglected here but not much difference
- detailed radiative balance $S \approx \overline{J}$
- much radiation from coronal rise down into chromosphere due to fairly large Λ, resulting in b_u increase to very large values
- radiation lock-in to $S \approx B$ only below 1000 km

93

start index

He I 10830 Å IN THE ALC7 CHROMOSPHERE

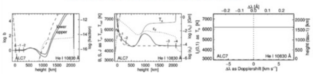

not of interest in ALC7

- high-excitation line supposedly obtaining visibility from coronal irradiation – not in ALC7
- minute fractional population from large Boltzmann factor
- upper-level b_1 set by He I 584 Å plus collisional coupling $2p^3P - 2p^1P$ with large He I 584 Å down-radiation from transition region into chromosphere
- total source function ≈ LTE H^- source function until Thomson scattering takes over
- nothing in the ALC7 spectrum

94

start index

CANONICAL CHROMOSPHERIC LINE FORMATION

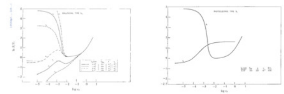

- CRD line source function including detour paths:

$$S^l_{\nu_0} = \frac{\overline{J}_{\nu_0} + \varepsilon'_{\nu_0} B_{\nu_0}(T) + \eta'_{\nu_0} B_{\nu_0}(T_{\rm d})}{1 + \varepsilon'_{\nu_0} + \eta'_{\nu_0}} = (1-\varepsilon_{\nu_0}-\eta_{\nu_0})\,\overline{J}_{\nu_0} + \varepsilon_{\nu_0} B_{\nu_0}(T) + \eta_{\nu_0} B_{\nu_0}(T_{\rm d})$$

- ε = upper-lower collisional destruction fraction of total extinction
  η = detour-path extinction fraction of total extinction
  ε', η' = idem as ratio to scattering extinction
  $\overline{J}$ = profile-averaged angle-averaged intensity
  $T_{\rm d}$ = formal detour excitation temperature: $(g_u\, D_{ul})/(g_l\, D_{lu}) \equiv \exp(h\nu_0/kT_{\rm d})$
- line source function split (Thomas 1957ApJ...125..260T):
  "collision type" (H & K) or "photoelectric type" (Hα, Balmer continuum feeding)

95

start index

Hα SOURCE FUNCTION IN THE ALC7 CHROMOSPHERE

after Rutten & Uitenbroek 2012A&A...540A..86R

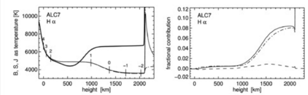

- $S^l_{\nu_0} = (1-\varepsilon_{\nu_0}-\eta_{\nu_0})\,\overline{J}_{\nu_0} + \varepsilon_{\nu_0} B_{\nu_0}(T) + \eta_{\nu_0} B_{\nu_0}(T_{\rm d}) = \overline{J}_{\nu_0} + \varepsilon_{\nu_0}[B_{\nu_0}(T) - \overline{J}_{\nu_0}] + \eta_{\nu_0}[B_{\nu_0}(T_{\rm d}) - \overline{J}_{\nu_0}]$
  The detour part $\eta_{\nu_0}[B_{\nu_0}(T_{\rm d}) - \overline{J}_{\nu_0}]/S^l_{\nu_0}$ exceeds the collision part $\varepsilon_{\nu_0}[B_{\nu_0}(T) - \overline{J}_{\nu_0}]/S^l_{\nu_0}$. However, their sum $[S^l_{\nu_0} - \overline{J}_{\nu_0}]/S^l_{\nu_0}$ (solid) reaches only a few percent so $S^l_{\nu_0} \approx \overline{J}_{\nu_0}$. Across the ALC7 chromosphere Hα is a scattering line, not "photoelectrically controlled".
- The Hα core is dominated by resonance scattering with a formation gap below the chromosphere filled by backscattered radiation. The ALC7 chromosphere acts as scattering attenuator building up its own irradiation. Most emerging photons are created in the deep photosphere where $\varepsilon_{\nu_0} \approx 1$ and $\overline{J}_{\nu_0} \approx B_{\nu_0}(T)$. The granulation pattern has larger contrast than the fibril pattern but is washed out in the scattering across the gap.
- The ALC7 Hα core formation is well described by the Eddington-Barbier approximation for an irradiated finite isothermal scattering atmosphere.

96

start index

HYDROGEN IN THE ALC7 and FCHHT-B PLANE-PARALLEL STARS

ALC7: 2008ApJS..175..229A FCHHT-B: 2009ApJ...707..482F discussion: 2017IAUS..327....1R

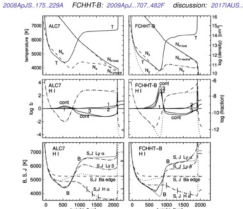

97

start index

Na I D_1 AND Mg I b_2

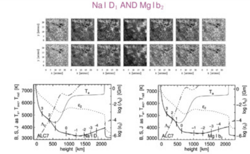

- similar NLTE formation $=$ heavy two-level scattering
- core intensities do not sense ALC7 chromosphere
- narrow Na I D_1 flanks reverse reversed granulation
- minority stages: recombination $\propto N_e$ senses non-E Lyα settling and scattering
- SST: Dopplergrams ≈ unsigned fluxtube magnetograms (Na I D_1 formation)
  non-E enhanced in cooling recombining downflows? (SE $=$ Bifrost snapshot OK)

98

start index

Lyα and Hα

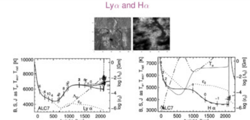

- both: heavy NLTE scatterers with $S \approx J$
- Lyα: boxed-in by enormous extinction ⇒ radiative detailed balance: $S = J$
  in shocks (≈ ALC7 chromosphere) collisional thermalization: $b_2 \approx b_1$
  in cool gas surrounding hot structures $b_2 \gg 1$ from Lyα surround scattering
  in post-hot cool gas slow $S \approx J$ thermalization with $b_2 \gg 1$: S^l memory of hot past
- Hα: photons created in granulation
  scatter 3D across upper-photosphere opacity gap and through chromosphere
  in shocks etc. Boltzmann extinction $b_2 \approx b_1$
  in post-hot cool gas $b_2 \gg 1$: extinction memory of hot past
- Lyα scene: heating events bright down-throat, cooling contrails dark from scattering?
  Hα scene: RBE/RRE heating events, cooling contrails dark from non-E opacity?

99

start index

Hα and Ca II 8542 Å

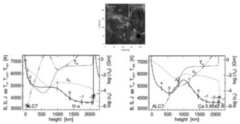

- both: heavy NLTE scatterers with $S \approx J$ sampled at similar $\tau = 1$ heights
- both: Saha-Boltzmann or larger extinction in shocks and ALC7
- core widths: both decrease away from network $=$ decreasing temperature
- Hα fibrils extend further, contradicting Saha-Boltzmann extinction sensitivities
- fibril opacity in Ca II 8542 Å instantenous, in Hα post-hot non-E?

Ca II K and Mg II k

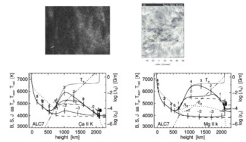

- both: heavy NLTE scatterers with PRD source function splits
- both: near-Saha-Boltzmann extinction everywhere; abundance ratio 18
- both: absence of non-E sensitivities $=$ instantaneous chromosphere
- both: slender fibrils emanating from network, in Ca II H & K better at narrower bandwidth, in Mg II k best in k_2 peak separation
- slender fibrils $=$ propagating heating events?

ALC7 ATMOSPHERE VERSUS FALC ATMOSPHERE

Avrett & Loeser 2008ApJS..175..229A *Fontenla, Avrett & Loeser* 1993ApJ...406..319F

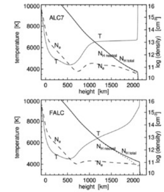

Mg I 4571 Fe I 6302 Mg I b_2 Na I D_1 Ba II 4554 Ca II 8542 Ca II K Mg II k Lyα Hα Hβ He I 584

Mg I 4571 Å IN ALC7 AND FALC

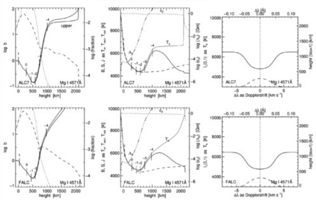

unique photospheric line with LTE source function

Fe I 6301.5 Å IN ALC7 AND FALC

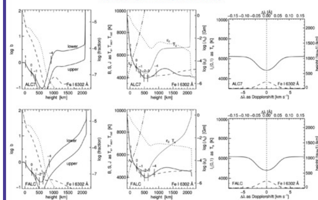

standard polarimetry line

Mg I b_2 5173 Å IN ALC7 AND FALC

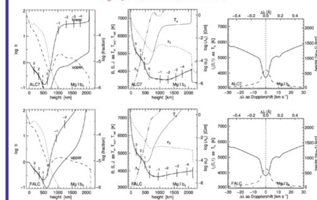

diagnostic of upper photosphere

Na I D_1 5896 Å IN ALC7 AND FALC

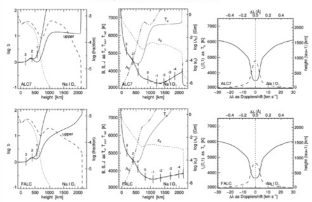

Na I D_1: darkest solar line in optical spectrum = textbook example of two-level scattering

Ba II 4554 Å IN ALC7 AND FALC

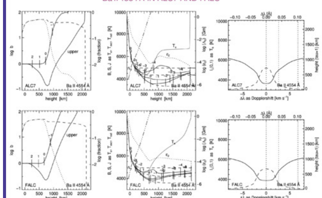

weakest PRD line, best velociy diagnostic, good Hanle diagnostic

Ca II 8542 Å IN ALC7 AND FALC

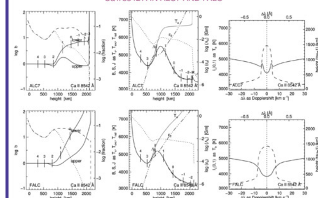

cleanest chromospheric diagnostic in the near infared

109

Ca II K 3934 Å IN ALC7 AND FALC

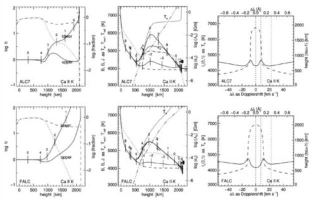

largest extinction in the optical spectrum

110

Mg II k 2796 Å IN ALC7 AND FALC

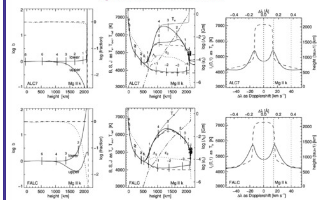

cleanest PRD line and yet larger extincton than Ca II K

111

Lyα 1216 Å IN ALC7 AND FALC

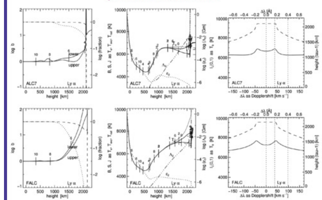

champion: largest extinction and most scattering of all lines

112

Hα 6563 Å IN ALC7 AND FALC

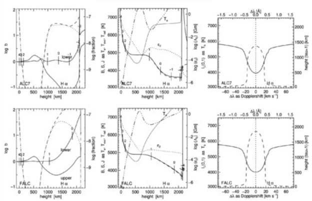

Hα: extraordinary from high excitation energy, huge element abundance, on top of Lyα

113

Hβ 4861 Å IN ALC7 AND FALC

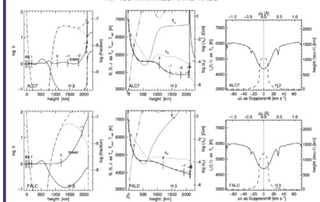

Hβ: analogon to Hα at 5.4$\times$ smaller oscillator strength and in the blue

114

He I 584 Å IN ALC7 AND FALC

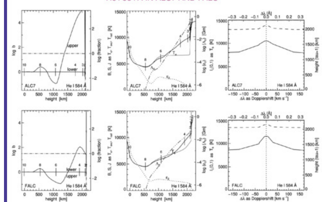

backradiator into chromosphere

115

FALC ATMOSPHERE VERSUS FALP ATMOSPHERE

Fontenla, Avrett & Loeser 1993ApJ...406..319F

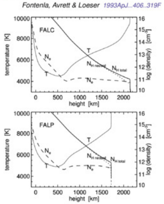

116

Mg I 4571 Å IN FALC AND FALP

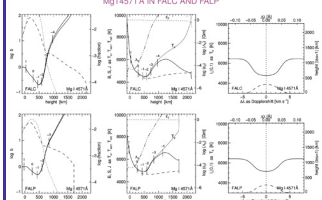

unique photospheric line with LTE source function

117

Fe I 6301.5 Å IN FALC AND FALP

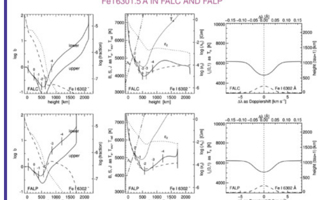

standard polarimetry line

118

Mg I b_2 5173 Å IN FALC AND FALP

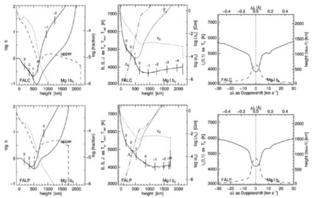

diagnostic of upper photosphere

start index

119

Na I D_1 5896 Å IN FALC AND FALP

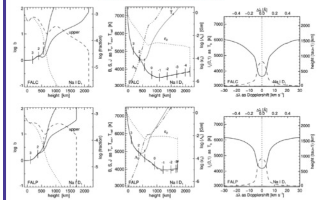

Na I D_1: darkest solar line in optical spectrum = textbook example of two-level scattering

start index

120

Ba II 4554 Å IN FALC AND FALP

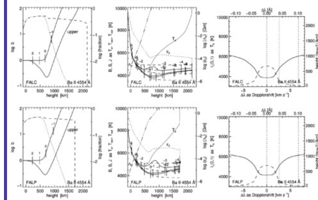

weakest PRD line, best velociy diagnostic, good Hanle diagnostic

start index

121

Ca II 8542 Å IN FALC AND FALP

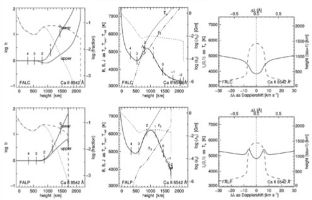

cleanest chromospheric diagnostic in the near infared

start index

122

Ca II K 3934 Å IN FALC AND FALP

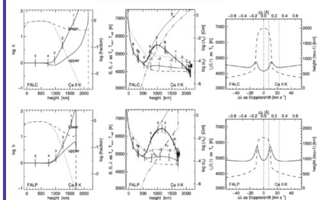

largest extinction in the optical spectrum

start index

123

Mg II k 2796 Å IN FALC AND FALP

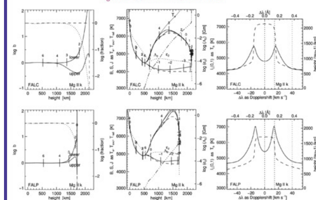

cleanest PRD line and yet larger extincton than Ca II K

start index

124

Lyα 1216 Å IN FALC AND FALP

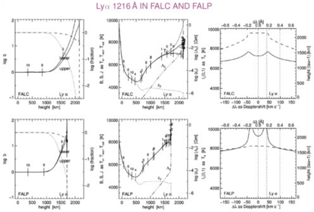

champion: largest extinction and most scattering of all lines

start index

125

Hα 6563 Å IN FALC AND FALP

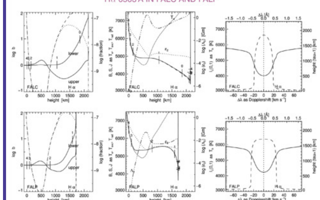

Hα: extraordinary from high excitation energy, huge element abundance, on top of Lyα

start index

126

Hβ 4861 Å IN FALC AND FALP

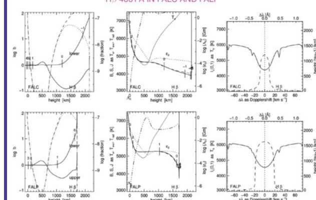

Hβ: analogon to Hα at 5.4× smaller oscillator strength and in the blue

start index

127

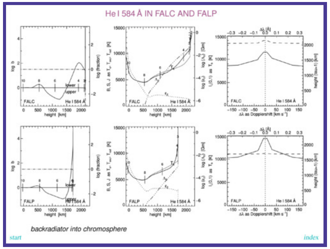

128

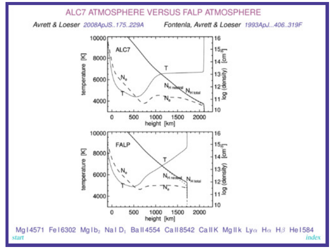

129

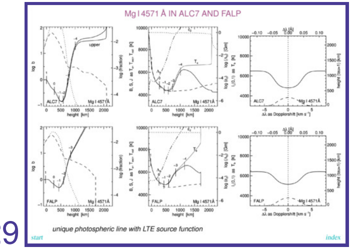

130

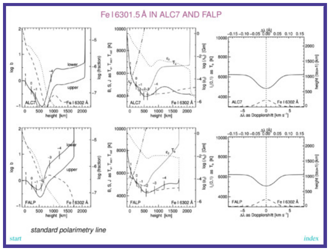

131

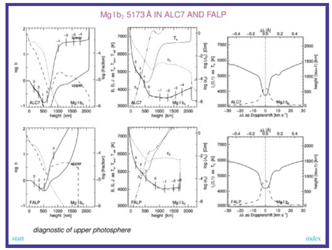

132

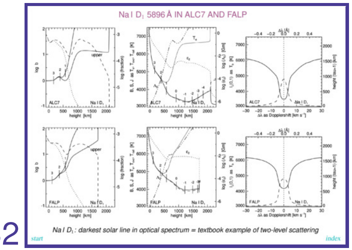

133

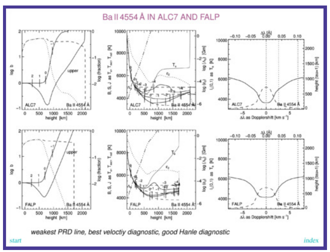

134

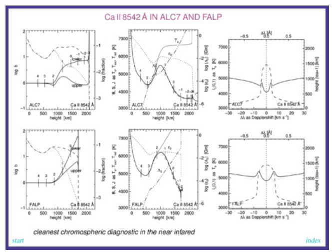

135

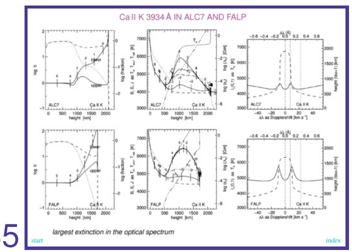

136
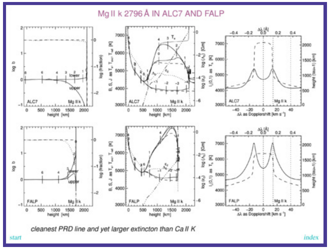

137
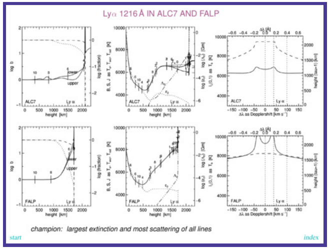

138
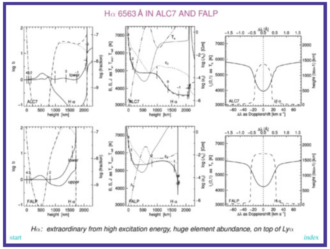

139
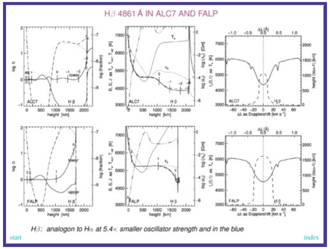

140
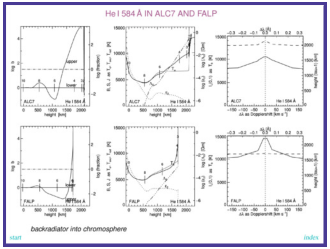

141

SOLAR SPECTRUM FORMATION: EXAMPLES

Robert J. Rutten

https://webspace.science.uu.nl/~rutte101

thin: cloud modeling corona chromosphere Rydberg per ALMA?

thick: UV line flip VAL3C temperature VAL3C spectrum Kurucz stars

photospheric lines: inversions bright points reversed granulation Na I D1 MGs limb emission lines

continua from VAL3C: Avrett models versus 3D MHD VAL3C continua VALII budget hydrogen budget all

lines from ALC7: model optical spectrum ultraviolet depletion hydrogen strong lines plot formats pops plot BSJ plot profile plot Mg I 4571 Fe I 6302 Mg I b_2 Na I D_1 Ba II 4554 Ca II 8542 Å Ca II K Mg II k Lyα Hα Hβ He I 584 He I 10830 canonical Hα Na I D_1–Mg I b_2 Lyα–Hα Hα–Ca II 8542 Å Ca II K–Mg II k versus FCHHT-B ALC7–FALC FALC–FALP ALC7–FALP

detour lines: pumping suction

Oslo-simulated dynamic atmosphere: 1D RADYN 3D Bifrost Bifrost line synthesis

LA-conjectured PSBE atmosphere: non-E Hα aureole boosting Hα extinction CE–SB EBs spicules-II contrail ALMA non-E chromosphere?

IRIS diagnostics: overview diagnostics

start index

142
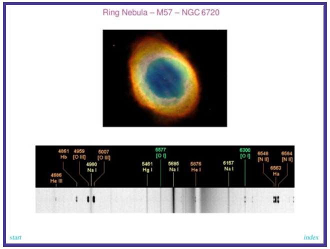

143
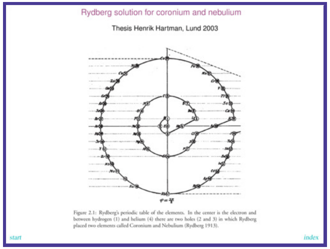

144

thumbs/thumb-ssf-pn-zanstra

145

Bowen nebulium lines

THE ASTROPHYSICAL JOURNAL

AN INTERNATIONAL REVIEW OF SPECTROSCOPY AND ASTRONOMICAL PHYSICS

VOLUME LXVII — JANUARY 1928 — NUMBER 1

THE ORIGIN OF THE NEBULAR LINES AND THE STRUCTURE OF THE PLANETARY NEBULAE

BY I. S. BOWEN

ABSTRACT

Identification of nebular lines.—Eight of the strongest nebular lines are classified as due to electron jumps from metastable states in N_{II}, O_{II} and O_{III}. Several of the weaker lines are identified with recently discovered lines in the spectrum of highly ionized oxygen and nitrogen.

Behavior of lines in nebulae.—The lines thus identified are shown to behave in various nebulae in a way consistent with the foregoing classifications. A similar study of the few lines yet unknown makes it possible to estimate the stage of ionization from which they arise.

Structure of the planetary nebulae.—On the basis of the foregoing identifications, the relative sizes and intensities of the monochromatic images of the planetary nebulae are explained by an extension and modification of the ideas developed by Zanstra for hydrogen in the diffuse nebulae.

start index

146

Bowen line pumping

Thesis Henrik Hartman, Lund 2003

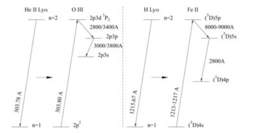

Figure 4.1: Principle for the Bowen mechanism in O III and a similar fluorescence case in Fe II.

start index

147

Pumped Fe II lines from symbiotic Mira RR Tel

Thesis Henrik Hartman, Lund 2003

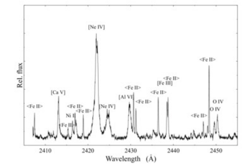

Figure 4.2: Part of the ultraviolet spectrum of RR Tel showing numerous fluorescent <Fe II> and high ionization lines.

start index

148

SOLAR SPECTRUM FORMATION: EXAMPLES

Robert J. Rutten

https://webspace.science.uu.nl/~rutte101

thin: cloud modeling corona chromosphere Rydberg per ALMA?

thick: UV line flip VAL3C temperature VAL3C spectrum Kurucz stars

photospheric lines: inversions bright points reversed granulation Na I D1 MGs limb emission lines

continua from VAL3C: Avrett models versus 3D MHD VAL3C continua VALII budget hydrogen budget all

lines from ALC7: model optical spectrum ultraviolet depletion hydrogen strong lines plot formats pops plot BSJ plot profile plot Mg I 4571 Fe I 6302 Mg I b$_2$ Na I D$_1$ Ba II 4554 Ca II 8542 Å Ca II K Mg II k Lyα Hα Hβ He I 584 He I 10830 canonical Hα Na I D$_1$–Mg I b$_2$ Lyα–Hα Hα–Ca II 8542 Å Ca II K–Mg II k versus FCHHT-B ALC7–FALC FALC–FALP ALC7–FALP

detour lines: pumping suction

Oslo-simulated dynamic atmosphere: 1D RADYN 3D Bifrost Bifrost line synthesis

LA-conjectured PSBE atmosphere: non-E Hα aureole boosting Hα extinction CE–SB EBs spicules-II contrail ALMA non-E chromosphere?

IRIS diagnostics: overview diagnostics

start index

149

PHOTON SUCTION IN ALKALI ATOMS

Bruls, Rutten, Shchukina 1992A&A...265..237B

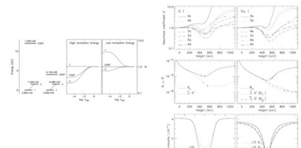

- minority atom: continuum = reservoir
- line photon losses drive replenishment recombination flow
- ground state gets overpopulated to reach photoionization balancing

start index

150

Mg I EMISSION FEATURES AT 12 MICRON

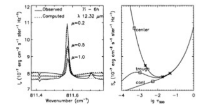

- *discovery*
  - Brault & Testerman 1980: McMath FTS, unpublished
  - Murcray, Murcray & Murcray 1981: South Pole FTS, handmasked
  - Brault & Noyes 1983ApJ...269L..61B: McMath FTS data
  - Chang & Noyes 1983ApJ...275L..11C: identification
- *explanation (Carlsson, Rutten, Shchukina 1992A&A...253..567)*
  - upper-level overpopulation toward laser rise
  - bound-bound suction and bound-free pumping
  - collisionally dominated recombination cascade

start index

151

12 MICRON EMISSION FEATURES

Carlsson, Rutten & Shchukina 1992A&A...253..567C, *Rutten & Carlsson* 1994IAUS..154..309R

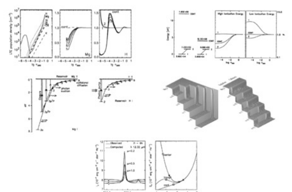

start index

152

THE SIMPLEST HYDROGEN PROBLEM

Auer & Mihalas 1969ApJ...156..157A 1969ApJ...156..681A

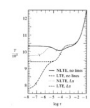

- *simple*
  - plane-parallel HE + RE
  - 2-level + continuum + CRD
- *straightforward*
  - Lyα photon-loss cooling
  - Balmer continuum heating
- *intricate*
  - Hα photon-loss cooling
  - Hα photon-loss heating

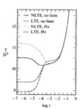

- work through final problem in RTSA course notes *(only 5 pages of questions + 3 pages of footnotesize answers)*
- explain every curve in every graph of Wiersma et al. 2003ASPC..288..130W

start index

153

SOLAR SPECTRUM FORMATION: EXAMPLES

Robert J. Rutten

https://webspace.science.uu.nl/~rutte101

thin: cloud modeling corona chromosphere Rydberg per ALMA?

thick: UV line flip VAL3C temperature VAL3C spectrum Kurucz stars

photospheric lines: inversions bright points reversed granulation Na I D1 MGs limb emission lines

continua from VAL3C: Avrett models versus 3D MHD VAL3C continua VALII budget hydrogen budget all

lines from ALC7: model optical spectrum ultraviolet depletion hydrogen strong lines plot formats pops plot BSJ plot profile plot Mg I 4571 Fe I 6302 Mg I b$_2$ Na I D$_1$ Ba II 4554 Ca II 8542 Å Ca II K Mg II k Lyα Hα Hβ He I 584 He I 10830 canonical Hα Na I D$_1$–Mg I b$_2$ Lyα–Hα Hα–Ca II 8542 Å Ca II K–Mg II k versus FCHHT-B ALC7–FALC FALC–FALP ALC7–FALP

detour lines: pumping suction

Oslo-simulated dynamic atmosphere: 1D RADYN 3D Bifrost Bifrost line synthesis

LA-conjectured PSBE atmosphere: non-E Hα aureole boosting Hα extinction CE–SB EBs spicules-II contrail ALMA non-E chromosphere?

IRIS diagnostics: overview diagnostics

start index

154

INTERNETWORK H_{2V} GRAINS = ACOUSTIC SHOCKS

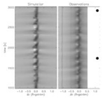

- *Ca II K_{2V} grains (Rutten & Uitenbroek 1991SoPh..134...15R)*
  - extended and confused literature (600 references)
  - most likely non-magnetic phenomenon
  - most likely acoustic shocks
  - wave interference reminiscent of "clapotis"
- *observation (Lites, Rutten & Kalkofen 1993ApJ...414..345L)*
  - sawtooth line-center shift
  - triangular whiskers
  - H_{2V} grains
- *simulation (Carlsson & Stein 1997ApJ...481..500C)*
  - 1D radiation hydrodynamics
  - subsurface piston derived from Fe I Doppler
  - emulation of observer's diagnostics
- *analysis*
  - source function breakdown
  - dynamical chromosphere

start index

155

CLAPOTISPHERE

Rutten 1995soho....1..151R "The internetwork chromosphere is inherently a clapotisphere"

"The extensive literature on the Ca II K_{2V} grains and related cell-interior phenomena leads us to the conclusion that bright cell grains are of hydrodynamical origin, due to oscillations that are present all over the solar surface but which produce grains only at places and moments set by pattern interference between the velocity oscillations in the K_3 layer and the evanescent wave trains of the p-mode oscillation deeper down. They remind us of what is called "clapotis" on sea charts for areas where wave interference produces waterspouts on the ocean (Dowd 1981)."

Rutten & Uitenbroek 1991SoPh..134...15R

"When the crests of such waves coincide, their amplitudes combine, creating huge standing waves, much steeper than traveling waves. This phenomenon is called "clapotis". Off the northern tip of New Zealand, where major wave patterns collide in deep water, clapotis is regularly seen. The pinnacling waves formed here have so much vertical power that they can throw a laden kayak clear out of the water."

Dowd 1981 (not on ADS)

start index

156

SHOCK GRAIN DIAGNOSIS

Carlsson & Stein 1997ApJ...481..500C

$$I_\nu(0) = \int_0^\infty S_\nu \, e^{-\tau_\nu} \, d\tau_\nu = \int_0^\infty S_\nu \; \tau_\nu \, e^{-\tau_\nu} \, \frac{d \ln \tau_\nu}{dz} \, dz$$

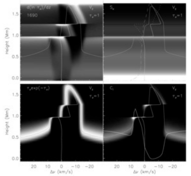

start index

157

SHOCK-RIDDEN COOL LOWER CHROMOSPHERE

Carlsson & Stein 1995ApJ...440L..29C

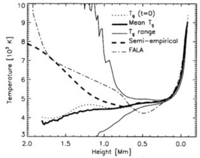

- mean T(h) (thick solid) remains close to RE starting model (dotted)
- bandwidth of T fluctuations (thin solid borders) very large above 1000 km
- a fit of the mean ultraviolet intensities needs a temperature rise (dashed)

start index

158

SOLAR SPECTRUM FORMATION: EXAMPLES

Robert J. Rutten
https://webspace.science.uu.nl/~rutte101

thin: cloud modeling corona chromosphere Rydberg per ALMA?

thick: UV line flip VAL3C temperature VAL3C spectrum Kurucz stars

photospheric lines: inversions bright points reversed granulation Na I D1 MGs limb emission lines

continua from VAL3C: Avrett models versus 3D MHD VAL3C continua VALII budget hydrogen budget all

lines from ALC7: model optical spectrum ultraviolet depletion hydrogen strong lines plot formats pops plot BSJ plot profile plot Mg I 4571 Fe I 6302 Mg I b_2 Na I D_1 Ba II 4554 Ca II 8542 Å Ca II K Mg II k Lyα Hα Hβ He I 584 He I 10830 canonical Hα Na I D_1–Mg I b_2 Lyα–Hα Hα–Ca II 8542 Å Ca II K–Mg II k versus FCHHT-B ALC7–FALC FALC–FALP ALC7–FALP

detour lines: pumping suction

Oslo-simulated dynamic atmosphere: 1D RADYN 3D Bifrost Bifrost line synthesis

LA-conjectured PSBE atmosphere: non-E Hα aureole boosting Hα extinction CE–SB EBs spicules-II contrail ALMA non-E chromosphere?

IRIS diagnostics: overview diagnostics

start index

159

BIFROST SOLAR-ANALOG STAR

- *Bifrost: a Modular Python/C++ Framework for Development of High-Throughput Data Analysis Pipelines* 2017AAS...22923605C
- *Vertical crustal motion observed in the BIFROST project* 2003JGeo...35..425S
- *BIFROST project: 3-D crustal deformation rates derived from GPS confirm post-glacial rebound in Fennoscandia* 2001EP&S...53..703S
- *"SP.ACE" 2013-2015: ASGARD Balloon and BIFROST Parabolic Flights: Latest Developments in Hands-On Space Education Projects for Secondary School Students* 2015ESASP.730..635D
- *BIFROST: conference hotel in Iceland* (not on ADS)
- Bifrost: computational star in Carlssonscandia, remarkably like the Sun in its spectral characteristics and likewise non-plane-parallel, inconstant, and inconsistent, with the virtue of showing much spatio-temporal fine structure similar to solar fine structure:
  - granules and intergranules
  - acoustic box modes similar to solar p-mode interference patterns
  - non-diagnosed internal gravity waves
  - clapotispheric internetwork shocks
  - magnetic network concentrations
  - dynamic fibrils
  - Ellerman reconnection bursts

  but lacking: spicules-II, long fibrils, k_2 - h_2 peak separation, Si IV in UV bursts, more?
- Bifrost analogs in chromosphere-formation stage: CO5BOLD MURaM Mancha

start index

160

BIFROST

- *heritage*
  - Nordlund & Stein 3D HD ⇒ granulation
  - Carlsson & Stein 1D HD RADYN ⇒ Ca II H_{2V} shocks
  - Nordlund et al. 2D MHD Stagger ⇒ MCs, internetwork
- *code*
  - Gudiksen et al. 2011A&A...531A.154G Bifrost description
  - Carlsson & Leenaarts 2012A&A...539A..39C cooling + heating approximations
  - Leenaarts et al. 2012A&A...543A.109L fast angle-dependent PRD
  - Martínez-Sykora et al. 2012ApJ...753..161M ambipolar diffusion
  - Pereira et al. 2013A&A...554A.118P 3D simulation better than standard 1D models
  - Olluri et al. 2013AJ....145...72O non-E 3D solver
  - Golding et al. 2014ApJ...784...30G non-E He ionization
  - Carlsson et al. 2016A&A...585A...4C publicly available snapshot
  - Sukhorukov & Leenaarts 2016A&A...597A..46S PRD in 3D simulations
  - Martínez-Sykora et al. 2017ApJ...847...36M 2D ("2.5D") ion-neutral
  - Leenaarts 2018arXiv180506666L tracer particles ⇒ Lagrangian flow lines
- *warnings*
  - if no Lyα RT no N_e boosting from Lyα surround scattering around hot structures
  - 3D RT may be needed (MULTI3D of Leenaarts & Carlsson 2009ASPC..415...87L) beyond columnwise (RH1.5D of Pereira & Uitenbroek 2015A&A...574A...3P)
  - non-E RT may be needed beyond snapshot-wise SE (especially H, He)

start index

161

BIFROST ANALYSES 1

Hayek et al. 2010A&A...517A..49H solar-type stars
Martínez-Sykora et al. 2011ApJ...732...84M EUV line asymmetries
Leenaarts et al. 2012ApJ...749..136L 3D Hα formation
Stepán et al. 2012ApJ...758L..43S Lyα Hanle
de la Cruz Rodriguez et al. 2012A&A...543A..34D Ca II 8542 Å inversion test
Olluri et al. 2013ApJ...767...43O non-E in O IV ratios
Martínez-Sykora et al. 2013ApJ...771...66M Ca II and Hα from a spicule-II
Leenaarts et al. 2013ApJ...772...89L Mg II h & k for IRIS I
Leenaarts et al. 2013ApJ...772...90L Mg II h & k for IRIS II
Pereira et al. 2013ApJ...778..143 Mg II h & k for IRIS
Hansteen & Archontis 2014ApJ...788L...2A reconnecting strong-field simulation
Olluri et al. 2015ApJ...802....5O optically thin emission lines
Leenaarts et al. 2015ApJ...802..136L Hα fibrils versus field
Stepán et al. 2015ApJ...803...65S scattering polarization Lyα
Pereira et al. 2015ApJ...806...14P MgII triplet formation
Carlsson et al. 2015ApJ...809L..30C Mg II k from plage
Hansteen et al. 2015ApJ...811..106H heating from footpoint braiding
Rathore et al. 2015ApJ...811...81R IRIS C II formation
Guerreiro et al. 2015ApJ...813...61G quiet-Sun heating events

start index

162

BIFROST ANALYSES 2

Martínez-Sykora et al. 2016ApJ...817...46M non-E Si IV/O IV ratios
Golding et al. 2016ApJ...817..125G non-E He ionization
Nóbrega-Siverio et al. 2016ApJ...822...18N 2D (Hα) surges
Kato et al. 2016ApJ...827.....7K waves from magnetic pumping
de la Cruz Rodriguez et al. 2016ApJ...830L..30D Mg II h & k + Mg II triplet inversions
Schmit+DePontieu 2016ApJ...831..158S IRIS Si IV QS internetwork versus IRIS
Leenaarts et al. 2016A&A...594A.104L spatial structure in He I 10830
Schmit & De Pontieu 2016ApJ...831..158S TR emission from internetwork
Martínez-Sykora et al. 2016ApJ...831L....1M 2.5D ambipolar misalignment fibrils-field
Fleischman et al. 2017ApJ...839...30F try NLFFF on Bifrost snapshot
Golding et al. 2017A&A...597A.102G He resonance lines
Kanella & Gudiksen 2017A&A...603A..83K detect reconnection sites and current sheets
Guerreiro et al. 2017A&A...603A.103G small-scale heating events
Martínez-Sykora et al. 2017Sci...356.1269M spicules from ambipolar diffusion
Hansteen et al. 2017ApJ...839...22H generation of bombs and nano/micro-flares
Nóbrega-Siverio et al. 2017ApJ...850..153N 2D non-E Si IV surges
Rouppe van der Voort et al. 2017ApJ...851L...6R plasmoids in UV-burst reconnection

start index

163

BIFROST ANALYSES 3

Bjørgen et al. 2018A&A...611A..62B Ca II H & K insufficient peak separation

Liu et al. 2018arXiv180402931L automatic swirl detection

Nóbrega-Siverio et al. 2018ApJ...858....8N 2D non-E Si IV, O IVsurges

Martínez-Sykora et al. 2018arXiv180506475M ion-neutral 2D: spicules-II

164

RECENT DEVELOPMENTS IN PRD LINE SYNTHESIS

- *RH code: Uitenbroek 2001ApJ...557..389U*
  - Rybicky & Hummer: not $\Lambda(S)$ but $\Psi(j)$ iteration; preconditioning
  - overlappping lines
  - 1D, 2D, 3D, spherical versions
- *RH 1.5D: Pereira & Uitenbroek 2015A&A...574A...3P*
  - 1.5D = column-by-column
  - massively parallel
  - also molecular lines (but Kurucz lines in LTE)
- *angle-dependent redistribution: Leenaarts et al. 2012A&A...543A.109L*
  - good summary PRD theory and equations
  - non-stationary atmosphere requires angle-dependent PRD
  - hybrid approximation: transform to gas parcel frame, assume angle-averaged PRD ($\approx$ angle dependent from deep isotropy), transform back
- *towards Bifrost PRD: Sukhorukov & Leenaarts 2017A&A...597A..46S*
  - hybrid approximation for small memory
  - linear frequency interpolation for speed
  - 252×252×496 grid, 1024 CPUs: 2 days for Mg II k $\approx$ doable
- *next: 3D PRD with multigrid (Bjørgen & Leenaarts 2017A&A...599A.118B)*

165

NON-EQUILIBRIUM HYDROGEN IONIZATION IN 1D SHOCKS

Carlsson & Stein 2002ApJ...572..626C

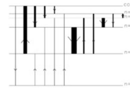

atom top ~ 3.4 eV alkali: NLTE-SE ionization loop
- driven by photon pumping Balmer continuum, scattering from deep, ≈5300 K, smooth
- closure by photon losses in n_α lines

atom bottom actually up to 10 eV: non-E Lyα
- tremendous scatttering from small ε
- tremendous opacity from huge H abundance
- small structures already detailed radiative balance
- non-E: fast settling at high T, slow at low T

- RADYN code: 1D(t) hydrodynamics, time-dependent, NLTE radiation, simple PRD
- observed subphotosphere piston drives acoustic waves up that shock near $h=1000$ km
- Lyα scatters in radiative balance and controls $n=2$. Within shocks $S \approx J$ saturates to B from radiation lock-in (increased ε from partial hydrogen ionization) so that $b_2 \approx 1$
- collisional Lyα balancing has Boltzmann temperature sensitivity: fast (seconds) in hot gas, slow (minutes) in cool gas, resulting in retardation: post-shock cooling gas maintains the high n_2 shock value at increasing b_2 during minutes, up to huge overpopulation ($b_2 \approx 10^{10}$)
- ionization from $n=2$: instantaneous statistical-equilibrium balance driven by Balmer continuum $J \neq B$ and closed by cascade recombination, with $b_{\rm cont}/b_2 \approx 10^{-1}$ in hot and $\approx 10^{+3}$ in cool gas, the latter adding to much larger retarded b_2
- between shocks hydrogen remains hugely overionized versus SE and LTE predictions

166

DETAILED BALANCING

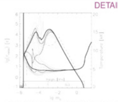

Hydrogen ionization/recombination relaxation timescale throughout the solar-like shocked Radyn atmosphere. The timescale for settling to equilibrium at the local temperature is very long, 15–150 min, in the chromosphere but much shorter, only seconds, in shocks in which hydrogen partially ionizes.
Carlsson & Stein 2002ApJ...572..626C

net radiative and collisional downward rates (Wien approximation)

$$n_u R_{ul} - n_l R_{lu} \approx \frac{4\pi}{h\nu_0}\, n_l^{\rm LTE}\, b_u\, \sigma^l_{\nu_0} \left(B_{\nu_0} - \frac{b_l}{b_u} \overline{J}_{\nu_0} \right) \quad \text{zero for } S = \overline{J},\ \text{no heating/cooling}$$

$$n_u C_{ul} - n_l C_{lu} = n_l C_{lu} \left(\frac{b_u}{b_l} - 1 \right) = b_u n_l^{\rm LTE} C_{lu} \left(1 - \frac{b_l}{b_u} \right) \quad \text{zero for } b_u = b_l,\ \text{LTE } S^l$$

dipole approximation for atom collisions with electrons (Van Regemorter 1962)

$$C_{ul} \approx 2.16 \left(\frac{E_{ul}}{kT} \right)^{-1.68} T^{-3/2} \frac{g_l}{g_u} N_e f$$

Einstein relation

$$C_{lu} = C_{ul} \frac{g_l}{g_u}\, e^{-E_{ul}/kT}$$

C_{ul} is not very temperature sensitive (any collider will do); C_{lu} has Boltzmann sensitivity

167

NON-E HYDROGEN IONIZATION IN 2D MHD SHOCKS

Leenaarts et al. 2007A&A...473..625L

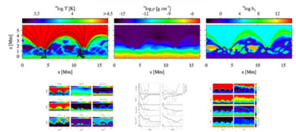

- in shocks Lyα has $S \approx B$ from high T (fast balancing) and N_e (10% H ionization)
- retarded collisional balancing in Lyα: n_2 hangs near high shock value $n_2 \approx n_2^{\rm LTE}$
- gigantic post-shock $n=2$ overpopulations versus LTE ("S-B underestimates")
- yet larger post-shock overionization from hydrogen-top Balmer balancing
- no Lyman RT: green arches artifacts, no lateral N_e boost from Lyα scattering

168

Hα IN BIFROST

1D plane-parallel SE: Rutten & Uitenbroek 2012A&A...540A..86R

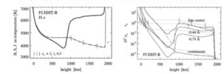

3D non-E MHD: Leenaarts et al. 2012ApJ...749..136L

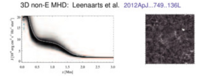

- Hα is a pure scattering line with $S \approx J$ and a deep opacity dip in the upper photosphere
- 3D scattering across the opacity gap enhances fibril visibility
- core darkness measures density, core width measures temperature
- caveats: Bifrost snapshot, no non-E RT, lacking spicules-II, long fibrils

169

OSLO SIMULATION VERSUS 1D STANDARD MODELS

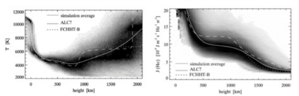

- simulation = state-of-the-art: 3D(t), $\vec{B}$, non-HE, SE populations but NE for H
  Leenaarts, Carlsson & Rouppe van der Voort 2012ApJ...749..136L
- ALC7 = UV fit: 1D static, no $\vec{B}$, HE + microturbulence, SE populations
  Avrett & Loeser 2008ApJS..175..229A
- FCHHT-B = UV fit: 1D static, no $\vec{B}$, HE + imposed acceleration, SE populations
  Fontenla, Curdt, Haberreiter, Harder & Tian 2009ApJ...707..482F

The T and J_ν(Hα) behavior seems arguably similar. However, the conceptual differences between plane-parallel static hydrostatic-equilibrium modeling and the 3D(t) MHD simulation are enormous (cf. Newtonian gravitation versus general relativity). The $T(h)$ stratifications in the simulation vary tremendously, with shocks propagating upwards and sideways and the increase to coronal temperature dancing up and down over a large height range.

170

He I and He II

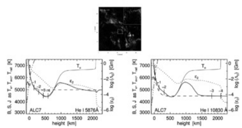

- optical He I lines: nothing in ALC7, nor in atlases, nor in Moore-Minnaert-Houtgast
- more complex non-E formation than H I: not only He I 584 acting as Lyα but ionization/recombination not limited to the atom top as for H I (smooth Balmer continuum driving from below) but sensing hot and structured irradiation from above
- see Bifrost He papers and more to come
- to-do for 2018 = 150 years after Lockyer: explain He I D_3 in flash spectrum

  long dark Hα-like He II 304 fibrils also memorial-opacity contrails?

171

HYDROGEN AUREOLE BOOSTING IN COOL GAS BESIDE HOT GAS

Fontenla et al. 2009ApJ...707..482F Rutten & Uitenbroek 2012A&A...540A..86R Rutten 2016A&A...590A.124R

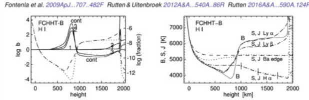

FCHHT-B: steep B rises to chromosphere and corona emulate adjacent cool and hot features

Lyα: scattering back-radiation boosts $S_{{\rm Ly}\,\alpha} \approx J_{{\rm Ly}\,\alpha}$ and Hα extinction $\propto b_2 \approx S_{{\rm Ly}\,\alpha}/B_{{\rm Ly}\,\alpha}$ towards hot-feature value (left: dotted $n_2^{\rm LTE}/N_{\rm Htot}$, dashed actual $n_2/N_{\rm Htot}$)

ionization: also b_2-boosted, with additional $b_{\rm cont}/b_2$ offset defined by the Balmer continuum

Lyβ: b_3 between b_2 and $b_{\rm cont}$ and sharing Hα photon losses

Hα: the FCHHT-B chromosphere is a back-scattering attenuator just as in the ALC7 atmosphere. The b_2 peak from Lyα irradiation does not affect Hα because even with this boost the Hα extinction in the temperature miminum remains negligible.

A hot feature embedded in cooler gas has a similar Lyα scattering aureole enhancing H ionization and Hα extinction around it. A temporary hot disturbance leaves such spread-out boost behind (a wake when moving).

172

Hα EXTINCTION RECIPE

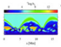

- *retarded Lyα balancing: extinction memory of hot moments*
  - $n_2 \gg n_2^{LTE}$ in hot shocks from fast Lyα balancing and increased ε
  - n_2 decays slowly, tracking high shock values
  - gigantic b_2 in post-shock cooling clouds until next shock

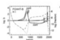

- *Lyα scattering: aureole boosting*
  - Lyα scattering defines $S_{L\gamma} \approx J_{L\gamma}$ with radiative balance
  - hot features in cool gas have Lyα scattering aureoles
  - H I top ($n \geq 2$ including n_{ion}) boosted in aureoles
- *Hα extinction recipe*
  - find hottest instance nearby (~300 km) and in recent past (~minutes)
  - compute Saha-Boltzmann fractional n = 2 population then and there
  - use this extinction value in cooler gas around it and afterwards
  - small hot features leave wider Hα marks (as the grin of the Cheshire cat)
  - fast small hot features leave wider Hα trails (as contrails from jet engines)

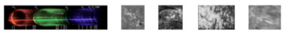

start index

173

SAHA-BOLTZMANN FOR CHROMOSPHERIC LINES

Rutten 2016A&A...590A.124R

Bachelor exercise "Cecilia Payne": compute N_e and κ^{LTE} for given $N_{H,total}$

"I taught making Saha-Boltzmann graphs to hundreds of students at Utrecht and elsewhere with a lab exercise "Cecilia Payne" (available on my website). It uses a fictitious and unpronounceable didactic element called "Schadeenium" after Utrecht astrophysicist Aert Schadee (1936–1999), who invented it for teaching in the 1970s."

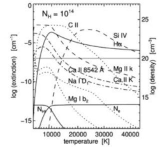

start index

174

CORONAL EQUILIBRIUM VERSUS SAHA-BOLTZMANN IONIZATION

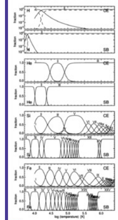

Rutten + Rouppe van der Voort 2017A&A...597A.138R
"Carole Jordan versus Cecilia Payne"

- *CE*
  - up: collisional excitation/ionization
  - down: radiative deexcitation/recombination
  - NB: dielectronic recombination
- *SB*
  - up: collisional excitation/ionization
  - down: collisional deexcitation/recombination
- $N_e = 10^{14}$ (other densities)
  - SB: N_e affects ionization, not excitation
  - CE: N_e affects excitation, not ionization
  - smaller N_e: SB peaks steepen and shift left
- *hydrogen*
  - long H I tail from no H III (log scales)
  - still competitive at 10^{-5} others
- *Mg III, C V, Si V, Si XIII, Fe XVII, Fe XXV*
  - wide hump from closed shell (atom configs)
  - extra recombination radiation into previous ion

index

175

ELLERMAN BURSTS OVERVIEW

- Mount Wilson: solar hydrogen bombs
  Ellerman 1917ApJ....46..298E ADS citation history (100=100?)
  - sudden brightenings in Hα wings
  - not in line core, only in Balmer and Ca II lines
  - between spots in complex emerging active regions

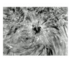

- DOT: pseudo Ellerman bombs
  Leenaarts et al. 2006A&A...449.1209L 2006A&A...452L..15L
  Rutten et al. 2013JPhCS.440a2007R
  - magnetic concentrations in sunspot moat
  - Spruit hole radiation plus small collisional damping
  - Hα blue-wing BPs better than G-band BPs

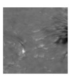

- SST: true Ellerman bombs
  Watanabe et al. 2011ApJ...736...71W
  - photospheric jets in rapid succession along network
  - shielded in Hα core by overlying fibrils
  - photospheric strong-field reconnection?
- interpretation: *reconnection per cartoon*

start index

176

ELLERMAN BOMB VISIBILITIES

Rutten 2016A&A...590A.124R

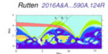

- *observations*
  - Ellerman bomb: Hα moustaches below core fibrils [example] [movie]
  - also bright but different in Ca II 8542 Å [example]
  - also bright but diffuse in AIA 1700 and 1600 Å [example]
  - not in optical continuum nor Fe I, Na I D, Mg I b lines [example]
  - also bright in IRIS C II and Si IV lines [example]
  - hot FAF-like aftermaths with cool blends [example] [EBs vs FAFs]
- *visibility recipes*
  - Balmer in hot and dense onsets: Saha-Boltzmann extinction
  - cooling aftermaths: long Balmer memory of large onset extinction
  - Hα wings: electron broadening (Stark + Holtsmark)
  - transition-region lines: at large N_e extinction closer to SB then CE
  - "cool" blends: surrounding cool clapotisphere in slanted viewing (above)
  - diffuse bright feet in 1700 Å: surround irradiation by EB + bound-free scattering

start index

177

ELLERMAN BOMBS PER LTE

Rutten 2016A&A...590A.124R

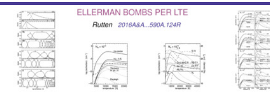

- *Hα*
  - extraordinary hot-gas opacity (large abundance, large excitation energy, no HIII)
  - extraordinary wide wings at large H ionization (Stark + Holtsmark)
  - extraordinary memory for hot past
- *ultraviolet Balmer continuum*
  - same hot-gas opacity and memory as Hα
  - fibrils transparent so no Stark moustaches needed
  - shielding by surrounding photosphere, but scatter-through in Mg I and Fe I edges
- *other lines*
  - Na I D and Mg I b absent above 10 000 K
  - Si IV absent below 20 000 K but may have hot-past memory in cooling gas
  - EB bottoms shielded by adjacent or overlying cooler gas, except Hα and Si IV

start index

178

STRAWS / SPICULES-II / RBEs / RREs

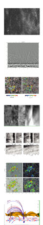

- *observations*
  - "straws", DOT Ca II H
    Rutten 2006ASPC..354..276R
  - "spicules-II", Hinode Ca II H
    De Pontieu et al. 2007Sci...318.1574D
  - "rapid blue excursions", SST Hα
    Rouppe van der Voort et al. 2009ApJ...705..272R
  - "coronal heating events", Hinode Hα + SDO EUV
    De Pontieu et al. 2011Sci...331...55D
  - "torsion-swaying jets", SST Hα + Ca II 8542 Å
    De Pontieu et al. 2012ApJ...752L..12D
  - "rapid red excursions", SST Hα
    Sekse et al. 2013ApJ...769...44S
- *simulation: Martinez-Sykora et al.* 2011ApJ...736....9M
  - feature called a spicule-II but questionable
  - no others in simulations so far
  - driver unknown (Pereira et al. 2012ApJ...759...18P)
- *upshot: ubiquitous small magnetic heating events possibly important in*
  - quiet-sun (also unipolar) coronal heating
  - fast solar wind driving
  - solar wind element segregation

start index

179

LONG FIBRILS AS CONTRAILS

Rutten & Rouppe van der Voort 2017A&A...597A.138R

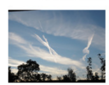

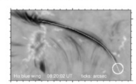

- Hα blue wing: fantail with slender extending dark thread = wide blueshifted core
- visible in IRIS 1400 Å (Si IV), AIA 304, 171, 193 Å, not in Ca II 8542 Å = hot
- three-four minutes later dark Hα core fibril = non-E H recombination
- large non-E Hα opacity in cooling post-hot-disturbance gas
- fibril ~ contrail: not representing cool present but much hotter precursor past
- line-tying by precursor H ionization: contrail maps preceding field topography

start index

180

SAHA-BOLTZMANN HYDROGEN EXTINCTION AT ALMA WAVELENGTHS

Rutten 2017A&A...598A..89R 2017IAUS..327....1R (tutorial)

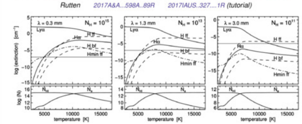

- LTE extinction: Lyα Hα H I continua H⁻ ff continuum 8542 other lines
- Hα at high T: LTE extinction from $n_2 \approx n_2^{LTE}$ enforced by enclosed Lyα
- H ionization: $n = 2$ population fixed by (actually non-E) Lyα; hydrogen top has additional NLTE-SE balancing between Balmer continuum and Balmer lines
- Balmer continuum $T_{rad} \approx 5250$ K: overionization below, underionization above ⇒ de-steepening of these LTE H ff Boltzmann increases around 5250 K pivot
- $\alpha_\nu^{ff} \sim \lambda^2 N_e N_{ion} T^{-3/2}$ (RTSA Eq. 2.79) gives steep H ff increase between ALMA bands
- features with non-E post-hot Hα extinction have larger to very much larger H ff extinction

start index

181

PREDICTIONS FOR SOLAR ALMA

2017A&A...598A..89R

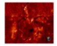

1. ALMA sun mostly covered by long fibrils (unlike simulated suns)
2. similar to Hα, good dark–dark correspondence, more opaque at longer ALMA wavelengths, less lateral contrast (no Dopplershifts)
3. temperatures: above 10 000 K in heating events propagating outward from activity, around 7000 K in initial fibrils, cooling down to 5000 K in long contrail fibrils (or less)
4. heating events best detectable with ALMA (if sufficient resolution)
5. if so, darker aureoles vanishing above 15 000 K (Lyα scattering)
6. small precursors produce 0.2–0.5 arcsec Hα and ALMA contrail widths (Lyα scattering)
7. precursors better field mappers than subsequent contrail fibrils (H ionization)
8. internetwork shocks only in quietest areas, with 4000 K cooling clouds (COmosphere)
9. no Ellerman bombs (hidden by fibrils)
10. flaring active-region fibrils poke through (@ measure reconnection temperature)
11. off-limb spicules-II more opaque than in Hα and Ca II H
12. coronal rain much more opaque than in Hα

start index

182

SOLAR RYDBERG LINES WITH ALMA?

Rutten 2017IAUS..327....1R

- *"linear thermometer"*
  - H⁻ free-free + H I free-free: $S = B$
  - thick feature: $T_b = T(\tau_\nu = 1)$
  - thin feature: cloud contribution $\Delta T_b = \tau T$
- *solar Rydberg lines so far*
  - in μm range Mg I stronger than H I
  - prediction H I α lines $n = 4 - 18$
  - H I 19α, 21α observed at limb
- *H I Rydberg lines with ALMA?*
  - candidate: H I 30α in Band 6 (1.3 mm)
  - much stronger than above predictions from large post-hot non-E extinction?
  - if so, unblendedly present since Mg I etc are not non-E boosted?
  - on disk as $T(\tau_\nu = 1)$ emission at steep $T(\tau)$ gradient
  - at limb as τT extension
  - Zeeman in I and Stokes: super-sensitive chromospheric magnetometer?

start index

183

NON-EQUILIBRIUM CHROMOSPHERE

cromosphere potpourri

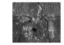

- *Hα chromosphere = past defined by Lyα*
  - long fibrils = post-hot cooling clouds
  - long-fibril contrast = different histories and Dopplershifts
  - long-fibril widths = Lyα scattering (0.2–0.5 arcsec)

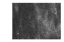

- *Ca II H & K chromosphere = present defined by temperature*
  - thin fibrils = horizontally launched heating events
  - thin-fibril widths = heating-event widths + scattering halo
  - @ corresponding IRIS Si IV, AIA EUV, ALMA mm features?

- *Hα versus Lyα = past versus present*
  - Lyα grains = heating events
  - Lyα short fribrils and comet heads = initial tracks
  - @ Lyα, ALMA heating-event imaging spectroscopy?

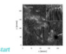

- *Hα versus Ca II 8542 Å versus He I D₃ versus He II 304 = idem*
  - Ca II instantaneous = short fibrils
  - He I D₃ ~ He II 304 = post-hot irradiated cooling gas?
  - @ time-delay image correlations

start index

184

IRIS DIAGNOSTICS OVERVIEW

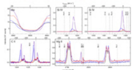

- *Si IV 1400 Å lines*
  - peak ratio 2: feature (not "lines") optically thin
  - if so: faithful Doppler mapping (e.g., EB bimodal jets)
  - gas temperature: 90 kK for CE, 20 kK for SB (ALMA at ratio ⇒ 1?)
- *Mg II h & k lines*
  - enormous SB opacity
  - strong PRD scatterers
  - SB opacity sampling classical chromosphere top to bottom
- *Mg II triplet lines*
  - bright suggests steep deep temperature rise
  - bright suggests (non-E?) recombination from wide Mg III reservoir
  - Mn I blend = photospheric gas along line of sight

start index

185

IRIS DIAGNOSTICS

- *Mg II h & k*
  - Leenaarts et al. 2013ApJ...772...89L
  - Leenaarts et al. 2013ApJ...772...90L
  - Pereira et al. 2013ApJ...778..143
  - Carlsson et al. 2015ApJ...809L..30C
- *other lines*
  - Mg II triplet Pereira et al. 2015ApJ...806...14P
  - C II doublet Rathore et al. 2015ApJ...811...80R
  - C II doublet Rathore et al. 2015ApJ...811...81R
  - C II doublet Rathore et al. 2015ApJ...814...70R
  - O I 1355.6 Å Lin et al. 2015ApJ...813...34L

start index

186

SOLAR SPECTRUM FORMATION: EXAMPLES

Robert J. Rutten

https://webspace.science.uu.nl/~rutte101

thin: cloud modeling corona chromosphere Rydberg per ALMA?

thick: UV line flip VAL3C temperature VAL3C spectrum Kurucz stars

photospheric lines: inversions bright points reversed granulation Na I D1 MGs limb emission lines

continua from VAL3C: Avrett models versus 3D MHD VAL3C continua VALII budget hydrogen budget all

lines from ALC7: model optical spectrum ultraviolet depletion hydrogen strong lines plot formats pops plot BSJ plot profile plot Mg I 4571 Fe I 6302 Mg I b₂ Na I D₁ Ba II 4554 Ca II 8542 Å Ca II K Mg II k Lyα Hα Hβ He I 584 He I 10830 canonical Hα Na I D₁–Mg I b₂ Lyα–Hα Hα–Ca II 8542 Å Ca II K–Mg II k versus FCHHT-B ALC7–FALC FALC–FALP ALC7–FALP

detour lines: pumping suction

Oslo-simulated dynamic atmosphere: 1D RADYN 3D Bifrost Bifrost line synthesis

LA-conjectured PSBE atmosphere: non-E Hα aureole boosting Hα extinction CE–SB EBs spicules-II contrail ALMA non-E chromosphere?

IRIS diagnostics: overview diagnostics

start index

187

thumbs/thumb-\par .jpg

1 .jpg

start index

thumbs/thumb-.jpg